

# **Encapsulation of Explant-Derived Cardiac Stem Cells in Agarose Nanoporous Gel Cocoons to Enhance Cardiac Repair**

Pushpinder Kanda, M.Sc.

This thesis is submitted as a partial fulfillment of the Ph.D program in Cellular and  
Molecular Medicine.

Department of Cellular and Molecular Medicine

Faculty of Medicine

University of Ottawa

**Supervisor:** Darryl R. Davis, MD

© Pushpinder Kanda, Ottawa, Canada, 2019

## **Copyright Statement:**

The introduction chapter (Chapter 1) has been published in the journal *Expert Opinion On Biological Therapy* and reprinted (adapted) with permission from Kanda P., and Davis DR. Cellular mechanisms underlying cardiac engraftment of stem cells. *Expert Opinion in Biological Therapy*, 2017, 17(9):1127-1143. Copyright (2017) Taylor & Francis. (See supporting information pg. 147)

Study 1 (Chapter 3) has been published in the journal *ACS Nano* and reprinted (adapted) with permission from Kanda P., *et al.* Deterministic Encapsulation of Human Cardiac Stem Cells in Variable Composition Nanoporous Gel Cocoons To Enhance Therapeutic Repair of Injured Myocardium. *ACS Nano*, 2018, 12 (5), pp 4338–4350. Copyright (2018) American Chemical Society.

(See supporting information pg. 148)

Study 2 (Chapter 4) is original work and has not been published at the time of thesis submission.

**Abstract:**

Micro-encapsulation of heart explant-derived stem cells (EDCs) within protective nanoporous gel (NPG) cocoons improves cardiac function and long-term retention of transplanted cells after ischemic injury by limiting detachment induced cell death and vascular clearance of intramyocardial injected cells. Although cocooned EDCs boost cardiac function, the fundamental mechanism is unclear. Here, we investigate the effects of altering cocoon stiffness and size on human EDC mediated repair of damaged myocardium using an immunodeficient mouse model of ischemic cardiomyopathy.

First, we found that increasing cocoon stiffness by altering NPG content boosted cell viability and migration; effectively forcing cocooned cells to adopt a migratory, invasive phenotype. Although cocooning improved retention of transplanted cells, increasing cocoon stiffness had no additional effects on long-term engraftment despite markedly improving cardiac function and fibrosis after myocardial infarction. Given increased cocoon stiffness boosted the production and microRNA cargo within EDC nanovesicles, the observed benefits in post-ischemic function are likely dependent more on paracrine production of transplanted cells rather than simply increasing the number of cells retained.

The effect of cocoon diameter on EDC phenotype and cell mediated repair of ischemic myocardium was evaluated using microfluidic-based cocooning enabling deterministic encapsulation within defined cocoon size and intracapsular cell number while maintaining a fixed cocoon stiffness. Increased cocoon size enhanced post-ischemic cardiac function by reducing clearance of transplanted cells and increased paracrine stimulation of endogenous repair. The latter being attributable to microfluidic

cocooning closely following the expected Poisson distribution with smaller cocoons having a greater proportion of single cells while larger cocoons contained greater proportions of multicellular aggregates which enhanced cell-cell interactions to increase the amount and breadth of cytokines/nanoparticles delivered to injured myocardium.

In conclusion, altering the biophysical properties of NPG surrounding cocooned cells provides a straightforward means of boosting the regenerative potential of heart EDCs for repair of injured myocardium.

## Table of Contents:

<b>1.0 General Introduction</b> .....	1
1.1 Ischemic Cardiomyopathy .....	1
1.2 Historical Background of Cell Therapy Treating Ischemic Cardiomyopathy .....	2
1.3 Cardiac Derived Stem Cells for Treating Ischemic Cardiomyopathy .....	6
1.3.1 Side Population.....	7
1.3.2 Antigenic Selection of Cardiac c-Kit+ Cells.....	8
1.3.3 Cardiospheres, cardiosphere-derived cells, and explant-derived cardiac stem cells.....	9
1.3.4 Clinical Trials Using Cardiac Derived Cells.....	14
1.4 Heterogeneity of Injured Myocardium .....	16
1.5 Engraftment of Transplanted Cells.....	20
1.6 Cellular Mechanisms Underlying Intra-Coronary Injected Cell Uptake in The Heart .....	27
1.7 Mechanism of Cell-Mediated Repair of Damaged Myocardium .....	28
1.8 Transplanted Cell Persistence Hypothesis.....	31
1.9 Mechanical Clearance of Transplanted Cells.....	32
1.10 Role of Transplanted Cell Pro-Survival Signalling.....	34
1.11 Role of Biomaterials in Transplanted Cell Engraftment.....	37

<b>2.0 Encapsulation of Explant-Derived Cardiac Stem Cells in Agarose Nanoporous Gel Cocoons</b> .....	40
2.1 Study 1: Introduction, Aim, and Hypothesis .....	40
2.2 Specific Objectives for Study 1: .....	43
2.3 Study 2: Introduction, Aim, and Hypothesis .....	43
2.4 Specific Objectives for Study 2: .....	45
2.5 Summary of Study 1 and 2:.....	45
<b>3.0 Study 1: Deterministic Encapsulation of Human Cardiac Stem Cells in Variable Composition Nanoporous Gel Cocoons to Enhance Therapeutic Repair of Injured Myocardium</b> .....	47
3.1 Abstract.....	47
3.2 Results.....	48
3.2.1 Characterization of Nanoporous Gel Capsules.....	48
3.2.2 Effects of Nanoporous Gel Encapsulation on Proliferation and Viability .....	50
3.2.3 Effects of Nanoporous Gel Encapsulation on Cell Morphology and Migration	53
3.2.4 Effects of Altered Nanoporous Gel Capsule Rigidity on EDC Engraftment and Myocardial Repair.....	60
3.2.5 Paracrine Profiling of Encapsulated EDCs.....	63
3.3 Conclusion .....	66
3.4 Methods .....	67
3.4.1 Patients and Cell Culture .....	67

3.4.2 Nanoporous Gel Encapsulation .....	68
3.4.3 Low Temperature Scanning Electron Microscopy, Atomic-Force Microscopy, Transmission Electron Microscopy, and Z-Stack Confocal Microscopy .....	69
3.4.4 Immunohistochemistry .....	71
3.4.5 Conditioned Media for Paracrine Profiling .....	71
3.4.6 Migration Assays .....	72
3.4.7 Myocardial Infarction, Cell Injection, and Functional Evaluation .....	73
3.4.8 Histology .....	75
3.4.9 Statistical Analysis .....	75
<b>4.0 Study 2: Enhanced Therapeutic Repair of Injured Myocardium by High- Throughput Microfluidic-Based Cocooning of Explant-Derived Cardiac Stem Cells</b> .....	<b>77</b>
4.1 Abstract.....	77
4.2 Results.....	78
4.2.1 Fabrication of Microfluidic Platform .....	78
4.2.2 Characterization of Nanoporous Gel Cocooned EDCs .....	80
4.2.3 Effects of Nanoporous Gel Encapsulation on Cell Migration and Viability .....	85
4.2.4 Effects of Altered Nanoporous Gel Capsule Size on Cell Retention and Myocardial Repair .....	85
4.2.5 Effects of Cell-Cell Contact on Paracrine Profile.....	89
4.3 Conclusion .....	91

4.4 Methods .....	91
4.4.1 Patients and Cell Culture .....	91
4.4.2 Vortex Encapsulation .....	92
4.4.3 Microdevice Design and Fabrication .....	93
4.4.4 Cell Viability, Migration Assay and Cytokine profile .....	96
4.4.5 Myocardial Infarction, Cell Injection, and Functional Evaluation .....	97
4.4.6 Viral Packaging and Transduction .....	99
4.4.7 Bioluminescent Imaging for <i>In Vivo</i> Cell Tracking .....	100
4.4.8 Histology .....	100
4.4.9 Statistical Analysis .....	101
<b>5.0 Discussion .....</b>	<b>102</b>
<b>6.0 Supporting Information .....</b>	<b>109</b>
<b>7.0 Bibliography .....</b>	<b>152</b>

## List of Tables

Table 1.	Advantages and disadvantages of stem cell therapy for cardiac regeneration.	12
Table 2.	Benefits and disadvantages of cell therapy.	29
Table 3.	Mechanism of enhancing cell retention and function using biomaterials.	37
Table S1.	Advantages of agarose NPG.	106
Table S2.	Study 1: Echocardiographic measurements of left ventricle dimensions and function.	108
Table S3.	Top 20 miRNAs present in EDC secreted nanovesicles regulating angiogenesis, fibrosis, cardiomyocyte proliferation and apoptosis.	109
Table S4.	Comparing miRNA expression in nanovesicles isolated from cocooned and adherent EDCs.	110
Table S5.	Comparing miRNA expression in nanovesicles isolated from EDCs cocooned in 3.5% and 2% NPG capsules.	115
Table S6.	Study 1: Summary of patient characteristics.	116
Table S7.	Study 2: Echocardiographic measurements of left ventricle dimensions and function.	118
Table S8.	Study 2: Summary of patient characteristics.	119

## List of Figures

Figure 1.	Cellular mechanisms limiting retention and survival of cells transplanted into the damaged heart.	22
Figure 2.	Mechanisms underlying cardiac repair by stem cell therapy.	30
Figure 3.	Cell encapsulated in nanoporous gel cocoon.	40
Figure 4.	Characterization of nanoporous gel capsules.	50
Figure 5.	Effect of nanoporous gel encapsulation on cell cytoskeletal structure.	54
Figure 6.	Effects of nanoporous gel encapsulation on cell migration.	56
Figure 7.	Characterizing cell egress from nanoporous gel capsules.	58
Figure 8:	Effects of altered nanoporous gel capsule composition on EDC engraftment and myocardial repair.	61
Figure 9.	Paracrine profiling of nanoporous gel encapsulated EDCs.	64
Figure 10.	Microfluidic schematics.	78
Figure 11.	Characterization of microfluidic nanoporous gel cocoons.	81
Figure 12.	Effects of cocoon size on cell migration and viability.	83
Figure 13.	Effects of changing cocoon size on EDC engraftment and myocardial repair.	86
Figure 14.	Effects of cell-cell interaction on cytokine profile.	89
Figure S1.	Size distribution of empty nanoporous gel capsules.	121
Figure S2.	Physical characterization of nanoporous gel capsules.	122
Figure S3.	Cell viability in post encapsulation.	124
Figure S4.	Measuring 2-D cell migration rate.	126
Figure S5.	Kinetics of EDC emerging out of capsules.	127
Figure S6.	Extracellular clustering in capsules.	128

Figure S7.	Study 1: Scar size.	129
Figure S8.	Study 1: BrdU staining.	130
Figure S9.	Study 1: Vessel density.	131
Figure S10.	Profiling the secretion of TIMPs and exosome nanovesicles in condition media.	132
Figure S11.	KEGG pathway analysis for encapsulated vs. non-encapsulated EDCs.	133
Figure S12.	KEGG pathway analysis for altering capsule composition.	134
Figure S13.	Microfluidic device setup.	135
Figure S14.	Empty cocoon size and ECM distribution.	137
Figure S15.	EDCs viability and migration.	138
Figure S16.	Left ventricular ejection fraction plot.	139
Figure S17.	Study 2: Scar size.	140
Figure S18.	Study 2: Vessel density.	142
Figure S19.	Study 2: BrdU staining.	143
Figure S20.	Transgenic EDCs expressing firefly luciferase.	145

## List of Abbreviations

Adh = Adherent

ATP = Adenosine triphosphate

BMMCs = Bone marrow mononuclear cells

Brdu = Bromodeoxyuridine

CDC = Cardiosphere-derived stem cell

CEM = Cardiac explant media

c-Kit = receptor tyrosine kinase

CSC = Cardiac-derived stem cell

cTnT = Cardiac troponin T

DAMPS = Damage-associated molecular patterns

EDC = Explant-derived stem cell

ECM = Extracellular matrix

eNOS = Endothelial nitric oxide synthase

EPC = Endothelial progenitor cell

ESC = Embryonic stem cells

FGF = Fibroblast growth factor

HSP = Heat shock protein

HIF-1 = Hypoxia inducible factor 1

IC = Intracoronary

ICM = Ischemic cardiomyopathy

IGF-1 = Insulin-like growth factor 1

IL = Interleukin

IM = Intramyocardial

iPSCs = Induced pluripotent stem cells

IV = Intravenous

LCA = Left coronary artery

MF = Microfluidic

MI = Myocardial Infarct

MSC = Mesenchymal stem cell

NOD/SCID = non-obese diabetic/severe combined immunodeficiency

NPG = nanoporous gel

PBMCs = Peripheral blood mononuclear cells

qPCR = Quantitative polymerase chain reaction

ROS = Reactive oxygen species

Sca-1 = Stem cells antigen-1

SDF-1 = Stromal cell-derived factor 1

SkMs = Skeletal myoblasts

Susp (or Sp) = Suspended

TLR = Toll-like receptors

TNF = Tumor necrosis factor

TGF = Transforming growth factor

Vx = Vortex

## Acknowledgments

I am deeply grateful to the following individuals for their contributions and support with my thesis project:

- Thesis Advisory Committee

Dr. Duncan J Stewart, Dr. David W Courtman, and Dr. Rob Beanlands

- Dr. Davis's Laboratory members:

Bin Yi (Training and experimental design)

Sandrine Parent (animal surgeries and *in vivo* data collection)

Tanya Yeuchykh (*In vitro* experiments and data collection)

Richard Seymour (animal surgeries and *in vivo* data collection)

Ghazaleh Rafatian (Optimizing experimental design)

Audrey Mayfield (Training and experimental design)

Alexandros Nikolaos Nantsios (experimental design and optimization)

- Collaborating members:

Dr. Ainara Benavente-Babace (Microfluidic platform design and *equal* contribution to experiments, and data analysis for microfluidic study)

Dr. Emilio I. Alarcon (Biomaterial characterization)

Dr. Fabio Variola (Biomaterial characterization)

Dr. Michel Godin (Microfluidic platform design)

Dr. Robert A. de Kemp (*In vitro* data analysis)

Nicholas Cober (Training and *in vivo* cell tracking data collection)

- University of Ottawa Heart Institute - Animal Care and Veterinary Services
- University of Ottawa Heart Institute - Cardiac surgeons for collecting of cardiac biopsy specimens:

Dr. Marc Ruel, Dr. Buu-Khanh Lam, Dr. Munir Boodhwani, Dr. Fraser Rubens, Dr. Vincent Chan, and Dr. Thierry Mesana

I would like to thank Dr. Duncan J Stewart's lab for providing the lentivirus vector for the expression of firefly luciferase.

I owe my deepest gratitude to my supervisor, Dr. Darryl R Davis. Without his continuous mentorship, advice, and support over the past three years, this work would not have been possible.

## **Sources of Funding**

This work was supported by the Canadian Institutes of Health Research (Operating Grant 229694) and the Heart and Stroke Foundation of Canada (NA-7346). D. R. Davis and P. Kanda are supported by the Canadian Institutes of Health Research Clinician Scientist Award (MC2-121291) and the Frederick Banting and Charles Best Canada Graduate Scholarship, respectively.

**Notes:** The authors declare the following competing financial interest(s): D.J. Stewart and D. Courtman are named inventors on a patent application detailing the technology described in this thesis dissertation.

# Chapter 1

## 1.0 General Introduction

### 1.1 Ischemic Cardiomyopathy

Heart failure is a major source of morbidity and mortality and affects over 26 million individuals worldwide.<sup>1</sup> Ischemic cardiomyopathy (ICM), a leading cause of heart failure, is a disease in which a myocardial infarct (MI) results in the conversion of dead myocardium into scar tissue. Ongoing cardiac-tissue remodeling progressively declines the heart's pumping function.<sup>2,3</sup> Although the development of new pharmaceutical drugs and medical management has improved disease outcome, the mortality rate remains high whereby 27% of the patients die within 1 year of diagnosis.<sup>2,4</sup> CM affects over 600 000 Canadians and costs the healthcare system over \$480 million annually -the cost is predicted to surpass \$1 billion/annum by 2030.<sup>5</sup> These observations rationalize a new focus on novel means to reverse, repair, and vascularize the damaged ICM heart.

To address this pressing need, cell therapy has emerged as a promising option to prevent adverse cardiac remodeling and reverse damage post MI. Just over a decade, the mammalian heart was thought to be a terminally differentiated organ with no capacity to regenerate. It was believed that a set number of cardiomyocytes determined at birth would slowly dwindle with aging or injury and no mechanism to replace lost cardiomyocytes. However, several studies challenged this dogma by providing evidence that the heart exhibited low level cardiomyocyte renewal.<sup>6-8</sup> Today, several pre-clinical studies in small and large animals have identified endogenous multipotent cardiac

progenitor cells within the adult heart with the capacity to differentiate into cardiomyocytes, endothelial and smooth muscle cells.<sup>9-13</sup>

Cardiac cell therapy is the treatment of injured myocardium with *ex vivo* expanded cells to improve cardiac function. The critical feature of this definition lies in the premise that transplanted cells must (at least transiently) remain in the heart to promote healing. Over the past decade, it has become clear that, in the absence of additional treatments designed to enhance cell survival, long-term engraftment of any transplanted cell is modest and all therapeutic regeneration is mediated by the stimulation of endogenous repair mechanisms rather than differentiation of transplanted cells into working myocardium.<sup>14-17</sup> This realization has led many to question the need for “cells” in cell therapy and has motivated the search for cell-sourced factors that can stimulate endogenous repair as a means of bypassing cell transplantation. Nevertheless, if robust engraftment could be achieved, cardiomyogenic cell products could be more engaged in direct cardiac repair and the efficacy of adult cell therapy could be markedly enhanced. This is particularly important for the therapy of established ischemic cardiomyopathy, which would likely require a substantial increase in contractile cells to reverse long-term functional and structural abnormalities. This chapter outlines the challenges confronting cardiac engraftment of *ex vivo* expanded cells and explore the potential of enhancing cell-mediated repair of injured myocardium by targeting the fundamental mechanisms limiting transplanted cell retention and survival.

## **1.2 Historical Background of Cell Therapy Treating Ischemic Cardiomyopathy**

At the turn of the century, the ability of cell based products to repair damaged hearts was first explored using unselected bone marrow mononuclear cells (BMMCs) which contain a mixture of endothelial, hematopoietic and mesenchymal progenitor cells.<sup>18,19</sup> In part, this strategy was chosen based on the widespread availability of hospital based bone marrow transplantation programs that could provide a clinically compatible cell source believed (at this time) to differentiate into a de novo vascular network (vasculogenesis) while also promoting the growth of new capillaries from pre-existing blood vessels (angiogenesis). Promising data from preclinical studies led to the start of several clinical trials<sup>20-24</sup> and, while these studies showed that BMMC administration was safe, clear evidence supporting the ability of BMMCs to repair injured myocardium is lacking.<sup>25</sup> Although, differences in patient demographics, cell dose/source, method/route/time of administration, and primary study endpoints make direct comparisons challenging,<sup>26</sup> this data has resulted in an ongoing large multinational phase III trial (BAMI, NCT01569178; study start date September 2013) powered to detect a decrease in all-cause mortality after intracoronary (IC) administration of BMMCs.

Based on early BMMC results and the belief that a “purified” cell product might provide greater cell-mediated repair, attention focused towards antigenically selecting (*i.e.*, CD34+ or CD133+)<sup>27,28</sup> or culture-guiding (*i.e.*, endothelial progenitor cells, EPCs)<sup>29</sup> cells that demonstrated marked pro-angiogenic and vasculogenic properties. Although promising studies show enhanced therapeutic potency<sup>30</sup> and cell homing to the injured heart,<sup>17</sup> the overall efficacy of antigenically selected cells remains comparable to unselected BMMCs.<sup>31</sup> In retrospect, this finding is not surprising as very few transplanted BMMCs are found after IC or intramyocardial (IM) injection<sup>17,32-34</sup> with the salutary effects

of cell transplantation attributable to indirect (paracrine mediated) repair via cytokines or exosomes.<sup>14</sup>

In recognition of the limited role of transplanted cell differentiation and to avoid the adverse effects of patient comorbidities on autologous (*i.e.*, self to self) cell products, the field transitioned towards “immune evasive” blood or bone marrow derived mesenchymal stem cells (MSCs).<sup>35</sup> MSCs have since been defined as cells that: 1) adhere under basic culture conditions; 2) express CD90, CD73 and CD105 without lineage (CD79 $\alpha$ , CD14 or CD11b, CD45, CD19, CD34 and HLA-DR) and 3) differentiate *in vitro* into chondrocytes, osteoblasts and adipocytes.<sup>36</sup> While the combination of immune evasive properties with multilineage potential of MSCs raised concerns that administration might result in non-cardiac tissues developing within the heart,<sup>36,37</sup> this fear was not realized as the long-term retention of transplanted MSCs is equivalent to other cell sources (<3.5% 6 weeks post injection) with the benefits conferred through paracrine mediated-reductions in fibrosis and inflammation.<sup>38</sup> Based on the hope that paracrine mediated repair will suffice, a Phase 3 trial is currently underway investigating the effects of purified STRO-3+ (DREAM HF-1; NCT02032004; study start date January 2014).

Rather than hindering clinical translation, the ephemeral nature of BMSCs and MSCs may have played a key role in promoting the development of these therapeutics as the past decade has also provided notes of caution regarding retention of transplanted cells- best exemplified by the skeletal myoblast (SkM) experience. SkMs are an abundant source of adult tissue stem cells that repair skeletal muscle after injury. The ability of these hardy cells to resist apoptosis and generate working skeletal muscle prompted use as one of the earliest therapies for ischemic cardiac injury.<sup>39,40</sup> Preclinical data

demonstrated that significant numbers of transplanted SkMs persisted in the injured heart (e.g., SkM grafted areas approaching more than half of the infarct area<sup>41</sup>) and increasing amounts of working skeletal muscle in the injured heart predicted enhanced myocardial function.<sup>41,42</sup> Clinical implementation followed very quickly but early clinical trials abruptly stalled when an alarming safety signal emerged indicating that SkM therapy was associated with an increased risk of ventricular pro-arrhythmia and sudden cardiac death.<sup>43-45</sup> Follow-up studies revealed that although SkMs form functional myofibrils, these islands of working skeletal tissue are incapable of electrically coupling with the surrounding myocardium leading to asynchronous contraction and the ideal substrate for cardiac rhythm disorders.<sup>46</sup> Somatic gene transfer of the ventricular gap junction protein connexin 43 to SkMs promotes electrical coupling and, as outlined below, has recently resulted in transplant of a genetically modified cell product back into patients.<sup>47</sup>

Interestingly, the pre-clinical embryonic stem cells (ESCs) literature has also provided a note of caution regarding attempts to promote the engraftment of non-cardiac cell products within the injured heart (reviewed in ref [45]). ESCs are isolated from the inner cell mass of blastocyst-stage embryos and display an unlimited capacity for self-renew while retaining the ability to differentiate into any cell type, including cardiomyocytes.<sup>48</sup> Partially in response to the ethics of using human fetuses, induced pluripotent stem cells (iPSCs) have been developed by introducing a cocktail of transcription factors to transform easily accessible somatic cells (such as dermal fibroblasts) into pluripotent stem cells.<sup>49</sup> These cells mirror ESCs as they readily self-renew and differentiate into any cell type. To date, cell purity has been a challenge and differentiation protocols have provided heterogeneous populations of cardiac cells that

include undifferentiated cells, immature ventricle-, atrial- and node-like cells.<sup>50</sup> Although several pre-clinical small animal studies suggested that the lineage infidelity of ESCs may have very little impact on therapeutic regeneration,<sup>51,52</sup> a recent study showed that, while ESC-derived cardiomyocyte grafts could extensively remuscularize infarcted primates (*i.e.*, macaques), coupling of immature electrically unstable cells with host myocardium significantly increased the burden of life-threatening ventricular pro-arrhythmia through slowed propagation of electrical wavefronts within damaged myocardium (*i.e.*, increased substrate for re-entry) and formation of ectopic beats (*i.e.*, automatic ectopic electrical foci).<sup>50,53</sup> Early small animal studies may not have identified this pro-arrhythmic potential because large grafts are needed for slow waves to propagate for electrical re-entry<sup>45,52,53</sup> and the inherently faster heart rates of small animal models (~600 beats per mins in mice vs. 100-130 in macaques) may have suppressed re-entrant beats or ectopic automaticity.<sup>53</sup>

### **1.3 Cardiac Derived Stem Cells for Treating Ischemic Cardiomyopathy**

The growing realization that engraftment of non-cardiac cell products may have inadvertent side effects, prompted several investigators to explore the therapeutic impact of cardiac-derived cell products. In the mid-2000's, several pre-clinical studies hinted that endogenous multipotent cardiac cells existed in the adult heart with a capacity to replace cardiomyocytes, endothelial and smooth muscle cells.<sup>6,10,54,55</sup> This finding was supported by convincing radioactive carbon 14 tracking demonstrating that human adult cardiomyocytes undergo continuous low grade replacement throughout adulthood (0.5-

1.0%/year).<sup>56</sup> To date, the identity of this endogenous myocyte cell source remains controversial with multiple candidates proposed based on cell surface markers characteristic of stem cells (*i.e.* tyrosine receptor kinase, stem cell antigen-1 [Sca-1], Endoglin [CD105], Islet-1, platelet-derived growth factor receptor-alpha or membrane transporters like ATP-binding cassette sub-family G member 2 or Multidrug resistance protein-1 involved in Hoechst dye efflux).<sup>54</sup> Despite this uncertainty, several groups have moved forward with the development of cardiac-derived stem cell (CSC) therapeutics based on the belief that administration of an intrinsically cardiac cell product would provide greater cell-mediated repair through direct differentiation into working myocardium and pro-healing paracrine factors.

### **1.3.1 Side Population**

The first population of heart-derived progenitor cells were isolated using methodology similar to established techniques used to identify skeletal and bone marrow progenitor cells.<sup>57</sup> These cells are termed 'Side Population (SP)' based on their ability to extrude Hoechst dye (a cell-permeable DNA binding dye) via multidrug resistance protein-1 transporters.<sup>10</sup> Flow cytometry analysis determined SP cells represent only a small fraction (~1%) within the heart which lacked typical cardiomyocyte lineage markers. These cells are multipotent as they differentiate into endothelial<sup>58,59</sup> or smooth muscle cells<sup>60</sup> and form beating cardiomyocytes when co-cultured with neonatal ventricular cardiomyocytes<sup>61</sup> or following small molecule stimulation.<sup>60</sup> SP cells co-express Sca-1 and platelet-derived growth factor receptor-alpha.<sup>11,61</sup> Preclinical studies have demonstrated that transplanted murine SP cells improve cardiac function and attenuate

myocardial scarring after ischemic injury in murine models.<sup>11,59,60,62</sup> Given long-term cell retention is limited (<1% two weeks after delivery), these benefits are attributable to paracrine stimulation of endogenous repair although the mediators of these effects have yet to be fully defined.<sup>11</sup> Despite these promising results, it is unlikely that Sca-1+ SP cells will be translated for clinical application as the human homolog of Sca-1 has yet to be identified and studies of Sca-1 have been uniformly been restricted to murine cells applied within murine models of cardiac damage.

### **1.3.2 Antigenic Selection of Cardiac c-Kit+ Cells**

The tyrosine receptor kinase (c-Kit) was initially identified as a marker for 'stemness' in hematopoietic cells and was naturally explored in the heart in hopes of identifying a cardiac progenitor population that mediates endogenous repair.<sup>63</sup> Beltrami and colleagues were the first to identify a non-hematopoietic c-Kit+ cell in the heart shown to be clonogenic, multipotent and capable of self-renewal.<sup>9</sup> Antigenic-sorted c-Kit+ cells were shown to expressed early cardiac developmental transcription factors (Nkx 2.5, GATA4, and MEF2C). Since, several pre-clinical studies have isolated c-Kit+ cells from small or large animals with techniques developed to isolate and expand human c-Kit+ cells from atrial and ventricular biopsies.<sup>16,64-70</sup> Antigenically, c-Kit+ cells represent a heterogeneous population as they co-express surface makers indicative of endothelial (e.g. CD31, CD34), mesenchymal (e.g. CD90, CD105) and progenitor (e.g. Sca-1, Abcg2), identity.<sup>66</sup> One report also suggests that two distinct populations of cardiac c-Kit+ cells exist with kinase domain receptor (KDR) co-expression indicating a vasculogenic ability while KDR- cells retain a true myogenic potential.<sup>71</sup>

Interestingly, early reports claimed that in situ (resident) c-Kit<sup>+</sup> cells account for a substantial fraction of new cardiomyocytes found after cardiac injury (up to ~70% of lost cardiomyocytes).<sup>9,67</sup> Recent lineage tracing studies suggested these early reports were mistaken as lineage cell fate analysis found tagged c-Kit<sup>+</sup> cells contribute very few new cardiomyocytes (0.016 or 0.007% of total cardiomyocytes in the heart) and primarily differentiate into endothelial cells.<sup>72,73</sup> Despite concerns regarding insufficient c-Kit labeling in lineage tracing studies,<sup>74</sup> these claims have been supported by independent studies using multiple recombinant mouse models<sup>73</sup> and complementary cell tagging methodology.

Unlike endogenous c-Kit<sup>+</sup> cells, antigenically sorted and ex vivo expanded c-Kit<sup>+</sup> cells have been shown to differentiate into cardiomyocytes.<sup>9,66,68</sup> While few conflicting studies have claimed robust engraftment and cardiomyogenesis by ex vivo expanded c-Kit<sup>+</sup> cells,<sup>67,68</sup> many follow up studies have failed to reproduce such results<sup>16,66,69,75</sup> as long-term engraftment approached ~1% 35 days after intramyocardial injection suggesting the contribution of transplanted c-Kit<sup>+</sup> cells to adopt a myocyte fate is physiologically irrelevant.<sup>16</sup> Therefore, functional gains seen in preclinical and clinical studies using ex vivo expanded c-Kit<sup>+</sup> cells are likely primarily dependent on paracrine stimulation of endogenous repair- which has yet to be robustly evaluated.

### **1.3.3 Cardiospheres, cardiosphere-derived cells, and explant-derived cardiac stem cells**

In 2004, Messina and colleagues adopted the established neurosphere culture technique to the heart and demonstrated ex vivo expansion of cardiac progenitor cells

directly from murine and human heart biopsies.<sup>76</sup> In this method, cardiac tissue was minced, enzymatically digested, and plated on fibronectin coated dish. Soon after, cells spontaneously migrated from plated tissue (*i.e.*, explant-derived cells, EDCs) to provide a monolayer covering the surrounding cultureware. EDCs were harvested using mild enzymatic digestion for suspension culture on poly-D-lysine coated plates. The weak electrostatic interactions between negatively charged cell membranes and positively charged poly-D-lysine results in adhesion of cell “stalks” that anchor 50-150  $\mu\text{m}$  diameter multicellular, spherical aggregates termed cardiospheres (CSp). CSps resemble embryonic stem cell niches with actively proliferating progenitor cells (c-Kit, CD34, or Sca-1 from murine sourced heart biopsies) in the core surrounded by supportive endothelial (CD31), cardiac (cardiac troponin, myosin heavy chain, connexin-43) and mesenchymal (CD105, CD90) cells at the periphery.<sup>76,77</sup> Similar to neurosphere culture, CSp formation was thought to provide an enrichment step to increase the proportion of progenitor cells expressing pluripotent transcription factors (SOX2, Nanog), stem cell related proteins (histone deacetylase 2, telomerase), stem cell associated growth factors (insulin-like growth factor), and extracellular-matrix/adhesion proteins (integrin- $\alpha$ 2, laminin- $\beta$ 1, collagen, matrix-metalloproteinase) compared to a monolayer culture.<sup>69</sup>

Although intramyocardial injection of CSps after myocardial injury provides a dose dependent improvement in cardiac function, sphere diameter and aggregation precludes intracoronary delivery secondary to the risk of occluding coronary vessels.<sup>78</sup> To circumvent this issue, CSps were expanded as a 2-dimensional monolayer culture termed, cardiosphere-derived cells (CDCs) for single-cell intracoronary delivery.<sup>12,77</sup> CDCs are CD105+/CD45- cells with subpopulations expressing CD90 (~30-40%), c-Kit

(~5-10%), and alpha smooth muscle actin (~5%).<sup>12,77,79</sup> Akin to cardiospheres, CDCs are clonogenic, self renewing, and multipotent cells that can differentiate into endothelial, cardiac and smooth muscle lineages.<sup>12,80,81</sup> CDC have also been shown to electrically couple with myocytes both in vitro and in vivo- a finding limiting the risk of malignant arrhythmias after transplantation.<sup>12,13,45</sup> Over 40 independent laboratories worldwide have validated the therapeutic bioactivity of CDCs and demonstrated that CDC administration of CDCs results in new cardiac tissue, reduces scar size, reduces adverse structural remodeling and improves hemodynamics.<sup>12,80-85</sup> Akin to other cardiac cell products, gains in cardiac function are leveraged upon paracrine stimulation of endogenous repair and not direct differentiation of transplanted cells into working cardiomyocytes. These promising preclinical results have lead to the development of many phase I/II clinical trials (discussed below).

Unsurprisingly, the upstream progenitor cells directly cultured from cardiac tissue and expanded to CDCs (EDCs) represent a heterogeneous population of cells that include significant cardiac (c-kit+), endothelial (CD34, CD31), and mesenchymal (CD105, CD90) subpopulations. In contrast to CDCs, EDCs may provide a more expedient and effective cardiovascular therapeutic as EDCs culture methods reduce in culturing time (1 vs. 5 weeks) which reduce the risk of phenotypic drift or malignant transformation. Head to head comparisons between CDCs and EDCs have shown that, while both cell products provide equivalent paracrine mediated repair of injured myocardium, EDCs possess a 100 fold greater capacity to adopt a cardiomyogenic lineage; rationalizing their use as a myocyte replacement therapeutic.<sup>80,86,87</sup>

Deciding which cell type is therapeutically superior is not straightforward as no clinical study provides a head-to-head comparison of cell types and pre-clinical studies are limited (Table 1). While two pre-clinical studies have suggested heart-derived cells may be superior to BMSCs or MSCs,<sup>88,89</sup> the one meta-analysis of the available pre-clinical data have shown similar efficacy between different heart and non-heart cell types.<sup>90</sup> Amongst the heart-derived cells products themselves, one study has shown that CDCs may be superior to antigenically selected and expanded c-Kit+ cells<sup>89</sup> but this effect was not confirmed when data was combined within a pre-clinical meta-analysis.<sup>90</sup>

Product	Cell source	Clinical translation status				Advantages	Disadvantages
		Pre-clinical	Phase I	Phase II	Phase III		
Cardiac-derived cells	Cardiac tissue					Evidence for myogenesis and paracrine mediated repair. <sup>54,81,91</sup>	All require surgical biopsy.
CDCs c-Kit+ cells sca-1+ cells		+	+	+		Autologous + allogeneic <sup>92</sup>	Autologous only Autologous only
Embryonic stem cells	Human embryo	+	+			Evidence for myogenesis and paracrine mediated repair.	Arrhythmias, <sup>53</sup> immune reactions, <sup>95</sup> imprinting, genetic modification. Tumors. <sup>96-98</sup> Difficult to obtain large number of homogeneous population of progenitor or
Induced pluripotent stem cells	Somatic cells	+				Potential to differentiate to all cell types need for cardiac repair. <sup>93,94</sup>	

							differentiated cells. <sup>50</sup>
Unselected MNCs	Blood and bone marrow	+	+	+	+	Relatively easy to isolate large number of cells. <sup>20</sup> Short processing time.	Evidence for paracrine mediated repair alone. <sup>14,99</sup> Heterogeneous population of cells. <sup>17</sup>
Selected MNCs (CD34+, CD133+)	Blood and bone marrow	+	+	+		Better purity compared to unselected MNCs. Evidence of enhanced cell homing to injured myocardium compared to unselected MNCs. <sup>17</sup>	Evidence for paracrine mediated repair alone. <sup>14</sup> Low abundance in blood or bone marrow. <sup>21,31</sup> Requires additional isolation steps (potential risk of exposing patients to beads and animal IgG used in enrichment steps). <sup>100</sup>
EPCs (or circulating angiogenic cells)	Blood and bone marrow	+	+	+		Promote neovascularization and angiogenesis. <sup>29</sup> Can be expanded in culture to increase yield. <sup>101</sup>	Low abundance in blood or bone marrow. <sup>101</sup> Markers identifying EPCs are not clearly defined and overlap with BMCs and endothelial cells. <sup>102</sup> Circulating pool diminished in patients with co-morbidities (e.g. hypertension). <sup>102</sup>

MSCs	Blood, bone marrow, adipose tissue, and umbilical cord	+	+	+	+	<p>Evidence for myogenesis and paracrine mediated repair.</p> <p>Autologous + allogeneic.</p> <p>Easily accessible and abundant number of cells.</p> <p>Cells can be acquired from multiple organ sources (e.g. bone marrow or adipose tissue)</p> <p>Can be expanded in culture to increase yield.<sup>35</sup></p>	<p>Broad differentiation potential with the risk of forming non-cardiovascular cells (e.g. chondrocytes, osteoblasts and adipocytes).<sup>35</sup></p>
------	--	---	---	---	---	--	--

**Table 1. Advantages and disadvantages of stem cell therapy for cardiac regeneration.** Cardiosphere-derived cells (CDCs); Mononuclear cells (MNCs); Endothelial progenitor cells (EPCs); Mesenchymal stem cells (MSCs). Plus sign (+) indicates published evidence for clinical translation. \* phase III trials currently underway.

### 1.3.4 Clinical Trials Using Cardiac Derived Cells

To date, three phase 1 clinical trials have been completed using cardiac derived cell products. The Cardiac Stem Cell Infusion in Patients With Ischemic Cardiomyopathy (SCIPIO, NCT00474461) trial demonstrated that antigen-selected cardiac progenitor cells (c-Kit+ cells) injected into the myocardium of patients with ischemic cardiomyopathy during routine surgical bypass was associated with a moderate improvement in global myocardial function and clinical status.<sup>103</sup> However, concerns raised regarding cell characterization and clinical follow-up<sup>104</sup> combined with several corrections/retractions by key co-investigators<sup>105</sup> have made interpretation and extension of this study challenging. In contrast, the CARDiosphere-Derived aUtologous Stem CElls to Reverse ventricUlar

dySfunction (CADUCEUS, NCT00893360) trial evaluated the safety of heterogeneous population of CD105+/CD45- CDCs after intra-coronary delivery 3-4 months following acute myocardial infarction.<sup>106</sup> One year after cell administration, CDC therapy was found to be safe with promising evidence of reduced scar sizes and increases in viable myocardial mass<sup>107</sup> but, similar to non-cardiac cell sources, long-term engraftment has been limited.<sup>84,108</sup> Based on this promising data, ongoing phase I/II trials are probing the efficacy of allogeneic CDCs in ischemic cardiomyopathy (Allogeneic Heart Stem Cells to Achieve Myocardial Regeneration, ALLSTAR; NCT01458405; start date October 2012), Duchenne muscular dystrophy cardiomyopathy (Halt cardiomyopathy progression in Duchenne, HOPE; NCT02485938; start date August 2015) and non ischemic cardiomyopathy (Dilated cardiomyopathy intervention With Allogeneic Myocardially-regenerative Cells, DYNAMIC; NCT02293603; start date November 2014).<sup>109</sup>

Interestingly, the 6-month pre-specified interim analysis for the ALLSTAR trial (allogeneic CDCs to treat ischemic cardiomyopathy) was recently released and demonstrated that IC administration of allogeneic CDCs had no detectable effect on MRI scar size or ejection fraction.<sup>110</sup> While company officials attributed this result to unforeseen improvements in the placebo group and technical variability in scar size measurements, other technical factors (such as immediate delivery of a cryogenically stored allogeneic cell product derived from donors with possible medical comorbidities) may have resulted in delivery of an attenuated cell product that requires a significant dose to realize therapeutic benefit.<sup>109</sup> More information will undoubtedly be forthcoming but ultimately this outcome highlights the futility of simply changing the cell product delivered without incorporating strategies designed to enhance cell engraftment.

A recently completed phase I trial called transc coronary infusion of cardiac progenitor cells in hypoplastic left heart syndrome (TICAP, NCT01273857), investigated the effects of delivering autologous CDCs in children born with hypoplastic left heart syndrome. Patients received CDCs via intracoronary infusion 4-5 weeks after second or third stage reconstructive surgery. The 18-month follow up demonstrated that CDC treatment was safe/feasible and improved the right ventricular ejection fraction while reducing heart failure status compared to control group (*i.e.*, standard care). These promising results lead to the development of a larger randomized phase II trial that assigned 41 patients in a 1:1 ratio to receive CDCs treatment or standard medical care 4-9 months after surgery or staged reconstruction (cardiac progenitor cell infusion to treat univentricular heart disease, PERSEUS, NCT01829750). At three months, CDC treated group showed significant improvement in right ventricular function compared to standard care.<sup>111</sup> Four months after surgery, the control group was provided with an alternative option of receiving late CDC intracoronary infusion. Akin to early delivery, late CDC delivery improved the right ventricular function compared to baseline. Overall, the 1 year follow up demonstrated that CDC infusion was associated with an improved right ventricular function, somatic growth, quality of life with reduced cardiac fibrosis and heart failure status.

#### **1.4 Heterogeneity of Injured Myocardium**

When considering the design of an ideal cell therapy, useful insights can be acquired by considering the harsh conditions in which cells are expected to survive. Oxygen is vital in the heart for both cell metabolism and survival. At rest, the adult human

heart beats 100-150K times per day as compared to ~864K in mice (the animal most used in preclinical studies). Therefore, a constant supply of energy is needed to meet this high metabolic demand. Nearly two-thirds of the adenosine triphosphate (ATP) made by each myocyte is used during contraction while the remainder is spent maintaining cellular homeostasis.<sup>112</sup> To sustain this aerobic demand, the human heart consumes 2.5-4.5 Liters of oxygen per minute and extracts ≈75% of the arterial oxygen.<sup>113</sup> After a myocardial infarct (MI), the oxygen concentration within ischemic cardiac tissue declines to 1-2% from physiologic non-infarcted tissue oxygen content of 5-10%. As such, oxygen starved cells switch to inefficient anaerobic metabolism with knock-on decreases in ATP production and stores. Ultimately, this leads to loss of the ATP-dependent ion transporters, cytoplasmic/mitochondrial calcium overload, release of lysosomal enzymes into the cytoplasm, accumulation of reactive oxygen species (ROS), disruption of membrane integrity, cell swelling, and rupture.<sup>114</sup> The magnitude of effect depends on the degree of oxygen restriction and the duration of interrupted blood flow with irreversible damage beginning within 20 minutes of ischemia.<sup>115</sup>

Mitochondrial sourced ROS promotes cell death by: 1) oxidizing proteins thus altering structure, 2) direct DNA damage, 3) direct membrane lipid peroxidation 4) clustering and activation of membrane bound death receptors (e.g. Tumor necrosis factor receptor 1 and Fas receptor) 5) activation of ROS-sensitive kinases (e.g. Apoptosis signal-regulating kinase 1) promoting endogenous apoptotic signalling, 6) increasing intra-cellular calcium dysregulation, 7) promoting inflammatory cytokine production (e.g. tumor necrosis factor alpha (TNF- $\alpha$ )) which induces cell death via extrinsic apoptosis pathway stimulation, 8) altering cellular redox homeostasis (e.g. low reduced-/oxidized-

glutathione ratio) and 9) boosting mitochondrial damage/dysregulation.<sup>116,117</sup> Infiltrating neutrophils further exacerbate oxidative stress by releasing oxidants and pro-inflammatory cytokines while also binding directly to myocytes to promote oxidative damage.<sup>118</sup>

Post-infarct myocardial remodeling is divided into three overlapping phases: inflammatory, proliferative and maturation.<sup>119</sup> During the inflammatory phase, damaged myocytes release damage-associated molecular patterns (DAMPs), such as high mobility group B1 and heat shock proteins (HSPs), which initiate an intense inflammatory response via pattern recognition receptors (*e.g.* toll-like receptors (TLR)) on innate immune cells.<sup>119</sup> Oxidative, mechanical and ischemic stress trigger the release of inflammatory cytokines (*e.g.* TNF- $\alpha$ , interleukin 1 beta (IL-1 $\beta$ ), IL-8 and IL-6) by damaged myocardium, endothelial cells, resident fibroblasts and cardiac mast cells<sup>119,120</sup> that promote neutrophil recruitment that help remove dead cells and break down damaged extracellular matrix (ECM). These cytokines also promote apoptosis (*e.g.*, TNF- $\alpha$  binding to tumor necrosis factor receptor-1 thus activating caspase-dependent apoptosis via Fas-associated death domain (FADD))<sup>120</sup> and recruit monocytes which subsequently trans-differentiate into M1 macrophages to phagocytose necrotic tissue.<sup>121</sup> ECM degradation in the presence of ongoing mechanical strain combine to promote thinning and expansion of the scar region while myocytes at the border of the scar hypertrophy to accommodate increases in intra-mural strain.<sup>122</sup> However, it is important to note that the effects of “inflammatory” factors are not strictly one sided. DAMPs recruit circulating MSCs to damaged sites while enhancing the immunosuppressive ability of MSCs through inhibition of T-cell proliferation and increased production of anti-inflammatory cytokines.<sup>123-126</sup>

Although this effect does not have substantial functional effects, these insights highlight the complex signalling needed to mediate post infarct healing.

By ~4-5 days, the inflammatory phase is largely resolved and neutrophils undergo apoptosis in preparation for phagocytic clearance by M1 macrophages.<sup>119</sup> This healing proliferative phase stimulates macrophages to switch into a reparative M2 phenotype which promotes the secretion of cytokines (such as transforming growth factor beta (TGF- $\beta$ ) and IL-10) that suppress inflammation while stimulating fibroblast growth and angiogenesis.<sup>119,121</sup> TGF- $\beta$  eventually stimulates fibroblast trans-differentiation into myofibroblasts that lay down healthy matrix protein to strengthen the developing mature scar.<sup>127</sup> By end of this maturation phase when scar formation is complete, endothelial cells and fibroblasts undergo apoptosis while myofibroblasts persist for many years in the scar to continue ECM turnover.<sup>119,127</sup>

These insights provide valuable guidance in understanding how transplanted cells promote myocardial repair and why long-term engraftment/differentiation is challenging. Proteolytic cleavage and clearance of ECM alone reduces the ability of transplanted cells to adhere and limits both cell retention and pro-survival integrin mediated signalling. Further changes in the 3-dimensional architecture and mechanical compliance of ECM severely compromises stem cell adhesion, mobility, and viability.<sup>128,129</sup> The hypoxic micro-environment itself limits transplanted cell function/viability as many cell types readily undergo apoptosis or cardiogenic gene silencing.<sup>130</sup> Depending on the timing of cell transplantation (*i.e.*, early or late after myocardial infarction), toxic infarct signalling needed to coordinate debris removal and scar strengthening will have direct effects on transplanted cell survival.<sup>131</sup> Interestingly, late delivery of MSCs (+1 week post infarct)

provides superior cell-mediated effects on cardiac function and angiogenesis as compared to 1 hour post-MI delivery,<sup>132</sup> -a finding that mirrors clinical experience with delayed delivery (4-7 days post-MI) providing superior effects on myocardial function and major adverse cardiac events as compared to early delivery of cells (1-3 days).<sup>133</sup>

### **1.5 Engraftment of Transplanted Cells**

Irrespective of cell type and means of delivery, any study transplanting suspended cells into injured hearts is fortunate if long-term retention (*i.e.*, 3-4 weeks) exceeds 2% of the initial injectate.<sup>16,17,32,33,108,134-136</sup> This discouraging reality reflects: 1) lasting pre-conditioning effects on cell viability that occur during mobilization for administration, 2) a limited capacity for cells proliferate *in vivo*, 3) clearance of cells from an inherently vascular and lymphatic rich organ, 4) off target injection into the blood stream, lymphatics or cavity, 5) mechanical extrusion from the site of injection and, as outlined above, 6) the harsh scar or infarct-micro environment where cells are expected to survive (Figure 1).

Interpretation of preclinical data is often complicated by the methodology used to quantify engraftment. Historically, stem cell reports have quantified cell retention by searching histological sections for chemical or genetically labeled cells.<sup>15</sup> Although immunohistochemistry permits tracking stem cell fate, viability and proliferation, it inherently precludes longitudinal cell tracking (*i.e.*, measurements can only be taken at a single time point) and absolute quantification of retained cell numbers are impossible. Furthermore, sampling biases and auto-fluorescence of myocardial tissue have been shown in the past to complicate interpretation.<sup>137</sup> In this method, tissue fixation, antigen retrieval and antibody panel selection are critical as each can introduce error because of

inefficient/lost cell labeling (under estimation) or off-target spread of cell labels (over estimation).<sup>138</sup> To overcome these drawbacks, recent papers have moved towards unbiased means of cell tracking using qualitative polymerase chain reactions for retained human ALU sequences (*i.e.*, xenograft models with human cells transplanted into non-human hearts)<sup>136</sup> or Y-chromosome genes (*i.e.*, sex-mismatch models with male donor cells transplanted into female recipients).<sup>139</sup> Although qualitative polymerase chain reaction can reliably detect small numbers of retained cells (~1% engrafted cells), it cannot inform on cell location/proliferation/viability/fate<sup>139</sup> and, akin to histological methods, provide only static measure of cell numbers.

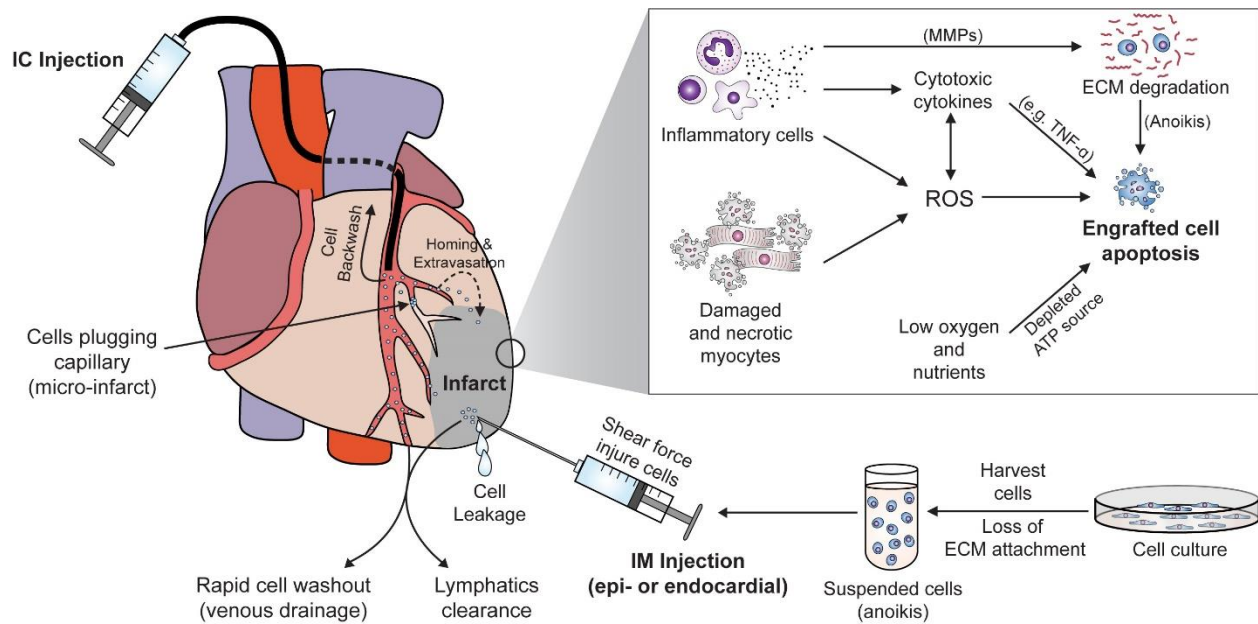


**Figure 1. Cellular mechanisms limiting retention and survival of cells transplanted into the damaged heart.** Cells are initially injured during preparation for transplant or as they undergo detachment induced cell death (*i.e.*, anoikis) while in suspension prior to injection. A further portion of cell attrition is attributable to the shear forces generated during injection through catheter and needle delivery systems. Immediately after injection, a number of cells are washed out via coronary venous (rapidly clearance) or lymphatic (slow clearance) drainage. Immediately after IM injection, cells can also be extruded from the needle-track while IC transplanted cells need to undergo transendothelial migration from coronary vessels to enter the parenchyma. Retained cells undergo apoptosis within the low oxygen and nutrient-deplete infarct environment. Depending on the timing of injection after myocardial injury, cell loss can also be exacerbated by inflammatory cells, reactive oxygen species (ROS), cytotoxic cytokines and the lack of cell-matrix attachment. Extracellular matrix (ECM); Matrix metalloproteinases (MMPs); Tumor necrosis factor alpha (TNF- $\alpha$ ).

These insights led to the development of non-invasive imaging techniques for longitudinal tracking of transplanted cells. Historically, radiolabeled white blood cells (WBCs) and glucose analogs have been used to visualize cardiac inflammation and perfusion using single-photon emission computed tomography or positron emission tomography imaging.<sup>140,141</sup> Based on this clinical experience, it was naturally extended for cardiac stem cell tracking.<sup>142</sup> Clinically, cell retention and biodistribution has been studied using labeled hematological stem cells.<sup>17,32,134,135,143,144</sup> Concerns regarding patient radiation exposure have limiting cell tracking studies to the use of short-lived radiotracers thereby permitting only short term cell tracking (*i.e.*, 1-3 days). Interpretation of study results are also confounded by: 1) radiotracer accumulation in macrophages/myocardium (over-estimate cell engraftment), 2) extra-cardiac diffusion of poorly retained radiotracers (under-estimate cell engraftment), 3) radiotoxicity to transplanted cells thus reducing transplanted cell viability and 4) inadequate tracer labelling of daughter progeny as cells divide (under-estimate cell engraftment).<sup>15,141,142</sup>

Despite these limitation, radiotracer labelled cell tracking has shown that IC injection of radiolabeled BMSCs at the time of acute MI results in ~0.5-5% of the initial injectate being retained 1 hour after delivery as most of the radioactive signal (> 85%) is detected in the liver and spleen- suggesting that cells are quickly washed into the systemic circulation for removal by the reticuloendothelial system.<sup>17,32,134,135,143,144</sup> Interesting, these clinical studies also showed that pre-clinical data may not replicate administration to patients. For example, IC injection of peripheral blood mononuclear cells (PBMCs) into porcine models of acute MI resulted in a large number of cells (47±1%)

being detected in the lungs 1 hour after injection<sup>33</sup> while multiple clinical studies demonstrated negligible amounts of IC injected PBMCs are trapped in the lung (even up to doses approaching 100 million cells). These findings may be attributable to the small size of hematopoietic stem cells (5-7  $\mu\text{m}$ ) that likely prevents cell clumping within “large” bore human capillaries.<sup>145-147</sup> Ultimately, this data highlights the effect of species on stem cell (*i.e.*, cell size, expression of adhesion surface molecule) and organ (*i.e.*, vessel diameter, homing signals, adhesion surface molecules expression) characteristics that make straightforward application of pre-clinical large animal data to clinical studies problematic.

Akin to blood stem cells, both MSCs and CSCs suffer from poor long-term cardiac retention. Experiments exploring IM injection of radiolabeled CDCs after coronary ligation demonstrated that while ~17% of transplanted cells are retained 1 hour after delivery this number declines to <5% by 3 weeks after injection.<sup>108</sup> Results from IC injection of cardiac-derived c-Kit<sup>+</sup> cells are no better with ~5% of transplanted cells persisting 1 day after injection and  $\leq 1\%$  persisting after 5 weeks.<sup>16</sup> In a manner similar to the experience with pre-clinical PBMCs, large numbers of labeled cardiac-derived cells and MSCs are found in the lungs shortly after delivery with clumps of cells navigating through the coronary sinus immediately after injection.<sup>16,148-150</sup> Based on the observation that vasodilating pulmonary vessels reduce lung trapping,<sup>151</sup> these findings may in part be attributable to the large size of cardiac-derived cells and MSCs (average diameter ~20-30  $\mu\text{m}$ ) as compared to the pulmonary arterioles (~average diameter 5-100  $\mu\text{m}$ ). But surface adhesion molecules expression also plays a role in lung trapping as inhibition of CD49d (a receptor for VCAM-1 expressed on endothelial cells) on MSCs also has been shown

to reduce retention of transplanted cell in the lung.<sup>146</sup> The extent to which this animal data extends to clinical application is uncertain but, to date, clinical trials using CSCs or MSCs have shown no detrimental pulmonary effects.

The nature of cell delivery also influences the degree of cell retention. The three most commonly used delivery methods are IC, IM and intravenous (IV) injection. IV injection is the least complicated and invasive delivery method; however, myocardial cell retention is extremely poor as the majority of cells are quickly distributed and trapped within the lungs, spleen, and liver.<sup>33,148-150,152</sup>

IC infusion is the most clinically practiced and preferred method for cell delivery. It can be performed with relative ease as the procedure is similar to balloon angioplasty, a widely-used method by interventional cardiologist to treat coronary artery occlusions. Because cells are often directly injected into the reperfused infarct related artery, they are homogeneously distributed within the infarct territory. Although cell retention remains greater than IV delivery,<sup>148,150</sup> cells are rapidly washed out from well perfused myocardium and the overall numbers of cells that can be delivered is limited by the risk of embolizing coronary arterioles.<sup>153</sup>

Direct IM injection offers the advantage of delivering large numbers of cells into areas with reduced perfusion and no risk for micro-infarction. While epicardial injection requires a sternotomy, transendocardial catheter based injection is possible in larger hearts (*i.e.*, humans or preclinical large animal models) but requires additional equipment, expertise and expense to localize scar regions.<sup>154</sup> While several mapping systems have been developed for transendocardial cell delivery, the most widely used system is based upon the non-fluoroscopic electro-anatomical platforms developed for catheter-based

ablation of cardiac arrhythmias (*i.e.*, the NOGA technology). In this system, combining of electro-anatomical maps of the left ventricle with temporal analysis of motion propagation provides estimates of endocardial scar size permitting targeted delivery of cells.<sup>154,155</sup> In small animal pre-clinical models, echocardiographic guided trans-thoracic epicardial injection is routine and permits the delivery of cells at any time after cardiac injury without the need for repeat sternotomy.<sup>156</sup> Taken as a whole, pre-clinical and clinical IM delivery of cells appears to provide greater acute and long-term cell retention as compared to IC or IV injection.<sup>33,34,157,158</sup> Discrepant results demonstrating equivalent or greater retention of IC delivered cells have been attributed to coronary plugging (with subsequent micro-infarction),<sup>148,150,159,160</sup> differences in animal model, variable cell types/dose, timing of delivery, cardiac injury (*e.g.*, arterial ligation vs. ischemic reperfusion) and delivery method.<sup>161</sup> Even amongst IM-injection delivery techniques, transendocardial delivery demonstrates superior cell retention compared to epicardial injection likely due to transmural heterogeneity hemodynamic and physical forces making the epicardial surface experience greater mechanical extrusion and venous washout.<sup>158,162</sup>

Finally, retrograde coronary venous via the coronary sinus cell delivery is another approach that is feasible and safe in both large animal<sup>33</sup> and humans.<sup>163</sup> In this approach, cells are injected into the coronary vein during balloon occlusion to minimize cell washout. Increased venous pressure enables retrograde flow and distributes cells homogeneously throughout the myocardium. While retrograde coronary sinus delivery permits a large number of cells to be delivered to the myocardium with minimal risk of embolization, rapid washout after balloon deflation limits cell retention to a degree similar to IC injection.<sup>33</sup>

## 1.6 Cellular Mechanisms Underlying Intra-Coronary Injected Cell Uptake in The Heart

Until recently, intravascular delivery of cells to injured myocardium was thought to involve transendothelial migration similar to leukocyte diapedesis, namely: 1) cell rolling along the endothelial lining of the vascular wall which is initiated through transient selectin-dependent attachments, 2) progressive integrin dependent binding leading to tight cell-endothelium attachments, 3) cell migration via gaps between endothelial cells (paracellular diapedesis) or the formation of pores directly through endothelial cells (transcellular diapedesis).<sup>164</sup> While both BMMCs<sup>165</sup> and MSCs<sup>166</sup> undergo transendothelial migration, many other stem cell products (*i.e.*, CSCs and EPCs) do not transmigrate despite marked endothelial cell interactions.<sup>167</sup> Infused cells are thought to accumulate within capillaries and, as they occlude the capillary, adhere to endothelium.<sup>168</sup> Endothelial cells then actively remodel to engulf the infused cells via membrane projections (termed endothelial pocketing) thus gradually shifting cells to the other side of the lumen. Once there, transplanted cell sourced metalloproteinases break down the vessel wall to expel the cells within the parenchyma. Extravasation is completed by 72 hours and vessel patency is restored. Termed angiopellosis, this alternative means of cell incorporation is mediated by endothelial integrin binding. Angiopellosis was first described as a means of removing of fibrin emboli in cerebral microvessels<sup>169</sup> -hinting this may be a conserved mechanism to recanalize vessels occluded by blood-clots, cancer cells and large foreign cells.

## 1.7 Mechanism of Cell-Mediated Repair of Damaged Myocardium

While the classical regenerative medicine paradigm lies in restoring cardiac function through engraftment and differentiation of stem cells into new functional cardiomyocytes, emerging evidence suggests the majority of cell-mediated repair occurs through indirect paracrine stimulation of endogenous repair.<sup>14</sup> This observation has prompted many to suggest that simply injecting cell conditioned media or recombinant cytokine preparations will provide the benefits of cell therapy without exposing patients to contaminated, expensive or oncogenic factors but this remains to be shown (Table 2). Cytokines, growth/differentiation factors and extracellular vesicles (e.g. exosomes) stimulate therapeutic regeneration through (Figure 2):

- 1) Cardiomyocyte protection from apoptosis through stimulation of endogenous pro-survival signaling pathways (e.g., phosphatidylinositol 3-kinase (PI3K)/Akt).<sup>170-174</sup>
- 2) Stimulation of angiogenesis.<sup>175</sup>
- 3) Recruitment/activation of endogenous stem cells to form new cardiomyocytes or blood vessels.<sup>176-178</sup>
- 4) Stimulation of existing myocyte re-entry into the cell cycle via PI3K/Akt signalling.<sup>179,180</sup>
- 5) Prevention of inflammation and fibrosis effects by directly inhibiting cardiac fibroblast or recruited leukocyte activation while promoting macrophage polarization from M1 to an M2 phenotype.<sup>180-184</sup>

Recent work has also highlighted the importance of cell-cell contact for therapeutic repair as integrin  $\beta$ 1 binding promotes both cardiomyocyte and hematopoietic stem cell

proliferation (via the MAPK/ERK and PI3K signalling pathways).<sup>185,186</sup> Transplanted cells also fuse with native cardiomyocytes to rejuvenate cells to a pluripotent state and rescuing them from apoptosis.<sup>187</sup>

<b>Benefits of cell transplantation</b>	<b>Disadvantages of cell transplantation</b>
Multiple complimentary cytokines/exosomes <sup>81,188</sup>	Expensive
Cell-contact mediated repair <sup>185</sup>	Contaminants (infectious, xenogenic)
Immuno-evasive permitting allogeneic therapy (some) <sup>35,82</sup>	Tumor
Potential for immune mediated clearance if malignant transformation	Potential for off-target effects
Engrafted cells continue to production cytokine/exosome over long period of time	

**Table 2. Benefits and disadvantages of cell therapy.**

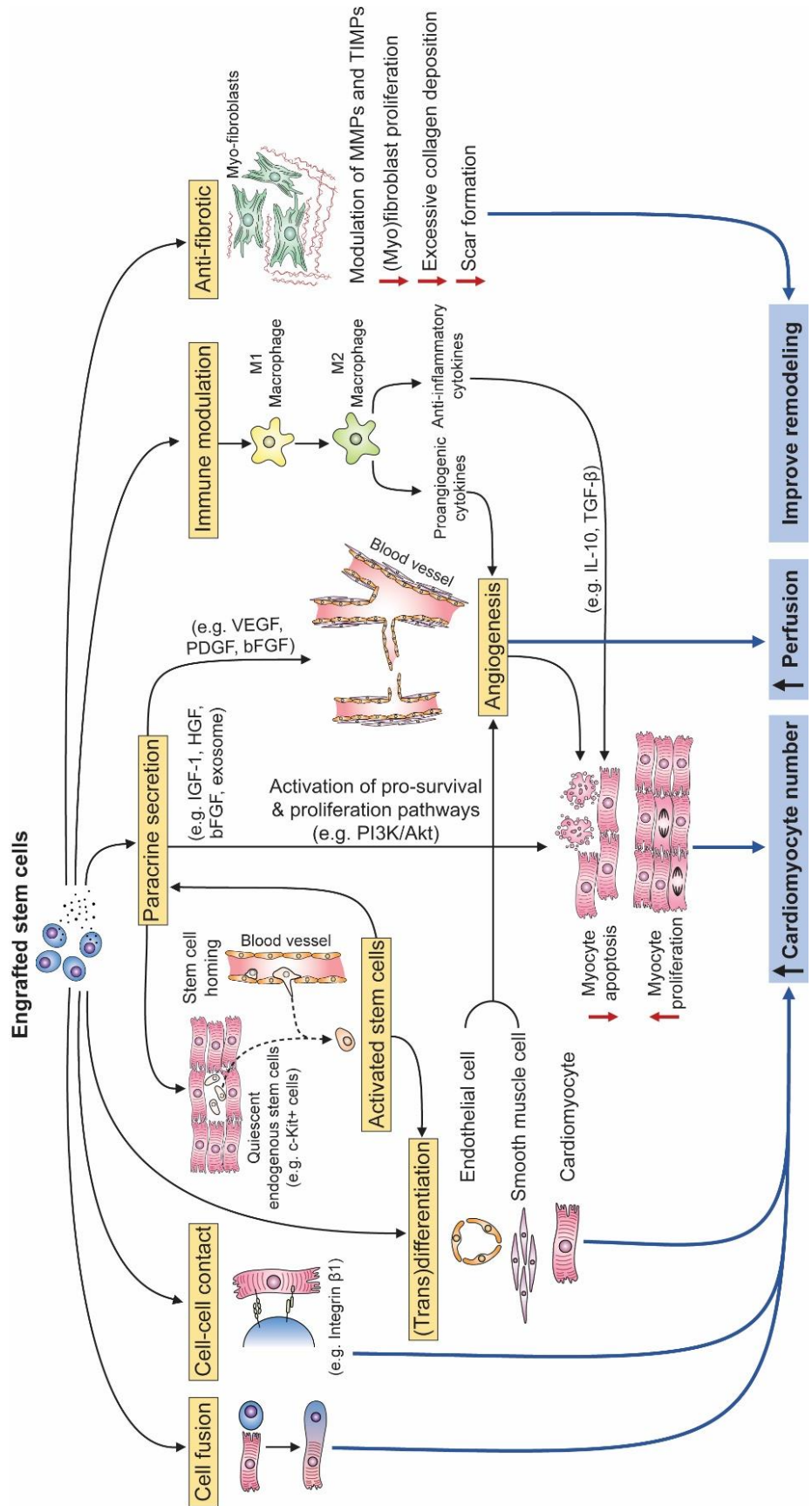


**Figure 2. Mechanisms underlying cardiac repair by stem cell therapy.** Engrafted stem cells promote direct cardiac regeneration by (trans) differentiating into cardiomyocytes, endothelial or smooth muscle cells. Cell-cell contact and fusion promote cardiomyocyte survival. Stem cells also promote indirect cardiac repair by secreting paracrine factors (cytokines/exosomes) which promote angiogenesis, activate pro-survival/pro-proliferative pathways, stimulate existing cells to re-enter the cell cycle and recruit endogenous stem cells. Paracrine factors also modulate the immune system by promoting an anti-inflammatory environment and inhibiting (myo)fibroblast proliferation/activation. Insulin-like growth factor 1 (IGF-1); Hepatocyte growth factor (HGF); Basic fibroblast growth factor (bFGF); Vascular endothelial growth factor (VEGF); Platelet-derived growth factor (PDGF); Interleukin (IL); Transforming growth factor beta (TGF- $\beta$ ); Matrix metalloproteinases (MMPs); Tissue inhibitors of metalloproteinases (TIMPs).

### **1.8 Transplanted Cell Persistence Hypothesis**

Given the above, the importance of transplanted cell persistence is controversial. One of the first clinical studies supporting the notion that enhancing acute cell retention boosts cell-mediated repair was reported by Vrtovec and colleagues.<sup>189</sup> Trans-endocardial injection of <sup>99m</sup>Tc-hexamethylpropylene-amine labeled CD34+ cells into patients with non-ischemic cardiomyopathy resulted in  $7.1 \pm 1.5\%$  of transplanted cells detected 2 hours after injection. The authors quantified the variability in the acute cell retention despite delivering similar number of viable cells. A direct correlation was seen between acute cell retention and improvements in cardiac function 3 and 12 months after

treatment. Preclinical data also supports a role for transplanted cells persistence in cell-mediated repair of injured myocardium. Ziebart and colleagues demonstrated that depletion of transplanted stem cells 2 weeks after injection reduced cell-mediated improvements in myocardial function and neovascularization.<sup>190</sup> The study used genetically modified EPCs that expressed a suicide gene (herpes simplex virus thymidine kinase) which activates a prodrug gancyclovir to induce cell apoptosis at specific timepoints. Similarly, ablating BMMCs or c-Kit<sup>+</sup> cardiac-derived cells abrogates therapeutic benefits suggesting that persistence of transplanted cells may play an important role in therapeutic regeneration.<sup>67,191</sup> But as a note of caution, straightforward interpretation of reports ablating transplanted cells is problematic as all methods of inducing “on demand” cell suicide are limited by off-target toxicity,<sup>192-194</sup> incomplete gene reprogramming,<sup>195</sup> and transgene silencing.<sup>196</sup> Taken as a whole, contemporary data supports the concept that engraftment of transplanted cells plays an important role in therapeutic regeneration but there must also be a critical time period where robust engraftment is no longer required to sustain gains in myocardial function. It follows that if engraftment can be markedly improved then unexploited mechanisms (such as differentiation into working myocardium) can be fully harnessed.

### **1.9 Mechanical Clearance of Transplanted Cells**

Techniques used to boost acute cell engraftment reflect how cells are being administered. When cells are infused through a catheter into the coronary circulation, it has been generally accepted in all cell therapy trials to date that flow needs to be stopped by balloon inflation to minimize backflow of cells. This concept was challenged

by Tossios and colleagues who reported that coronary occlusion in pigs did not improve acute (1 hour) or short term (24 hours) retention of BMNCs as compared to simple non-occlusive IC delivery.<sup>161</sup> This result likely stems from the observation that, although early cell retention is greater with upstream occlusion, the rapid clearance of cells from the well vascularized hearts immediately after balloon deflation negates any marginal advantage in early cell retention gained through occlusive delivery. In contrast, BMNC retention is superior following IM injection and, given the cells are often extra-vascular, clearance occurs at a slower linear rate. A portion of IM injected cells are immediately lost after injection through extrusion from the needle track or delivery into micro-vessels leading to direct washout via lymphatic or venous drainage.<sup>150</sup> To address this loss, strategies designed to limit mechanical extrusion (such as epicardial application of fibrin glue at the site of injection site) reduce cell leakage and enhance acute (~2 fold in the case of fibrin glue) and long term (~4 fold in the case of fibrin glue) engraftment of IM transplanted cells.<sup>108</sup>

Lastly, the heart is a lymphatic rich organ which likely plays a significant role in the clearance of transplanted cells.<sup>197-199</sup> The force generated during each contraction pushes the lymph from the myocardium into the subepicardial lymphatics which then drains into the mediastinum lymph nodes. The lymph flow rate in the heart is ~10 fold greater than other tissue which likely push cells along the lymphatic system.<sup>200</sup> Intramyocardial injection of radiolabeled cardiac derived cells (c-Kit+ cells) demonstrated that transplanted cells egress into the lymphatic vessels and drain into the mediastinal lymph nodes.<sup>198</sup> Interestingly, cells (e.g. MSCs) that engraft in the lymphovascular system limit

cardiac edema by promoting lymphangiogenesis that results in therapeutic repair after ischemia injury.<sup>201</sup>

### **1.10 Role of Transplanted Cell Pro-Survival Signalling**

Numerous genetic engineering and preconditioning strategies have been explored to enhance stem cell engraftment and function. Genetic modification is used to tailor the expression of genes that regulate apoptosis/proliferation (e.g. Akt,<sup>202</sup> Bcl-2,<sup>203</sup> caspase 8<sup>204</sup> and Pim-1<sup>205</sup>), ECM binding (e.g. tissue transglutaminase<sup>206</sup>), homing/migration (e.g. chemokine receptor,<sup>207</sup> endothelial nitric oxide synthase (eNOS)<sup>208</sup> and CD18<sup>209</sup>), immunomodulation (e.g. IL-10<sup>210</sup>), paracrine secretion (e.g. fibroblast growth factor (FGF),<sup>211</sup> HGF,<sup>212</sup> insulin-like growth factor 1 (IGF-1),<sup>212-214</sup> stromal cell-derived factor 1 alpha (SDF-1 $\alpha$ ),<sup>213,215</sup> vascular endothelial growth factor (VEGF)<sup>216</sup>) and stress proteins (e.g. hypoxia inducible factor 1 (HIF-1)<sup>217</sup> and HSPs<sup>218</sup>). Mangi and colleagues first demonstrated that constitutive over-expression of Akt in bone marrow derived-MSCs protected cells from apoptosis when challenged with hypoxic stress.<sup>219</sup> Transplantation of Akt-overexpressing MSCs into infarcted rat hearts improved systolic function, reduced scar volume, fibrosis, and cardiomyocyte hypertrophy in a dose-dependent manner. Akt exerts its cardioprotective effects through the activation of a downstream serine/threonine kinase, Pim-1 kinase. As such, overexpression of Pim-1 has also been reported to boost cell engraftment, long-term persistence, and differentiation to myocytes with salutary effects that enhance endogenous stem cell recruitment, neovascularization, reduce fibrosis, and improve cardiac function.<sup>75</sup>

Among the paracrine factors, IGF-1 is a key cardioprotective cytokine that promotes post-infarct cardiac repair via the Akt and ERK/MAPK pathways.<sup>177,220</sup> It follows that over-expression by transplanted progenitor cells has been shown to not only increase the survival of transplanted cells (and enhance long-term engraftment) but also limit apoptosis in surrounding reversibly damaged myocardium.<sup>221</sup> Interestingly, increasing long-term cell persistence is not always required to promote therapeutic regeneration as we recently demonstrated that transplantation of CSCs genetically programmed to overexpress SDF-1 $\alpha$  improved cardiac function in absence of longer-term cell engraftment by promoting the recruitment of endogenous stem cells and endogenous repair mechanisms.<sup>222</sup>

Despite the growing pre-clinical evidence supporting the benefits of genetically enhanced cell therapy, clinical translation has been limited because of regulatory and safety concerns.<sup>223</sup> The first in man report using genetically modified stem cells was recently reported using SkMs genetically programmed to over-express connexin 43.<sup>224</sup> Unlike previous studies using unmodified SkMs,<sup>43,44</sup> this early phase I study did not detect a meaningful increase in ventricular pro-arrhythmia although the number of treated patients was small (n=6). The ongoing ENACT AMI trial (NCT00936819) will be the first to use genetically modified blood-derived stem cells for cardiac disease.<sup>29</sup> This study will administer EPCs transfected with human eNOS to enhance cell function and promote neovascularization.

Similar to direct genetic modification, physiological preconditioning strategies have been used to modify stem cell function and promote resistance to the harsh environment of the ischemic myocardium. Exposure to cytokines and small molecules (such as TGF-

$\beta$ 1 + BMP-4 + FGF-2 + activin-A + retinoic acid + IGF-1 +  $\alpha$ -thrombin + IL-6) that prevent apoptosis has been shown to enhance long-term cell engraftment and myocardial function.<sup>225,226</sup> Clinical implementation is ongoing with the safety and efficacy of cytokine-cocktail treated MSCs just recently demonstrated in a phase II/III clinical trial (C-CURE; NCT00810238) for patients with chronic heart failure.<sup>227</sup>

In contrast, hypoxic pre-treatment is a simpler (and less expensive) alternative to boost cell viability and function. Exposure to low oxygen tension (0.5% oxygen) for a short period upregulates the expression of hypoxia inducible factor 1 which translocates to the nucleus and stimulates the expression of anti-apoptotic genes to activate pro-survival signalling pathways.<sup>228</sup> Hypoxic pre-treatment also enhances secretion of proangiogenic factors,<sup>229</sup> resistance to oxidative stress<sup>230</sup> and migration/homing by upregulating chemokine receptors.<sup>231</sup>

Finally, heat shock is another attractive approach to make stem cells more resilient to harsh environments. Preconditioning cells at high temperatures (39-45°C) increases the production of HSPs. HSPs are versatile proteins that act molecular chaperones to help protect cells from proteolytic degradation of denatured protein while also exerting cytoprotective effects by activating pro-survival pathways, reducing apoptosis and triggering anti-oxidative pathways.<sup>232,233</sup> Feng and colleagues recently demonstrated that heat shock preconditioning of Sca-1+ CSCs upregulates HSP 70 which protects cells from apoptosis.<sup>233</sup> Interestingly, heat shocked CSCs secrete exosomes enriched with heat shock factor 1 which, in turn, protects cardiomyocytes from apoptosis.

### 1.11 Role of Biomaterials in Transplanted Cell Engraftment

The ideal biomaterial used for cell therapy should be safe, nonimmunogenic, mimic mechanical properties of the heart, contain only chemically defined components (for clinical translation), biodegradable, cost-effective, require minimal amounts of exogenous biomaterials and employ a simple methodology. Moreover, it should enhance cell survival while also promoting cell release, migration and engraftment. Although no single biomaterial possesses all these properties, many have been designed for the cardiac applications including injectable hydrogels, cardiac patches, cell surface engineering, and microencapsulation. The types of biomaterial include natural materials like ECM proteins (e.g. fibrin, hyaluronan, collagen, and platelet-gel),<sup>78,234-236</sup> decellularized cardiac matrix,<sup>237</sup> polysaccharides (e.g. agarose, alginate, and chitosan),<sup>136,238,239</sup> synthetic materials (e.g. copolymer like polyethylene glycol),<sup>240</sup> self assembling peptides,<sup>241</sup> and electroconductive polymers;<sup>242</sup> covered in more detail in the following reviews [<sup>128,243</sup>]. The mechanism by which biomaterials enhance cell viability and acute retention is multifactorial and summarized in Table 3.

<b>Mechanical Factors</b>
<ol style="list-style-type: none"> <li>1. Bulk size and viscosity of the material act as a plug to prevent mechanical extrusion from initial site of injection.</li> <li>2. Prevents washout of cells through lymphatics and vessels.<sup>136,244</sup></li> <li>3. Protect cells from shearing force during administration.<sup>245</sup></li> </ol>
<b>Biological Factors</b>
<ol style="list-style-type: none"> <li>1. Biomaterials increase cell viability by providing crucial anchorage sites for cells to reduced detachment induced cell death (<i>i.e.</i>, anoikis).<sup>136</sup> This is particularly important for adherent cells (<i>e.g.</i> MSCs and CSCs) which are more dependent on cell-matrix anchorage for survival as compared to circulating cells (<i>e.g.</i> CD34+ cells)</li> <li>2. Biomaterials provide essential matrix proteins for cell anchorage after transplantation (<i>vs.</i> disrupted or remodeled extra-cellular matrix).<sup>136,244</sup></li> <li>3. Biomaterials act as a protective shell against the harsh inflammatory environment.<sup>246</sup></li> <li>4. Provide instructive cues for cells to proliferate, mobilize and differentiate.<sup>244,247-249</sup></li> <li>5. Modulates the secretion of trophic factors to enhance indirect myocardial repair.<sup>248,250</sup></li> </ol>

**Table 3. Mechanism of enhancing cell retention and function using biomaterials.**

Our group has recently developed a single cell microencapsulation method to enhance acute and long term persistence of transplanted CSCs.<sup>136</sup> This a clinically translatable microencapsulation technique cocoons cells within an agarose-based hydrogel supplemented with matrix proteins (fibrinogen and fibronectin). Microencapsulation provides several advantages over other bulkier biomaterial (*i.e.*, cardiac patches) as it readily permits the diffusion of growth factors/nutrients/oxygen, requires less biomaterial which minimizes the risk of foreigner body immune reaction, and encapsulated cells can easily be injected through small needle. We demonstrated that microencapsulation protects CSCs from anoikis and enhances acute cell retention (1 hour post-injection) by 3±1 fold over standard cell suspension. This boost in acute cell retention

led to greater long term cell persistence ( $2\pm 1$  fold by 21 days post-injection) and was associated with marked increase in CSC-mediated cardiac repair.

In addition to providing a protective niche for transplanted cells, biomaterials also deliver mechanical support to the injured myocardium. After an infarct, the left ventricle dilates to adopt a spherical geometry to reduce greater mechanical stress on the myocardium.<sup>122</sup> Biomaterials alone can act as bulking agents to provide mechanical support within the scar region to limit left ventricle expansion.<sup>251</sup> However, biomaterials are also biologically active as (depending on the material used) they have been shown to reduce post-infarct apoptosis and inflammation while promoting angiogenesis and endogenous stem cell recruitment.<sup>252</sup>

To date, clinical studies have found that combining biomaterials with cell therapy is safe with hints of enhanced efficacy (collagen patch + BMMCs, MAGNUM trial;<sup>253</sup> fibrin gel + CD15+/Isl1+ ESCs, ESCORT trial, NCT02057900). Others studies have taken the advantage of supplementing the materials with growth factors to support engrafted cell survival and promote angiogenesis.<sup>254</sup> In the ALCADIA trial (NCT00981006), gelatin-sheet was applied over the site of injection to slowly released basic fibroblast growth factor to support transplanted CDC survival.<sup>255</sup>

## Chapter 2

### 2.0 Encapsulation of Explant-Derived Cardiac Stem Cells in Agarose Nanoporous Gel Cocoons

#### 2.1 Study 1: Introduction, Aim, and Hypothesis

Infarcted heart tissue is inhospitable to transplanted cells and cell-based therapeutics are limited by very poor short-term retention and long-term engraftment.<sup>256</sup> As such, many of the benefits seen after delivery of cell products appear to rely on paracrine secretion of pro-healing cytokines and nano-sized exosomes that exert trophic effects on resident host tissue through the transfer of biological material (*i.e.*, microRNAs [miRNAs]).<sup>256-259</sup>

In response to this challenge, biomaterial approaches have been explored as a means of enhancing short- and long-term retention of transplanted cells (outlined in Chapter 1).<sup>260</sup> Of these approaches, individual micro-capsules have attracted attention as they permit diffusion of growth factors, nutrients and oxygen while protecting cells from mechanical stress and detachment induced cell death (*i.e.*, anoikis) during injection.<sup>261-263</sup> We developed a technique to encapsulate cells within extracellular matrix (ECM) supplemented nanoporous gels (NPG) to provide a temporary “home” from which cells can exit after a defined period (*i.e.* cocoons) (Figure 3).<sup>264,265</sup> Single cell encapsulation provides a miniscule amount of biomaterial as compared to more classic multi-cellular encapsulation- thus limiting the injectate required for transplant.<sup>78,234,266</sup> Agarose was chosen as the inert NPG for testing based on ease of encapsulation, the ability of cells to migrate through the material and free exchange

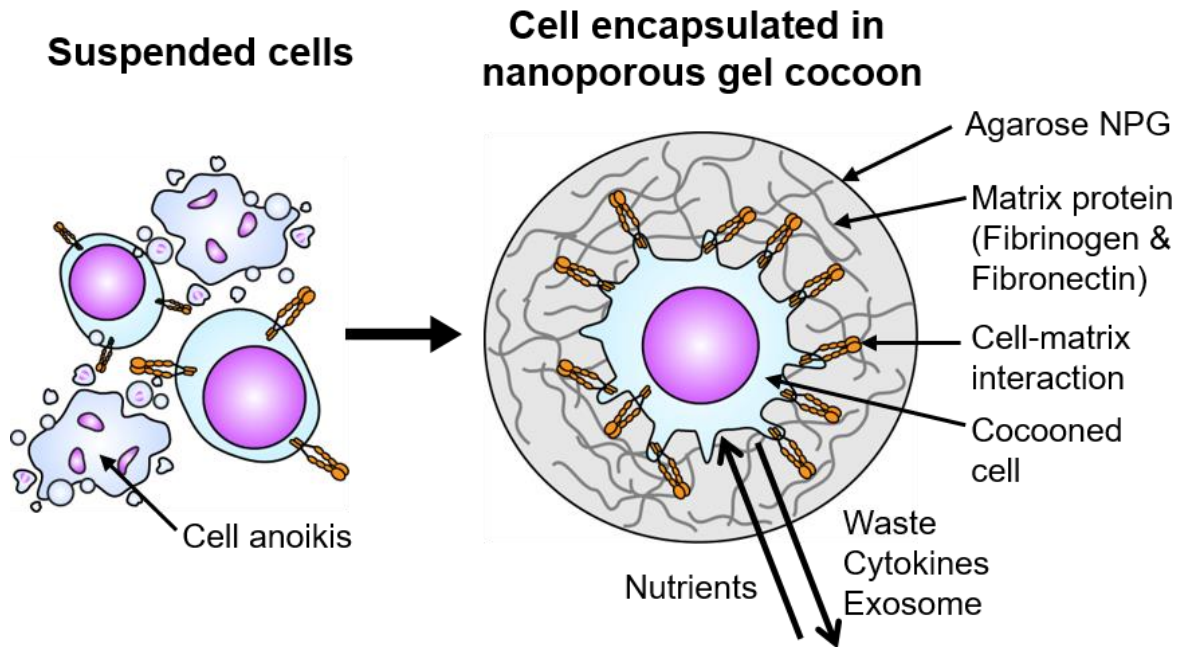


**Figure 3. Cell encapsulated in nanoporous gel cocoon.** Cartoon portraying suspended cells undergoing detachment induced cell apoptosis (anoikis). Cocoons supplemented with extracellular-matrix protein provide attachment sites to protect cells from anoikis. Nutrients/waste and cytokine/exosomes can freely diffuse through the agarose nanoporous gel (NPG).

cytokines/nutrients through the permeable shell (see Supporting information Table S1 for advantages of agarose).<sup>264,265,267</sup> Previous work showed that polymerization of fibrinogen and fibronectin, the de facto proteins of wound healing, within cocoon walls provides critical traction for attached cells to escape anoikis.<sup>264</sup>

Although cocooning increased retention of explant-derived cardiac stem cells (EDCs) and improved long-term gains in function after myocardial infarction,<sup>264</sup> it is

unclear if this improvement was attributable to enhanced cell engraftment or a change in the paracrine activity of cocooned cells. While various studies have investigated the influence of NPG physical properties on cell behaviour in 2- or 3-dimensional cultures,<sup>268-275</sup> few publications have considered the effects of altering the physical properties of NPGs on cells confined within 30-100 µm diameter capsules.<sup>267,276-279</sup> Studies altering mechanical properties of biomaterials (*i.e.*, hydrogel stiffness) have demonstrated significant biochemical changes within encapsulated cells including migration,<sup>280</sup> viability/proliferation,<sup>281,282</sup> differentiation<sup>283</sup> and secretion of cytokines.<sup>284,285</sup> Moreover, given that changes in agarose based biomaterial properties can trigger drastic metabolic changes in chondrocytes,<sup>273</sup> we rationalized that altering the physical properties of cocoons surrounding cells by varying NPG content would force cells to adopt an invasive/migratory phenotype that promotes cell-mediated repair of infarcted myocardium by altering the paracrine signature of cocooned cells.

**Aim 1:** To explore the effect of varying NPG content on the mechanical properties (*i.e.*, stiffness) of the NPG cocoons.

**Aim 2:** To explore how changing the physical properties of cocoons influences human EDC viability, proliferation, migration and paracrine output of EDCs.

**Aim 3:** To explore the effect of varying cocoon stiffness on the ability of human EDCs to improve cardiac function and structure using an immunodeficient mouse model of myocardial injury.

**Hypothesis:** Increasing cocoon stiffness forces cells to not only adopt a migratory/invasive phenotype but also increase the production of pro-healing cytokines,

exosome nanovesicles and altering the content of exosome miRNA to promotes cell-mediated repair of ischemic injury

## **2.2 Specific Objectives for Study 1:**

- 1) Characterize the physical properties of cocoons of varying agarose concentration (measuring cocoon diameter, stiffness, and pore size)
- 2) Examine the effects of altering cocoon agarose concentration on cell viability, proliferation, and their ability to extravasate the cocoons.
- 3) To evaluate the effects altering NPG composition on the cell's ability to adopt a migratory/invasive phenotype (measuring cell migration rates using Boyden chamber assay, and 2-D cell tracking analysis).
- 4) Determining the effects of altering cocoon's physical properties on EDC's ability to secrete cytokines, exosomes (nanovesicles), and their miRNA cargo.
- 5) Examining the effects of altering cocoon agarose concertation on EDC's ability to improve cell engraftment after injecting into an immunodeficient mouse model of ischemic myocardium.
- 6) Assess the effects of altering cocoon's physical properties on EDC mediated myocardial repair (measuring ventricular function, scar burden, peri-infarct vessel density, and myocyte proliferation).

## **2.3 Study 2: Introduction, Aim, and Hypothesis**

Although encapsulating human EDCs in NPG cocoons boosts cardiac function after intramyocardial injection, vortex-based cocooning is inconsistent, inefficient and

requires long processing time; thus, limiting straightforward application to the clinical setting. Microfluidic (MF) cocooning offers an attractive alternative means of encapsulating cells as:

- 1) The use of less biomaterial, reagents, and cells;
- 2) Provides control over cocoon size and cell occupancy;
- 3) Minimizes shear stresses during cocooning;
- 4) High-throughput and; capable of running parallel devices to permit large scale manufacturing of cocooned cell for clinical applications.

In study 2, we engineered a microfluidic platform to cocoon human EDCs within capsules of varying size with predictable cell occupancy for direct comparison to vortex cocooned cells.

**Aim 1:** To develop a high throughput microfluidic device that produces consistent capsule size while improving cocooning efficiency and minimizing processing time.

**Aim 2:** To investigate the impact of varying NPG cocoon size on human EDC viability, proliferation, migration and paracrine output of EDCs.

**Aim 3:** To explore the impact of NPG cocoon size on human EDC-mediated repair of injured myocardium using an immunodeficient mouse model of recent myocardial injury.

**Hypothesis:** Increasing cocoon size improves cardiac function by boosting transplanted cell retention and paracrine stimulation of endogenous repair.

## **2.4 Specific Objectives for Study 2:**

- 1) Design a microfluidic device to precisely control the size of agarose NPG cocoons with predictable number of cocooned cells.
- 2) Compare the yield and efficiency of cocooning cells using classic vortex method to microfluidic device.
- 3) While keeping the agarose concentration fixed, characterize the physical properties of cocoons of varying sizes (measuring cocoon stiffness, and pore size).
- 4) Examine the effects of altering cocoon size concentration on cell viability, proliferation, and their ability to extravasate the cocoons.
- 5) Examining the effects of cocoon size on cell engraftment after injecting into an immunodeficient mouse model of ischemic myocardium.
- 6) Determine the effects of cocoon size on cell engraftment after injecting into an immunodeficient mouse model of ischemic myocardium using a real-time *in vivo* cell tracking technique (Bioluminescence imaging)
- 7) Assess the effects of cocoon size on cell-mediated myocardial repair of ischemic heart (measuring ventricular function, scar burden, peri-infarct vessel density, and myocyte proliferation).
- 8) Determining the effects of cocoon size and cell-cell contact on the composition and number of cytokines/exosomes produced by cocooned cells.

## **2.5 Summary of Study 1 and 2:**

To test our hypothesis for both Study 1 and 2, we injected NPG cocooned human EDCs into an immunodeficient mouse model of ICM. We primarily used non-obese

diabetic/severe combined immunodeficiency (NOD SCID) mice in order to study clinically relevant human EDCs.<sup>136,286</sup> Cells were injected seven days post-MI because it has shown to be optimal for survival as it avoids the harsh inflammatory environment during the early stage of an MI; roughly 7 days post-MI, a switch to pro-healing cytokine milieu promotes survival of transplanted cells.<sup>287</sup> Approximately 1 week of cardiac remodeling in mouse is equivalent to 1 month in humans.<sup>122,288</sup> Current clinical trials administer cardiac-derived stem cells 1-2 months post-MI which is the time required to culture an effective dose of cells from patient cardiac biopsies.<sup>79,103</sup> Thus, transplanting cells 7 days post-MI in mice mimics clinical practice of autologous cell delivery.

We identified that altering NPG content played a major role in regulating the production of pro-healing paracrine factors to increase the generation of new blood vessels and cardiomyocytes while reducing scar burden. By using microfluidic device, we improved the cocooning efficacy and yield while producing homogeneous sized cocoons. We demonstrated that larger cocoons significantly boosted short-term cell persistence resulting in improved cardiac repair, effects attributable to changes in the amount and composition of cytokine factors. Further investigations are ongoing to determine the role of exosomes secreted by EDCs encapsulated in difference sized cocoons.

Ultimately, our work shows that by simply varying NPG content surrounding encapsulated cells or changing cocoon size provides a straightforward means of boosting engraftment and the regenerative potential of cardiac-derived stem cells without recourse to genetic manipulation<sup>289</sup> or multiple cell injections.<sup>290,291</sup>

## **Chapter 3**

### **3.0 Study 1: Deterministic Encapsulation of Human Cardiac Stem Cells in Variable Composition Nanoporous Gel Cocoons to Enhance Therapeutic Repair of Injured Myocardium**

#### **3.1 Abstract**

Although cocooning explant-derived cardiac stem cells (EDCs) in protective nanoporous gels (NPG) prior to intramyocardial injection boosts long-term cell retention, the number of EDCs that finally engraft is trivial and unlikely to account for salutary effects on myocardial function and scar size. As such, we investigated the effect of varying the NPG content within capsules to alter the physical properties of cocoons without influencing cocoon dimensions. Increasing NPG concentration enhanced cell migration and viability while improving cell-mediated repair of injured myocardium. Given the latter occurred with NPG content having no detectable effect on the long-term engraftment of transplanted cells, we found that changing the physical properties of cocoons prompted explant-derived cardiac stem cells to produce greater amounts of cytokines, nanovesicles and microRNAs that boosted the generation of new blood vessels and new cardiomyocytes. Thus, by altering the physical properties of cocoons by varying NPG content, the paracrine signature of encapsulated cells can be enhanced to promote greater endogenous repair of injured myocardium.

## 3.2 Results

### 3.2.1 Characterization of Nanoporous Gel Capsules

Figure 4A summarizes the process of encapsulating human EDCs within a NPG cocoons using the vortex-agitation method. Representative bright field images of cell-free aqueous suspended NPG capsules illustrate the inherent heterogeneity of capsule sizes resulting from vortex agitation (Figure 4B). The capsular diameter of cell-free suspensions varied from 30 to 100  $\mu\text{m}$  with the upper limit reflecting filtration through 100  $\mu\text{m}$  pore filters to remove clumped NPG (Supporting Information Figure S1). Increasing NPG content from 2 to 3.5% had no effect on the average diameter of cell-free capsules as measured using bright field microscopy ( $58\pm 2$  and  $62\pm 1$   $\mu\text{m}$ , respectively,  $p=0.11$ ) and electron microscope images of individual spheres ( $60\pm 5$  and  $71\pm 6$   $\mu\text{m}$ , respectively,  $p=0.17$ ). Incorporation of EDCs within 2 or 3.5% NPG cocoons had also no effect on the average diameter of the cocoons ( $57\pm 1$  and  $59\pm 1$   $\mu\text{m}$ , respectively;  $p=0.14$  vs. empty capsules, Figure 4B and C). Although vortex-based agitation provides limited control over the number of cells within a single cocoon, reproducible proportions of cells were found within both 2 and 3.5% NPG encapsulated preparations (Figure 4D). Altering NPG content had no effect on the proportion of empty capsules ( $31\pm 2\%$  and  $30\pm 1\%$  of total 3.5% and 2% NPG cocoons, respectively) or the very few free cells that escaped cocooning ( $2\pm 1\%$  and  $3\pm 1\%$  of total encapsulated cells in 3.5% and 2% NPG cocoons, respectively). While discerning if cells were truly inside NPG cocoons rather than adherent to the outer surface using light microscopy is challenging, confocal imaging confirmed that cells were truly located inside the NPG cocoons (Supporting Information Figure S2A).

Scanning electron microscopy (SEM) showed spherical structures (Supporting Information Figure S2B) with clear porous submicrometer structural features (Supporting Information Figure S2C). Porous sizes for the 3.5% NPG capsules were smaller ( $0.75\pm 0.07\ \mu\text{m}$ ) than the 2.0% NPG capsules ( $1.07\pm 0.07\ \mu\text{m}$ ,  $p < 0.0001$ , Figure 4E) with values that were closer to what has been reported for other 3D NPG structures.<sup>292,293</sup> As shown in the representative images in Supporting Information Figure S2D, the surface of the 3.5% NPG cocoon was considerably more homogeneous and organized than the 2% NPG counterpart.

Atomic force microscopy (AFM) confirmed that changing the NPG content altered the cocoon's stiffness ( $2.2\pm 0.01 \times 10^{-3}$  vs.  $1.5\pm 0.02 \times 10^{-3}$   $\mu\text{N}/\text{nm}$ ;  $p < 0.0001$  vs. 2% NPG cocoons, Figure 4F), as previously shown using NPG-based encapsulation of chondrocytes.<sup>273</sup> Interestingly, the addition of ECM increased cocoon stiffness by  $\approx 0.5 \times 10^{-3}$   $\mu\text{N}/\text{nm}$  for both 3.5 and 2.0% capsules ( $1.56\pm 0.01 \times 10^{-3}$  and  $1.08\pm 0.01 \times 10^{-3}$   $\mu\text{N}/\text{nm}$  for 3.5% and 2% NPG cocoons, respectively); an observation potentially attributable to additional ECM-mediated crosslinking during capsule formation. From a physical standpoint, the stiffness of a 3D fibrous network is directly connected to its porosity (*i.e.*, mesh size). In general, a higher stiffness corresponds to a smaller mesh size as a result of greater intermolecular bonding (*e.g.* resulting from cross-linking).<sup>294</sup> In the case of our NPG, SEM and AFM data indicate that the observed interconnection between concentration-dependent stiffness and pore size most likely derives from variations in the 3D organization of agarose chains and the amount of intermolecular hydrogen bonds. Thus, a higher NPG concentration leads to a more densely packed organization of the

polymer chains that expedites intermolecular interactions, which stiffens the 3D mesh and reduces pore size.

### **3.2.2 Effects of Nanoporous Gel Encapsulation on Proliferation and Viability**

Vortex cocooning was well tolerated by EDCs as evidenced by ~90% of cells remaining viable 1 hour after encapsulation ( $p=0.96$  for effect of cocooning and NPG content, Supporting Information Figure S3A). Cell counts at 48 hours after encapsulation revealed that increasing NPG content prompted a  $1.6\pm 0.2$  fold increase in EDC numbers ( $p=0.015$  vs. 2% NPG cocoons; Figure 4G). This finding was attributable to a combination of reduced apoptosis ( $p=0.02$ ; Figure 4G and Supporting Information Figure S3B) and increased proliferation ( $p=0.04$ ; Figure 4G and Supporting Information Figure S3C). Mechanistically, this effect was mediated through integrin-dependent pro-survival signalling as cocooned EDCs culture conditions demonstrated a  $2.5\pm 0.2$  ( $p=0.003$ ; Figure 4H) or  $2.6\pm 0.2$  ( $p=0.003$ ) fold increase in metabolic activity compared to EDCs within ECM-free cocoons or suspension (poly-2-hydroxyethyl methacrylate), respectively. Pre-treatment of EDCs with  $\alpha V$ ,  $\alpha 5$ ,  $\beta 1$  and  $\beta 3$  integrin blocking antibodies further established the importance of integrin-matrix interactions as the metabolic activity of these cells decreased by  $1.5\pm 0.1$  fold when compared to EDCs encapsulated in ECM supplemented NPG capsules ( $p=0.023$ ; Figure 4H).

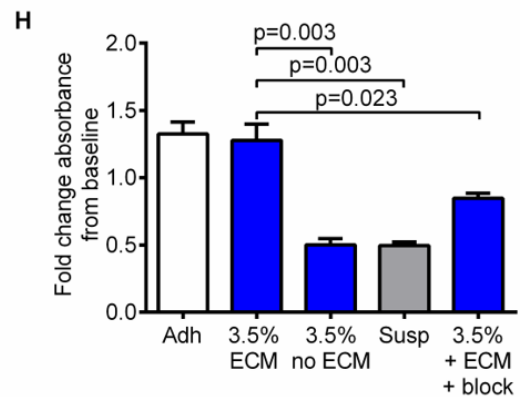
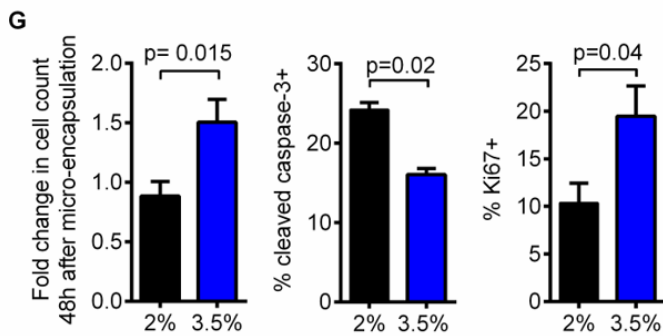
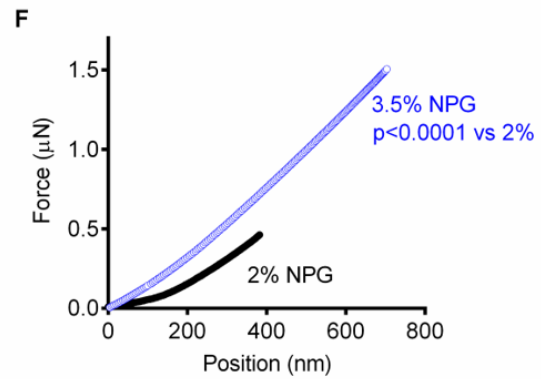
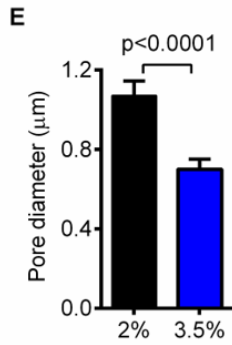
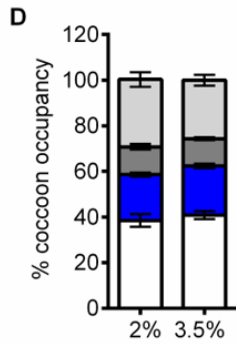
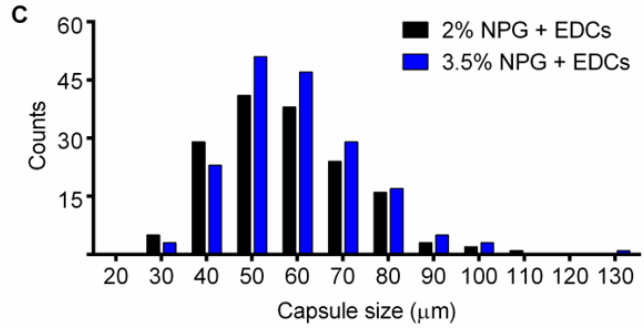
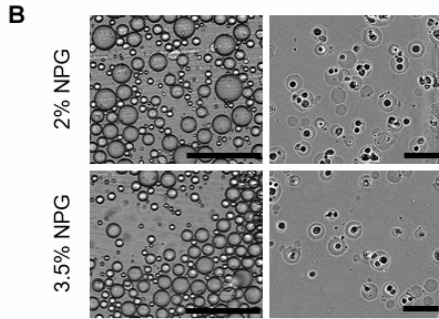
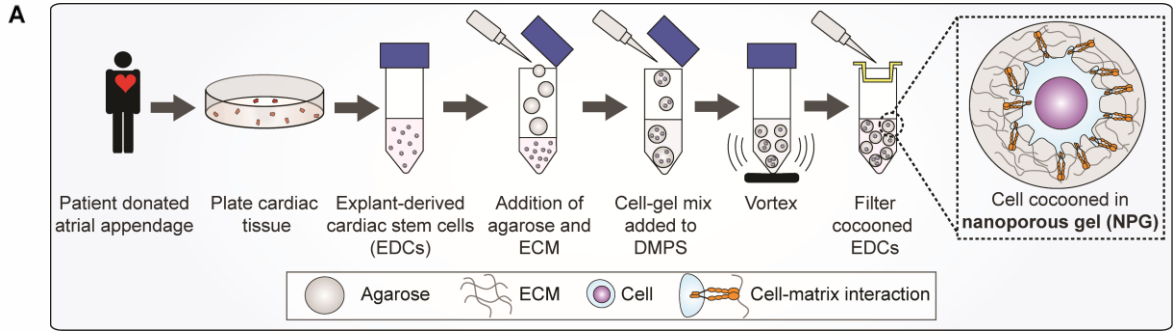


**Figure 4. Characterization of nanoporous gel capsules.** (A) Schematic summarizing encapsulation of human EDCs within NPG cocoons using vortex-based agitation. DMPS=dimethylpolysiloxane. (B) Representative images of empty cocoons (scale bar 500  $\mu\text{m}$ ) and EDCs encapsulated in 2 and 3.5% NPG cocoons (scale bar 100  $\mu\text{m}$ ). (C) Size distribution histograms for 2% and 3.5% NPG encapsulated EDCs. Size distributions were calculated from measuring >100 individual capsules from three different samples. (D) The distribution of cells found within 2 and 3.5% NPG cocoons (measured >1500 cocoons from 6 different samples). (E) Mean pore diameter calculated from measuring >100 pores. (F) AFM force-displacement curves for NPG capsules. Reported values for AFM were calculated from averaging 45 independent points randomly selected from the DPFM maps. (G) Cell growth quantified as fold change after 48h in culture (1% oxygen and 1% serum); cells were counted using a hemocytometer (n=8). Cell apoptosis and proliferation was quantified by measuring the number of cells positive for active-caspase 3 (n=3), and Ki67 positive nucleus (n=5), respectively. (H) Colorimetric cell viability assay (CCK-8) shows that pre-treatment of EDCs with  $\alpha\text{V}$ ,  $\alpha\text{5}$ ,  $\beta\text{1}$  and  $\beta\text{3}$  integrin blocking antibodies reduces cell viability by  $1.5\pm 0.1$  folds. +ECM= capsules containing matrix protein fibronectin and fibrinogen; Susp=non-encapsulated suspended cells; Adh=non-encapsulated cells adhered to cultureware; +Block= antibody cocktail used to block integrin-matrix interactions. (n=5 cell lines/assay). All error bars correspond to standard error mean SEM.

### 3.2.3 Effects of Nanoporous Gel Encapsulation on Cell Morphology and Migration

To explore the effects of variable capsule NPG composition on EDC phenotype, immunohistochemistry and electron microscopy were used to profile the cytoskeleton structure of cocooned cells. As shown in Figure 5A, encapsulation within NPG devoid of ECM prompted cells to assume a spherical shape with a diffuse halo of actin monofilaments at the periphery and no visible membrane protrusions into the surrounding capsule. The addition of ECM resulted in multiple small membrane protrusions and increased organization of the actin filaments throughout the cell with no apparent differences between 2 or 3.5% NPG cocooned cells. Transmission electron microscopy confirmed that cells within ECM supplemented cocoons possessed robust micrometer sized membrane protrusions that were not present in cells encapsulated within NPG alone (Figure 5B). Increasing NPG content doubled the number of membrane protrusions per cell seen on each encapsulated cell (Figure 5C).

Sequential *in vitro* imaging of plated NPG encapsulated EDCs demonstrated that increasing capsule NPG concentration markedly delayed cocoon occupancy half-time (*i.e.*, the time required for half of the encapsulated EDCs to emerge from the capsules) from  $15.8 \pm 1.7$  to  $41.8 \pm 11.9$  h for 2% and 3.5% NPG cocoons, respectively ( $p < 0.05$ ; Figure 6A). When comparing representative images after comparable numbers of EDCs exited the capsules (*i.e.*, 18 vs. 40 hours for cells cocooned within 2% or 3.5% NPG, respectively), similar proportions of rounded and flattened cells can be appreciated. Real time Boyden chamber imaging revealed that straightforward application of suspended non-encapsulated EDCs resulted in immediate and consistent migration across the membrane when cells were plated in basal media and exposed to a 20% serum gradient

(lower chamber, Figure 6B). Exponential curve fitting of cell migration over time demonstrated that encapsulation of EDCs within 3.5% NPG decreased the population migration time of cells within the lower well to  $27 \pm 1$  h (Figure 6C) from  $49 \pm 4$  h for non-encapsulated ( $p=0.001$ ) and  $46 \pm 3$  h ( $p=0.02$ ) for 2% NPG. To confirm if increasing NPG content confers a greater migratory potential, individual cells were tracked for 11 h after emergence from capsules. As displayed in Figure 6D and Supporting Information Figure S4A and B, EDCs encapsulated within 3.5% NPG demonstrated a  $\approx 1.5$ -fold greater extra-capsular migration velocity as compared to 2% NPG or suspended EDCs ( $p < 0.0001$ ). Taken together, this data suggests that, although increasing capsule NPG content delays capsule exit, it also instructs cells to adopt a migratory phenotype.

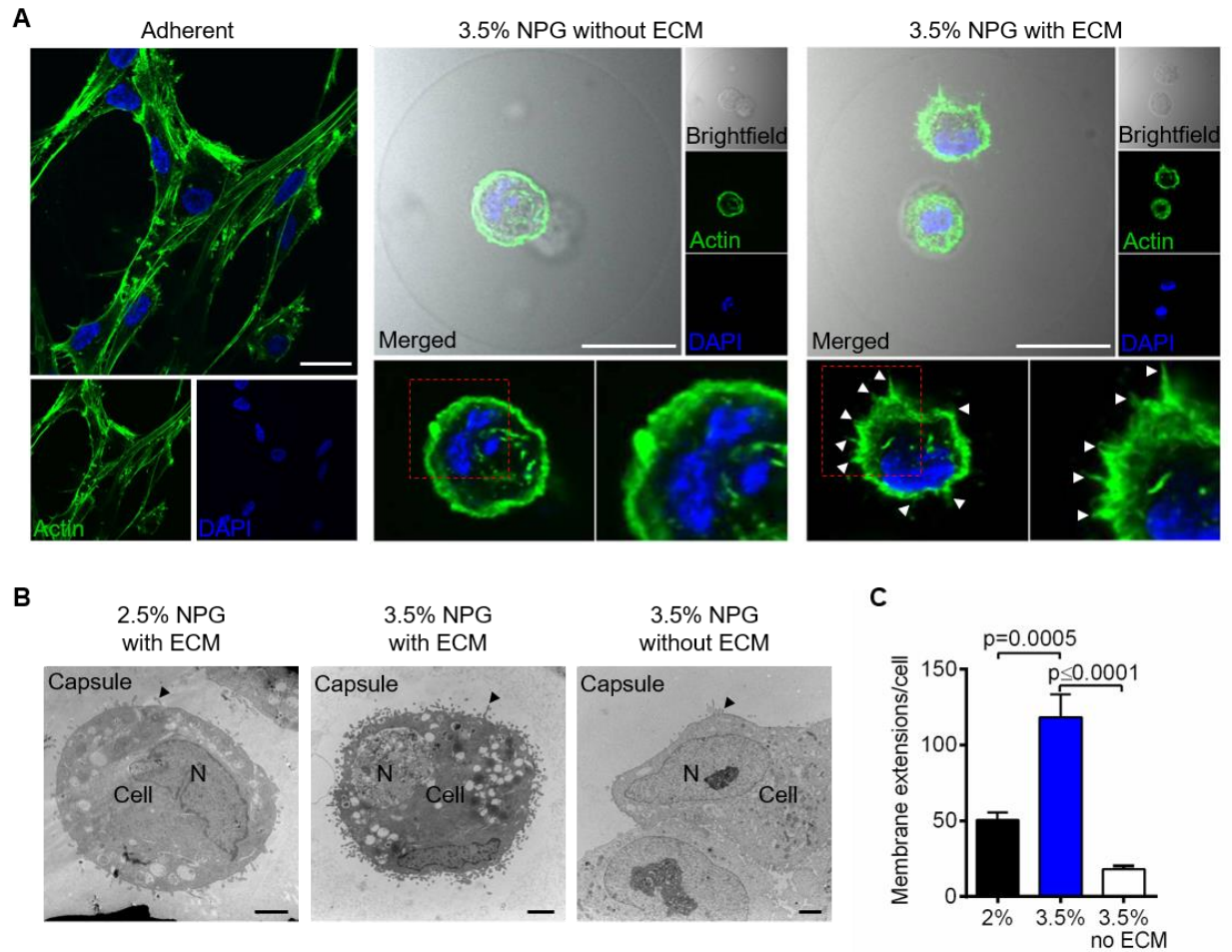
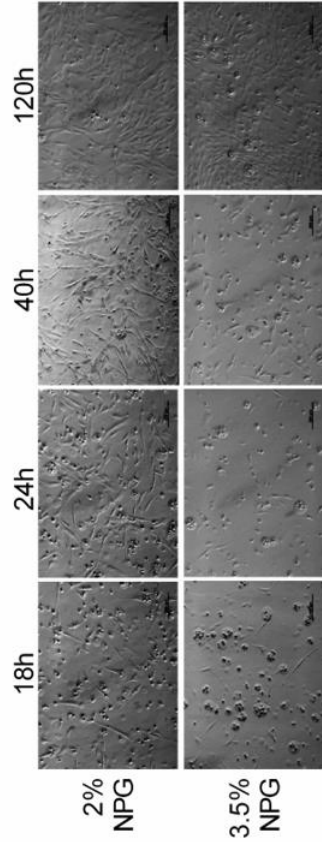
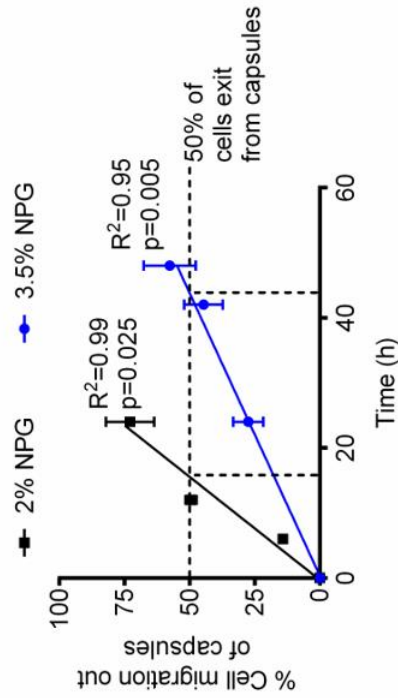


**Figure 5. Effect of nanoporous gel encapsulation on cell cytoskeletal structure.** (A) Actin filaments are stained using phalloidin (green) for non-encapsulated EDCs (Adherent) and EDCs within capsules supplemented with extra-cellular matrix (ECM) or without ECM proteins (fibronectin and fibrinogen). For the cocooned cells, corresponding brightfield, single stain actin and DAPI images are shown (right panels) while lower panels display magnified views with the dashed area indicating the area of increased magnification displayed in the bottom right panel. Small membranous projection are highlighted by the arrows. EDCs within capsules containing no extracellular matrix protein display a smooth cell surface with minimal membrane projections (scale bar 20  $\mu\text{m}$ ). (B)

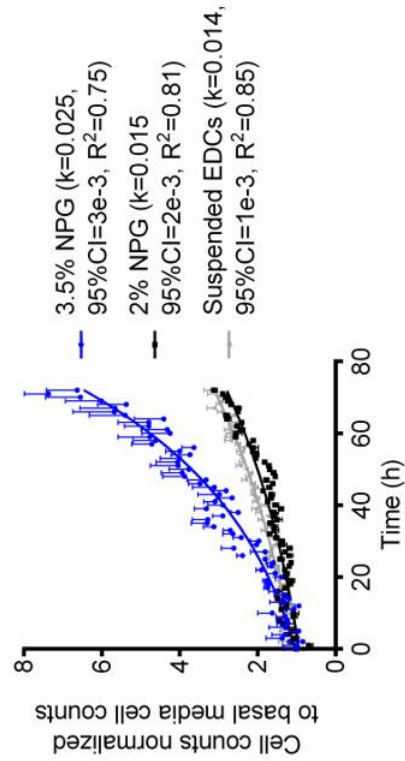
TEM images showing EDCs within capsules with or without extracellular matrix protein (scale bar 2  $\mu\text{m}$ ). Highlighted on the images are the nucleus (N), cell, capsule and the arrow showing a membrane protrusion. (C) The number of membrane projection identified with TEM images are quantified (n=5) (see methods and Supporting Information Figure S2E for details) Error bar correspond to standard error mean SEM.

Real-time live cell microscopy was used to profile serial changes in morphology as cells emerged from the 3.5% NPG capsules. Cells adopted a spherical shape immediately after encapsulation but as time progressed, small membranous protrusions sprouted from the cell surface which eventually projected through the cocoon wall (Figure 7A). These membranous protrusions developed into large flat membranous structures morphologically similar to lamellipodia as the cell extravasated through the capsule wall and attached to the underlying culture plate. Consistent with the notion that probing lamellipodia require integrin-ECM attachments to enable cell movement, plating encapsulated EDCs on uncoated cultureware prolonged capsular occupancy half-life by  $23\pm 6$  h as compared encapsulated cells plated on fibronectin coated cultureware ( $p=0.03$ ; Supporting Information Figure S5). Figure 7B and Supporting Information Figure S6, suggests that that within the cocoon, fibrinogen clustered around EDCs and bound to  $\beta 1$  integrins. As EDCs elongated through the capsule wall and adhered to the cultureware, a portion of the capsular ECM tracked with the emerging cells (Figure 7C); suggesting that the tightly bound ECM tracks with cells to maintain pro-survival signaling outside the capsule.

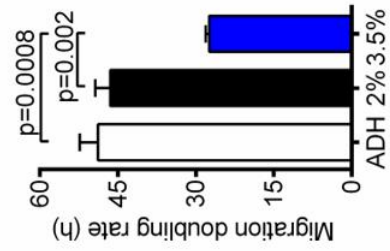
A



B



C



D

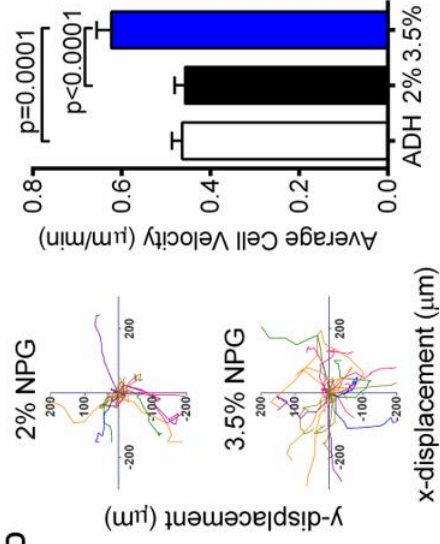


**Figure 6. Effects of nanoporous gel encapsulation on cell migration.** (A) EDCs were encapsulated with increasing NPG concentration of 2% and 3.5% and plated on fibronectin-coated cultureware within low oxygen/serum conditions. Random field images were acquired at 10X magnification to count the number of cells inside and outside of the capsules at various time points. Dashed lines highlight the time required for half of the cells to migrate out of the capsules (n=3). Representative bright field images compare cells exiting capsules of different NPG concentration (scale bar 200  $\mu\text{m}$ ). (B) The number of EDCs which cross the 8 $\mu\text{m}$  pore membrane from the top chamber into the lower chamber. Data was analyzed using exponential curve fitting with Prism v6 (n=4). (C) Curve fitting analysis was used to determine cell migration doubling rate (i.e., the doubling time of the exponential curve). Smaller migrating doubling rate corresponds to quicker cell migration across the pores. (D) Left: Displacement plots showing the path of cell migration. Right: Graph compares the rate of 2D-cell migration as EDCs emerge from capsules of different NPG concentrations or suspension culture conditions alone. Migration rate was determined by manual cell tracking software (Image J; n=52). Error bar correspond to standard error mean SEM.

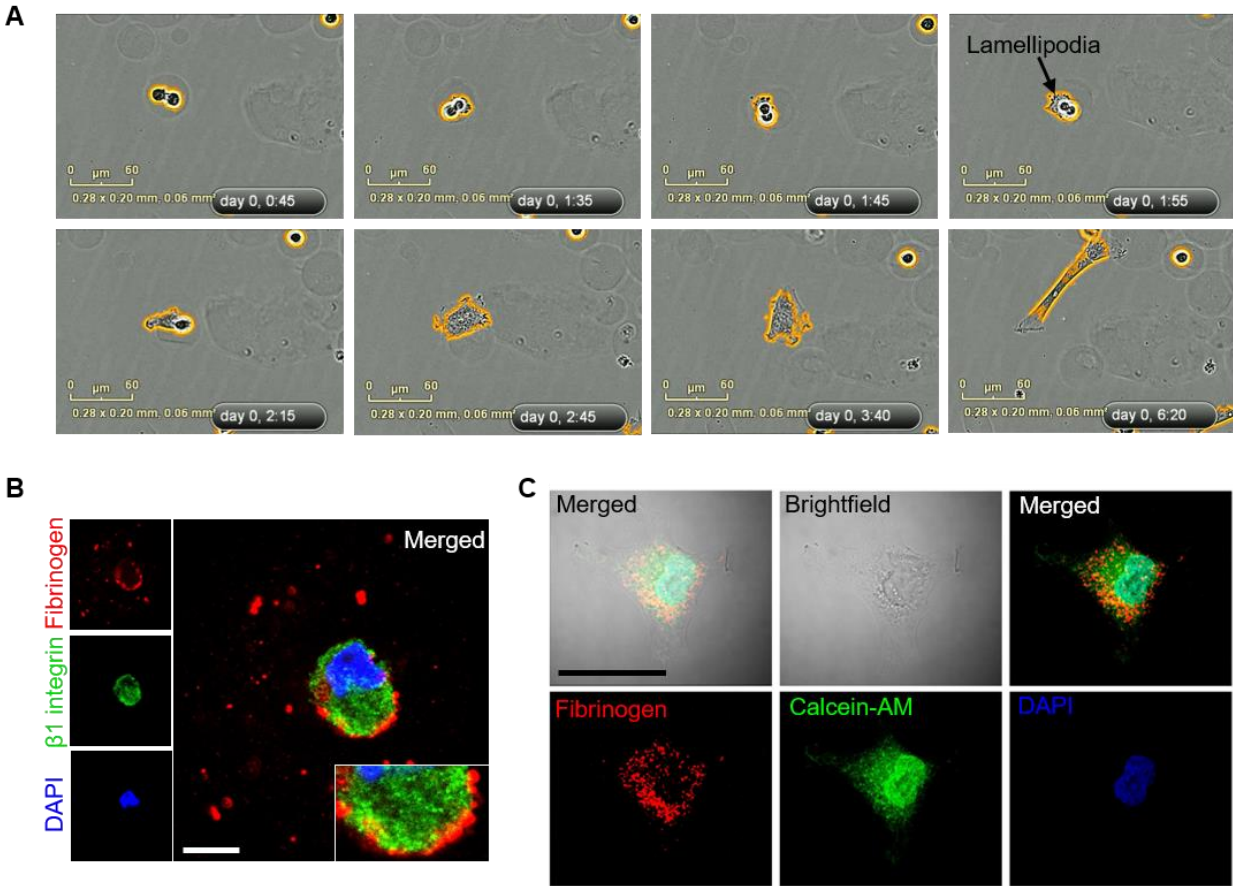


**Figure 7. Characterizing cell egress from nanoporous gel capsules.** (A) Images acquired at different time points using the IncuCyte System. Cells are outlined in orange. (B) EDCs are stained for  $\beta 1$  integrin (green) and capsules contain DsRed tagged fibrinogen (red), scale bar 10  $\mu\text{m}$ . The fibrinogen can be seen diffusely present within the capsule but also clusters around the cell. Overlap between fibrinogen and  $\beta 1$  integrin at the cell surface is highlighted in the magnified panel. Image taken 1 day after encapsulation. (C) Cells (labeled with Calcein-AM, green) retained a coat of fibrinogen (red) after exiting the capsules (scale bar 30  $\mu\text{m}$ ).

### 3.2.4 Effects of Altered Nanoporous Gel Capsule Rigidity on EDC Engraftment and Myocardial Repair

As shown in Figure 8A, the impact of capsular NPG content on cell-mediated repair of ischemic myocardium was evaluated using echocardiographic-guided intra-myocardial injection of human EDCs into an immunodeficient mouse 1 week after left coronary artery (LCA) ligation.<sup>264,286,295-297</sup> LCA is a well-established and clinically relevant mouse model for myocardial infarction.<sup>298</sup> NPG encapsulation increased the acute retention of EDCs by  $4\pm 1$  fold ( $p=0.04$  vs. suspended EDCs; Figure 8B). This boost was associated with enhanced long-term retention of cells as cocooning cells within 2 or 3.5% NPG increased long term retention (at day 21 post-MI) by  $18\pm 4$  fold ( $p=0.001$ ) or  $22\pm 8$  fold ( $p=0.03$ ), respectively. Increasing capsule NPG content had no detectable effect on the long-term retention of transplanted cells.

Despite negligible additive effects on cell engraftment, increasing capsule NPG content enhanced the ability of transplanted EDCs to repair injured myocardium. As shown in Supporting Information Table S2, all animals had comparable cardiac function as measured by left ventricular ejection fraction, and chamber dimensions 1 week after LCA ligation. Three weeks after intra-myocardial injection, animals randomized to receive intra-myocardial injection of cell-free ECM-supplemented cocoons or vehicle underwent progressive adverse cardiac remodeling. Although all animals transplanted with EDCs demonstrated better cardiac function 4 weeks after LCA ligation (Figure 8C), encapsulation within dense 3.5% NPG cocoons achieved the greatest improvement in left ventricular ejection fraction ( $p<0.0001$  vs. vehicle, 2% NPG cocooned EDCs, suspended EDCs or cell-free ECM-supplemented cocoons). Interestingly, transplant of

2% NPG cocooned EDCs or suspended EDCs provided equivalent degrees of myocardial repair 4 weeks after LCA ligation. Estimates of scar size mirrored this outcome as animals treated with 3.5% NPG encapsulated EDCs experienced the greatest reduction in scar burden while comparable scar sizes were seen in animals injected with 2% NPG encapsulated or suspended EDCs (Figure 8D and Supporting Information Figure S7).

To evaluate the effect of cell transplant on the generation of new myocytes within the peri-infarct region, all mice received daily intra-peritoneal injections of bromodeoxyuridine (BrdU) for the first week after cell or vehicle injection. As depicted in Figure 8E and Supporting Information Figure S8, animals that received EDCs encapsulated within 3.5% NPG cocoons demonstrated greater overall and cardiomyocyte proliferation when compared to animals that received either 2% NPG cocooned or suspended EDCs. Similar results were seen when comparing peri-infarct vascular density as animals that received 3.5% NPG cocooned cells demonstrated greater peri-infarct vessel density as compared to animals that received 2% NPG cocooned or suspended EDCs (Figure 8F and Supporting Information Figure S9).

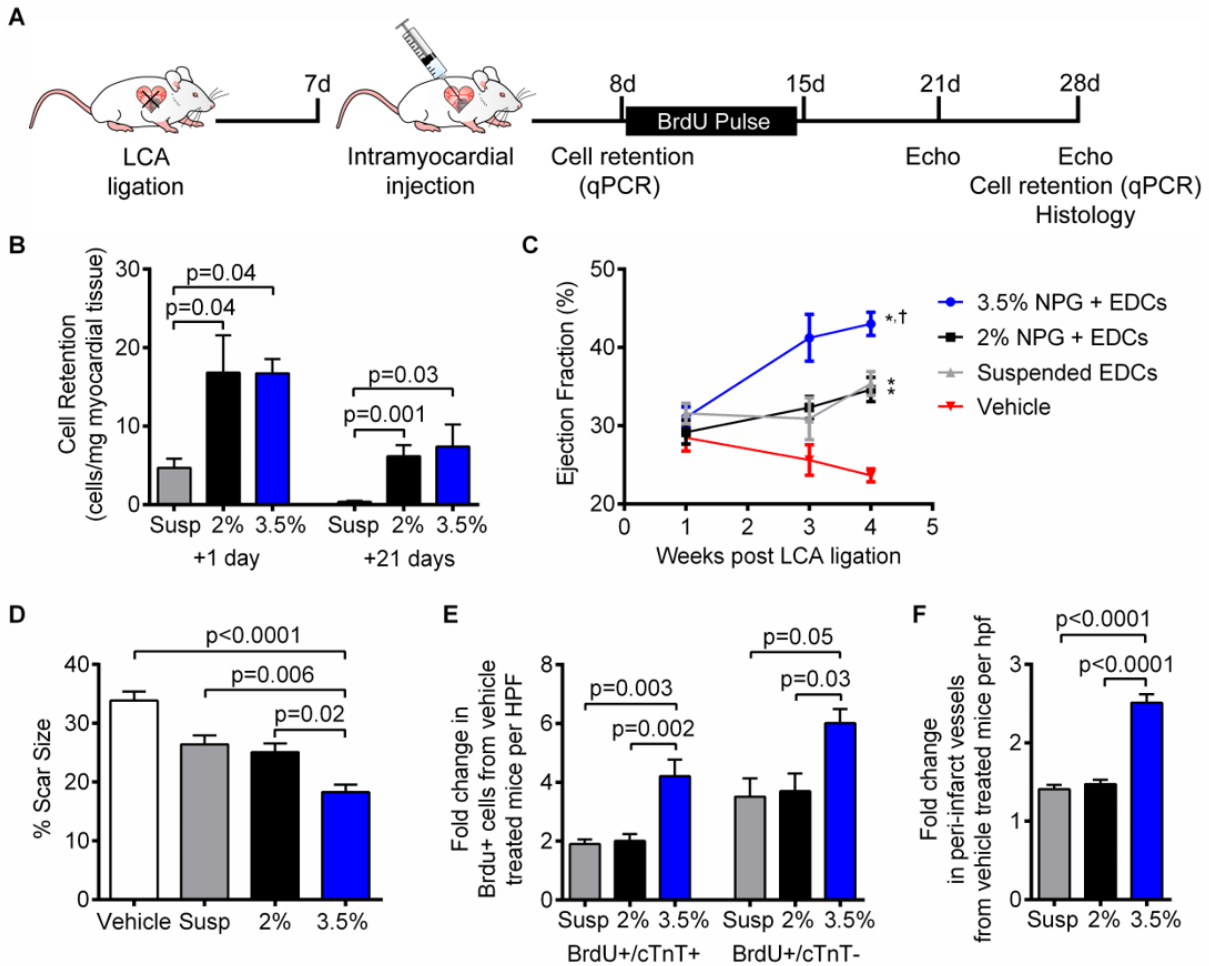


**Figure 8: Effects of altered nanoporous gel capsule composition on EDC engraftment and myocardial repair.** (A) Schematic summary of animal study. LCA=left coronary artery ligation. (B) Quantitative PCR analysis for retained human ALU sequences in mouse ventricles at 1 day and 21 days post injection to provide an estimate of the number of human cells retained after intra-myocardial injection (n=5 mice/group at day 1 and n=8 mice/group at day 21). (C) Echo analysis showing left ventricle ejection fraction (n=10-9 mice/cell and saline (vehicle) treated group); \*p<0.05 vs. vehicle, †p<0.05 for 3.5% vs. 2% NPG cocooned or suspended EDCs. (D) Quantification of percent scar size (n=5). (E) The number of proliferating cardiomyocytes (BrdU+/cTnT+)

and non-cardiomyocyte cells (BrdU+/cTnT-) quantified using random field analysis at high power field (HPF; 40X magnification; n=5). Graph represented as fold change over vehicle control group. (F) Isolectin staining used to quantify vessel density within infarct region. Graph represented as fold change over vehicle control group (n=5). Susp= Suspended EDCs. Vehicle control= Phosphate-buffered saline. All error bars correspond to standard error mean SEM.

### 3.2.5 Paracrine Profiling of Encapsulated EDCs

The mechanisms accounting for the discrepancy between cell engraftment and function outcomes were evaluated using proteomic profiling of media collected during EDC capsular migration for cytokines and proteases typically produced by migratory invasive cells.<sup>299-304</sup> While encapsulation alone promoted the expression of ECM metalloproteinase inducer (EMMPRIN), matrix metalloproteinase 1 (MMP1) and MMP10 (Figure 9A), NPG capsule content had no effect on MMP or tissue inhibitor of MMP production (Supporting Information Figure S10A). When compared to adherent or 2% NPG cocoons, increasing NPG content increased the secretion of beta fibroblast growth factor (bFGF) and interleukin-6 (IL-6) (Figure 9B); two cytokines implicated in post infarct healing.<sup>286,305,306</sup>

While encapsulation and cocoon NPG content had no effect on characteristic markers of nanovesicles lineage or size (Supporting Information Figure S10B-D), increasing NPG content boosted exosome production by  $2.2 \pm 0.3$  and  $1.6 \pm 0.3$  fold as compared to adherent and 2% NPG cocooned EDCs, respectively (Figure 9C). Within

non-cocooned EDC exosomes, the most abundant miRNAs were associated with cardiomyocyte salvage (e.g. hsa-miR-146a-5p, miR-23a-3p and hsa-miR-125b-5p), stimulating angiogenesis (hsa-miR-126-3p), and reducing fibrosis (e.g. hsa-miR-22-3p and hsa-miR-132-3p) (Supporting Information Table S3). NPG encapsulation increased the expression of 69 miRNAs while the expression of 6 miRNAs was decreased (3.5 or 2% NPG encapsulated EDCs vs. adherent EDCs, fold change > 1.5, p-adjusted <0.05, Figure 9D, Supporting Information Table S4). These miRNAs typically clustered within ECM matrix biosynthesis, cell adhesion, fatty acid biosynthesis, Ras signalling, TGF- $\beta$  signaling, Hippo signaling, Wnt signaling, and stem cell pluripotency pathways (Supporting Information Figure S11). Increasing cocoon NPG content altered the expression of 8 miRNAs (fold change >1.5; p-adjusted <0.05, Figure 9E and Supporting Information Table S5) involved in the promotion of cell adhesion, cell cycle re-entry, TGF- $\beta$  signaling, Hippo signaling and maintenance of stem cell pluripotency (Supporting Information Figure S12). This data suggests that, while NPG encapsulation promotes a rejuvenated migratory miRNA expression profile, increasing NPG content boosts both the production and pro-survival profile of EDC sourced nanovesicles.

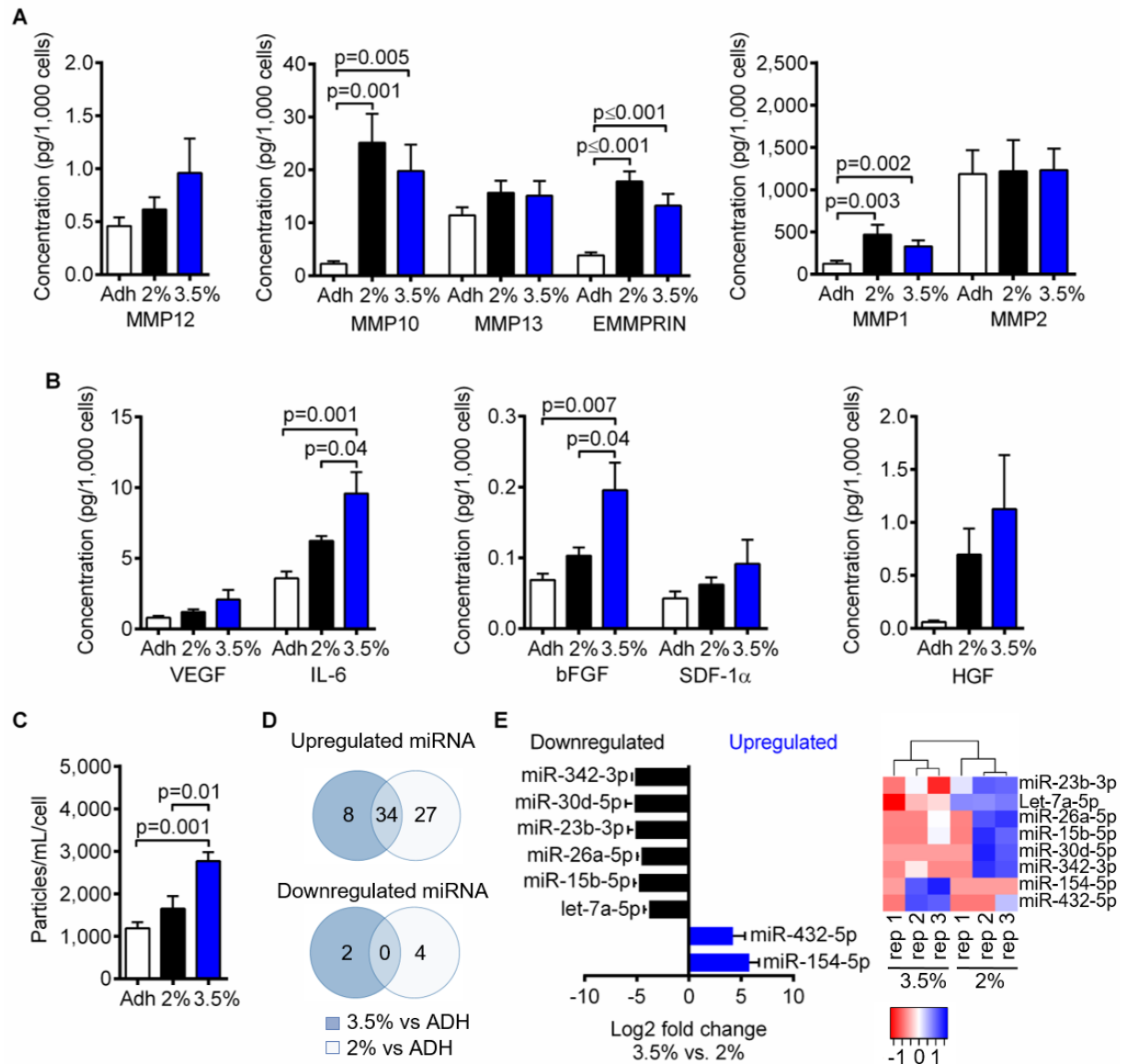


**Figure 9. Paracrine profiling of nanoporous gel encapsulated EDCs.** (A) MMP and EMMPRIN secreted into conditioned media was obtained from adherent (Adh), 2% and 3.5% NPG encapsulated EDCs after 48h of culture in hypoxic conditions (1% oxygen). Magnetic Luminex Performance Assay was used to quantify protein concentration. Protein concentration was standardized to the number of cells (n=9 biological samples with 3 technical replicates each). (B) The amount of secreted cytokines and growth factors

was measured in conditioned media (n=5). Fibroblast growth factor (FGF); Hepatocyte growth factor (HGF); Interleukin (IL); Vascular endothelial growth factor (VEGF); stromal cell-derived factor (SDF). (C) Number of exosome nanovesicles secreted into conditioned media quantified using particle-tracking analysis (Nanosight; n=5). (D) Venn diagram showing the number of up and downregulated miRNA present in nanovesicles isolated from cocooned (3.5 and 2% NPG capsules) and non-encapsulated EDCs. (E) Left: Up and downregulated miRNAs in nanovesicles isolated from 3.5% NPG encapsulated EDCs compared to 2% NPG encapsulation (n=3). Right: Heat map showing hierarchical clustering of differentially expressed miRNA between EDCs cocooned in 2 and 3.5% NPG capsules. Colour scale at bottom shows relative expression level of miRNA; blue= upregulation; red= downregulation. All error bars correspond to standard error mean SEM.

### 3.3 Conclusion

Encapsulation of EDCs within NPG cocoons boosts acute and long-term retention of cells after intra-myocardial injection into a clinically relevant mouse model that mirrors post infarct healing. Increasing NPG content improves cell viability and cell-mediated repair of ischemic myocardium by expanding both the production and pro-healing signature of transplanted cells. Akin to our animal model, patients with a myocardial infarct undergoing cell therapy will benefit from the enriched paracrine signature provided by encapsulation of EDCs in dense NPG cocoons.

The strategy presented here provides a simple method of regulating stem cell function compared to other less clinically applicable methods like genetic manipulation of cells. As such, our NPG encapsulation method is not just restricted just to cardiac applications, but it has the potential to be optimized and applied to other areas of regenerative medicine.

### **3.4 Methods**

#### **3.4.1 Patients and Cell Culture**

Human EDCs were cultured from atrial appendages obtained from patients undergoing clinically-indicated surgery using established methods<sup>80,264,286,296</sup> under a protocol approved by the University of Ottawa Heart Institute Research Ethics Board. Briefly, the atrial tissue was minced, digested and plated in standard media (Iscove's Modified Dulbecco's Medium, 20% Fetal Bovine Serum, 100 U/ml penicillin, 100 µg/ml streptomycin, 2mmol/l L-glutamine and 0.1 mmol/l 2-mercaptoethanol (all from ThermoFisher). Cells were collected using mild enzymatic digestion (TrypLE, ThermoFisher) every 7 days for 4 weeks. To limit possible experimental variation attributable to differences in the regenerative potency of individual cell lines, all cell lines were used in parallel as controls or experimental groups. As shown in the Supporting Information Table S6, the donor cohort was largely non-diabetic with good glycemic control (HbA1c =6.2±0.3) and several patient comorbidities (Long Term Stratification for survivors of acute coronary syndromes score =7.0±1.3) that directly reflect the population potentially in need of future cell therapy.<sup>296,307</sup> All experimental evaluations were conducted and analyzed by individuals blinded to treatment allocation.

EDC adherent or suspension culture was performed in fibronectin or Poly-HEMA (2-hydroxyethyl methacrylate) coated cultureware (ThermoFisher). Integrin neutralizing experiments were performed after pre-treating EDCs with integrin  $\alpha$ 3 (MAB1952P, EMD Millipore), integrin  $\alpha$ V (ab16821, Abcam), integrin  $\beta$ 1 (ab24693, Abcam) and integrin  $\beta$ 3 (ab78289, Abcam) blocking antibodies. A colorimetric WST-8 assay (Dojindo) was used to evaluate metabolic activity. Trypan blue exclusion was used to identify cell death (Sigma-Aldrich).

### **3.4.2 Nanoporous Gel Encapsulation**

Cells were encapsulated as previously described.<sup>264,265</sup> Briefly, human EDCs were suspended in media and mixed with low melt agarose at variable concentrations, human fibronectin and human fibrinogen as indicated (all from Sigma-Aldrich); the liquified agarose/ECM mix was added to the cells at a 2:1 ratio. To form capsules, the cell/nanoporous gel mixture was added to agitated dimethylpolysiloxane (Sigma-Aldrich) prior to rapid cooling. The mixture was then centrifuged and capsules were filtered from the coalesced NPG using a 100 $\mu$ m filter (Fisher Scientific) and were re-suspended in appropriate media for testing. In this report, we elected to compare NPG capsules of 2.0 and 3.5% (weight/volume) agarose with equivalent ECM content; a decision rationalized by prior work demonstrating marked effects of variable NPG content on the time of EDC emergence from the capsule and clear evidence underscoring the ability of 3.5% NPG capsules to promote EDC-mediated repair of ischemic myocardium.<sup>264</sup> Capsule sizes were estimated from measuring the diameter of individual capsules using a JuLI digital microscope. Briefly, samples were placed onto a glass slide and covered with a coverslip using 200  $\mu$ m plastic spacers. Reported values correspond to the average of three

independent batches, each measured by triplicated with >100 individual particles were measured in all cases.

### **3.4.3 Low Temperature Scanning Electron Microscopy, Atomic-Force Microscopy, Transmission Electron Microscopy, and Z-Stack Confocal Microscopy**

Capsule pore sizes were measured using scanning electron microscopy (SEM). The samples were prepared by delivering 50  $\mu\text{l}$  of the capsules suspensions (2.0 or 3.5% NPG) onto aluminum stubs covered with a carbon coating. The samples were dried under vacuum for 48h and then coated with a 5.0 nm electro-generated ultrapure gold using a low vacuum coater Leica EM-ACE200. The samples were imaged by using the secondary emission detector in a JSM-7500F FESEM from JEOL Inc., operating at 5.0 kV. Pore sizes from the capsules surfaces were measured using ImageJ software<sup>308</sup> from measuring >100 individual pores from different areas in the grid, similar to the description for determining material porosity for other materials.<sup>309</sup>

An Alpha 300 Raman/AFM microscope (WITec, Germany) was used to carry out Atomic Force Microscopy (AFM) measurements using Digital Pulsed Force Mode (DPFM). Samples for the capsules (with or without ECM) were prepared as described for SEM experiments (see above). For each condition, three (5x5)  $\mu\text{m}^2$  DPFM images were obtained with a cantilever characterized by a tetrahedral tip (tip radius  $\sim 10$  nm), a resonance frequency of 75 kHz and a nominal spring constant of 2.8 N/m (Arrow<sup>TM</sup> FM Nanoworld, Switzerland). Set point and amplitude ranged between 1-2 V and 3-6 V, respectively, with a frequency of 1000 Hz. Selected DPFM curves were converted from deflection [V]-phase [ $^\circ$ ] into force [N]-displacement [nm] according to a previously published procedure.<sup>310</sup> From these curves, the stiffness was calculated ( $\mu\text{N/m}$ ). At least

45 independent points from three images were randomly selected to calculate the stiffness values.

To observe EDC morphology within capsules of varying NPG composition, samples were first fixed overnight in a primary fixative (2.5% glutaraldehyde in 0.1M cacodylate buffer (pH 7.4), at 4°C. Following primary fixative, the samples were washed in cacodylate buffer and then placed for 2 hours in a post fixative solution (2% OsO<sub>4</sub> in 0.1M cacodylate buffer). After washing in cacodylate buffer the samples were dehydrated in a series of (acetone and remove) ethanol, transferred to acetone, and then embedded in Spurr's resin. Ultra-thin sections mounted on formvar coated grids were stained with 2% alcoholic uranyl acetate followed with Reynold's lead citrate and examined with a transmission electron microscope (Jeol JEM-1230, Japan). Membrane protrusions extending from cell surface were quantified (ImageJ; Supporting Information Figure S2E). Given that membrane protrusions (similar density to the cytoplasm) may appear as non-contiguous structures with the cell membrane as they orientate in space while being captured within ultra-thin cell sections used for electron microscopy, structures not contiguous with the cell membrane having average diameter less than 100 nm or more than 1000 nm from the cell surface were excluded.<sup>311,312</sup>

To confirm that cells were completely within the NPG cocoons, z-stack images were acquired using a 63X oil objective lens on the Zeiss LSM 880 confocal microscope. Briefly, EDCs labeled with calcein-AM were cocooned in NPG containing DsRed labeled fibrinogen (ThermoFisher), fixed using 4% paraformaldehyde (Alfa Aesar) and DAPI stained for nucleus. For imaging, z-stacks were acquired with slice thickness of 1 µm, for

a total of 104 slices, and were reconstructed into a 3-dimensional image using ZEN 2.3 (blue edition) software.

#### **3.4.4 Immunohistochemistry**

The effects of NPG encapsulation on proliferation and apoptosis was evaluated by staining for Ki-67 (ab15580; Abcam) or caspase-3 (mAb9664; Cell Signaling Technology), respectively. Images were acquired using Zeiss Axio Observer A1 microscope and analyzed in AxioVision Version 4.8. Incorporation and migration of fibrinogen within capsules was evaluated by including DsRed labeled fibrinogen (ThermoFisher) during encapsulation. The effects of NPG encapsulation on the cytoskeleton re-arrangements was evaluated by staining cells for actin (Phalloidin conjugated to Alexa Fluor 488; ThermoFisher). Images were acquired using Olympus IX81 confocal microscope and analyzed using FluoView10-ASW Version 4.2. For all quantitative analysis, 5 random fields from a minimum of 3 cell lines were counted.

#### **3.4.5 Conditioned Media for Paracrine Profiling**

Conditioned media was obtained after 48 hours of culture in 0.5% serum 1% oxygen– conditions designed to mimic ischemic myocardium. Conditioned media used to profile exosome production/identity was generated using exosome depleted serum (ThermoFisher). Matrix metalloproteinase (MMP) and cytokine content were profiled on a Bio-Plex 200 system (Bio-Rad Technologies) using custom Luminex Procarta Immunoassay kits (Affymetrix, CA, USA).<sup>286</sup> All immunosorbent measures were normalized to the number of plated cells and media volume. Nanovesicles were isolated from a separate aliquot of conditioned media using ExoQuick-TC polymer-based exosome precipitation (System Biosciences). Nanovesicle content was quantified using

Nanoparticle Tracking Analysis (Nanosight V2.3). Nanovesicle miRNA content was profiled and analyzed using multiplex fluorescent oligonucleotide-based miRNA detection (Human v3, Nanostring). Briefly, total RNA was extracted using miRNeasy Micro Kit (QIAGEN) and RNA quantity and quality was assessed using Nanodrop (ThermoFisher) and Agilent 2100 Bioanalyzer (Agilent). A total of 25ng of RNA was loaded for each reaction using nCounter Human V3 miRNA Expression Assay. Prior to differential gene expression analysis, data was imported into nSolver for image quality control metrics, as described by manufacture. No data was flagged for percent field of view (FOV) less than 75% and, binding density of samples ranged between 0.05-2.25. Background subtraction on the data was performed using the mean of negative controls plus two standard deviation. The counts were then normalized using trimmed-mean of M values (TMM)<sup>313</sup> and differentially expressed miRNA were identified using the generalized liner model (GLM) likelihood-ratio-test<sup>314</sup> using EdgeR in the online DEBrowser tool (<https://debrowser.umassmed.edu/>). Heat map was created in DEBrowser tool using the “complete” clustering method.

### **3.4.6 Migration Assays**

Cocooned or non-cocooned EDCs were plated directly on a fibronectin coated 8 $\mu$ m pore plate (Essen BioScience) at a density of 1200 cells per well in 0.5% serum and 1% oxygen media. Cell migration to a chemoattractant (20% serum media) was imaged every hour (IncuCyte ZOOM, Essen BioScience). To account for passive transwell migration, cell counts were normalized to basal media condition and exponential curve fitting was used to determine the cell migration rates.

Quantification of 2D-cell migration was performed using live cell imaging with cells placed into a matrigel coated cultureware and allowed to grow in 1% O<sub>2</sub> containing 0.5% serum media. Images were taken every 45mins, and cells were manually tracked in ImageJ software.<sup>315</sup> Cells were tracked for entirety of the experiment unless the cell could not be tracked due to either clustering with other cells or hidden under the capsules. Cell tracking less than 8 frames were discarded.

### **3.4.7 Myocardial Infarction, Cell Injection, and Functional Evaluation**

The effect of NPG capsule composition on human EDC retention and post infarct repair was investigated in a series of male non-obese diabetic severe combined immunodeficient (NOD SCID, Charles River) mice (6-8 weeks old, average weight of 23±2g) under a protocol approved by the University of Ottawa Animal Care Committee. Animals were injected with buprenorphine, sustained-release formula (1.2 mg/kg; subcutaneous) and meloxicam (0.2 mg/kg) 1 hour prior to surgery, and then meloxicam once daily thereafter for 2 more days. All animals underwent surgical ligation of the left coronary artery (LC). During surgery and echocardiographic assessment, mice were anesthetized with isoflurane (2-3%), intubated (not intubated for echos) and maintained under physiologic temperature control (37°C). Immediately after surgery, animals were placed in a 30°C incubator with supplemental oxygen and moistened food to recover. Once animals returned to physiological state, they were returned to their normal holding room. All animals were housed in Techniplast ventilated cages with at least bi-weekly cage changes and were given food and water ad libitum. The food is supplied by Envigo (irradiated #2019 extruded chow) and the water is autoclaved and prepared on site. The overhead lighting in the holding room was alternated every 12 hours between light and

dark cycles. A University of Ottawa Animal Care Technician monitored animals at least twice daily for 3 days post surgery and then at least once per day until the end of the study. One week after LC ligation, mice were randomized to receive echocardiographic guided injection of 100,000 EDCs in suspension, 100,000 EDCs encapsulated in 2% NPG, 100,000 EDCs encapsulated in 3.5% NPG, empty 2% and 3.5% NPG capsules or an equivalent volume of saline. The effect of cell therapy on cardiac function was evaluated in the remaining animals using echocardiography (VisualSonics V1.3.8, VisualSonics) 14 and 21 days after cell or vehicle injection. At the end of the study, mice were sacrificed by cervical dislocation once the animal were anesthetized (2-3% isoflurane anesthesia) and displayed absence of withdrawal reflex to toe pinch. Investigators were blinded to animal's treatment group when conducting experiments and analyzing data.

The myocardial retention of transplanted cells was assessed 1 and 21 days after cell injection in a random subset of mice using quantitative polymerase chain reaction (qPCR) for non-coding human alu repeats <sup>286,295,297</sup>. The left ventricle was excised, weighed and homogenized to extract genomic DNA (DNeasy kit; Qiagen) for performing qPCR using transcript specific hydrolysis primer probes (Primer 1: 5'-GCCTCAGCCTCCCGAGTAG-3'; Primer 2: 5'-CATGGTGAAACCCCGTCTCTA-3'; Probe: 5'-56-FAM ATTAGCCGG/ZEN/GCGTGGTGGCG-31ABkFQ-3', Integrated DNA Technologies). To determine the absolute number of cells, a standard curve was generated by making a serial log dilution of human genomic DNA extracted from EDCs spiked with mouse genomic DNA extracted from ventricular lysates. To account for the

difference in heart size, the number of engrafted EDCs was expressed as cells per mg of myocardial tissue.

### **3.4.8 Histology**

After the final assessment of myocardial function, the remaining hearts were excised, fixed with 4% paraformaldehyde, embedded in optimal cutting temperature compound and sectioned. Tissue viability within the infarct zone was calculated from Masson's trichrome; lung tissue, pericardium, and pooled blood in the ventricles were carefully removed prior to quantification using Image J.<sup>264,286,295-297</sup> Infarct vascularization was evaluated using isolectin B4 (B-1205, Vector Laboratories).

To evaluate the effects of encapsulation on endogenous repair, a series of NOD SCID mice were injected with 5-bromo-2'-deoxyuridine (BrdU; 100 mg/kg intra-peritoneal; ThermoFisher) once daily for 7 days after intra-myocardial injection of EDCs or vehicle. Twenty-one days after EDC or vehicle injection, mice were sacrificed, and hearts were sectioned for immunohistochemical analysis of BrdU (ab6326; Abcam) co-segregation with cTnT.

### **3.4.9 Statistical Analysis**

All data is presented as mean  $\pm$  SEM. To determine if differences existed within groups, data was analyzed by a one or two-way ANOVA, as appropriate. In all cases, variances were assumed to be equal and normality was confirmed prior to further post-hoc testing. If differences existed, Sidak's or Tukey's corrected t-test was used to determine the group(s) with the difference(s) (Prism v6). Differences in categorical

measures were analyzed using Fischer's exact test. A final value of  $P \leq 0.05$  was considered significant for all analyses.

## Chapter 4

### 4.0 Study 2: Enhanced Therapeutic Repair of Injured Myocardium by High-Throughput Microfluidic-Based Cocooning of Explant-Derived Cardiac Stem Cells

#### 4.1 Abstract

Encapsulation of explant-derived cardiac stem cells (EDCs) in micrometer nanoporous gel (NPG) based cocoons boosts therapeutic regeneration by abrogating detachment induced cell death and vascular clearance of cocooned cells. Previously, we have shown increasing NPG content improves cell viability and cell-mediated repair of ischemic myocardium by expanding both the production and pro-healing signature of transplanted cells. The impact of altering other modifiable cocoon properties, such as cocoon size or intracapsular cell number, on the regenerative potential of transplanted cells is unknown and represents the focus of this study. Increased cocoon size enhanced post-ischemic cardiac function by reducing clearance of transplanted cells and increased paracrine stimulation of endogenous repair. The latter being attributable to microfluidic cocooning closely following the expected Poisson distribution with smaller cocoons having a greater proportion of single cells while larger cocoons contained greater proportions of multicellular aggregates which enhanced cell-cell interactions to increase the amount of pro-healing cytokines delivered to injured myocardium. Thus, by altering cocoon size and occupancy using high-throughput microfluidics, the paracrine signature of encapsulated EDCs can be enhanced to promote greater endogenous repair of injured myocardium.

## 4.2 Results

### 4.2.1 Fabrication of Microfluidic Platform

The microfluidic (MF) chip platform consisted of: 1) two inlets, one for cell/NPG mix and the other for oil, 2) a nozzle, 3) a serpentine stage and 4) two outlets (Figure 10A; Supporting Figure S13). Up-front filtration within the inlet prevented micro-channel obstruction from cell and/or NPG clumping (Figure 10B). The cells/NPG mixture then entered a short serpentine mixing stage to align cells within the center of the micro-channel for sequential cocooning. Using an established flow-focused design,<sup>316</sup> two oil channels then joined the cell/NPG microchannel at a perpendicular angle (Figure 10A). Given the aqueous cell/NPG mixture is immiscible within oil, passage through the cylindrical nozzle moulded circular NPG droplets (cocoon) about the cells (Figure 10D). NPG cocoon size was defined a priori by varying nozzle diameter (30 or 50  $\mu\text{m}$ ) and the perfusion pressure ratio between the sample (cell/NPG) and oil micro-channels. To prevent temperature fluctuations that influence cocooning consistency and efficiency, inlet and nozzle temperatures were maintained at 37° Celsius. Cocooned cells then travelled within a 4° Celsius serpentine stage to ensure all cocoons completed gelation prior to collection (Figure 10A). Post hoc filtration within the outlet filter removed unwanted cocoon aggregates and ensured collection of uniform sized cocooned cells (Figure 10C). Throughout the experiments, this design provided consistent uniform cocoon production at throughput rates approximating 300,000 cells/second.

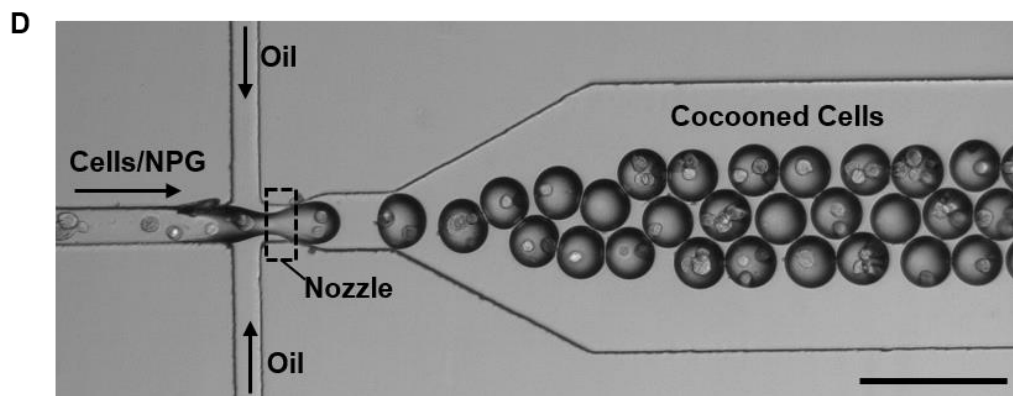
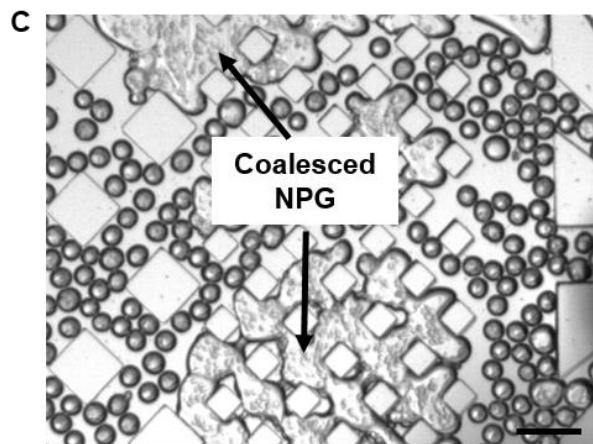
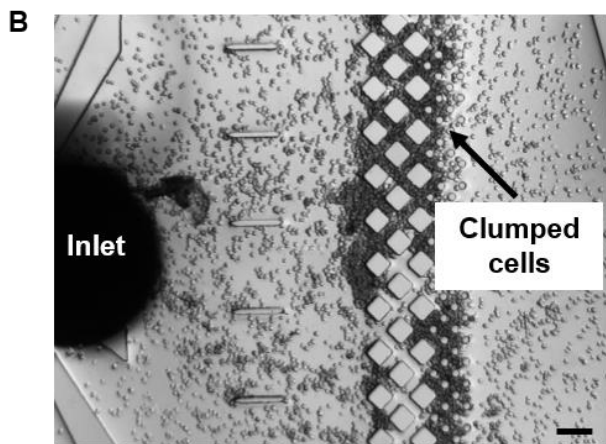
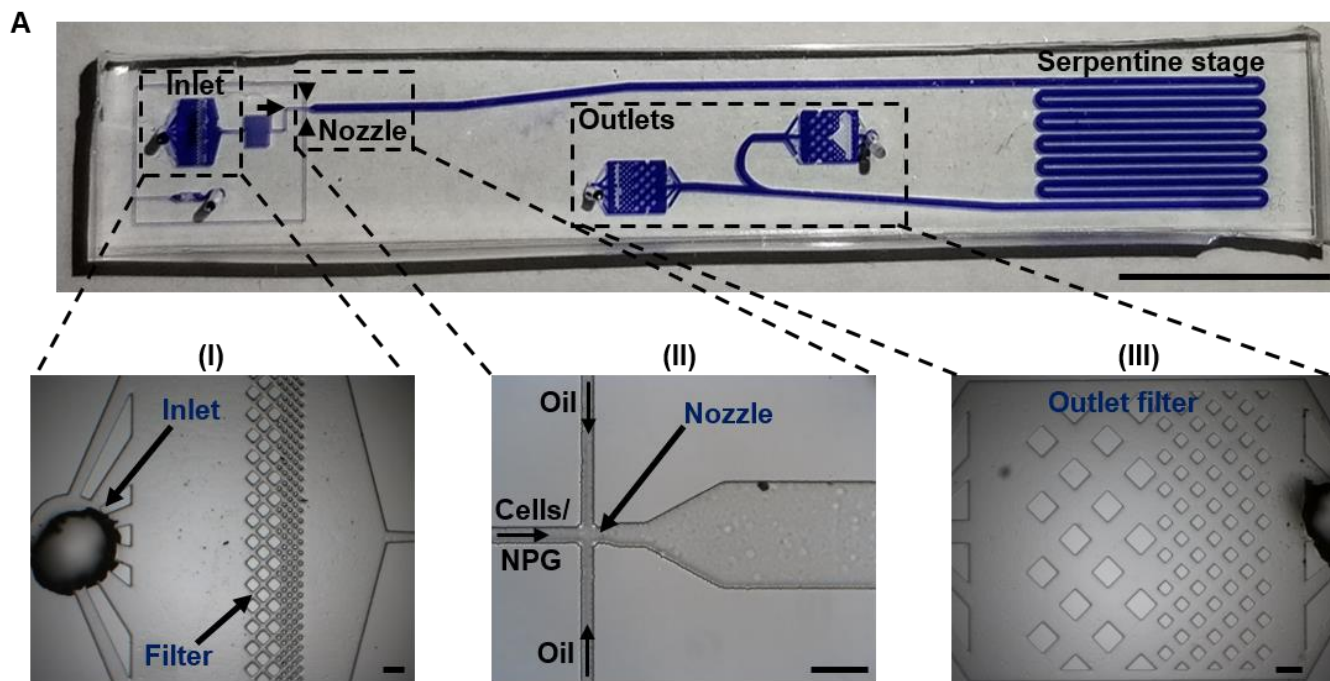


**Figure 10. Microfluidic schematics.** (A) Microfluidic chip filled with a blue dye within the aqueous (cells/NPG) stream to help visualize the micro-channels (scale bar 1 cm). The microfluidic chip is divided into four main regions, inlet, nozzle, serpentine stage, and outlet. Magnified images show (I) cell/NPG inlet filter, (II) nozzle and (III) outlet filter; scale bar 200  $\mu\text{m}$ . Arrow and arrow heads show direction of flow of cell/NPG and oil into the nozzle, respectively. (B) Debris and large cell clumps are trapped by the inlet filter; representative image taken ~30 minutes after starting encapsulation (scale bar 200  $\mu\text{m}$ ). (C) Representative image showing outlet filter trapping of large coalesced cocoons prior to collection (scale bar 200  $\mu\text{m}$ ). (D) Representative image demonstrating the formation of droplets (cocoons) at the nozzle as the cell/NPG mixture flows across two perpendicularly placed oil inlets (scale bar 200  $\mu\text{m}$ ). Depending on the cocoon size, the nozzle's width (dotted box) was changed to 30  $\mu\text{m}$  or 50  $\mu\text{m}$  (see methods).

#### 4.2.2 Characterization of Nanoporous Gel Cocooned EDCs

As previously shown,<sup>317</sup> vortex-based encapsulation (Vx) inherently provides cocoons of varying size (30-100  $\mu\text{m}$ ) that are normally distributed about the mean (67.5 $\pm$ 1.5  $\mu\text{m}$ ) with the upper limit capped after filtration through a 100  $\mu\text{m}$  pore filter to avoid adverse effects attributable to clumped biomaterials (Figure 11A). By varying micro-channel flow pressure ratios and nozzle diameters within the chip, MF-based encapsulation provided precise control over cocoon size with equivalent distribution of ECM proteins between cocoons (Supporting Figure S14A). Given that altering the physical properties of cocoons alters the ability of encapsulated cells to improve cardiac function, the influence of variable cocoon diameter on cells was explored by comparing

small ( $50.7 \pm 0.2 \mu\text{m}$ ) and large ( $90.1 \pm 0.2 \mu\text{m}$ ) with the standard Vx-defined ( $70.7 \pm 0.2 \mu\text{m}$ ) cocoon diameters (Figures 11A and B). Akin to Vx cocooning, the addition of cells did not alter cocoon size (Supporting Figure S14B). As shown in Figure 11C, MF increased the yield (proportion of cocooned cells divided by the total number of cells) of cocooned cells from  $32.5 \pm 1.8$  to  $71.5 \pm 3.0\%$  ( $p < 0.0001$  vs.  $70 \mu\text{m}$  MF diameter cocoons) with no effect seen when manufacturing different cocoon sizes ( $p > 0.20$  for MF capsule size). MF cocooning closely followed the expected Poisson distribution with smaller cocoons having a greater proportion of single cells while larger diameter cocoons contained greater proportions of multicellular aggregates (Figure 11D). The average cell occupancy of  $70 \mu\text{m}$  MF cocoons faithfully mirrored Vx cocoon occupancy ( $\sim 60\%$ ; Figure 11E). Very few cells ( $< 2\text{-}3\%$ ) escaped MF or Vx cocooning to be found as free cells within the cocooned cell suspension immediately after processing (Figure 11F). Both MF and Vx cocooning was well tolerated by cells as  $\approx 92\%$  of cells were viable 1 hour (Figure 11G) and over 48 hours (Figure 11H) after cocooning.

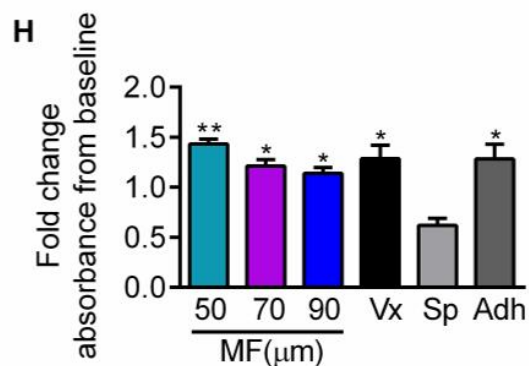
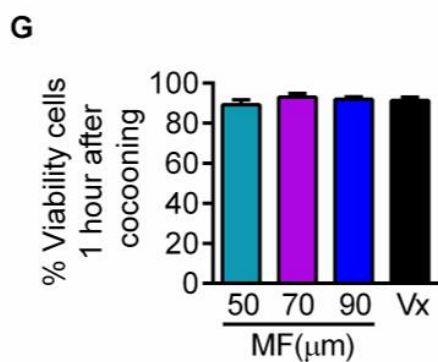
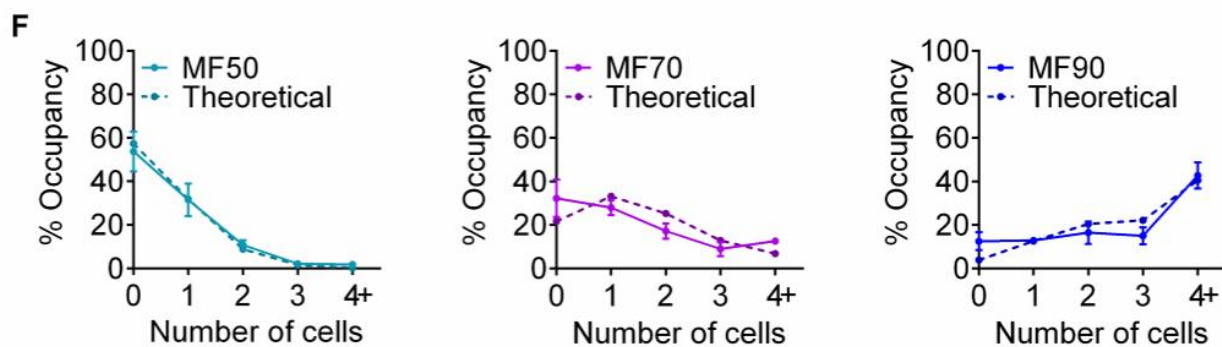
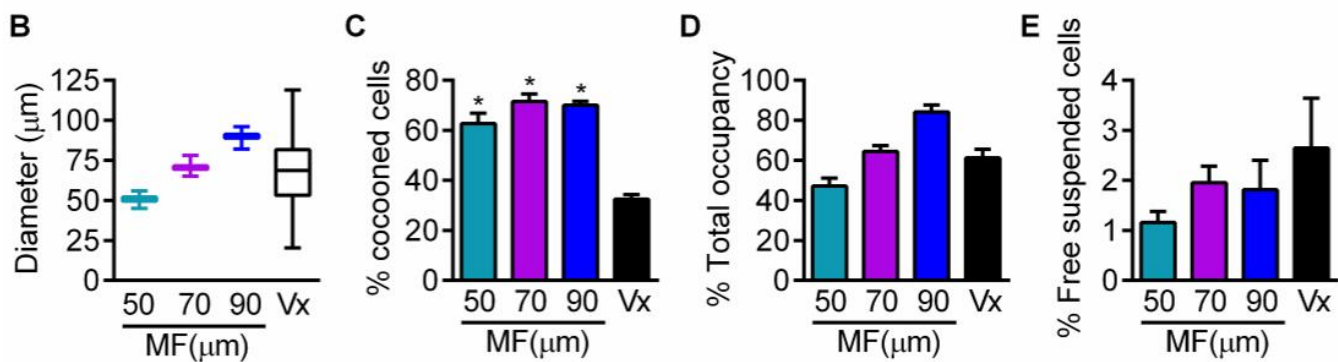
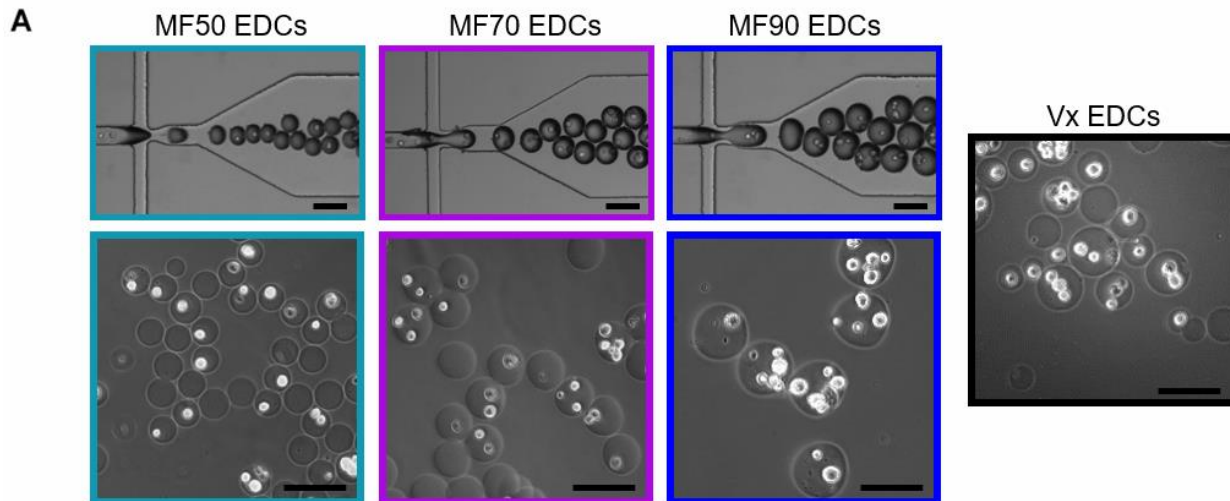


**Figure 11. Characterization of microfluidic nanoporous gel cocoons.** (A) Representative images showing microfluidic encapsulation of cells in NPG cocoons with 50, 70, 90  $\mu\text{m}$  diameter (top panels) and magnified images taken by confocal microscope (bottom panels). Confocal microscope image of Vx cocooned cells shown in the right image panel. (Scale bar 100  $\mu\text{m}$ ). (B) Box and whiskers plot showing the size distribution of MF and Vx cocooned EDCs. Size distributions were calculated from >100 individual cocoons using three independent samples. (C) Percent yield of MF or Vx cocooned cells (n=6; \*p<0.001 vs. Vx cocoons). (D) Plot showing the percentage of cocoons that are occupied with either 0, 1, 2, 3, or 4+ cells. The occupancy was calculated from measuring >200 individual cocoons using three independent samples. The measured occupancy (solid line) was compared to the theoretical values (dotted line) calculated by the Poisson distribution model. (E) Bar graph showing the percentage of cocoons occupied by cells (n=6). (F) The percentage of free suspended cells that are not cocooned after MF or Vx cocooning (n=6; p=0.42). (G) Quantification of viable (live/dead) cells 1 h after cocooning (n=3; p=0.48). (H) Colorimetric dehydrogenase activity assay demonstrating the effect of cocooning, adherent (Adh) and suspended (Sp) cell culture conditions on cell viability (n=4; \*p<0.05 and \*\*p<0.01 vs. Sp). Error bars correspond to standard error mean SEM.

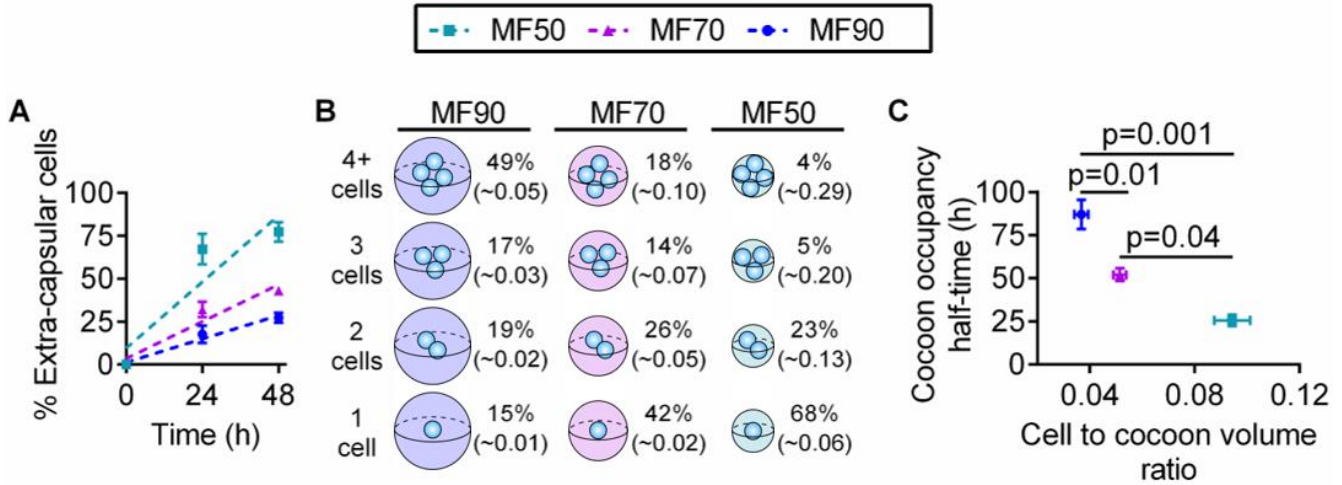


**Figure 12. Effects of cocoon size on cell migration and viability.** (A) EDCs were encapsulated with increasing cocoon size and grown on fibronectin-coated chamber slides within low serum (0.5% CEM) and 5% oxygen conditions. Random field images with were acquired using a confocal microscope at 10X magnification to count the number of viable EDCs inside and outside of the capsules at various time points (n=3). Viability of cells was assed using live/dead stain. For linear regression,  $R^2=0.80$ ,  $0.88$ , and  $0.82$  for MF50, 70, and 90, respectively. (B) Schematic showing the cell to cocoon volume ratio (ratio shown in brackets), and the percentage of cocoons containing either 1, 2, 3 or 4+ EDCs (n=3). The cell and cocoons are drawn to proportions. (C) Plot demonstrating that as the cocoon size decreased (*i.e.* increasing cell to cocoon volume ratio), cells escaped cocoons quicker (*i.e.* decreased occupancy half-time) (n=3). Error bars correspond to standard error mean SEM.

### **4.2.3 Effects of Nanoporous Gel Encapsulation on Cell Migration and Viability**

Given the impact of biomaterials on the kinetics of cell delivery within injured tissue<sup>318-320</sup>, the influence of cocoon size on cell egress was evaluated. As shown in Figure 12A and Supporting Figure S15, increasing cocoon size delayed the time needed for cells to emerge and adhere to the cultureware. Linear curve fitting of cell migration as a function of time from cocoon enclosure revealed that increasing cocoon size increased the occupancy half-time (*i.e.* time needed for half the cells to emerge from the cocoons) from  $26 \pm 3$  h to  $52 \pm 4$  h or  $87 \pm 8$  h for MF50, MF70 and MF90, respectively ( $p < 0.05$  MF50 vs. all). Greater disparity in the ratio of cell(s) to cocoon volumes was seen in larger diameter cocoons (Figure 12B and C) making it unsurprising that more time was needed for cells to extravasate through the thicker NPG cocoon shell. Reassuringly, and in keeping with previous reports,<sup>279</sup> increasing cocoon size had no effect on cell viability up to 48 hours after encapsulation obviating concerns regarding the effect of increased cocoon diameters on molecular diffusion and exchange ( $p > 0.34$  for effect of cocoon diameter on cell viability 1, 24 and 48 hours after cocooning).

### **4.2.4 Effects of Altered Nanoporous Gel Capsule Size on Cell Retention and Myocardial Repair**

The impact of cocoon size on cell-mediated repair was explored using an established preclinical model of ischemic myocardial injury.<sup>136,214,296,317</sup> As shown in Figure 13A, immunodeficient mice underwent left coronary artery (LCA) ligation 1 week before randomization to echocardiographic guided intra-myocardial injection of EDCs (suspended or variable diameter cocoons) or vehicle. All animals had comparable echocardiographic left ventricular chamber dimensions and ejection fractions at the time

of cell or vehicle injection (Supporting Table S7). Three weeks after intra-myocardial injection, animals that receive vehicle alone underwent progressive adverse ventricular remodeling whereas all animals treated with EDCs had better myocardial function ( $p < 0.0001$  vs. vehicle; Figure 13B and Supporting Figure S16). Interestingly, EDCs encapsulated within 90  $\mu\text{m}$  cocoons achieved the greatest improvement in left ventricle ejection fraction (LVEF;  $+12 \pm 1\%$  from baseline,  $p < 0.001$  vs. vehicle, suspended or cocooned EDCs). While histological analysis confirmed that all animals treated with either EDCs had smaller ventricular scars 3 weeks after cell treatment ( $p < 0.0001$  vs. vehicle; Figure 13C and Supporting Figure S17), the greatest reduction in scar burden was seen in animals treated with MF90 cocooned EDCs ( $p < 0.05$  vs. all groups). Similarly, more viable tissue within the infarct region ( $p < 0.05$  vs. all groups; Figure 13D) and greater vessel density within the peri-infarct region ( $P < 0.05$  vs. all groups; Figure 13E and Supporting Figure S18) was seen in animals that received MF90 cocooned EDCs.

To determine the effects of transplanted cells on the generation of new cardiomyocytes within the peri-infarct region, all mice received daily intra-peritoneal injections of bromodeoxyuridine (BrdU) for 1 week after cell or vehicle injection. As shown in Figure 13F and Supporting Figure S19, animals that received MF90 EDCs demonstrated greater overall and cardiomyocyte proliferation compared to animals that received MF50, MF70, or suspended EDCs.

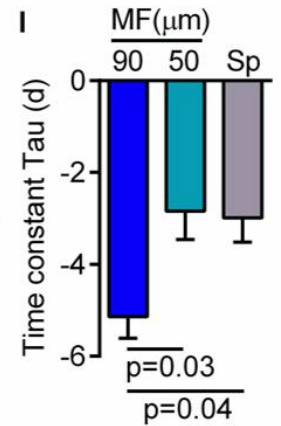
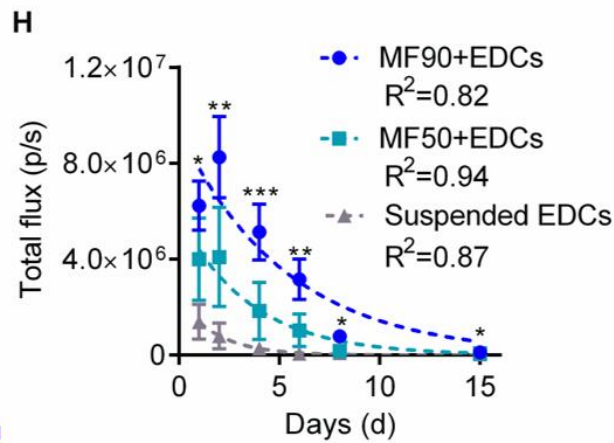
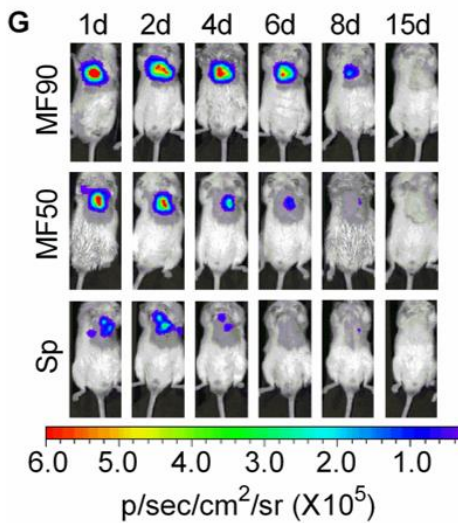
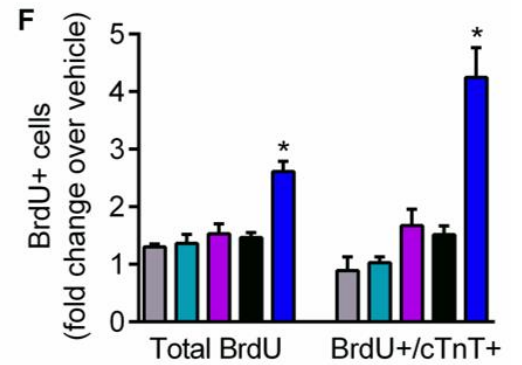
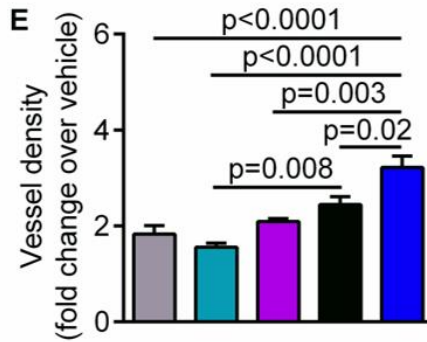
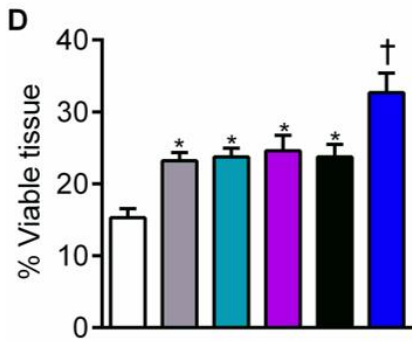
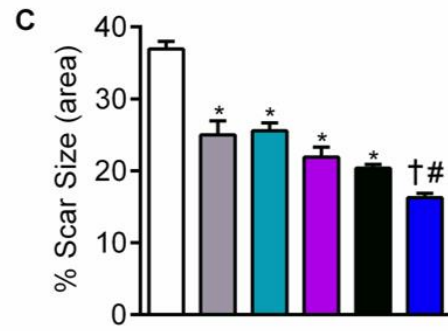
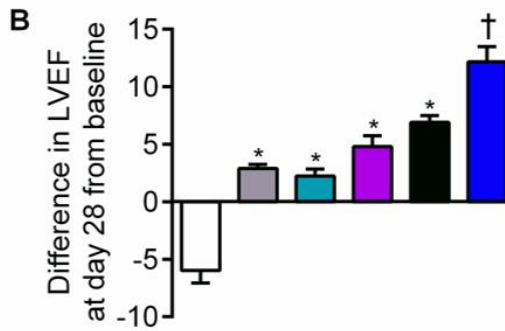
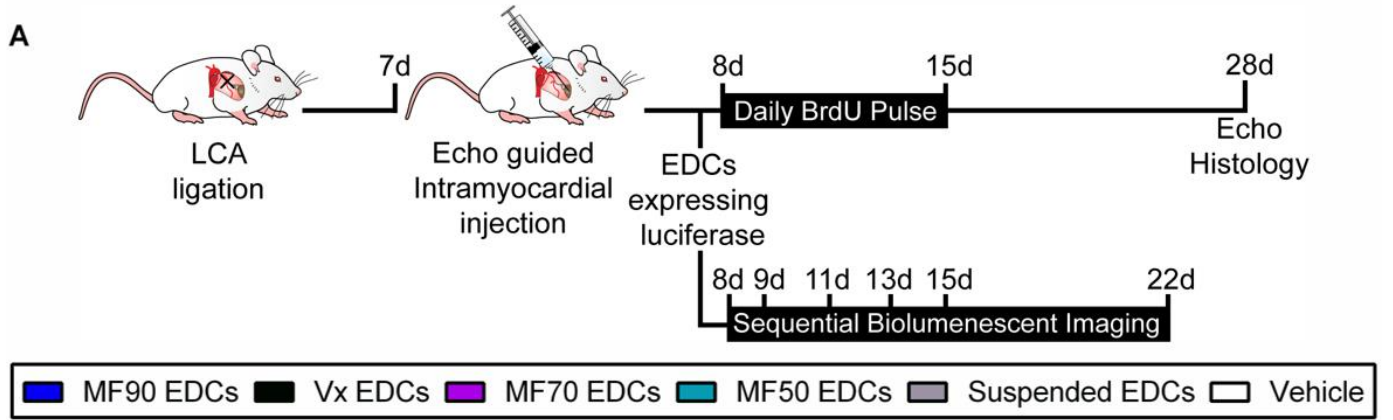


**Figure 13. Effects of changing cocoon size on EDC engraftment and myocardial repair.** (A) Schematic summary of animal study. In a subset of animals, transgenic EDCs expressing firefly luciferase were tracked *in vivo* using bioluminescent imaging. LCA = left coronary artery ligation. (B) Echo analysis showing the difference between left ventricle ejection fraction at day 28 and baseline (day 7) (n=8-10 mice/cell and saline (vehicle) treated group; \*p<0.0001 vs. vehicle, †p<0.001 MF90 vs. all groups). (C) Quantification of percent scar size using masson trichrome stained section (n=5; \*p<0.0001 vs. vehicle, †p<0.05 MF90 vs. MF70, #p<0.001 MF90 vs. MF50 or suspended group). (D) Quantification of percentage of viable tissue within the infarct region (n=5; \*p<0.05 vs. vehicle, †p<0.05 MF90 vs. all groups). (E) Isolectin b4 staining used to quantify vessel density within infarct region (n=5). Graph represented as a fold change over vehicle control group. (F) Graph showing the total number of proliferating cells (BrdU+) or cardiomyocytes (BrdU+/cTnT+) in the infarct/peri-infarct regions (n=5; \*p<0.0001 vs. all). Random field images were acquired using an inverted fluorescent microscope at high power field (40X objective lens). Graph represented as fold change over vehicle control group. (G) Representative bioluminescent images over time showed significantly reduced clearance for MF90 cocooned EDCs. Quantification of bioluminescent intensity over time (n=4-5; \*p<0.05, \*\*p<0.01, \*\*\*p<0.001 MF90 vs. MF50 or suspended group). (I) Exponential curve fitting analysis was used to determine the time constant Tau. Larger negative Tau value corresponds to slower clearance of EDCs from the heart (n=4-5). Error bars correspond to standard error mean SEM.

*In vivo* bioluminescent imaging of transplanted luciferase labelled EDCs was used to evaluate the effect of increasing cocoon size on the kinetics of transplanted cell retention. As shown in Figure 13G and H, encapsulation within larger cocoons increased acute cell retention ( $2.5 \pm 1.1$  and  $10.5 \pm 4.7$  folds greater vs. MF50, and suspended EDCs respectively at day 1;  $p < 0.05$  MF90 vs. all). Exponential fitting of bioluminescent flux from luciferase tagged cells as a function of time following cell injection revealed that large 90  $\mu\text{m}$  capsule diameters also reduced the rate of cell clearance (smaller cell clearance constant) from injured tissues ( $p < 0.05$  vs. suspended or MF50 cells; Figure 13I).

#### **4.2.5 Effects of Cell-Cell Contact on Paracrine Profile**

Given the importance of cell-cell contact in regulating paracrine secretion,<sup>321,322</sup> the effects of abrogating these interactions on the cytokine profile in conditioned media was characterized using a proteomic array. Cell-cell contact between EDCs in MF90 cocoons was blocked using an antibody cocktail to block E/P-selectin and N-cadherin without effecting cell viability (Figure 14A). As shown in Figure 14, blocking cell-cell interactions (+Block) decreased the secretion of FGF-19, HGF, and SDF-1 $\alpha$  which are previously shown to promote cardiac repair ( $7.2 \pm 2.1$ ,  $2.1 \pm 0.1$ , and  $1.6 \pm 0.1$  fold decrease for MF90 - block vs. +block,  $p = 0.04$ ,  $p = 0.01$ , and  $p = 0.02$ , respectively).<sup>212,215,323</sup> Interestingly, abrogating cell-cell contact also enhanced the proinflammatory cytokine profile known to negatively effect cardiac remodeling *e.g.* ENA-78, IFNG, IL-6, IL-8, MCP-1, PTX3, and Serpin E1.<sup>324-328</sup> This data suggests that multicellular aggregates in large cocoons enhances cell-cell interactions to increase the amount of pro-healing cytokines delivered to injured myocardium.

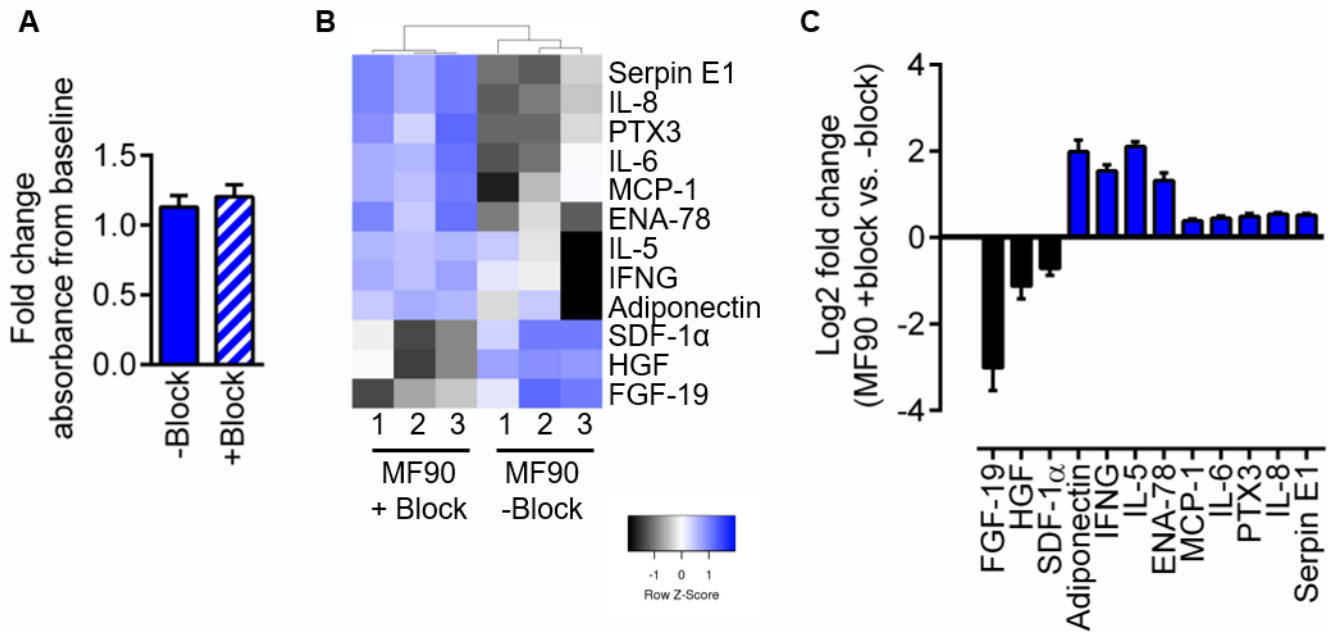


**Figure 14. Effects of cell-cell interaction on cytokine profile.** (A) Colorimetric dehydrogenase activity assay demonstrating that blocking cell-cell contact using anti-E/P-selectin and anti-N-cadherin antibodies (+Block) did not affect cell viability (n=3). (B) Heat map showing hierarchical clustering of differentially expressed cytokine in condition media (48h of culture in 1% O2 and 0.5% serum) between MF90 cocooned EDCs with and without blocking antibodies (n=3). Colour scale shows relative expression level of cytokines; blue= upregulation; black= downregulation. (C) Graph represents Log2 fold change between differentially expressed cytokines present in condition media from MF90 cocooned EDCs with and without blocking antibody (p<0.05 for +Block vs. -Block; n=3). Cocooned EDCs lacking cell-cell contact decrease secretion of pro-healing cytokines (e.g. FGF-19, HGF, SDF-1 $\alpha$ ) while increasing pro-inflammatory cytokines (e.g. IL-8, ENA-78, IL-5, MCP-1). All error bars correspond to standard error mean SEM. ENA= epithelial-derived neutrophil-activating peptide; IFNG= Interferon gamma; IL= Interleukin; MCP= monocyte chemoattractant protein; PTX3= Pentraxin 3.

### **4.3 Conclusion**

In this study, we engineered a MF device to produce large quantities of encapsulated EDCs in NPG cocoons with precisely defined size, and cell occupancy. Cocooned EDCs were transplanted intramyocardially into clinically relevant NOD SCID mice that modelled ischemic cardiomyopathy. Enlarging the cocoon size increased the intracapsular cell number, and enhanced cell-mediated repair of ischemic myocardium by providing greater stimulation for blood vessel growth and endogenous cardiomyocyte proliferation. Although large cocoons boosted cell engraftment, this effect alone could not account for the improved cardiac gains. Instead, larger cocoons likely promoted greater number of cell-cell interactions that boosted EDC's paracrine repertoire to promote cardiac healing.

### **4.4 Methods**

#### **4.4.1 Patients and Cell Culture**

Human EDCs were cultured from atrial appendages obtained from patients undergoing clinically-indicated surgery using established methods<sup>80,264,329,330</sup> under a protocol approved by the University of Ottawa Heart Institute Research Ethics Board. Briefly, the atrial tissue was minced, digested and plated in standard cardiac explant media (CEM) containing Iscove's Modified Dulbecco's Medium, 10% Fetal Bovine Serum, 100 U/ml penicillin, 100 µg/ml streptomycin, 2mmol/l L-glutamine and 0.1 mmol/l 2-mercaptoethanol (all from ThermoFisher). Cells were collected using mild enzymatic digestion (TrypLE, ThermoFisher) every 7 days for 4 weeks; trypan blue exclusion was used to identify cell death (Sigma-Aldrich). To limit possible experimental variation

attributable to differences in the regenerative potency of individual cell lines, all cell lines were used in parallel as controls or experimental groups. As shown in the Supporting Information Table 8, the donor cohort was largely non-diabetic with good glycemic control (HbA1c=  $6.2 \pm 0.3$ ) and several patient comorbidities (Long Term Stratification for survivors of acute coronary syndromes score=  $6.3 \pm 0.8$ ) that directly reflect the population potentially in need of future cell therapy.<sup>307,330</sup> All experimental evaluations were conducted and analyzed by individuals blinded to treatment allocation.

EDC adherent or suspension culture was performed in fibronectin or Poly-HEMA (2-hydroxyethyl methacrylate) coated cultureware (ThermoFisher). To compare cell growth overtime, the metabolic activity of cell was measured using colorimetric WST-8 assay (Dojindo).

#### **4.4.2 Vortex Encapsulation**

Cells were encapsulated as previously described.<sup>264,265</sup> Briefly, human EDCs were suspended in media and mixed with low melt agarose human fibronectin and human fibrinogen (all from Sigma-Aldrich). To form capsules, the cell/NPG mixture was added to agitated dimethylpolysiloxane (Sigma-Aldrich) prior to rapid cooling. The mixture was then centrifuged and cocoons were filtered from the coalesced NPG using a 100  $\mu\text{m}$  filter (Fisher Scientific) and were re-suspended in appropriate media for testing. In this report, we used NPG cocoons of 2.5% (weight/volume) agarose with 0.15 mg/ml of fibrinogen and 0.25 mg/ml fibronectin. We elected to use an NPG agarose concentration of 2.5% w/v to maximize cocoon stiffness (a decision rationalized by prior work demonstrating stiffer cocoons enhance EDC pro-healing paracrine profile) and minimize clogging of the inlet filters and microfluidic channels. The liquified agarose/ECM mix was add to the cells

at a 2:1 ratio. Cocoon diameter was measured using a digital microscope (VWR). Briefly, several images were taken every 10 mins within the microfluidic device to calculate the average cocoon diameter using Image J software; >200 cocoons were measured from at least three independent batches.

#### **4.4.3 Microdevice Design and Fabrication**

A microfluidic device for cell encapsulation was developed as shown in (Supporting Information Figure S13). The polydimethylsiloxane (PDMS) based platform consisted of two inlets, two outlets, a nozzle (where the cocoons are formed), and a serpentine section which allowed time for the NPG cocoons to properly gel before collection. The dimensions of the nozzle width varied from 30 to 50  $\mu\text{m}$  to allow proper size control of the cocoons. The 30  $\mu\text{m}$  and 50  $\mu\text{m}$  nozzle was used to produce cocoons with diameter of 50  $\mu\text{m}$  or 90  $\mu\text{m}$ , respectively, while any of the two nozzles were used to produce cocoons of 70  $\mu\text{m}$  diameter. The height of the micro-channels ranged from 100 to 110  $\mu\text{m}$ . All inlets and outlets contained a filtering stage to avoid passage of undesired debris, cell clumps, or coalesced agarose.

Standard photolithography and soft lithography procedures were used to create the master moulds onto silicon wafers. The photo mask (CAD/Art Services) containing the designs (Supporting Information Figure S13) was drawn with AutoCAD (Autodesk). A negative photoresist SU-8-2050 (MicroChem Co., USA) was deposited onto clean silicon wafer. Then, patterns were exposed to UV light (OAI DUV/NUV mask aligner) through the photo mask. PDMS devices were made by mixing the elastomer to the curing agent (at a 10:1 ratio), according to manufacturer's protocols (Sylgard184, Ellsworth) and poured into the mould master. Subsequently, the mixture was degassed and cured overnight at 70°C.

Finally, PDMS devices were cut, inlets and outlets were punched with 0.75mm inner diameter biopsy punches, and permanently bonded to clean glass slides by air-plasma bonding at 50W for 45s (Glow Research Autoglow Oxygen Plasma System). Devices were kept at 70°C for 2 days, to ensure PDMS devices returned to a hydrophobic state.

A schematic of the complete device setup is available in the Supporting Information Figure S13. Briefly, the setup includes the microfluidic droplet device mounted on a custom-made aluminum heat sink, which itself is mounted on a trinocular inverted microscope (VWR International). Thermoelectric modules (TE Technology Inc.) attached to the heat sink supply a constant temperature gradient across the microfluidic device, which maintained the temperature at ~37°C over the inlets (keeping the agarose liquid and the cells viable) and at ~4°C over the serpentine channels to help gel the agarose. A pump (Thermaltake AquaBay M5) drives warm (~37°C) water from a water bath through the heat sink continuously. This hydraulic system has two purposes: it allows for dissipation of heat from the device as well as maintenance of the cell/NPG mix at 37°C on the platform.

Flow of fluid (oil or cell/NPG mix) is driven into the microfluidic chip by pressure. Unlike syringe pumps, air pressure driven flow generated higher amounts of monodispersed droplets due to the absence of pulsation effects induced by the stepper motors. Temperature, solenoid valves controlling the pressure, and image acquisition are controlled by a DAQ card (National Instruments) and custom written LabVIEW (NI LabVIEW 2013) module. Droplet formation rate, droplet size, and efficiency of encapsulation are measured using Image J; images acquired using a high-speed

monochrome camera (Blackfly Color 1.3 MP GigE) capturing images at (a reduced frame rate) set to 60 fps during droplet formation.

Sterile filtered (0.2 micron pore size) mineral oil and deionized water were used to test the device for leaks and to ensure proper droplet formation prior to cell encapsulation. Following confirmation of flows stabilization and droplet formation, cells were harvested and collected in an eppendorf in a total volume of 65  $\mu\text{L}$  of appropriate media at a concentration of  $8.5 \times 10^6$  cells/mL. The NPG mixture (agarose:EMC) was added to cells in a 2:1 ratio and carefully mixed to avoid formation of air bubbles. The cell/NPG mixture was carefully transferred to a sterile, glass insert (0.15mL conical glass insert, VWR International), which was kept warm at 37°C. Air pressure (~0.15-0.20MPa) was used to control the flow of the cell/NPG mixture and the oil into the microfluidic droplet device. Following 5 mins for droplet stabilization, and prior to introducing the cell/NPG mixture, the device is coated for 40 mins with 10% filtered BSA to reduce cell adhesion to the tubing or filters. Subsequently, the cell/NPG mixture is inserted, and the encapsulation process starts. By regulating the pressure of the cell and oil inlets different throughputs are obtained. Finally, cocooned cells are collected by placing outlet tubing (PEEK, 1/32" OD, 0.007" ID) into an ice cooled microcentrifuge tube containing media. A typical collection time lasts for 0.5-1 hour. Once the cocoons are collected, the oil is removed by centrifugation at 300 g for 3 mins and the cocoons are resuspend in appropriate media for further experiments.

Confocal microscopy was used confirm that ECM was imbedded within the cocoons and that size of cocoons did not alter the ECM distribution. Briefly, empty cocoons supplemented with DsRed labeled fibrinogen (ThermoFisher) were placed into

a chamber slide (ThermoFisher) and images at 20X objective lens using the Zeiss LSM 880 confocal microscope.

To determine cell occupancy in different sized cocoons, samples were placed into a chamber slide and imaged using a confocal microscope (Zeiss LSM 880) with a 10X objective lens. The number of cells in each cocoon (or free cells) was counted in image J; >200 individual cocoons were counted from three different samples.

#### **4.4.4 Cell Viability, Migration Assay and Cytokine profile**

To monitor viability, cocooned cells were plated on a fibronectin coated chamber slide (ThermoFisher) and were labeled with live/dead stain (ThermoFisher) at 1, 24, 48h post-encapsulation. Cocooned cells were grown in 1% serum CEM and 5% Oxygen. A minimum of 5 random field images were acquired using a 10X objective lens on the Zeiss LSM 880 confocal microscope. The number of viable cells in the cocoons were counted in Image J software. To measure the rate of cell extravasating the cocoon, the number of viable cells inside and outside of the cocoons were counted (Image J) at the different time points and was represented as the percentage of cell migrating out of cocoons.

To determine the cell to cocoon volume ratio, EDC diameter was estimated as ~20  $\mu\text{m}$ . Both cells and cocoons were assumed to be spherical in geometry based on detailed z-stack images from confocal microscopy.<sup>317</sup> The spherical volume of cocoon and EDC was calculated using the formula  $\text{volume} = \frac{4}{3}\pi(\text{radius})^3$ . Cell to cocoon volume ratio was calculated by dividing cell volume with cocoon volume. To account for differences in cell occupancy, the volume ratio was calculated for cocoons containing 1,2,3 or 4+ cells and the weighted average of cell-to-cocoon volume ratio was calculated:

$$WVR = \frac{[(O_1)(R_1)]_{1 \text{ cell}} + [(O_2)(R_2)]_{2 \text{ cells}} + \dots + [(O_n)(R_n)]_{n \text{ cells}}}{(O_1 + O_2 + \dots + O_n)}$$

WVR = weighted cell to cocoon volume ratio

$O$  = percentage of cocoons occupied with 1, 2, 3, 4, or  $n$  number of cells

$R$  = cell to cocoon volume ratio for cocoons occupied with 1, 2, 3, 4, or  $n$  number of cells

The relative abundance of cytokines within conditioned media was measured using a Proteome Profiler Array capable of detecting 105 cytokines (Human XL Cytokine Array Kit; R&D Systems). Conditioned media was obtained from MF90 cocooned EDCs after 48 h culture in 0.5% serum and 1% oxygen– conditions designed to mimic ischemic myocardium. Cell-cell interactions was blocked using anti-N-Cadherin antibody (C2542; Sigma) and anti-E/P-Selectin antibody (BBA1; R&D Systems).<sup>322</sup> Briefly, prior to cocooning, EDCs were incubated for 1h with 10  $\mu\text{g}/\text{mL}$  of anti-E/P-Selectin antibody and 40  $\mu\text{g}/\text{mL}$  of anti-N-Cadherin antibody. Post-cocooning, an additional 5  $\mu\text{g}/\text{mL}$  of anti-E/P-Selectin and 20  $\mu\text{g}/\text{mL}$  of anti-N-Cadherin was added to the media.

#### **4.4.5 Myocardial Infarction, Cell Injection, and Functional Evaluation**

The effect of cocoon size on human EDC retention and post infarct repair was investigated in a series of male non-obese diabetic severe combined immunodeficient (NOD SCID, Charles River) mice (6-8 weeks old, average weight of  $22.5 \pm 0.2$  g) under a protocol approved by the University of Ottawa Animal Care Committee. Animals were injected with buprenorphine, sustained-release formula (1.2 mg/kg; subcutaneous) and meloxicam (0.2 mg/kg) 1 hour prior to surgery, and then meloxicam once daily thereafter for 2 more days. All animals underwent surgical ligation of the left coronary artery (LC).

During surgery and echocardiographic assessment, mice were anesthetized with isoflurane (2-3%), intubated (not intubated for echos) and maintained under physiologic temperature control (37°C). Immediately after surgery, animals were placed in a 30°C incubator with supplemental oxygen and moistened food to recover. Once animals returned to physiological state, they were returned to their normal holding room. All animals were housed in Techniplast ventilated cages with at least bi-weekly cage changes and were given food and water ad libitum. The food is supplied by Envigo (irradiated #2019 extruded chow) and the water is autoclaved and prepared on site. The overhead lighting in the holding room was alternated every 12 hours between light and dark cycles. A University of Ottawa Animal Care Technician monitored animals at least twice daily for 3 days post surgery and then at least once per day until the end of the study. One week after LC ligation, mice were randomized to receive echocardiographic guided injection of 100 000 EDCs in suspension, 100 000 vortex cocooned EDCs, 100 000 microfluidic encapsulated EDCs in cocoon size of 90, 70, or 50 µm, or equivalent volume of phosphate-buffer saline. The effect of cell therapy on cardiac function was evaluated in the remaining animals using echocardiography (VisualSonics V1.3.8, VisualSonics) 14 and 21 days after cell or vehicle injection. At the end of the study, mice were sacrificed by cervical dislocation once the animal were anesthetized (2-3% isoflurane anesthesia) and displayed absence of withdrawal reflex to toe pinch. Investigators were blinded to animal's treatment group when conducting experiments and analyzing data.

#### 4.4.6 Viral Packaging and Transduction

The third-generation packaging system was used to construct lentivirus (Addgene). Briefly, 293T human embryonic kidneys (HEK; Clontech) cells were transfected using lipofectamine 2000 (Invitrogen) with packaging plasmids, envelope plasmid, and transfer plasmid containing gene of interest *i.e.*, firefly luciferase (Supporting Information Figure S20). Lentivirus was harvested at 48 and 72 h after transfection and concentrated using Lenti-X concentrator (Clontech) as per manufacture's protocol.

The lentivirus concentration was determined by qPCR of viral gene (IDT primer); (LV2 forward primer: 5'-ACCTGAAAGCGAAAGGGAAAC-3'; LV2 reverse primer: 5'-CACCCATCTCTCTCCTTCTAGCC-3'). Briefly, the HEK 293T cells were transduced and grown for 72 h followed by genome DNA was extracted (DNeasy kit, Qiagen). To quantify stably integrated lentivirus genes in the genomic DNA by qPCR and standard curve was created using plasmids containing lentiviral genes.

For EDC transduction, cells were first treated with 0.8 µg/ml polybrene (Sigma) for 10 mins followed by the addition of lentivirus. Cells were allowed to recover for at least 48 h. Stably expressing transgenic EDCs were further selected by a 24 h treatment of 2 µg/ml puromycin. The amount of puromycin need for selection was determined empirically, *i.e.* the concentration at which ~100% of non-transduced were killed after 24 h (see Supporting Information Figure S20). The multiplicity of infection (MOI) needed to achieve maximal transduction efficiency was determined by measuring the luciferase activity in transduced cell (Supporting Information Figure S20). Briefly, 48 h after puromycin selection, EDCs were lysed, mixed with luciferase assay reagents (Promega), and the light generated by the reaction was measured by a luminometer.

#### **4.4.7 Bioluminescent Imaging for *In Vivo* Cell Tracking**

After Viral transduction and puromycin selection, cells were allowed to recover for at least 48 h. Hundred thousand suspended, MF50, or MF90 cocooned transgenic EDCs were delivered intramyocardially into NOD SCID mice 1-week post-infarction. One day after cell injection, mice were anesthetized with isoflurane (2-3%) followed by intraperitoneal injection of d-luciferin sodium salt (Gold Biotechnology) with a dose of 150mg/kg. Mice were then transferred into the IVIS Spectrum (PerkinElmer), maintained under the anesthesia, and bioluminescent images were acquired every 5 mins until signal emission reached peak or plateaued (typically occurred within 20-40 mins); mice were kept under anesthesia for no longer than 1 h. Images from peak signal were analyzed with Living Image software V3.2 (PerkinElmer) and the total photon flux was reported.

As shown in Supporting Information Figure 20, both colorimetric dehydrogenase assay (measured after 24 h) and quantification of genomic DNA demonstrated that we injected equal amounts of cells into the hearts therefore, eliminating the possibility that the differences in the bioluminescent signal intensity might be the result of injecting different number of cells.

#### **4.4.8 Histology**

After the final assessment of myocardial function, the remaining hearts were excised, fixed with 4% paraformaldehyde, embedded in optimal cutting temperature compound and sectioned. Scar size and tissue viability within the infarct zone was calculated from Masson's trichrome stained sections; lung tissue, pericardium, and pooled blood in the ventricles were carefully removed prior to quantification using Image J.<sup>222,264,295,329,330</sup> Infarct vascularization was evaluated using isolectin B4 (B-1205, Vector

Laboratories); random field images were acquired using Zeiss Axio Observer A1 microscope.

To evaluate the effects of encapsulation on endogenous repair, a series of NOD SCID mice were injected with 5-bromo-2'-deoxyuridine (BrdU; 100 mg/kg intra-peritoneal; ThermoFisher) once daily for 7 days after intra-myocardial injection of EDCs or vehicle. Twenty-one days after EDC or vehicle injection, mice were sacrificed, and hearts were sectioned for immunohistochemical analysis of BrdU (ab6326; Abcam) co-segregation with cTnT. Wide-field fluorescent images were acquired using the Zeiss Axio Observer A1 microscope. To confirm that BrdU was truly present in the nucleus (co-localized stained with DAPI), z-stack images were acquired using a 63X oil objective lens on the Zeiss LSM 880 confocal microscope. The z-stacks were acquired with slice thickness of 1  $\mu\text{m}$ , for a total of 10-11 slices, and were reconstructed into a 3-dimensional image using ZEN 2.3 (blue edition) software.

#### **4.4.9 Statistical Analysis**

All data is presented as mean  $\pm$  SEM. To determine if differences existed within groups, data was analyzed by a one or two-way ANOVA, as appropriate. In all cases, variances were assumed to be equal and normality was confirmed prior to further post-hoc testing. If differences existed, Sidak's or Tukey's corrected t-test was used to determine the group(s) with the difference(s) (Prism v6). Differences in categorical measures were analyzed using Fischer's exact test. A final value of  $P \leq 0.05$  was considered significant for all analyses.

## Chapter 5

### 5.0 Discussion

In these studies, we focused on improving the NPG cocooning technology to enhance cell-mediated repair of ischemia injured hearts. Overall, we investigated two key cocoon physical properties, namely NPG content and cocoon size. In the first study, we found that increasing NPG agarose concentration from 2 to 3.5% drastically increased capsule stiffness with knock-on benefits towards cell viability, motility, and paracrine output. These effects increased cardiac function by promoting the formation of new blood vessels and myocytes while also limiting scar expansion. Interestingly, benefits occurred despite capsule NPG concentration having no detectable effect on the long-term retention of transplanted cells; suggesting that transplant outcomes are more dependent on exposure to a potent paracrine cell product rather than simply increasing the number of cells retained.

It follows that, the physical properties of the microenvironment likely play a fundamental role in dictating cell activity and that the outcome of cell injection is not solely dependent on specific characteristics of the cells (*i.e.*, contractility, formation of cell-cell junctions, the ability to degrade and remodel the extracellular matrix) but instead on a dynamic interaction between cocooned cells and extracellular factors. Stiffness and mesh size in particular have proven to be critical parameters that influence cell function in normal and pathological conditions.<sup>331-333</sup> For example, increasing stiffness in lung fibrotic lesions plays an important role in progressive pulmonary fibrosis through regulation of fibroblast migration and accumulation.<sup>280</sup> Mechanistically, changes in cytokine and

exosome production/cargo can be attributed to increased traction (and membrane stretching) applied on cocooned cells as integrins pull on the ECM imbedded throughout the rigid 3.5% NPG capsules,<sup>331,334,335</sup> an observation reflecting prior work exploring the effects of matrix elasticity/stiffness on cytokine production by hematological cells.<sup>284,285,336</sup> Both IL-6 and bFGF enhance cardiac function after ischemic injury by reducing apoptosis and increasing the generation of new cardiomyocytes or blood vessels.<sup>305,306,337</sup> Thus, increasing production of nanovesicles rich in transcripts associated with proliferation,<sup>259</sup> development<sup>338</sup> and cell migration<sup>339</sup> likely provided additive paracrine stimulation.

Interestingly, treatment with either suspended or 2% NPG cocooned cells had equivalent effects on myocardial function despite a marked increase both acute and long-term cell engraftment ( $4\pm 1$  and  $18\pm 4$  fold greater, respectively). This observation suggests that cell-mediated effects on endogenous repair are maximized and further increases, in the absence of an expanded paracrine repertoire, may not be possible. It follows that boosting the engraftment of a cell product with a restricted paracrine repertoire, solely reliant on indirect cardiac repair, would have no further benefits once a threshold cell dose had been reached. Only broadening the paracrine repertoire of these cells through biomaterial interactions, genetic engineering,<sup>295,297</sup> or inductive pre-treatment strategies<sup>233,340,341</sup> can hope to improve cell treatment outcomes once sufficient cells have been administered. These observations may help to explain the clinical failure (to date) of autologous cell products as accumulating medical comorbidities significantly restrict the paracrine signature of all adult stem cells.<sup>307,342</sup> Given that only ~10 cells/mg of myocardium (or 1,320 cells total engrafted cells) are found 21 days after injection, it is unrealistic to expect that this small number would have any meaningful contribution to

myocardial function. Although, it is unclear how many cells need to engraft for differentiation of cardiomyogenic cell products (*i.e.*, cardiac-derived or pluripotent stem cells) to have any impact on cardiac function. Finally, the impact of intracapsular cell number and variable cocoon size may influence the regenerative performance of cells and while these variables cannot be altered using vortex technology this represented an intriguing avenue for our next study.

In study 2, a MF-based means of encapsulating EDCs within NPG cocoons was developed to explore the influence of cocoon size and occupancy on EDC-mediated repair of ischemic myocardium. Unlike standard vortex-based cocooning, MF encapsulation enhanced: 1) cocooning throughput with ~2 fold more cells retrieved, 2) control over cocoon occupancy/size, and 3) injectate purity as MF encapsulation required ~30 fold less oil. When the effect of vortex cocooned EDCs on ischemic myocardium was compared to EDCs within similar MF encapsulated cocoons (*i.e.*, 70  $\mu\text{m}$  diameter vs. MF70), comparable gains in cardiac function and scar burden were realized. Increasing cocoon diameter enhanced cell-mediated repair of ischemic injury by slowing clearance and enhancing the paracrine signature of transplanted cocooned cells.

The importance of slowing clearance of transplanted cells is debatable. Previously, we have shown that, while increasing cocoon density improves cells mediated repair of ischemic myocardium, these benefits occurred despite capsule NPG content having no detectable effect on the long-term retention of transplanted cells. Thus, suggesting that transplant outcomes are dependent on exposure to a potent paracrine cell product rather than simply increasing the number of cells retained. It follows that cell-cell interactions which are increased in large diameter cocoons may play an important role in regulating

the 'stemness' and paracrine activity of MF90 EDCs.<sup>69,321,343</sup> The EDC literature supports this notion as culture within multicellular spheroids (cardiospheres) to recapitulate the stem cell niche environment simulates the formation of interconnected networks *via* gap junctions (connexin 43) and cell-cell adhesion molecules (E-selectins).<sup>77,321,344</sup> Cardiosphere conditions promote the expression of multipotent (Nanog, SOX2), stem-cell (Telomerase), cytokine (IGF-1, VEGF) and adhesion (integrin- $\alpha$ 2, laminin- $\beta$ 1, procollagen, E-selectins) transcription factors with reduced expression after cardiosphere dissociation into single cells or cell-cell contact inhibition.<sup>344</sup> Unlike single cell transplantation into infarcted hearts, spheroids demonstrate increased resistance to oxidative stress with improved paracrine stimulation of endogenous repair. Collectively, these studies underscore the importance of cell-cell interactions in the regulation stem cell function and highlight the need to incorporate these concepts within the design of biomaterial technologies. Here we demonstrated that encapsulating multiple cells in cocoons is important for cell-cell contact which enhances the secretion of pro-healing cytokines. Inhibiting cell-cell contact using blocking antibodies for N-Cadherins and E/P-Selectins (both expressed on EDCs surface<sup>321</sup>) diminished the production pro-healing cytokines and promoted the expression of inflammatory cytokines. Given that EDCs are composed of a heterogeneous cell population, the role of cell-cell contact in individual cell type remains unclear.

These studies have several important limitations that include the use of an immune deficient recipient that may limit immune clearance of cells. While this approach provides a relatively easy means of demonstrating "proof of principle" using cells sourced from patients possibly in need of future cell therapy, clinical translation will require proof in

autologous immunocompetent models to establish the additive benefit of encapsulation. Given that cardiac derived progenitor cells are immune-invasive, we suspect that cardiac gains will be similar in immunocompetent animals as demonstrated in previous studies.<sup>82,345</sup> Furthermore, when extrapolating AFM data one should account for the experimental limitations such as cantilever, frequency, and scanned area.<sup>346</sup> The timing of cell delivery also represents an important limitation as the benefits conferred by an enhanced paracrine profile may not be realized when cells are administered to an extensively scarred and remodelled myocardium rather than newly damaged or stunned tissue. Recent work has shown that direct cell-to-cell contact plays a role in the benefits seen after cardiac-derived cell delivery.<sup>185,347</sup> As such, more work is needed to dissect the important kinetic relationship between transplanted cell membrane exposure to injured myocytes and contact mediated salvage of reversibly damaged cells. One must also consider the limitation of luciferase reporter gene when interpreting *in vivo* cell tracking.<sup>348</sup> The quenching and scattering of light as it passes through deep tissue and chest wall make it difficult to detect less than 10000 retained cells;<sup>15,348</sup> although the physiological importance of less than 1% of the initial injectate is debatable. In our studies, cocooned-cells were primarily delivered intramyocardially because short-term cell retention has shown to be superior to IC delivery (see Chapter 1.5 and 1.9 for more details). It is possible that IC delivery may have resulted in greater cell retention due to entrapment of large cocooned cells in the small coronary micro-vessels but, this risks further myocardial damage by occluding blood flow.

Although agarose NPG biomaterials can augment cell-based regenerative therapies, macrophage and foreign body giant cells mediated immune reactions to injected material

(i.e., foreign body reactions) can have unintended consequences.<sup>349</sup> The magnitude of inflammatory response depends on the size, shape, charge and how closely the material mimics natural tissue composition.<sup>350</sup> Although negatively charged polymers (like agarose) are less likely than positively charged polymers to induce a foreign body reaction, subcutaneous implant of high concentration agarose induces new vessel and fibrous tissue formation rich in neutrophils.<sup>351,352</sup> Given these limitations, we identified hyaluronan hydrogels as an excellent alternative to cocooning EDCs because:

- 1) The glycosaminoglycan component of the extracellular matrix is present in all connective tissues especially the heart.<sup>353</sup>
- 2) It is highly expressed in embryonic and adult stem cells niches.<sup>354</sup>
- 3) Increases transplanted cell viability in diverse target tissues such as adipose tissue, brain, and myocardium.<sup>234,355-357</sup>
- 4) Promotes repair of injured myocardium by transplanted human cardiac stem cells.<sup>234,357</sup>
- 5) It is biodegradable, biocompatible, with minimal activation of immune response.<sup>358,359</sup>
- 6) Hydrogel degradation products that promote angiogenesis.<sup>360</sup>
- 7) Used in clinical practice for treating of osteoarthritis, burn wounds and provides surgical aid for abdominal or ophthalmological procedures.<sup>361-364</sup>

Hystem-C (Sigma) is a commercially available hyaluronan-based hydrogel that is crosslinked using thiol-reactive poly(ethylene glycol) diacrylate and covalently linked to thiolated collagen. The biomaterial is chemically-defined and nonimmunogenic while the collagen is porcine derived.<sup>365</sup> Given that Hystem-C system has also been shown to

enhance myocardial repair by cardiac stem cells,<sup>234,357</sup> it is an excellent candidate for cocooning EDCs using the microfluidic platform.

The implications of these studies on the future design of NPG for cell transplantation are evident as the reductionist agarose platform demonstrates not only is the cell:NPG contact important for cell-treatment outcomes but physical cues from the NPG, size of the cocoons, and cell-cell interaction play pivotal roles in guiding cell phenotype, and ultimately their regenerative potency. Hence, our work illustrates how deterministic nanostructural properties (such as porosity and stiffness) and macroscopic properties (such as cocoon size) dictate the regenerative properties of microsized structures.<sup>260</sup> Exciting avenues for future exploration include designing a microfluidic device that embeds or coats the surface of the cocoons with responsive polymers whose properties change in response to alterations in physiological pH, physical stress, or specific enzyme degradation (MMP for instance). Finally, optimization of the microfluidic device to perform multiple encapsulation in parallel will production of large dosages of cocooned cells necessary to carry out experiments in more clinically relevant large animal models (such as swine modeling ischemic cardiomyopathy).

# Chapter 6

## 6.0 Supporting Information

**Table S1. Advantages of agarose NPG.**

<p><b>Biocompatibility</b></p> <ul style="list-style-type: none"><li>• MSC encapsulated in composite agarose gel produced a weak immune reaction after intramyocardial injection.<sup>278</sup></li><li>• Compared to other biomaterials (e.g. hyaluronan or collagen), subcutaneous injection of agarose scaffold elicited a reduced immune response.<sup>366</sup></li><li>• Use in humans for cosmetic lip augmentation and showed great compatibility over 3 years.<sup>367</sup></li><li>• Phase I/II clinical trial used a composite cellular agarose scaffold to create an artificial cornea for treating advanced corneal trophic ulcers (NCT01765244).<sup>368</sup></li><li>• Used as a scaffold for cartilage regeneration in preclinical,<sup>369,370</sup> and phase II clinical<sup>371</sup> studies.</li><li>• Supports motor axon regeneration.<sup>372</sup></li><li>• Phase II clinical trial using agarose beads containing mouse renal adenocarcinoma cells to treat patients with advanced colorectal cancer (NCT02046174).</li></ul>
<p><b>Simplicity of encapsulation</b></p> <ul style="list-style-type: none"><li>• Gelation is controlled by temperature.</li></ul>

- Gelation does not require cytotoxic cross-linkers (e.g. collagen or hyaluronan gels), pH neutralization (e.g. collagen gels), enzymatic proteolytic cleavage (e.g. fibrin gels), or metal ions (e.g. Calcium for alginate gelation) that may harm cardiomyocytes.

#### **Immuno-protective**

- Agarose scaffold are shown to protect cells (e.g. pancreatic islets cells) from immune rejection.<sup>373</sup> This is especially important for allogenic or xenografts (i.e. humans to animals in preclinical studies) cell therapy.

#### **Ease of controlling physical properties**

- Can control matrix stiffness and pore size by simply altering agarose concentration.

#### **Cost effective**

#### **Compatible with various cell types**

- Mesenchymal cells<sup>265,278</sup>
- Explant-derived cardiac stem cells<sup>136,317</sup>
- Neuronal cells<sup>374</sup>
- Chondrocytes<sup>273</sup>

**Table S2. Study 1: Echocardiographic measurements of left ventricle dimensions and function.**

	3.5% NPG cocooned EDCs (n=10)		2% NPG cocooned EDCs (n=9)		Suspended EDCs (n=9)		Vehicle (n=9)		3.5% empty capsules (n=6)		2% empty capsules (n=6)	
	+7	+28	+7	+28	+7	+28	+7	+28	+7	+28	+7	+28
Days post LCA ligation:												
Left Ventricular End Diastolic Volume (µl)	56±3	64±4	67±3	77±4	64±7	75±10	71±5	82±6	58±5	60±4	55±1	58±4
Left Ventricular End Systolic Volume (µl)	39±3	37±3 <sup>#</sup>	47±3	51±3	47±6	50±8	51±5	63±7	41±4	43±4	38±1	41±3
Stroke Volume (µl)	17±1	27±1 <sup>#</sup> \$	19±1	27±2 <sup>#</sup> \$	21±1	26±2 <sup>#</sup> \$	20±1	18±1	17±1	17±1	17±1	17±1
Fractional Area Change (%)	19±1	26±1 <sup>†</sup> #	16±1	21±1 <sup>#</sup>	18±1	20±1 <sup>#</sup>	16±1	14±2	18±1	17±1	19±1	18±1
Left Ventricular Ejection Fraction (%)	31±1	43±2 <sup>*</sup> †#	29±2	35±2 <sup>#</sup>	32±1	35±5 <sup>#</sup>	29±2	24±3	30±1	30±1	31±1	29±1

\*p<0.05 vs. suspended EDCs; †p<0.05 vs. 2% encapsulated EDCs; #p<0.01 vs. vehicle;

\$p<0.05 vs. 2 and 3.5% empty capsules.

**Table S3. Top 20 miRNAs present in EDC secreted nanovesicles regulating angiogenesis, fibrosis, cardiomyocyte proliferation and apoptosis.**

<b>Name</b>	<b>Biological role</b>
hsa-miR-23a-3p	Promotes CM proliferation <sup>375</sup>
hsa-miR-125b-5p	Protects against p53 mediates CM apoptosis and protects MSCs from anoikis <sup>376</sup>
hsa-let-7b-5p	Protects transplanted MSCs from apoptosis <sup>377</sup>
hsa-miR-199a-3p+hsa-miR-199b-3p	Promotes adult CM to enter cell-cycle <sup>378</sup>
hsa-miR-21-5p	Protects CM from oxidative stress-related apoptosis <sup>379</sup>
hsa-miR-130a-3p	Involved in promoting blood derived endothelial progenitor cell angiogenesis <sup>380</sup>
hsa-miR-29b-3p	Regulates fibrotic response of fibroblast <sup>381</sup>
hsa-miR-146a-5p	Antiapoptotic and cardiomyogenic <sup>259</sup>
hsa-miR-22-3p	Regulates cardiac fibrosis <sup>382</sup>
hsa-miR-126-3p	Promotes angiogenesis <sup>380,383</sup>
hsa-miR-93-5p	Protects against ischemia-reperfusion injury induced CM apoptosis <sup>384</sup>
hsa-miR-125a-5p	Promotes M2-type (anti-fibrotic) macrophage phenotype <sup>385</sup>
hsa-let-7g-5p	Protects against hypoxia induced CM apoptosis <sup>386</sup>
hsa-miR-222-3p	Protect against adverse cardiac remodeling and dysfunction <sup>387</sup>
hsa-miR-378d	Promotes MSC survival and vascularization under hypoxic-ischemic conditions. Also promote cardiac-derived stem cell survival through Akt/FAK/CTGF signaling pathway. <sup>388</sup>
hsa-miR-132-3p	Promotes cardiac repair (boosts angiogenesis, reduces fibrosis, and enhances cardiac functional) <sup>389</sup>
hsa-miR-23b-3p	Promotes CM proliferation <sup>375</sup>
hsa-miR-24-3p	Protects against CM apoptosis <sup>390</sup>
hsa-miR-873-3p	Inhibit RIPK1/RIPK3-mediated necrotic cell death in CMs <sup>391</sup>

hsa-miR-199a-5p

Promote CM proliferation<sup>392</sup>

CM=cardiomyocytes.

**Table S4. Comparing miRNA expression in nanovesicles isolated from cocooned and adherent EDCs.**

Name	p-adjusted	p-value	log2 (Fold change)
<b>Upregulated 3.5% vs. ADH</b>			
hsa-miR-28-5p	1.05E-06	2.29E-09	8.35
hsa-miR-145-5p	1.05E-06	2.62E-09	8.32
hsa-miR-423-5p	1.57E-06	5.85E-09	8.11
hsa-miR-424-5p	2.06E-06	1.03E-08	7.97
hsa-miR-376c-3p	3.52E-06	2.34E-08	7.76
hsa-miR-642a-3p	3.52E-06	2.63E-08	7.73
hsa-miR-432-5p	4.58E-06	4.00E-08	7.62
hsa-miR-337-5p	6.22E-06	6.19E-08	7.51
hsa-miR-148b-3p	1.64E-05	1.84E-07	7.22
hsa-miR-136-5p	3.91E-05	6.34E-07	6.89
hsa-let-7c-5p	7.68E-05	1.38E-06	6.67
hsa-miR-140-5p	8.30E-05	1.65E-06	6.62
hsa-miR-29a-3p	1.85E-05	2.31E-07	6.06
hsa-miR-374a-5p	2.13E-05	2.92E-07	5.93
hsa-miR-154-5p	1.09E-03	2.99E-05	5.79
hsa-miR-323a-3p	2.49E-03	8.68E-05	5.45

hsa-miR-19b-3p	2.77E-03	1.00E-04	5.41
hsa-miR-29b-3p	7.68E-05	1.43E-06	5.39
hsa-miR-222-3p	1.66E-04	3.52E-06	5.38
hsa-miR-377-3p	4.03E-03	1.56E-04	5.27
hsa-miR-15a-5p	2.67E-04	6.31E-06	5.2
hsa-miR-151a-3p	5.14E-03	2.11E-04	5.17
hsa-let-7i-5p	3.02E-04	7.52E-06	5.06
hsa-miR-127-3p	2.67E-04	6.12E-06	5.04
hsa-miR-148a-3p	7.82E-03	3.41E-04	5
hsa-miR-20a-5p+hsa-miR-20b-5p	1.06E-02	4.76E-04	4.89
hsa-miR-199a-5p	1.46E-03	4.92E-05	4.84
hsa-miR-106a-5p+hsa-miR-17-5p	1.65E-02	8.03E-04	4.71
hsa-miR-382-5p	1.17E-03	3.36E-05	4.66
hsa-miR-376a-3p	1.17E-03	3.49E-05	4.51
hsa-miR-1915-3p	3.32E-02	1.69E-03	4.43
hsa-miR-379-5p	4.30E-02	2.52E-03	4.28
hsa-miR-4516	5.14E-03	2.09E-04	4.04
hsa-miR-495-3p	6.13E-03	2.60E-04	3.89
hsa-miR-337-3p	4.27E-02	2.45E-03	3.78
hsa-miR-181a-5p	1.28E-02	5.89E-04	3.66
hsa-miR-130a-3p	2.52E-02	1.26E-03	3.36
hsa-miR-574-3p	4.26E-02	2.36E-03	3.36
hsa-miR-22-3p	4.26E-02	2.24E-03	3.21
hsa-miR-543	4.26E-02	2.32E-03	3.19
hsa-miR-25-3p	4.26E-02	2.39E-03	3.17
hsa-miR-199a-3p+hsa-miR-199b-3p	4.81E-02	2.87E-03	3.06

**Downregulation 3.5% NPG vs. ADH**

hsa-miR-4286	3.65E-03	1.37E-04	-4.68
hsa-miR-626	1.40E-02	6.62E-04	-4.57
<b>Upregulation 2% NPG vs. ADH</b>			
hsa-miR-145-5p	1.75E-10	2.18E-13	9.42
hsa-miR-28-5p	4.89E-08	1.22E-10	8.19
hsa-miR-376c-3p	1.24E-07	4.62E-10	7.92
hsa-miR-19b-3p	3.91E-07	3.91E-09	7.47
hsa-miR-423-5p	7.20E-07	9.87E-09	7.28
hsa-let-7c-5p	1.36E-06	2.03E-08	7.12
hsa-miR-148b-3p	2.78E-06	4.85E-08	6.93
hsa-miR-218-5p	2.78E-06	4.85E-08	6.93
hsa-miR-140-5p	3.18E-06	5.93E-08	6.89
hsa-miR-222-3p	2.42E-07	1.20E-09	6.47
hsa-miR-15b-5p	1.76E-05	4.38E-07	6.44
hsa-miR-1915-3p	1.89E-05	4.94E-07	6.41
hsa-miR-29a-3p	2.80E-07	2.09E-09	6.31
hsa-miR-374a-5p	2.80E-07	1.95E-09	6.23
hsa-miR-15a-5p	3.91E-07	4.38E-09	6.18
hsa-let-7d-5p	4.24E-05	1.37E-06	6.17
hsa-miR-575	6.79E-05	2.37E-06	6.04
hsa-miR-29b-3p	3.91E-07	3.47E-09	5.96
hsa-miR-136-5p	1.76E-04	6.57E-06	5.79
hsa-miR-424-5p	1.98E-04	7.66E-06	5.75
hsa-miR-337-5p	3.04E-04	1.23E-05	5.63
hsa-miR-20a-5p+hsa-miR-20b-5p	4.90E-04	2.38E-05	5.45
hsa-miR-199a-5p	2.39E-05	6.55E-07	5.4
hsa-let-7i-5p	9.45E-06	1.88E-07	5.28

hsa-miR-377-3p	8.54E-04	4.78E-05	5.27
hsa-miR-379-5p	8.54E-04	4.78E-05	5.27
hsa-miR-30d-5p	9.80E-04	5.73E-05	5.22
hsa-miR-99b-5p	4.24E-05	1.36E-06	5.06
hsa-miR-23b-3p	2.72E-05	7.80E-07	5.04
hsa-miR-126-3p	3.88E-05	1.16E-06	5.01
hsa-miR-181a-5p	1.60E-05	3.59E-07	4.97
hsa-let-7g-5p	4.79E-05	1.61E-06	4.92
hsa-miR-342-3p	1.23E-03	7.64E-05	4.74
hsa-miR-361-5p	9.96E-04	5.95E-05	4.68
hsa-miR-29c-3p	8.48E-03	6.44E-04	4.5
hsa-miR-125a-5p	1.44E-04	5.21E-06	4.47
hsa-miR-199b-5p	3.04E-04	1.25E-05	4.32
hsa-miR-26a-5p	2.80E-03	1.88E-04	4.27
hsa-miR-574-3p	6.78E-04	3.46E-05	4.15
hsa-miR-127-3p	4.72E-04	2.23E-05	4.12
hsa-miR-16-5p	4.18E-04	1.82E-05	4.07
hsa-miR-376a-3p	4.65E-04	2.14E-05	4.07
hsa-miR-130a-3p	4.18E-04	1.79E-05	4.02
hsa-miR-93-5p	7.08E-04	3.70E-05	4.01
hsa-let-7a-5p	4.53E-04	2.03E-05	3.98
hsa-miR-382-5p	1.25E-03	7.91E-05	3.92
hsa-miR-4516	1.09E-03	6.67E-05	3.86
hsa-miR-337-3p	1.13E-02	8.69E-04	3.83
hsa-miR-25-3p	8.63E-04	4.94E-05	3.82
hsa-miR-320e	7.53E-04	4.03E-05	3.79
hsa-miR-21-5p	1.96E-03	1.27E-04	3.53

hsa-miR-27b-3p	2.35E-03	1.55E-04	3.51
hsa-miR-24-3p	3.26E-03	2.23E-04	3.48
hsa-miR-34a-5p	5.66E-03	4.10E-04	3.29
hsa-miR-22-3p	1.39E-02	1.12E-03	3.02
hsa-miR-199a-3p+hsa-miR-199b-3p	1.26E-02	9.91E-04	2.98
hsa-let-7b-5p	1.56E-02	1.30E-03	2.91
hsa-miR-100-5p	1.56E-02	1.32E-03	2.9
hsa-miR-495-3p	2.01E-02	1.75E-03	2.89
hsa-miR-630	2.93E-02	2.59E-03	2.74
hsa-miR-125b-5p	4.62E-02	4.26E-03	2.56
<b>Downregulation 2% NPG vs. ADH</b>			
hsa-miR-585-3p	2.96E-02	2.69E-03	-3.82
hsa-miR-6721-5p	1.56E-02	1.28E-03	-4.28
hsa-miR-184	4.82E-03	3.36E-04	-4.71
hsa-miR-548e-5p	8.48E-03	6.44E-04	-4.5

**Table S5. Comparing miRNA expression in nanovesicles isolated from EDCs cocooned in 3.5% and 2% NPG capsules.**

<b>Name</b>	<b>p-adjusted</b>	<b>P-value</b>	<b>Log2 (Fold change)</b>
<b>Upregulated 3.5% vs. 2%</b>			
hsa-miR-154-5p	7.78E-03	2.12E-05	5.79
hsa-miR-432-5p	1.83E-02	1.63E-04	4.21
<b>Downregulated 3.5% vs. 2%</b>			
hsa-let-7a-5p	1.83E-02	1.82E-04	-3.82
hsa-miR-15b-5p	1.30E-02	8.01E-05	-4.81
hsa-miR-26a-5p	2.10E-02	2.36E-04	-4.57
hsa-miR-23b-3p	3.41E-03	4.24E-06	-5.13
hsa-miR-30d-5p	1.83E-02	1.39E-04	-5.22
hsa-miR-342-3p	1.30E-02	8.12E-05	-5.17

**Table S6. Study 1: Summary of patient characteristics.**

<b>Atrial Appendage donors</b>	
<b>(n=19)</b>	
Age (yrs)	64±2
BMI (kg/m <sup>2</sup> )	31±2
Sex (%male)	74%
Diabetes	42%
Hypertension	90%
Dyslipidemia	68%
Ongoing smoking	26%
Thyroid disease	17%
Peripheral vascular disease	21%
Coronary artery disease	79%
History of MI	42%
Valvular heart disease	74%
Congestive heart failure	21%
NYHA class	1.4±0.2
LV Ejection Fraction (%)	44±4
CCS class	2.1±0.5
Creatinine (µmol/L)	100±11
Hemoglobin A1c	6.2±0.3

Medications:	
Anti-platelet therapy	90%
Beta-blocker	79%
Statins	74%
ACEI or ARB	74%

BMI= Body Mass Index; MI= Myocardial infarction; NYHA= New York Heart Association; LV= Left ventricle; CCS= Canadian Cardiovascular Society; ACEI= Angiotensin-converting enzyme inhibitor; ARB= Angiotensin receptor blocker; Error corresponds to standard error mean.

**Table S7. Study 2: Echocardiographic measurements of left ventricle dimensions and function.**

	Vx (n=9)		MF70 (n=10)		MF50 (n=9)		MF90 (n=10)		Sp (n=8)		Vehicle (n=10)	
	+7	+28	+7	+28	+7	+28	+7	+28	+7	+28	+7	+28
<b>Days Post LCA ligation</b>												
<b>Left Ventricular End Diastolic Volume (μl)</b>	62±3	75±5	57±4	63±5	61±4	65±5	62±3	74±7	61±4	70±6	68±4	81±4
<b>Left Ventricular End Systolic Volume (μl)</b>	44±2	49±5	40±4	42±5 <sup>*</sup>	43±3	44±4	45±3	46±6	44±4	49±6	48±3	62±4
<b>Stroke Volume (μl)</b>	17±4	26±1 <sup>**</sup>	17±1	22±2	18±1	21±1	16.5±0.4	28±2 <sup>***†#</sup>	17±1	21±1	20±1	19±1
<b>Fractional Area Change (%)</b>	17±1	22±1 <sup>**</sup>	18±1	22±2 <sup>***</sup>	18±1	19±1 <sup>*</sup>	16±1	24±2 <sup>****</sup>	17±1	19±2	17±1	13±1
<b>Left Ventricular Ejection Fraction (%)</b>	28±2	35±2 <sup>**</sup>	31±2	35±2 <sup>**</sup>	31±2	33±2 <sup>*</sup>	27±2	40±2 <sup>****</sup>	29±2	32±3	29±1	23±1

\*p<0.05, \*\*p<0.01, \*\*\*p<0.001, \*\*\*\*p<0.0001 vs. vehicle; †p<0.01 vs. MF70; #p<0.01 vs. MF50; §p<0.01 vs. Sp. Error corresponds to standard error mean. Sp= Suspended EDCs; Vx= Vortex cocooned EDCs; MF= Microfluidic cocooned EDCs; Vehicle= Phosphate-buffered saline

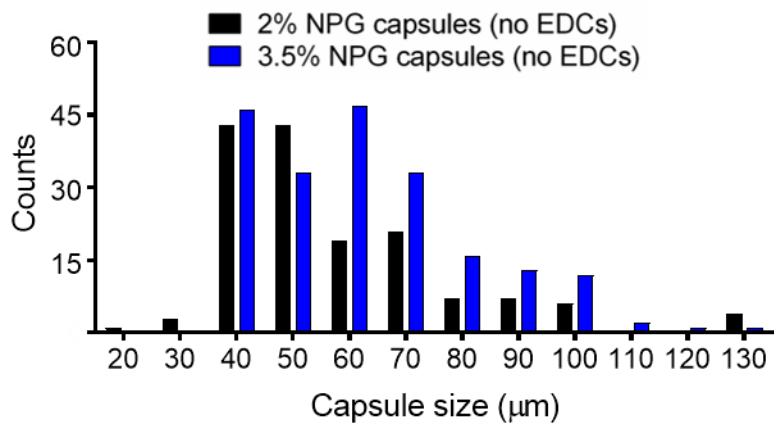
**Table S8. Study 2: Summary of patient characteristics.**

<b>Atrial Appendage donors</b>	
<b>(n=22)</b>	
Age (yrs)	67±2
BMI (kg/m <sup>2</sup> )	31±2
Gender (%male)	77%
Diabetes	36%
Hypertension	86%
Dyslipidemia	73%
Ongoing smoking	27%
Thyroid disease	14%
Peripheral vascular disease	23%
Coronary artery disease	82%
History of MI	46%
Valvular heart disease	68%
Congestive heart failure	18%
NYHA class	1.6±0.2
LV Ejection Fraction (%)	45±4
CCS class	2.5±0.4
Creatinine (µmol/L)	99±10
Hemoglobin A1c	6.2±0.3

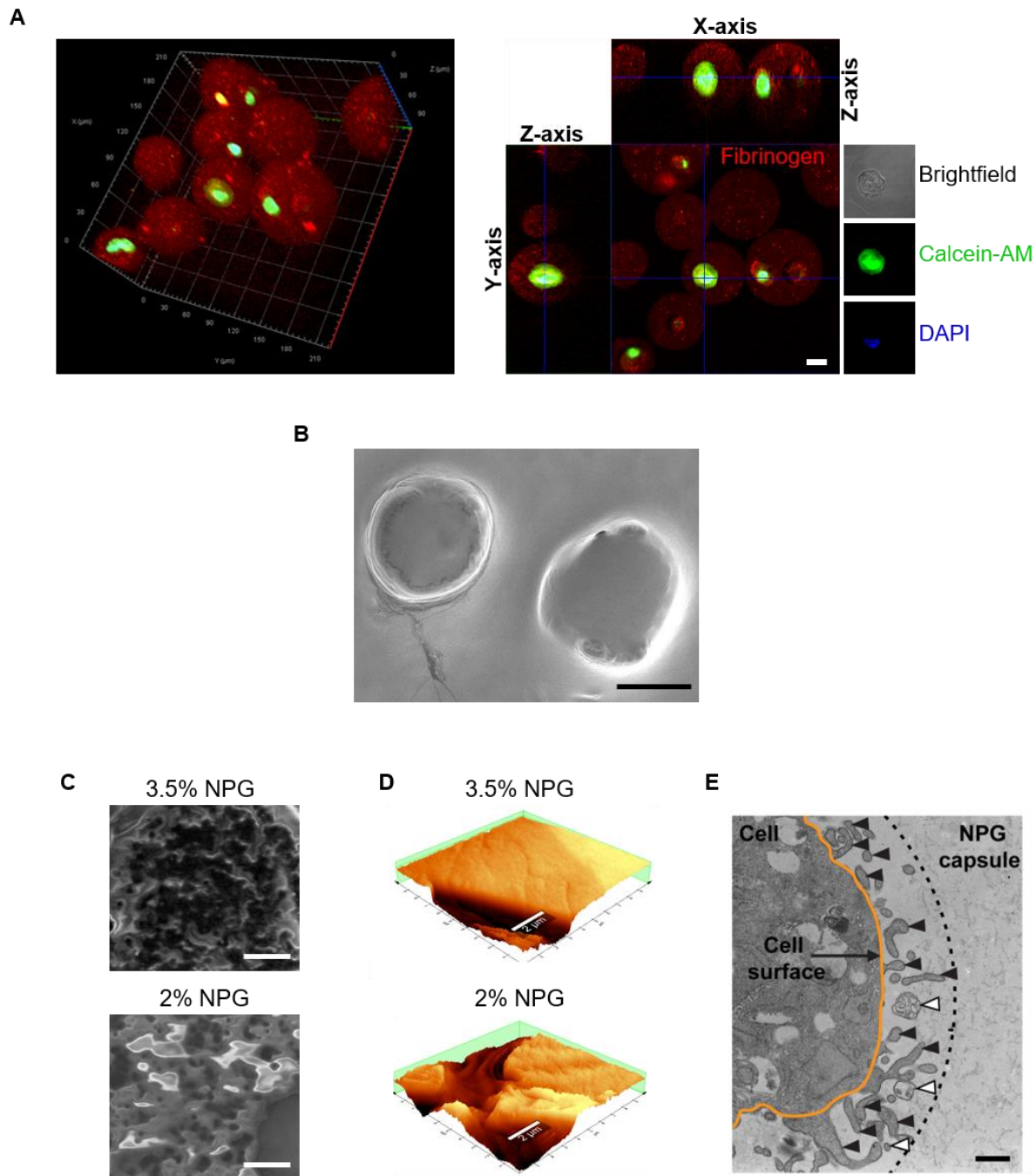
Medications:

Anti-platelet therapy	91%
Beta-blocker	82%
Statins	77%
ACEI or ARB	73%

BMI= Body Mass Index; LV= Left ventricle; MI=Myocardial infarction; NYHA= New York Heart Association; CCS= Canadian Cardiovascular Society; ACEI= Angiotensin-converting enzyme inhibitor; ARB= Angiotensin receptor blocker; Error corresponds to standard error mean.

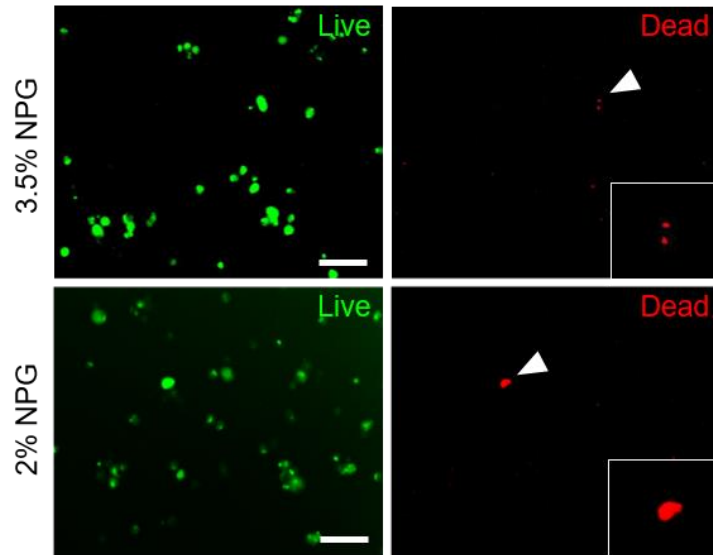
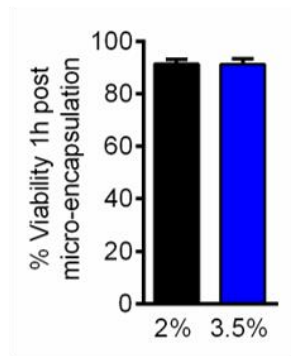
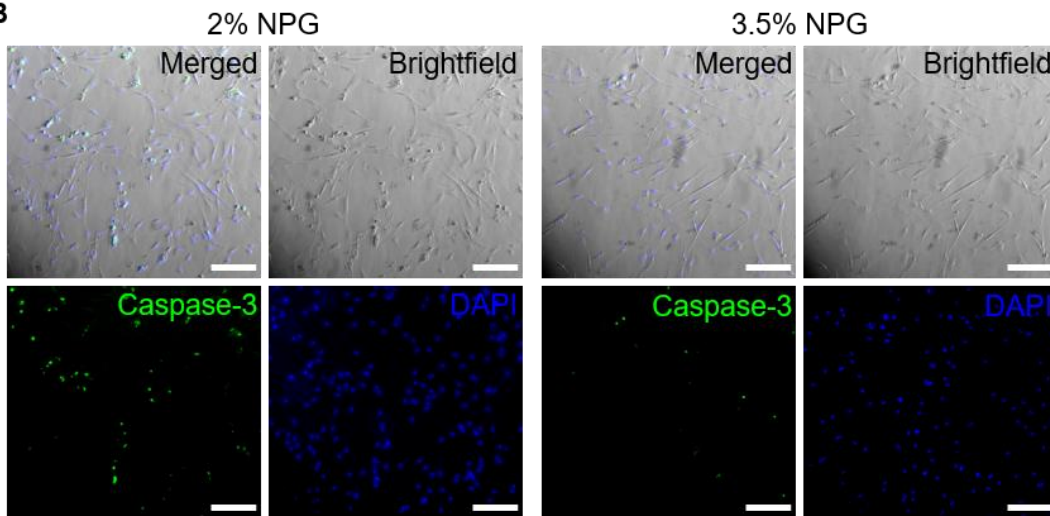
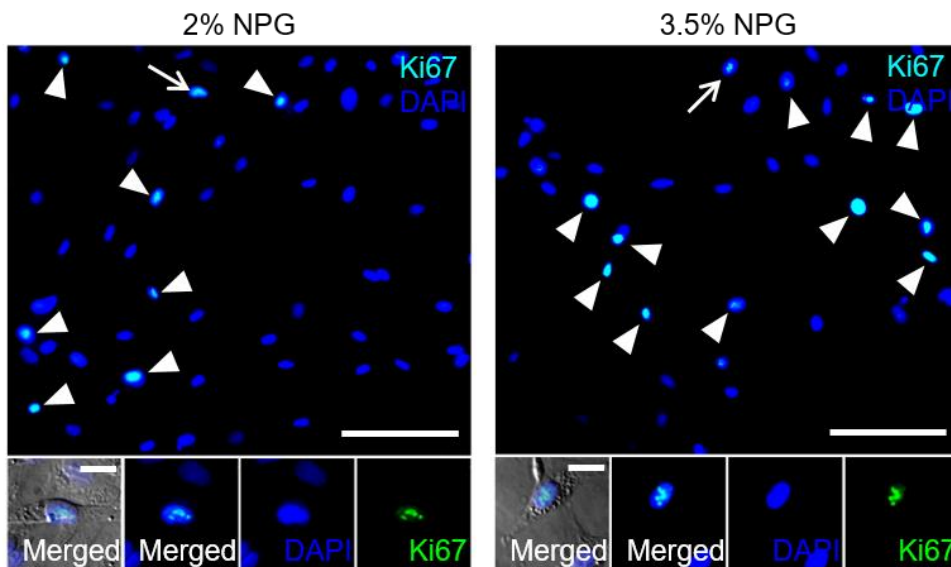


**Figure S1. Size distribution of empty nanoporous gel capsules.** Size distribution histograms for 2% and 3.5% NPG capsules without cells. Size distributions were calculated from measuring >100 individual capsules from three different samples.

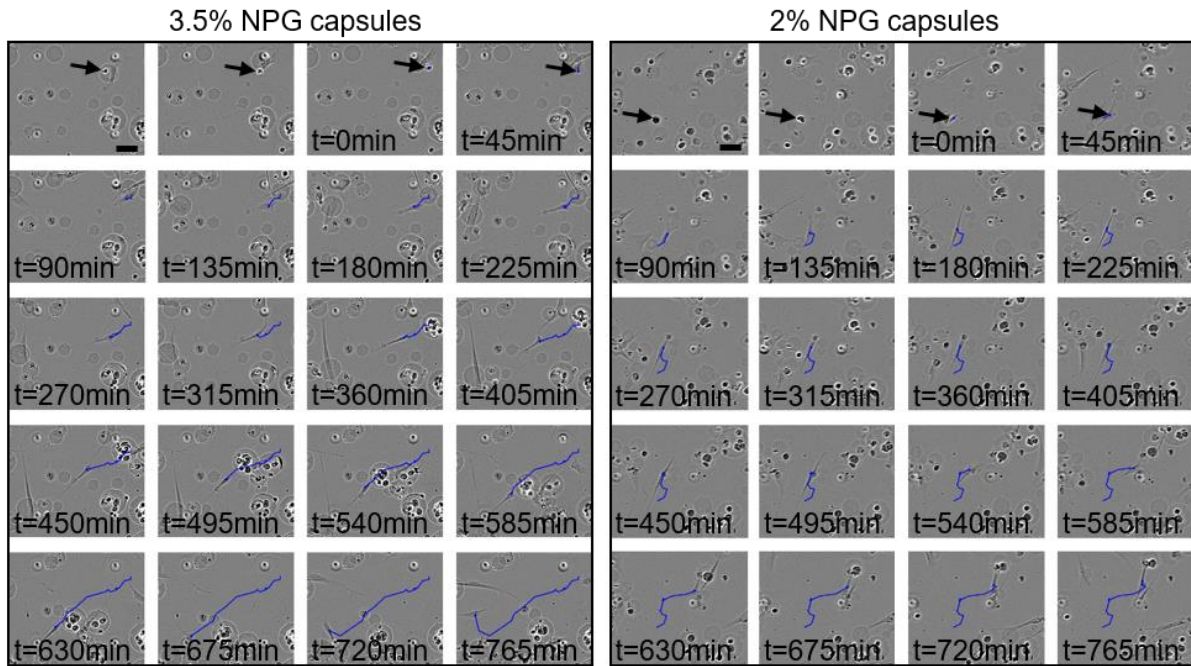
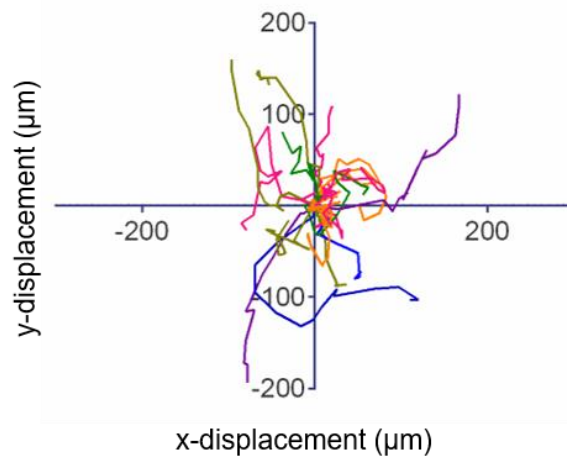


**Figure S2. Physical characterization of nanoporous gel capsules.** (A) Ortho-representation z-stack images (right panels) and 3D reconstruction (left panels) of cells within 3.5% NPG cocoon confirming cells are completely encapsulated by NPG. Cells are

labeled with Calcein-AM (green), DAPI (blue) while cocoons are demarcated by DsRed tagged fibrinogen (red). Scale bar 20  $\mu\text{m}$ . (B) Selected SEM image for 3.5% NPG capsules (scale bar 100  $\mu\text{m}$ ). (C) Representative SEM images for porous regions of NPG capsules (scale bar 10  $\mu\text{m}$ ). (D) Surface morphology maps for NPG capsules measured by AFM (10x10  $\mu\text{m}$ ). The false color represents changes in intensity of the tint indicates areas of higher stiffness (scale bar 2  $\mu\text{m}$ ). (E) A transmission electron microscope image of an ultra-thin cell section showing membrane protrusions (black arrow heads). Membrane protrusions extend out from the cell surface (finger like projections) but may appear as non-contiguous structures (elongated sphere that are not continues with the cell surface) depending on their orientation in three-dimensional space. White arrow heads show secreted extracellular vesicles, non-contiguous structure with average diameter less than 100 nm, and any structures at a distance greater than 1000 nm (dashed line) from the cell surface were excluded (Scale bar 500 nm).

**A****B****C**

**Figure S3. Cell viability in post encapsulation.** (A) Left: Quantification of percentage of viable cells 1hr post-encapsulation (n=3). Right: Representative images showing EDCs 1hr post-encapsulation and labeled with live (green)/dead (red) stain. Arrow highlight an example of a dead cell shown in the magnified panel. Scale bar 100 $\mu$ m. (B) Representative images show cells undergoing apoptosis (active-caspase 3, green) under stress conditions (1% serum and 1% oxygen). Scale bar 200  $\mu$ m. (C) Representative images showing Ki67+ nucleus (arrow heads); long arrow shows a cell at a higher magnification (n=5 per sample). Scale bar 100  $\mu$ m in large panel and 20 $\mu$ m in small panel. All error bars correspond to standard error mean.

**A****B**

**Figure S4. Measuring 2-D cell migration rate.** (A) Representative time lapse images of cells emerging out from the capsule and migrating on matrigel coated cultureware. Cell within the NPG cocoon is indicated by the arrow. Cells were manually tracked using Image J software (migration path traced in blue). Scale bar 50 $\mu$ m. (B) Displacement plot showing the path of cell migration of non-encapsulated (adherent) cells.

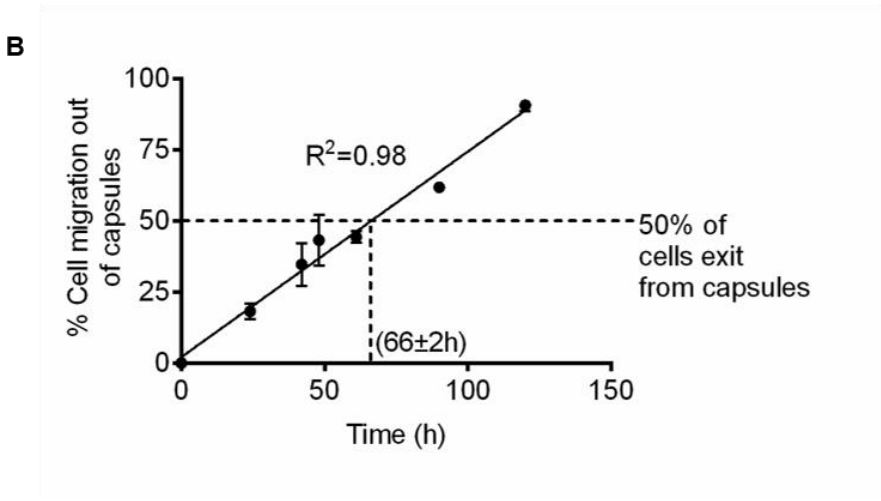
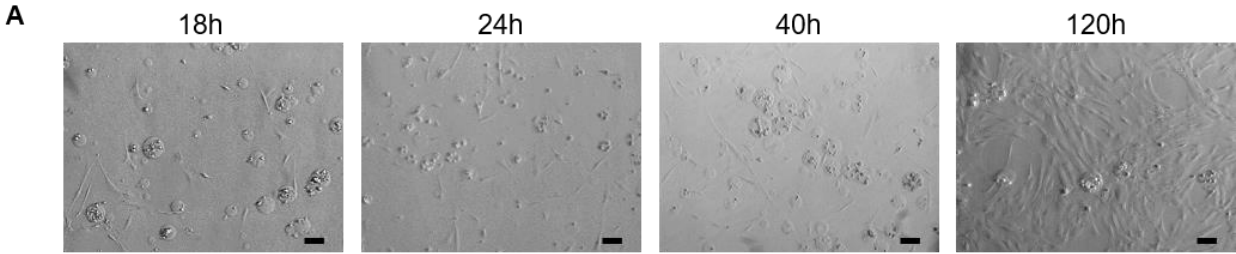


**Figure S5. Kinetics of EDC emerging out of capsules.** (A) Representative bright field images showing cells exiting the capsules at different time points on cultureware lacking fibrinogen coating. Scale bar 200 $\mu$ m. (B) Graph represents the number of EDCs that emerged from 3.5% NPG capsules on cultureware lacking fibrinogen coating (n=3). Error bar correspond to standard error mean.

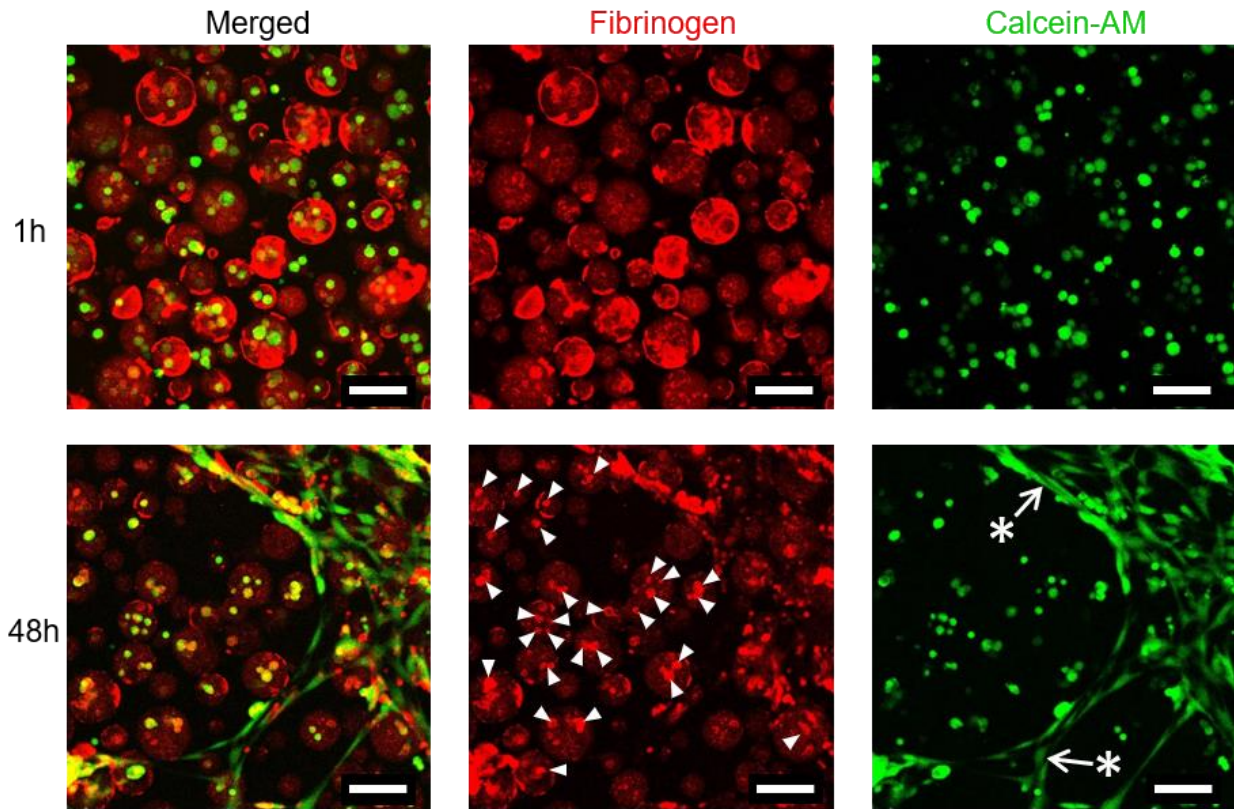


**Figure S6. Extracellular clustering in capsules.** Cells (labeled with Calcein-AM, green) in cocoons (3.5% NPG) supplemented with DsRed tagged fibrinogen (red) 1 and 48 hr post-encapsulation. Arrow heads show fibrinogen clustering around the cells within capsules. Arrows (asterisk) highlight cells that have migrated out of capsules. Scale bar 100 $\mu$ m.

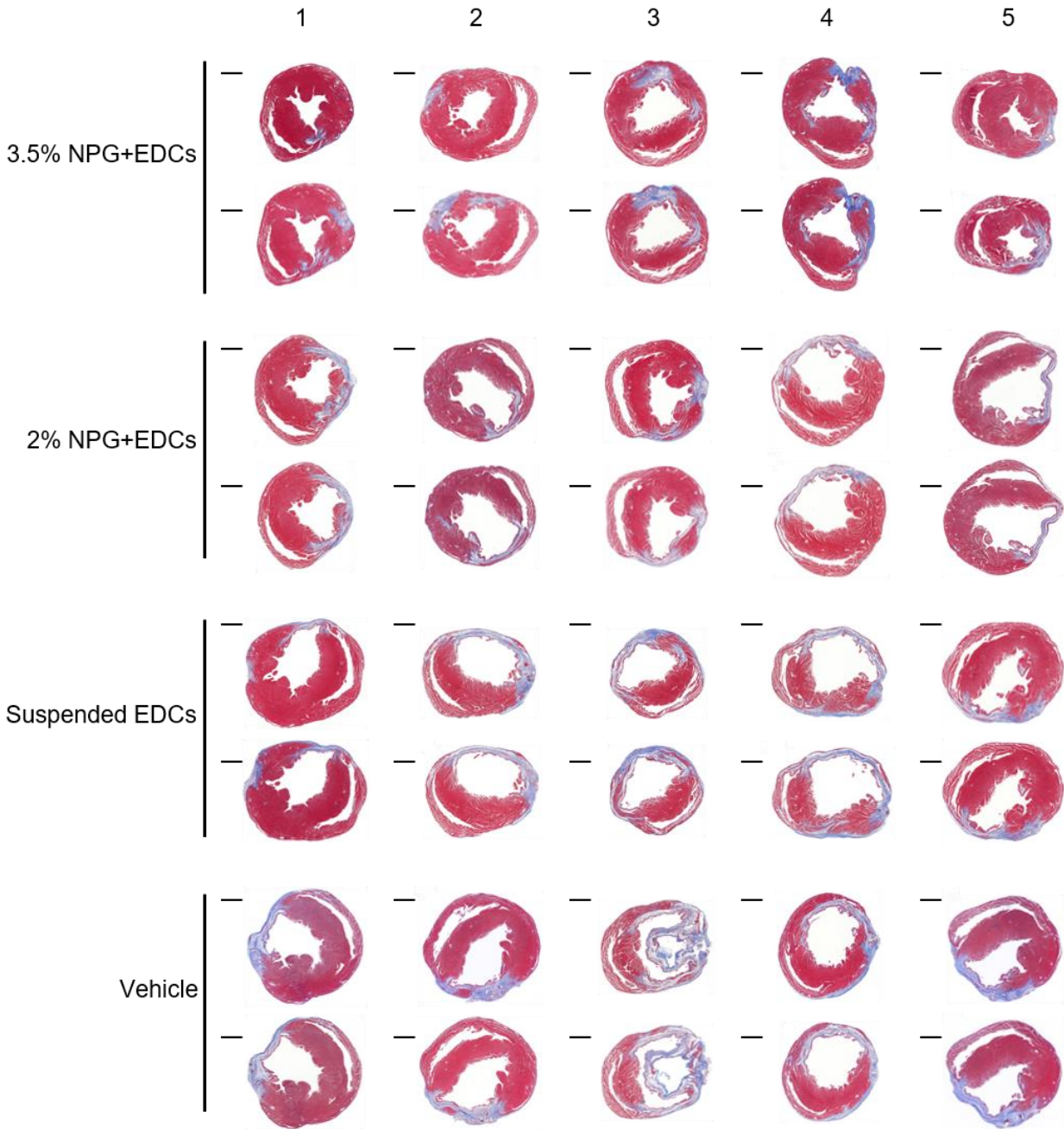


**Figure S7. Study 1: Scar size.** Representative Masson's trichrome images showing scar burden (blue= scar, red= viable myocardium) from 5 different animals and 2 sections per heart. Scale bar 1000 $\mu$ m.

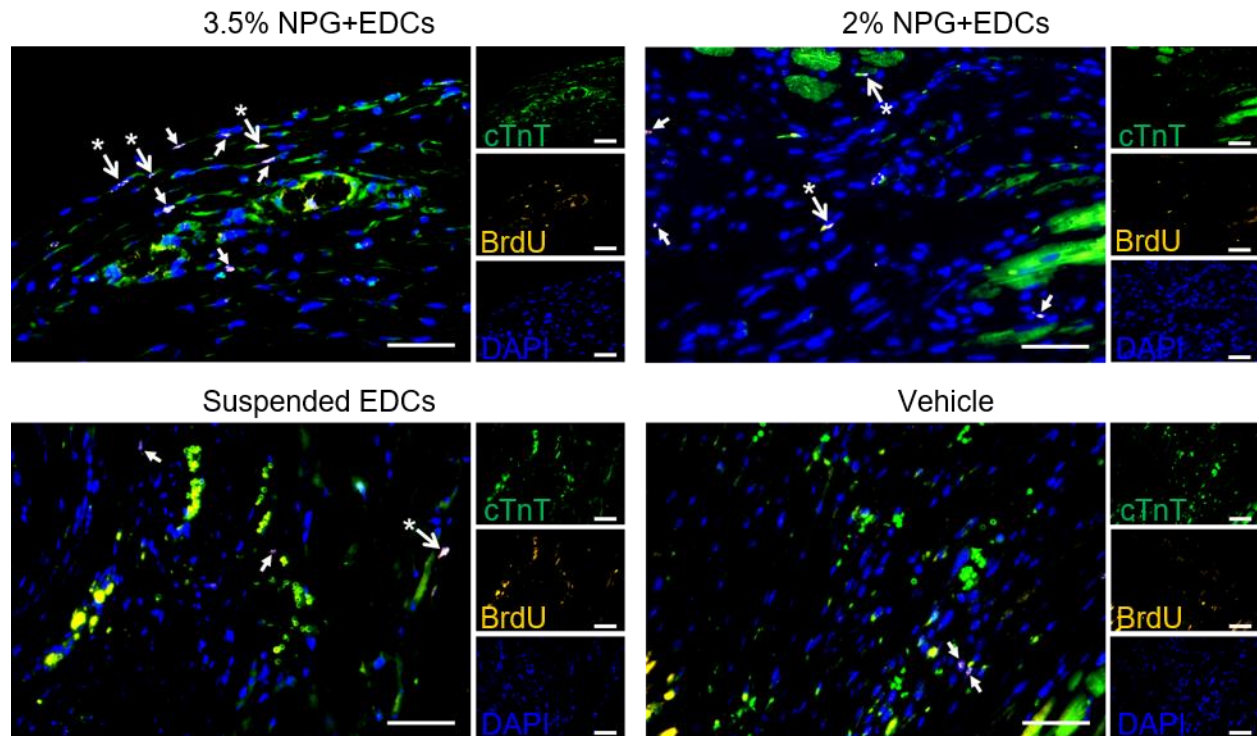


**Figure S8. Study 1: BrdU staining.** Representative images showing proliferating cells (BrdU positive cells) within infarct/peri-infarct region of the heart section. Non-cardiomyocyte proliferating cells (BrdU+/cTnT-) are indicated by solid arrow heads, and proliferating cardiomyocytes (BrdU+/cTnT+) are indicated by arrows with asterisk. Scale bar 50 $\mu$ m.

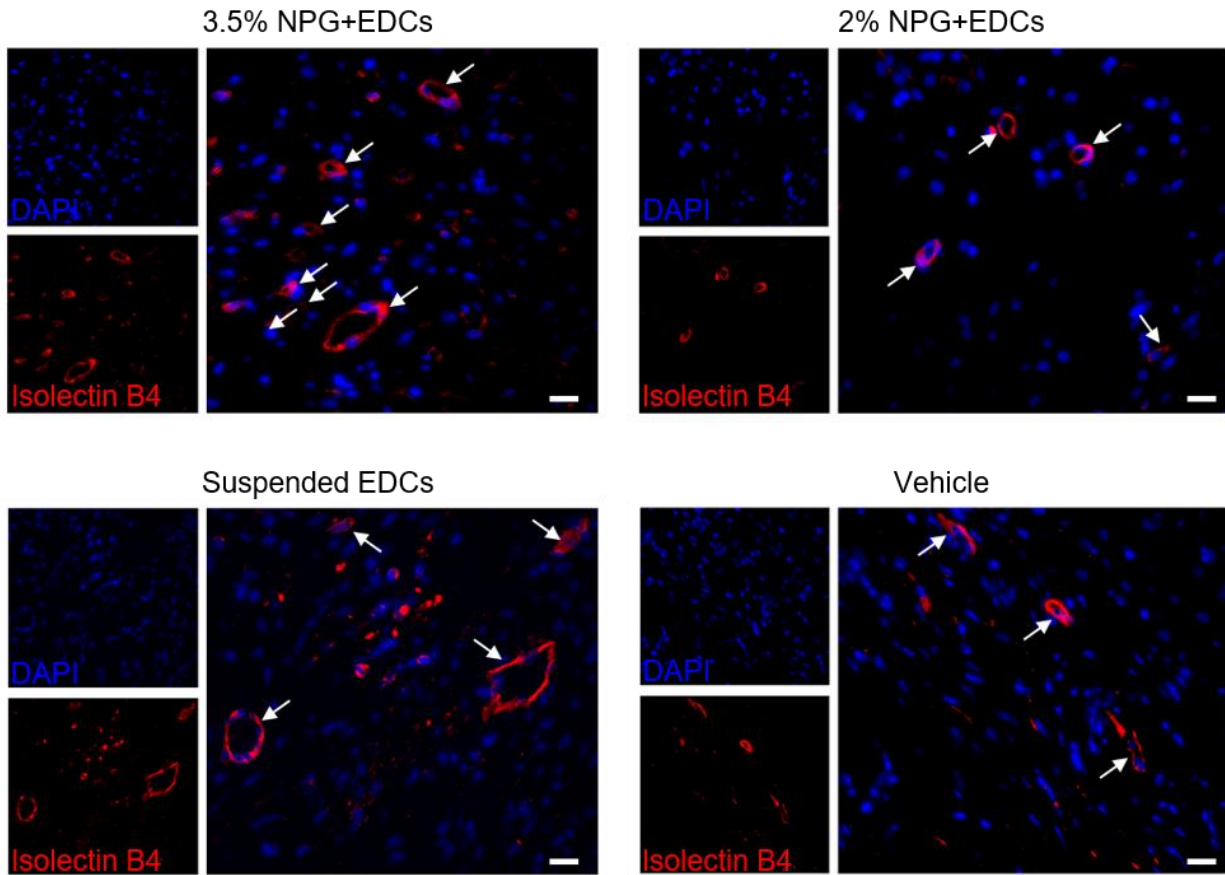


**Figure S9. Study 1: Vessel density.** Representative images showing blood vessels (indicated by the arrows) within infarct/peri-infarct region of the heart section. Scale bar 20µm.

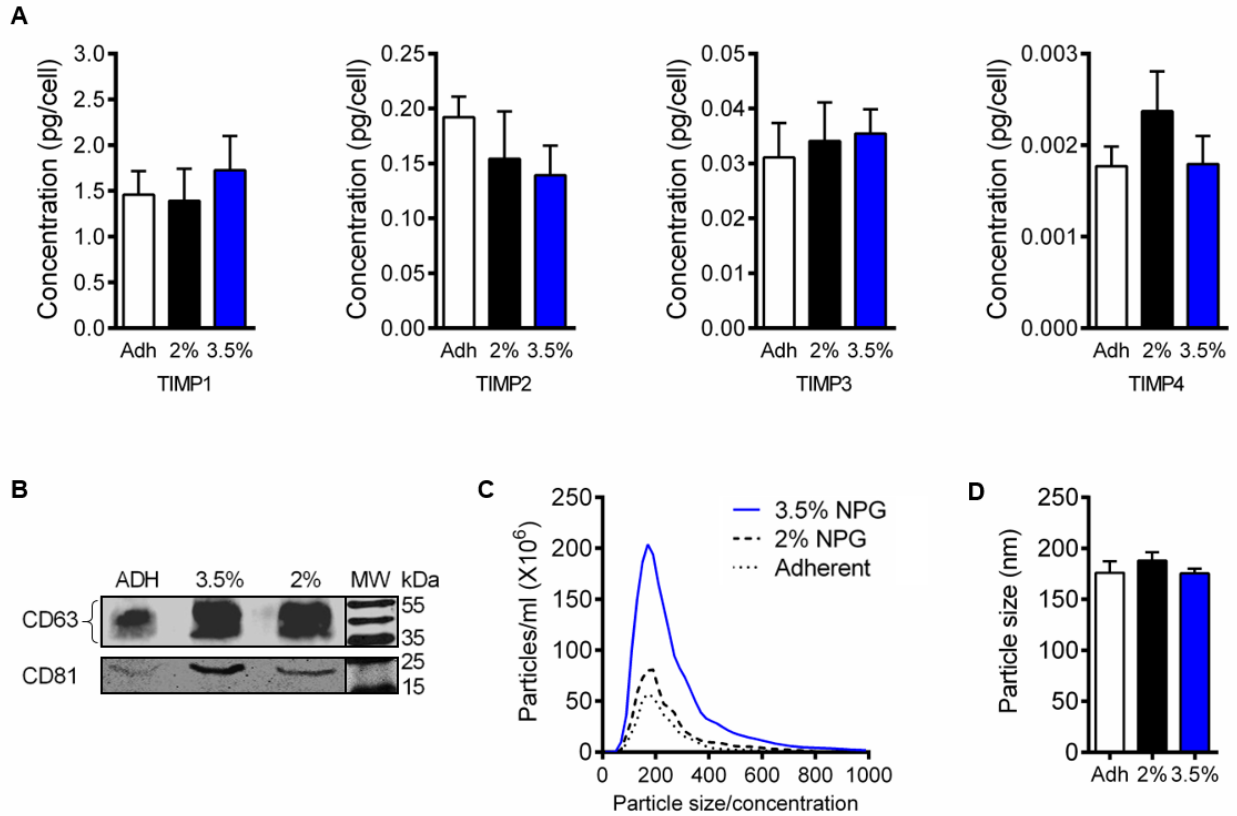


**Figure S10. Profiling the secretion of TIMPs and exosome nanovesicles in condition media.** (A) TIMP secreted into conditioned media was obtained from adherent (Adh), 2% and 3.5% NPG encapsulated EDCs after 48h of culture in hypoxic condition (1% oxygen). Magnetic Luminex Performance Assay was used to quantify protein concentration. Protein concentration was standardized to the number of cells (n=6 with 3 technical replicates each). (B) Western Blot showing the presence of exosome markers CD63 and CD81. (C) Number of nanovesicles secreted into condition media quantified using particle-tracking analysis (Nanosight; n=5). (D) Average size of secreted nanovesicles (n=5). Error bars correspond to standard error mean.

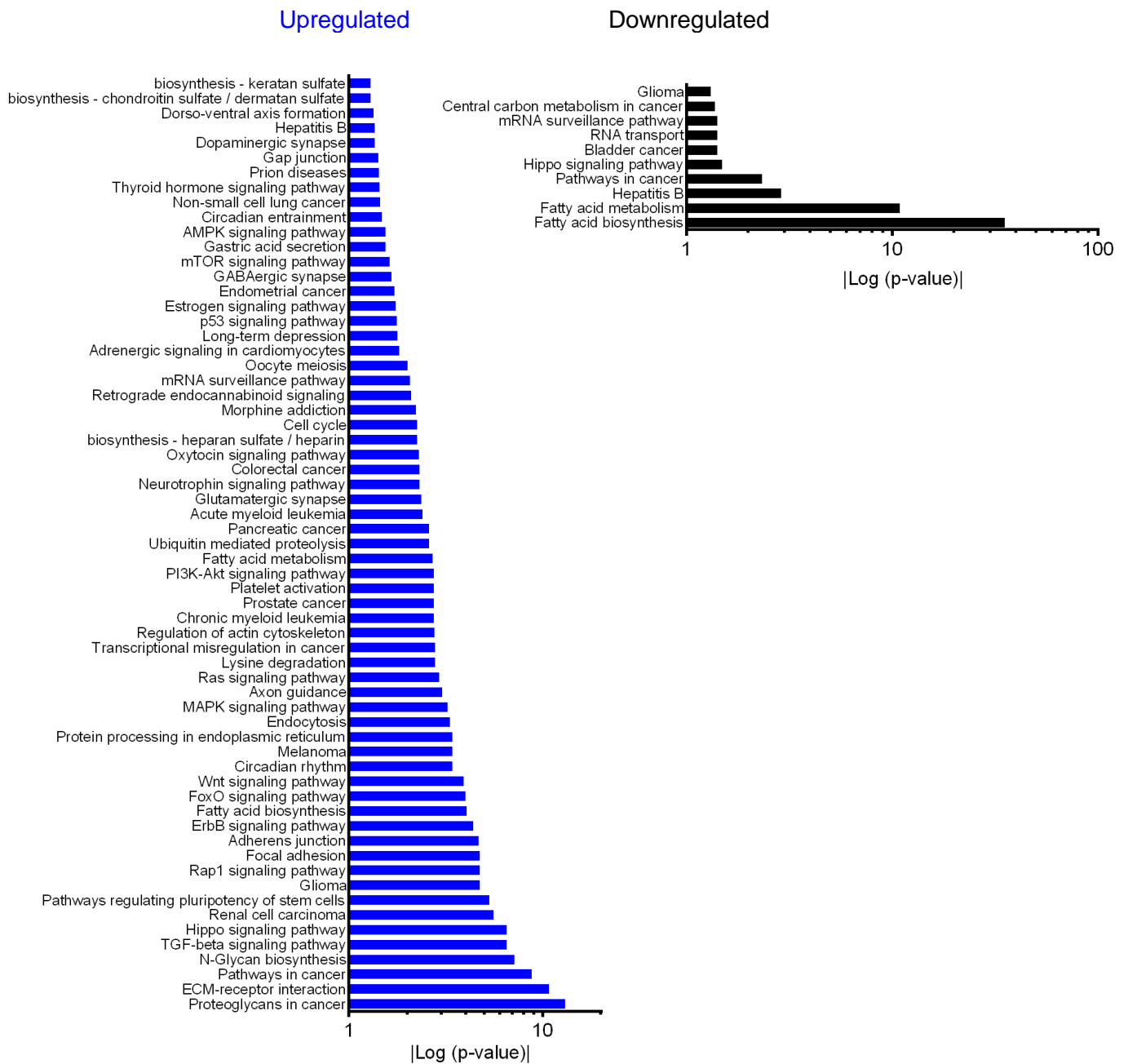


**Figure S11. KEGG pathway analysis for encapsulated vs. non-encapsulated EDCs.**

Pathways associates with up- and down-regulated miRNAs in nanovesicles isolated from 3.5% and 2% NPG encapsulated EDCs compared to non-encapsulated EDCs (mirPath v.3 using DIANA Tools).<sup>393</sup>

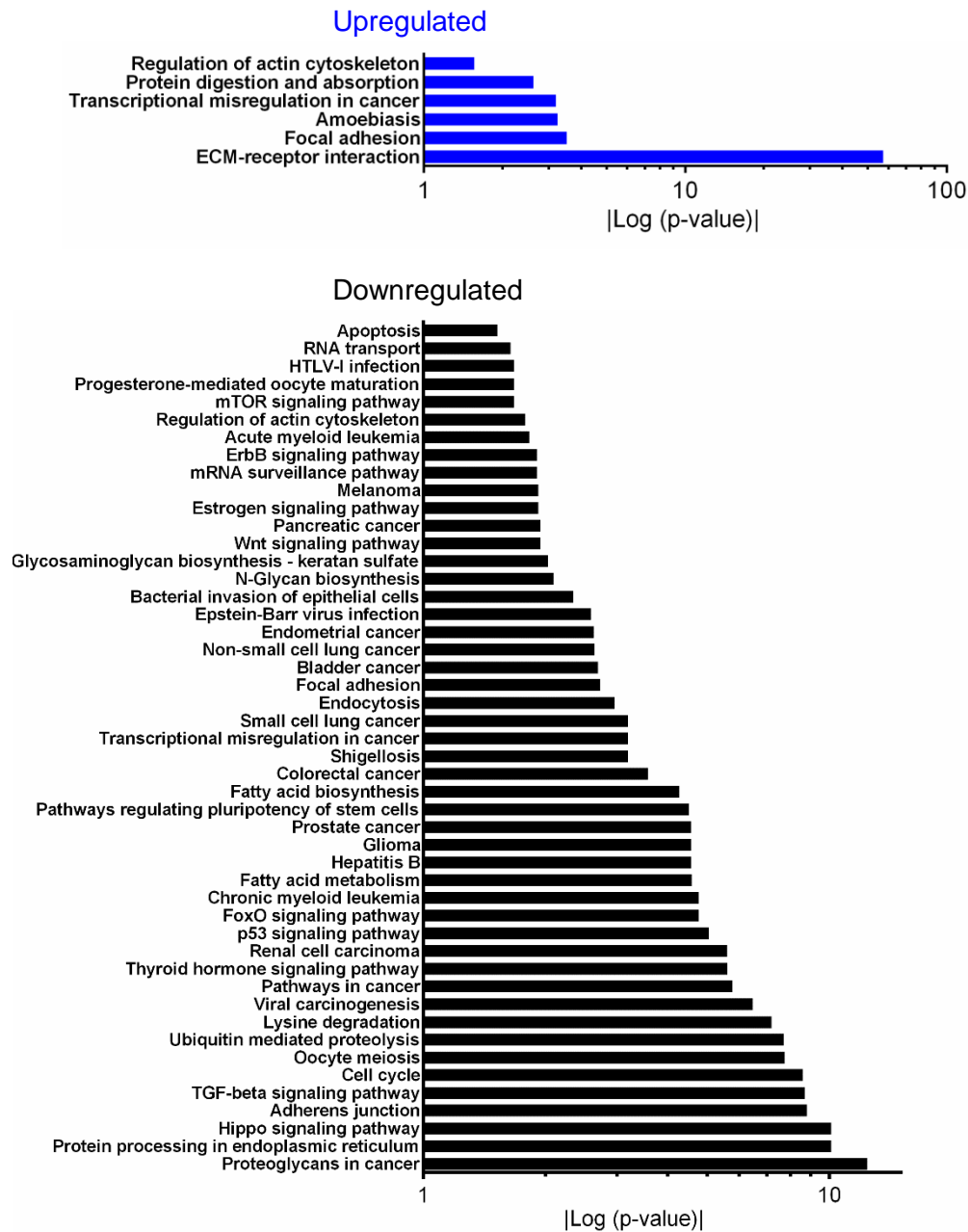


**Figure S12. KEGG pathway analysis for altering capsule composition.** Pathways associates with up- and down-regulated miRNAs in nanovesicles isolated from 3.5% NPG encapsulated EDCs compared to 2% NPG encapsulation (mirPath v.3 using DIANA Tools).<sup>393</sup>

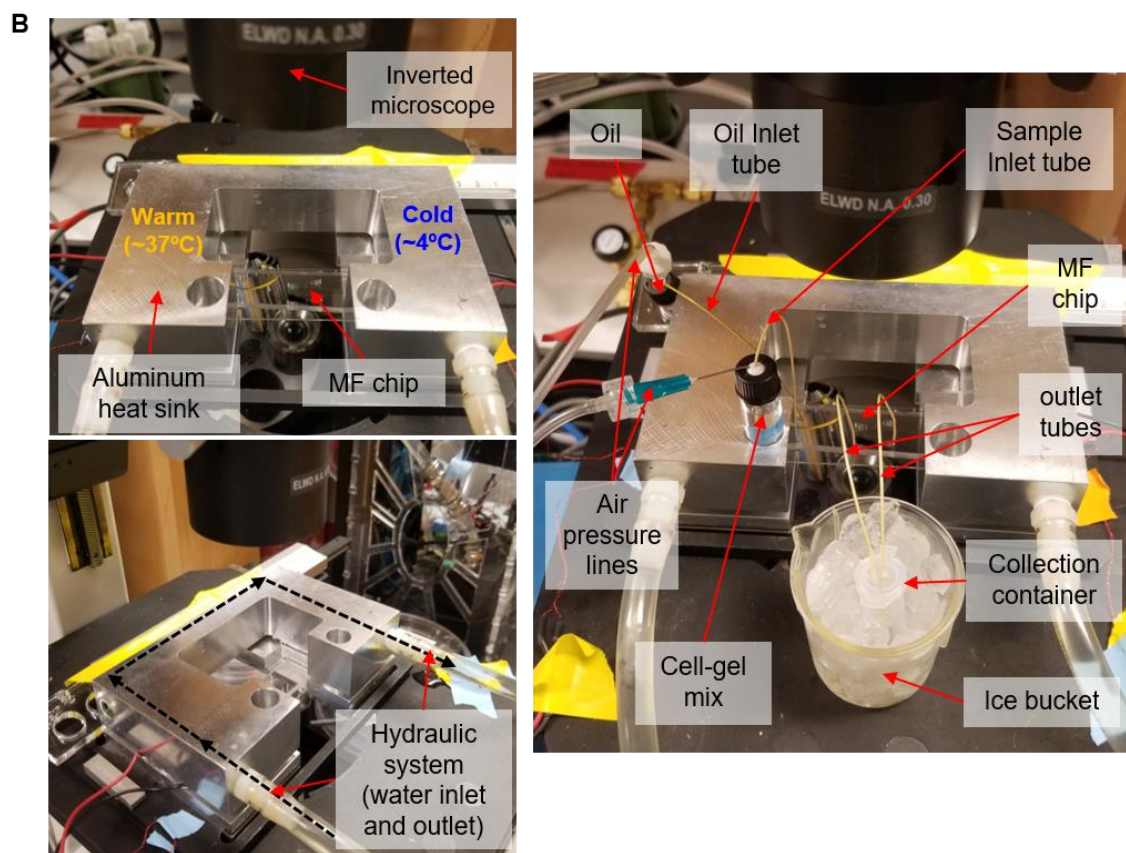
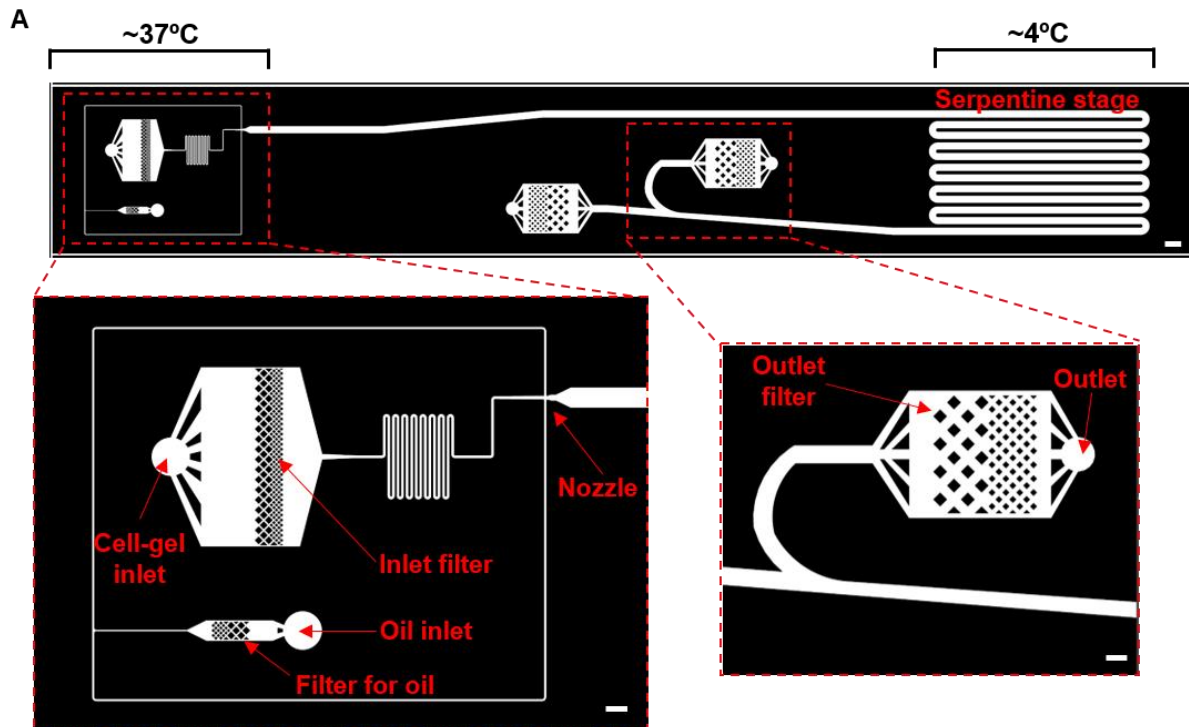


**Figure S13. Microfluidic device setup.** (A) Schemata of microfluidic chip (top panel scale bar=800  $\mu\text{m}$ ) drawn with AutoCAD; this blueprint was used as the photomask to develop the microfluidic (MF) chip. Magnified panel (scale bar= 400 $\mu\text{m}$ ) highlight key areas on the microfluidic chip. The inlet and the outlet were maintained at a temperature of  $\sim 37^{\circ}\text{C}$  and  $\sim 4^{\circ}\text{C}$ , respectively. (B) Image showing the microfluidic device setup. The top and bottom left image panels show different angles of the aluminum heat sink which holds the MF chip. The left side of the aluminum heat sink is warmed to  $\sim 37^{\circ}\text{C}$  by a hydraulics system which pumps in warmed water ( $\sim 37^{\circ}\text{C}$ ); the path of the water is indicated in black dotted lines. The right side of the aluminum block is maintained at  $4^{\circ}\text{C}$ . The image panel on the right shows the cell-gel mix and the oil container connected to the air pressure lines. Note that the cell-gel temperature is maintained at  $37^{\circ}$  by the heating block to prevent premature agarose gelation. The air pressure drives the movement of fluid (cell-gel mix or oil) into the microfluidic chip *via* the inlet tubes. The outlet tubes carry the cocoons into the ice chilled collection container (filled with appropriate culture media or buffer).

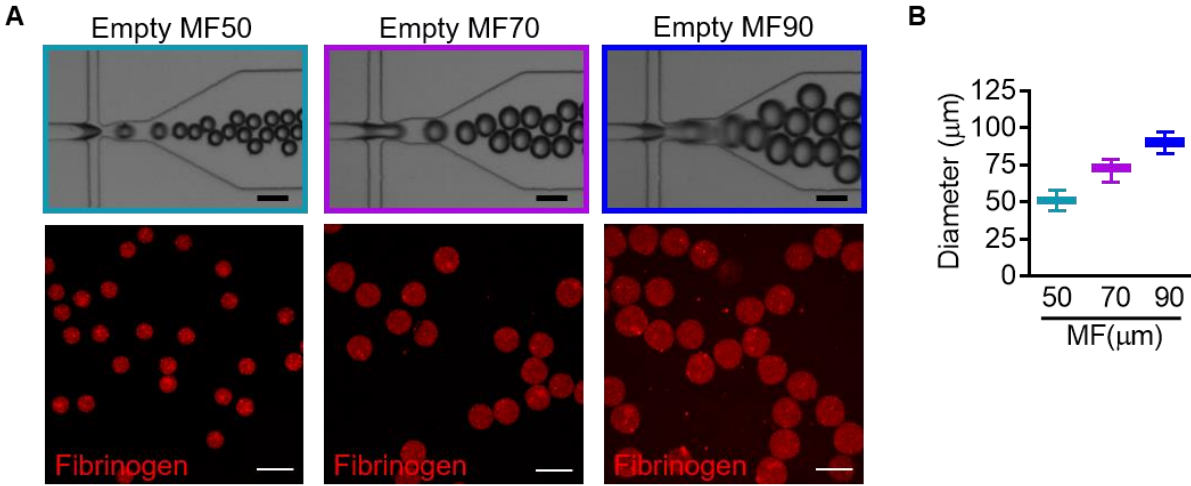


**Figure S14. Empty cocoon size and ECM distribution.** (A) Top panels show empty cocoons being formed at the nozzle while the bottom panels show confocal microscope images of empty cocoons supplemented with DsRed labeled fibrinogen (Scale bar=100 μm). Extracellular matrix proteins were homogeneously distributed throughout the cocoons; cocoon size did not effect protein distribution. (B) Box and whiskers plot showing the size distribution of MF90, MF70, and MF50 cocooned EDCs. Size distributions were calculated from measuring >100 individual cocoons from three different samples.

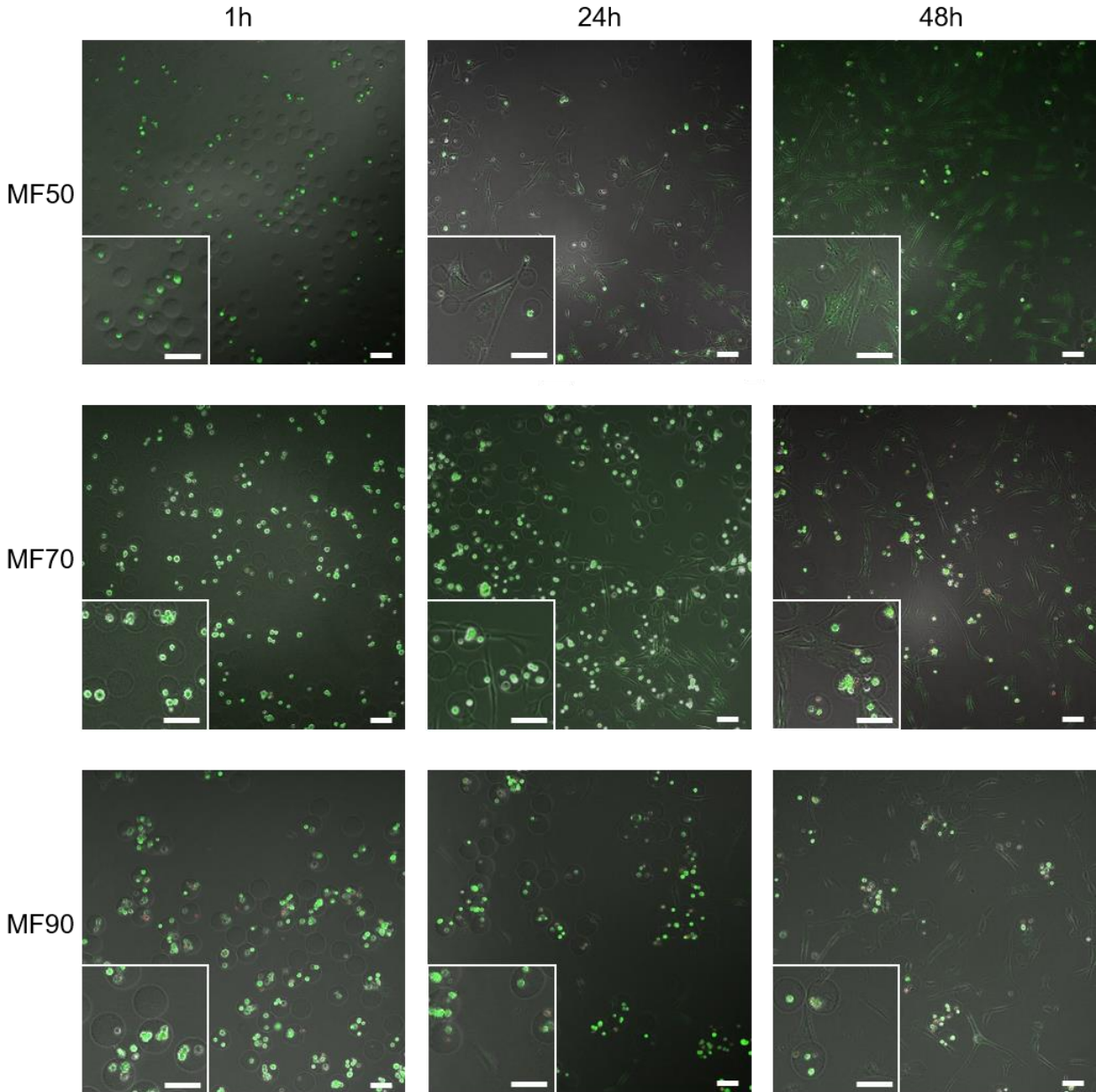


**Figure S15. EDCs viability and migration.** Representative images showing EDCs 1, 24, and 48 h post-encapsulation and labeled with live (green)/dead (red) stain. Images were acquired using confocal microscope (10X objective lens) with an enlarged image shown at the bottom left corner. Over one hundred live/dead stained cells from three different samples were counted to quantify intracapsular EDC viability. To measure the rate of cell escaping the cocoons (*i.e.* occupancy half-time), the number of cells inside

(rounded cell morphology) and outside (spindle cell morphology) of the cocoons were counted at various time points. Scale bar=100  $\mu$ m.

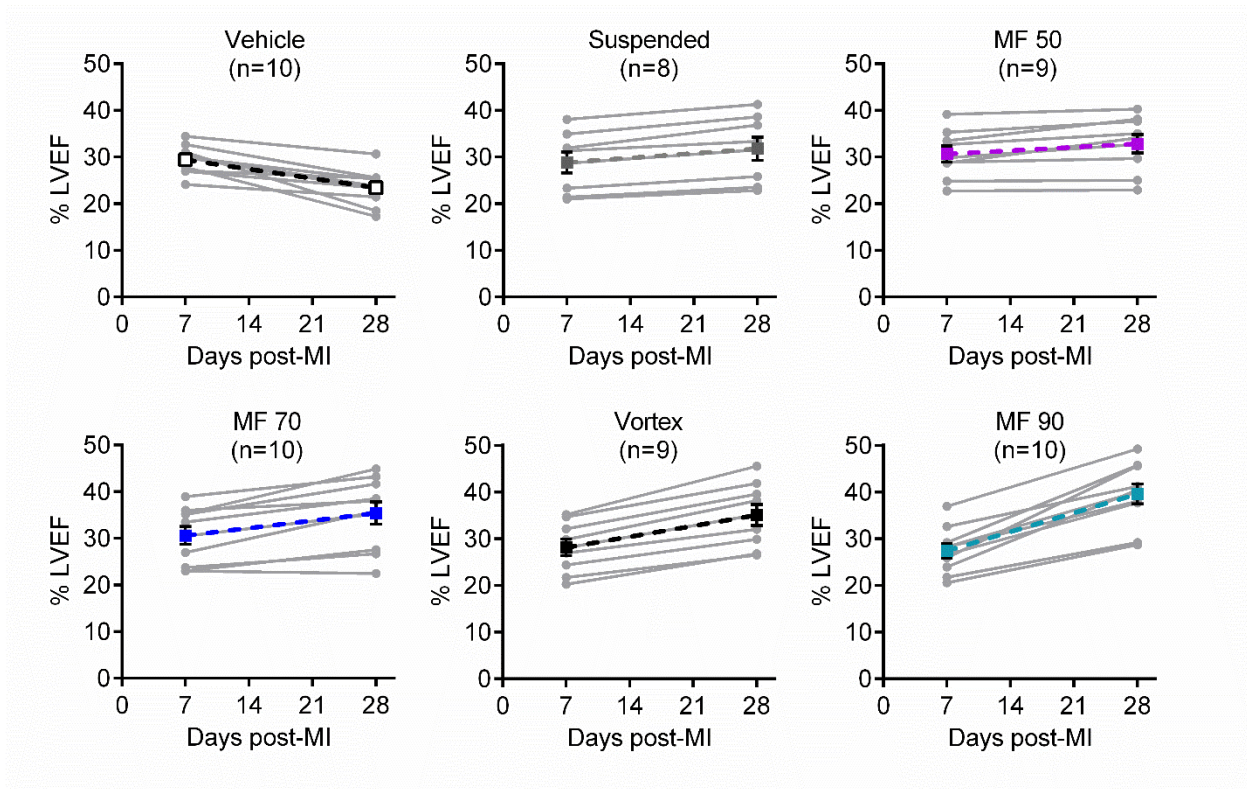


**Figure S16. Left ventricular ejection fraction plot.** Echo analysis showing left ventricle ejection fraction (LVEF) for each animal (solid grey lines) in the group and the averaged values (dotted lines). Error corresponds to standard error mean.

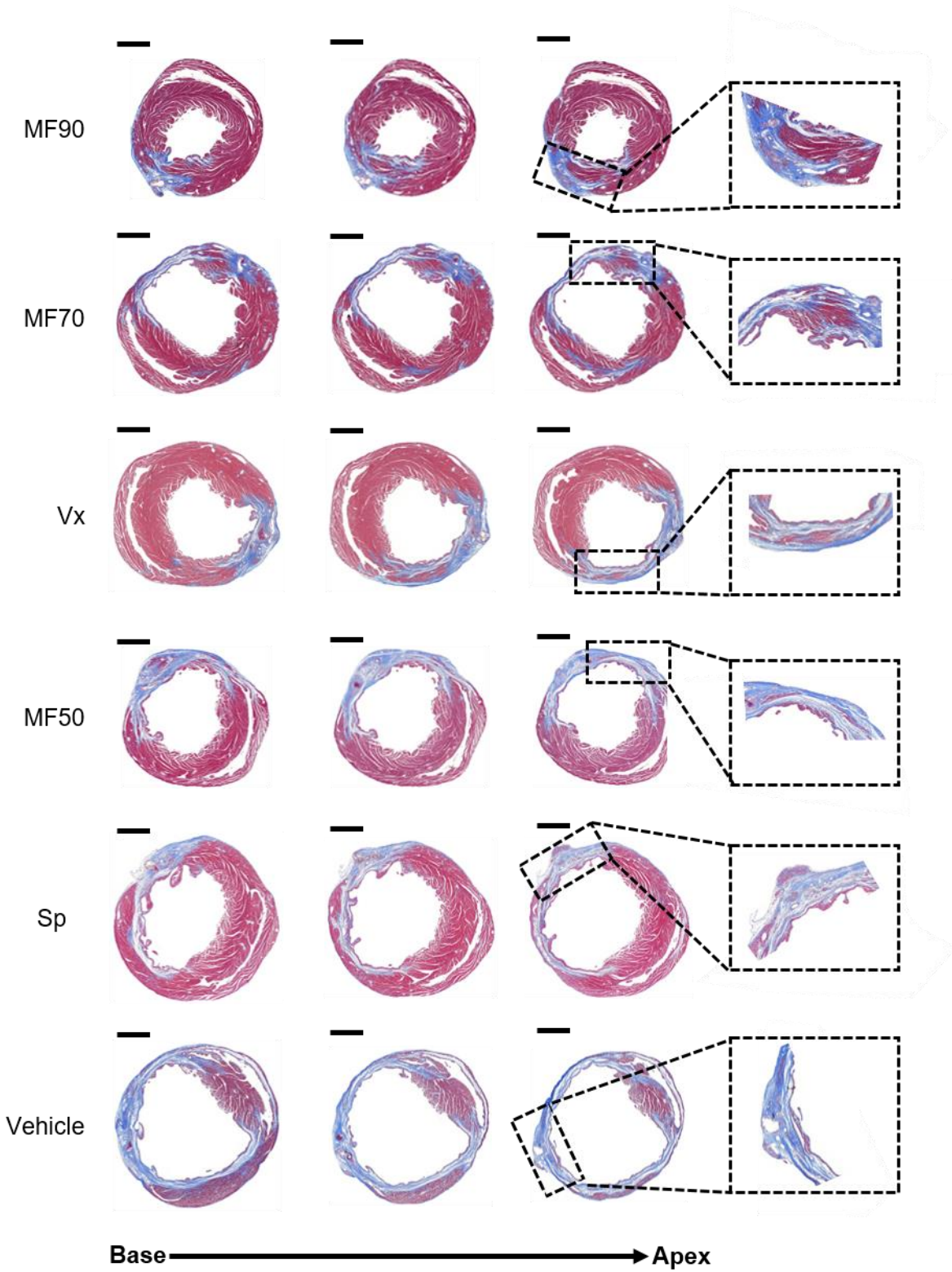


**Figure S17. Study 2: Scar size.** Representative Masson's trichrome images showing scar burden (blue= scar, red= viable myocardium) from 3 different section of the heart (scale bar= 1000  $\mu$ m). Box highlights areas of viable tissue within the infarct region.

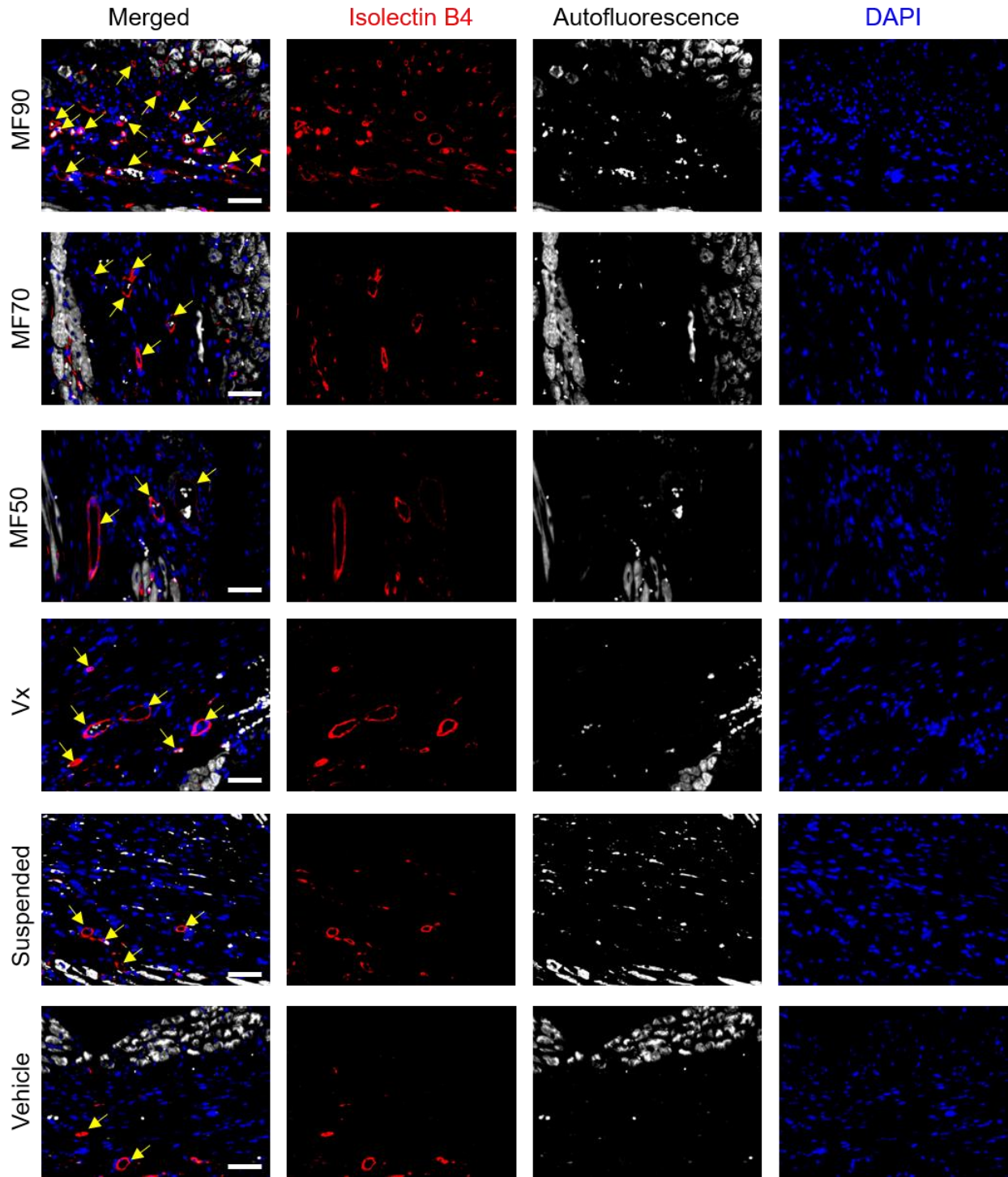


**Figure S18. Study 2: Vessel density.** Representative images showing blood vessels (indicated by the yellow arrows) within infarct/peri-infarct regions of the heart. Vessels were stained with Isolectin B4 (scale bar=50  $\mu$ m).

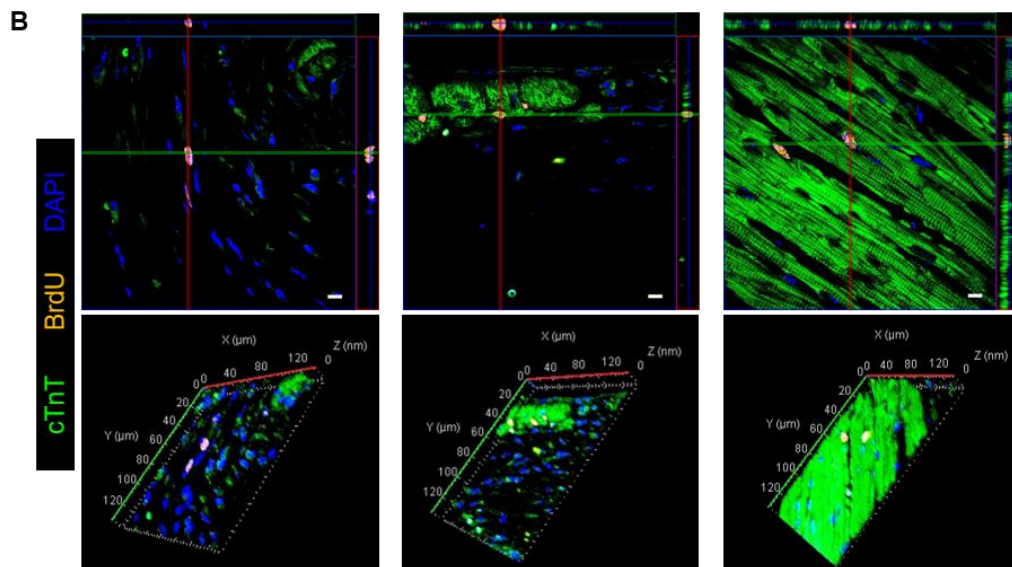
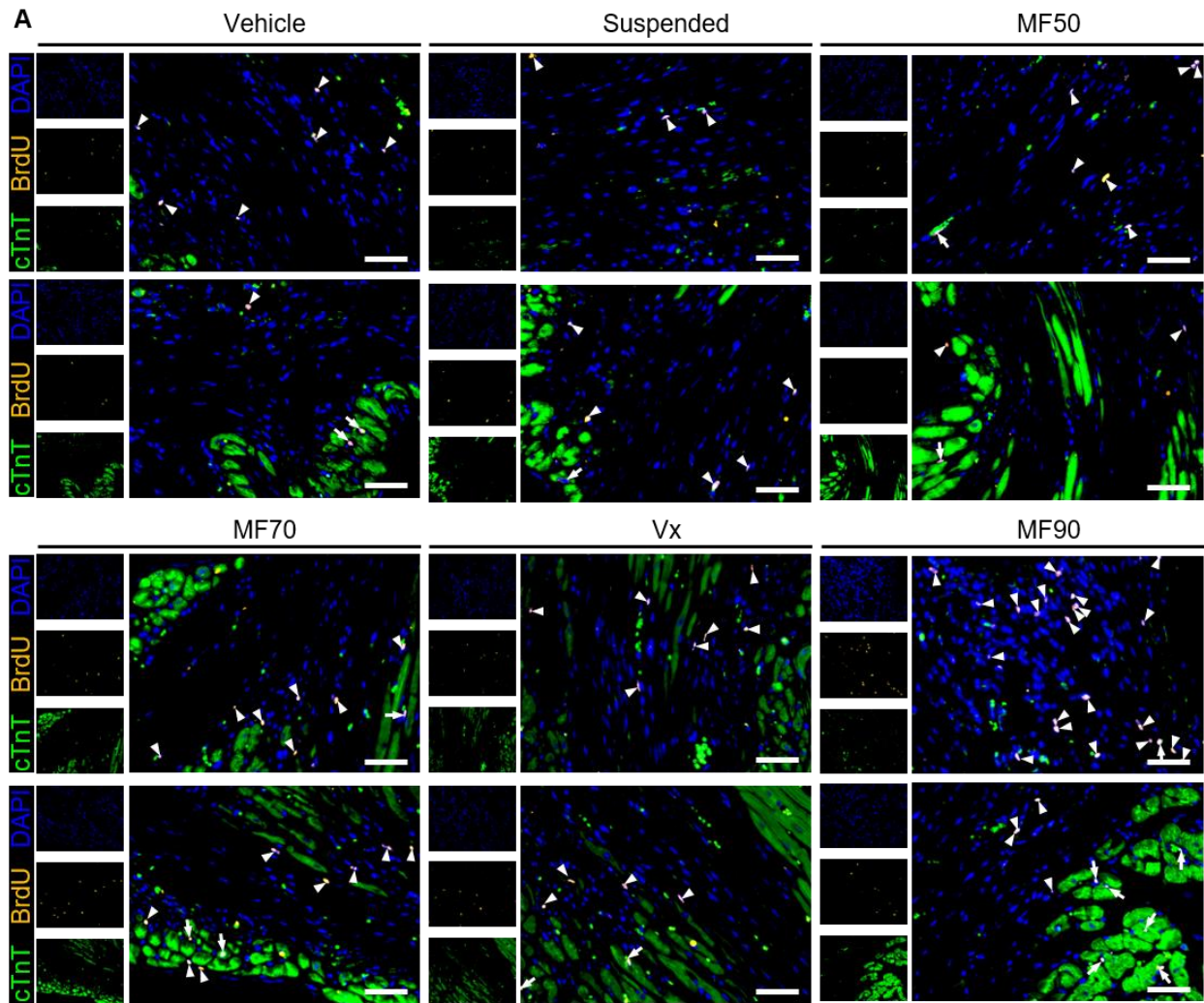


**Figure S19. Study 2: BrdU staining.** (A) Representative images showing proliferating cells (BrdU positive cells) within infarct/peri-infarct region of the heart; two images are shown for each group. Non-cardiomyocyte proliferating cells (BrdU+/cTnT-) are indicated by solid arrow heads, and proliferating cardiomyocytes (BrdU+/cTnT+) are indicated by arrows (scale bar=50  $\mu$ m). (B) Ortho-representation of z-stack images (top panels) and three dimensional reconstruction (bottom panels) confirm co-localization of BrdU stain (orange) within nucleus (DAPI; blue). Images left to right are taken from the infarct, border, and remote regions of the heart, respectively.

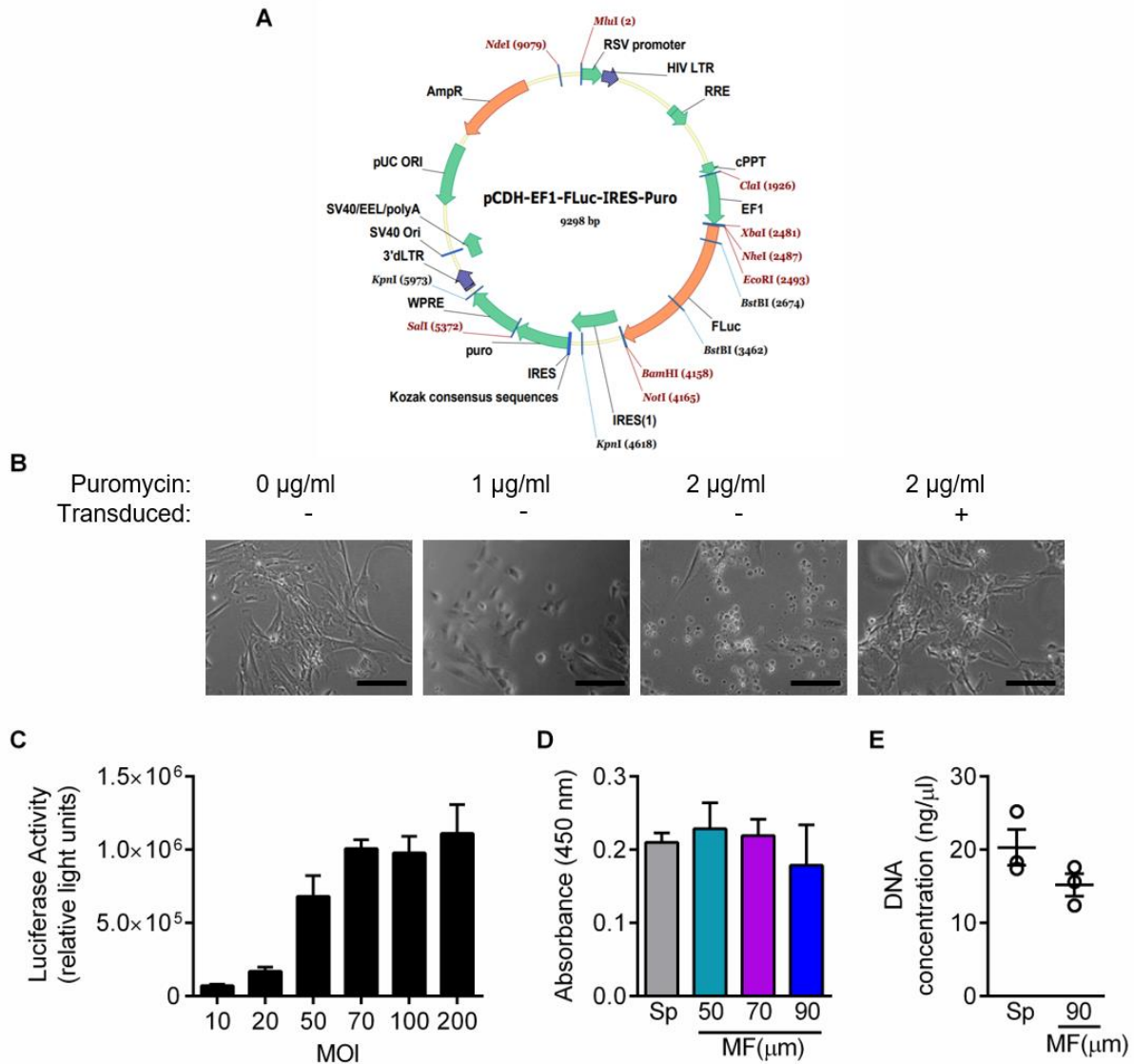


**Figure S20. Transgenic EDCs expressing firefly luciferase.** (A) Diagram of transfer plasmid containing firefly luciferase (FLuc). This vector was used to construct a third-generation virus used to transduce EDCs. The expression of luciferase was driven by constitutive elongation factor 1 (EF1) promoter. With the insertion of internal ribosome entry site (IRES), puromycin (puro) resistance gene was co-expressed with firefly luciferase. (B) Transgenic EDCs expressing luciferase were purified by eliminating non-transduced cells using puromycin. First, we determined that 2.0  $\mu\text{g/ml}$  puromycin was

sufficient to eliminate 100% of non-transduced EDCs within 24. Transduced-EDCs were then incubated with 2.0 µg/ml puromycin for 24 h. (C) EDC luciferase activity plotted against the different virus-to-cell ratio (*i.e.* multiplicity of infection (MOI) used for transduction. Maximal viral transduction efficiency was achieved with MOI 50 (*i.e.*, the luciferase activity plateaued at this point). All future virus transduction experiments were carried out using MOI of 50. (D) Colorimetric cell viability assay (CCK-8) shows that roughly equal amounts of cells were counted using hemocytometer and loaded into each well; measurements taken 24 h after plating cells (n=4; no statistical significance was observed between the groups). (E) The graph showed that similar amount of DNA was extracted from 100 000 hemocytometer counted MF90 cocooned or suspended (Sp) EDCs (n=3; no statistical significance was observed between the groups). Error corresponds to standard error mean.

Copyright statement for published review article: Cellular mechanism underlying cardiac engraftment of stem cells. *Expert Opinion in Biological Therapy*, 2017, 17(9):1127-1143.

6/13/2018

Rightslink® by Copyright Clearance Center



RightsLink®

[Home](#)

[Account Info](#)

[Help](#)



**Title:** Cellular mechanisms underlying cardiac engraftment of stem cells

**Author:** Pushpinder Kanda, Darryl R Davis

**Publication:** Expert Opinion on Biological Therapy

**Publisher:** Taylor & Francis

**Date:** Sep 2, 2017

Rights managed by Taylor & Francis

Logged in as:  
Pushpinder Kanda  
Mr. Pushpinder Kanda

[LOGOUT](#)

#### Thesis/Dissertation Reuse Request

Taylor & Francis is pleased to offer reuses of its content for a thesis or dissertation free of charge contingent on resubmission of permission request if work is published.

Copyright statement for published original research: Deterministic Encapsulation of Human Cardiac Stem Cells in Variable Composition Nanoporous Gel Cocoons To Enhance Therapeutic Repair of Injured Myocardium. *ACS Nano*, 2018, 12 (5), pp 4338–4350.



RightsLink®

Home

Account Info

Help



ACS Publications  
Most Trusted. Most Cited. Most Read.

**Title:** Deterministic Encapsulation of Human Cardiac Stem Cells in Variable Composition Nanoporous Gel Cocoons To Enhance Therapeutic Repair of Injured Myocardium

Logged in as:  
Pushpinder Kanda  
Mr. Pushpinder Kanda

LOGOUT

**Author:** Pushpinder Kanda, Emilio I. Alarcon, Tanya Yeuchy, et al

**Publication:** ACS Nano

**Publisher:** American Chemical Society

**Date:** May 1, 2018

Copyright © 2018, American Chemical Society

#### PERMISSION/LICENSE IS GRANTED FOR YOUR ORDER AT NO CHARGE

This type of permission/license, instead of the standard Terms & Conditions, is sent to you because no fee is being charged for your order. Please note the following:

- Permission is granted for your request in both print and electronic formats, and translations.
- If figures and/or tables were requested, they may be adapted or used in part.
- Please print this page for your records and send a copy of it to your publisher/graduate school.
- Appropriate credit for the requested material should be given as follows: "Reprinted (adapted) with permission from (COMPLETE REFERENCE CITATION). Copyright (YEAR) American Chemical Society." Insert appropriate information in place of the capitalized words.
- One-time permission is granted only for the use specified in your request. No additional uses are granted (such as derivative works or other editions). For any other uses, please submit a new request.

## 7.0 Bibliography

1. Ambrosy AP, Fonarow GC, Butler J, Chioncel O, Greene SJ, Vaduganathan M, Nodari S, Lam CS, Sato N, Shah AN, Gheorghiade M: **The global health and economic burden of hospitalizations for heart failure: Lessons learned from hospitalized heart failure registries.** *Journal of the American College of Cardiology* (2014) **63**(12):1123-1133.
2. Yeung DF, Boom NK, Guo H, Lee DS, Schultz SE, Tu JV: **Trends in the incidence and outcomes of heart failure in ontario, canada: 1997 to 2007.** *CMAJ : Canadian Medical Association journal = journal de l'Association medicale canadienne* (2012) **184**(14):E765-773.
3. Roger VL: **Epidemiology of heart failure.** *Circulation research* (2013) **113**(6):646-659.
4. ICES: **Cardiovascular health & services in ontario: An ices atlas.** (2006).
5. Tran DT, Ohinmaa A, Thanh NX, Howlett JG, Ezekowitz JA, McAlister FA, Kaul P: **The current and future financial burden of hospital admissions for heart failure in canada: A cost analysis.** *CMAJ open* (2016) **4**(3):E365-E370.
6. Beltrami AP, Urbanek K, Kajstura J, Yan SM, Finato N, Bussani R, Nadal-Ginard B, Silvestri F, Leri A, Beltrami CA, Anversa P: **Evidence that human cardiac myocytes divide after myocardial infarction.** *The New England journal of medicine* (2001) **344**(23):1750-1757.
7. Kajstura J, Gurusamy N, Ogorek B, Goichberg P, Clavo-Rondon C, Hosoda T, D'Amario D, Bardelli S, Beltrami AP, Cesselli D, Bussani R *et al*: **Myocyte turnover in the aging human heart.** *Circulation research* (2010) **107**(11):1374-1386.
8. Urbanek K, Cesselli D, Rota M, Nascimbene A, De Angelis A, Hosoda T, Bearzi C, Boni A, Bolli R, Kajstura J, Anversa P *et al*: **Stem cell niches in the adult mouse heart.** *Proceedings of the National Academy of Sciences of the United States of America* (2006) **103**(24):9226-9231.
9. Beltrami AP, Barlucchi L, Torella D, Baker M, Limana F, Chimenti S, Kasahara H, Rota M, Musso E, Urbanek K, Leri A *et al*: **Adult cardiac stem cells are multipotent and support myocardial regeneration.** *Cell* (2003) **114**(6):763-776.

10. Hierlihy AM, Seale P, Lobe CG, Rudnicki MA, Megeney LA: **The post-natal heart contains a myocardial stem cell population.** *FEBS letters* (2002) **530**(1-3):239-243.
11. Nosedá M, Harada M, McSweeney S, Leja T, Belian E, Stuckey DJ, Abreu Paiva MS, Habib J, Macaulay I, de Smith AJ, al-Beidh F *et al*: **Pdgfr $\alpha$  demarcates the cardiogenic clonogenic sca1<sup>+</sup> stem/progenitor cell in adult murine myocardium.** *Nature communications* (2015) **6**(6930).
12. Smith RR, Barile L, Cho HC, Leppo MK, Hare JM, Messina E, Giacomello A, Abraham MR, Marban E: **Regenerative potential of cardiosphere-derived cells expanded from percutaneous endomyocardial biopsy specimens.** *Circulation* (2007) **115**(7):896-908.
13. Davis DR, Ruckdeschel Smith R, Marban E: **Human cardiospheres are a source of stem cells with cardiomyogenic potential.** *Stem cells* (2010) **28**(5):903-904.
14. Hodgkinson CP, Bareja A, Gomez JA, Dzau VJ: **Emerging concepts in paracrine mechanisms in regenerative cardiovascular medicine and biology.** *Circulation research* (2016) **118**(1):95-107.
15. Terrovitis JV, Smith RR, Marban E: **Assessment and optimization of cell engraftment after transplantation into the heart.** *Circulation research* (2010) **106**(3):479-494.
16. Hong KU, Guo Y, Li QH, Cao P, Al-Maqtari T, Vajravelu BN, Du J, Book MJ, Zhu X, Nong Y, Bhatnagar A *et al*: **C-kit<sup>+</sup> cardiac stem cells alleviate post-myocardial infarction left ventricular dysfunction despite poor engraftment and negligible retention in the recipient heart.** *PloS one* (2014) **9**(5):e96725.
17. Hofmann M, Wollert KC, Meyer GP, Menke A, Arseniev L, Hertenstein B, Ganser A, Knapp WH, Drexler H: **Monitoring of bone marrow cell homing into the infarcted human myocardium.** *Circulation* (2005) **111**(17):2198-2202.
18. Kamihata H, Matsubara H, Nishiue T, Fujiyama S, Tsutsumi Y, Ozono R, Masaki H, Mori Y, Iba O, Tateishi E, Kosaki A *et al*: **Implantation of bone marrow mononuclear cells into ischemic myocardium enhances collateral perfusion and regional function via side supply of angioblasts, angiogenic ligands, and cytokines.** *Circulation* (2001) **104**(9):1046-1052.

19. Tomita S, Li RK, Weisel RD, Mickle DA, Kim EJ, Sakai T, Jia ZQ: **Autologous transplantation of bone marrow cells improves damaged heart function.** *Circulation* (1999) **100**(19 Suppl):II247-256.
20. Cao F, Sun D, Li C, Narsinh K, Zhao L, Li X, Feng X, Zhang J, Duan Y, Wang J, Liu D *et al*: **Long-term myocardial functional improvement after autologous bone marrow mononuclear cells transplantation in patients with st-segment elevation myocardial infarction: 4 years follow-up.** *European heart journal* (2009) **30**(16):1986-1994.
21. Lunde K, Solheim S, Aakhus S, Arnesen H, Abdelnoor M, Egeland T, Endresen K, Ilebakk A, Mangschau A, Fjeld JG, Smith HJ *et al*: **Intracoronary injection of mononuclear bone marrow cells in acute myocardial infarction.** *The New England journal of medicine* (2006) **355**(12):1199-1209.
22. Strauer BE, Brehm M, Zeus T, Kostering M, Hernandez A, Sorg RV, Kogler G, Wernet P: **Repair of infarcted myocardium by autologous intracoronary mononuclear bone marrow cell transplantation in humans.** *Circulation* (2002) **106**(15):1913-1918.
23. Grajek S, Popiel M, Gil L, Breborowicz P, Lesiak M, Czepczynski R, Sawinski K, Straburzynska-Migaj E, Araszkievicz A, Czyz A, Kozłowska-Skrzypczak M *et al*: **Influence of bone marrow stem cells on left ventricle perfusion and ejection fraction in patients with acute myocardial infarction of anterior wall: Randomized clinical trial: Impact of bone marrow stem cell intracoronary infusion on improvement of microcirculation.** *European heart journal* (2010) **31**(6):691-702.
24. Hirsch A, Nijveldt R, van der Vleuten PA, Tijssen JG, van der Giessen WJ, Tio RA, Waltenberger J, ten Berg JM, Doevendans PA, Aengevaeren WR, Zwaginga JJ *et al*: **Intracoronary infusion of mononuclear cells from bone marrow or peripheral blood compared with standard therapy in patients after acute myocardial infarction treated by primary percutaneous coronary intervention: Results of the randomized controlled hebe trial.** *European heart journal* (2011) **32**(14):1736-1747.
25. Fisher SA, Zhang H, Doree C, Mathur A, Martin-Rendon E: **Stem cell treatment for acute myocardial infarction.** *The Cochrane database of systematic reviews* (2015) 9:CD006536.
26. Rosen MR, Myerburg RJ, Francis DP, Cole GD, Marban E: **Translating stem cell research to cardiac disease therapies: Pitfalls and prospects for**

- improvement.** *Journal of the American College of Cardiology* (2014) **64**(9):922-937.
27. Poglajen G, Sever M, Cukjati M, Cernelc P, Knezevic I, Zemljic G, Haddad F, Wu JC, Vrtovec B: **Effects of transendocardial cd34+ cell transplantation in patients with ischemic cardiomyopathy.** *Circulation Cardiovascular interventions* (2014) **7**(4):552-559.
  28. Mansour S, Roy DC, Bouchard V, Stevens LM, Gobeil F, Rivard A, Leclerc G, Reeves F, Noiseux N: **One-year safety analysis of the compare-ami trial: Comparison of intracoronary injection of cd133 bone marrow stem cells to placebo in patients after acute myocardial infarction and left ventricular dysfunction.** *Bone marrow research* (2011) **2011**(385124).
  29. Taljaard M, Ward MR, Kutryk MJ, Courtman DW, Camack NJ, Goodman SG, Parker TG, Dick AJ, Galipeau J, Stewart DJ: **Rationale and design of enhanced angiogenic cell therapy in acute myocardial infarction (enact-ami): The first randomized placebo-controlled trial of enhanced progenitor cell therapy for acute myocardial infarction.** *American heart journal* (2010) **159**(3):354-360.
  30. Kawamoto A, Iwasaki H, Kusano K, Murayama T, Oyamada A, Silver M, Hulbert C, Gavin M, Hanley A, Ma H, Kearney M *et al*: **Cd34-positive cells exhibit increased potency and safety for therapeutic neovascularization after myocardial infarction compared with total mononuclear cells.** *Circulation* (2006) **114**(20):2163-2169.
  31. Tendera M, Wojakowski W, Ruzyllo W, Chojnowska L, Kepka C, Tracz W, Musialek P, Piwowarska W, Nessler J, Buszman P, Grajek S *et al*: **Intracoronary infusion of bone marrow-derived selected cd34+cxcr4+ cells and non-selected mononuclear cells in patients with acute stemi and reduced left ventricular ejection fraction: Results of randomized, multicentre myocardial regeneration by intracoronary infusion of selected population of stem cells in acute myocardial infarction (regent) trial.** *European heart journal* (2009) **30**(11):1313-1321.
  32. Blocklet D, Toungouz M, Berkenboom G, Lambermont M, Unger P, Preumont N, Stoupele E, Egrise D, Degaute JP, Goldman M, Goldman S: **Myocardial homing of nonmobilized peripheral-blood cd34+ cells after intracoronary injection.** *Stem cells* (2006) **24**(2):333-336.
  33. Hou D, Youssef EA, Brinton TJ, Zhang P, Rogers P, Price ET, Yeung AC, Johnstone BH, Yock PG, March KL: **Radiolabeled cell distribution after intramyocardial, intracoronary, and interstitial retrograde coronary venous**

- delivery: Implications for current clinical trials.** *Circulation* (2005) **112**(9 Suppl):1150-156.
34. Vrtovec B, Poglajen G, Lezaic L, Sever M, Socan A, Domanovic D, Cernelc P, Torre-Amione G, Haddad F, Wu JC: **Comparison of transendocardial and intracoronary cd34+ cell transplantation in patients with nonischemic dilated cardiomyopathy.** *Circulation* (2013) **128**(11 Suppl 1):S42-49.
  35. Singh A, Singh A, Sen D: **Mesenchymal stem cells in cardiac regeneration: A detailed progress report of the last 6 years (2010-2015).** *Stem cell research & therapy* (2016) **7**(1):82.
  36. Dominici M, Le Blanc K, Mueller I, Slaper-Cortenbach I, Marini F, Krause D, Deans R, Keating A, Prockop D, Horwitz E: **Minimal criteria for defining multipotent mesenchymal stromal cells. The international society for cellular therapy position statement.** *Cytotherapy* (2006) **8**(4):315-317.
  37. Parivar K, Baharara J, Sheikholeslami A: **Neural differentiation of mouse bone marrow-derived mesenchymal stem cells treated with sex steroid hormones and basic fibroblast growth factor.** *Cell journal* (2015) **17**(1):27-36.
  38. Muller-Ehmsen J, Krausgrill B, Burst V, Schenk K, Neisen UC, Fries JW, Fleischmann BK, Hescheler J, Schwinger RH: **Effective engraftment but poor mid-term persistence of mononuclear and mesenchymal bone marrow cells in acute and chronic rat myocardial infarction.** *Journal of molecular and cellular cardiology* (2006) **41**(5):876-884.
  39. Menasche P, Hagege AA, Scorsin M, Pouzet B, Desnos M, Duboc D, Schwartz K, Vilquin JT, Marolleau JP: **Myoblast transplantation for heart failure.** *Lancet* (2001) **357**(9252):279-280.
  40. Marelli D, Desrosiers C, el-Alfy M, Kao RL, Chiu RC: **Cell transplantation for myocardial repair: An experimental approach.** *Cell transplantation* (1992) **1**(6):383-390.
  41. Ghostine S, Carrion C, Souza LC, Richard P, Bruneval P, Vilquin JT, Pouzet B, Schwartz K, Menasche P, Hagege AA: **Long-term efficacy of myoblast transplantation on regional structure and function after myocardial infarction.** *Circulation* (2002) **106**(12 Suppl 1):1131-136.

42. Brasselet C, Morichetti MC, Messas E, Carrion C, Bissery A, Bruneval P, Vilquin JT, Lafont A, Hagege AA, Menasche P, Desnos M: **Skeletal myoblast transplantation through a catheter-based coronary sinus approach: An effective means of improving function of infarcted myocardium.** *European heart journal* (2005) **26**(15):1551-1556.
43. Menasche P, Alfieri O, Janssens S, McKenna W, Reichenspurner H, Trinquart L, Vilquin JT, Marolleau JP, Seymour B, Larghero J, Lake S *et al*: **The myoblast autologous grafting in ischemic cardiomyopathy (magic) trial: First randomized placebo-controlled study of myoblast transplantation.** *Circulation* (2008) **117**(9):1189-1200.
44. Veltman CE, Soliman OI, Geleijnse ML, Vletter WB, Smits PC, ten Cate FJ, Jordaens LJ, Balk AH, Serruys PW, Boersma E, van Domburg RT *et al*: **Four-year follow-up of treatment with intramyocardial skeletal myoblasts injection in patients with ischaemic cardiomyopathy.** *European heart journal* (2008) **29**(11):1386-1396.
45. Mount S, Davis DR: **Electrical effects of stem cell transplantation for ischaemic cardiomyopathy: Friend or foe?** *The Journal of physiology* (2016) **594**(9):2511-2524.
46. Abraham MR, Henrikson CA, Tung L, Chang MG, Aon M, Xue T, Li RA, B OR, Marban E: **Antiarrhythmic engineering of skeletal myoblasts for cardiac transplantation.** *Circulation research* (2005) **97**(2):159-167.
47. Fernandes S, van Rijen HV, Forest V, Evain S, Leblond AL, Merot J, Charpentier F, de Bakker JM, Lemarchand P: **Cardiac cell therapy: Overexpression of connexin43 in skeletal myoblasts and prevention of ventricular arrhythmias.** *Journal of cellular and molecular medicine* (2009) **13**(9B):3703-3712.
48. Mummery C, Ward-van Oostwaard D, Doevendans P, Spijker R, van den Brink S, Hassink R, van der Heyden M, Opthof T, Pera M, de la Riviere AB, Passier R *et al*: **Differentiation of human embryonic stem cells to cardiomyocytes: Role of coculture with visceral endoderm-like cells.** *Circulation* (2003) **107**(21):2733-2740.
49. Takahashi K, Yamanaka S: **Induction of pluripotent stem cells from mouse embryonic and adult fibroblast cultures by defined factors.** *Cell* (2006) **126**(4):663-676.

50. Hartman ME, Dai DF, Laflamme MA: **Human pluripotent stem cells: Prospects and challenges as a source of cardiomyocytes for in vitro modeling and cell-based cardiac repair.** *Advanced drug delivery reviews* (2016) **96**(3-17).
51. Laflamme MA, Chen KY, Naumova AV, Muskheli V, Fugate JA, Dupras SK, Reinecke H, Xu C, Hassanipour M, Police S, O'Sullivan C *et al*: **Cardiomyocytes derived from human embryonic stem cells in pro-survival factors enhance function of infarcted rat hearts.** *Nature biotechnology* (2007) **25**(9):1015-1024.
52. Shiba Y, Fernandes S, Zhu WZ, Filice D, Muskheli V, Kim J, Palpant NJ, Gantz J, Moyes KW, Reinecke H, Van Biber B *et al*: **Human es-cell-derived cardiomyocytes electrically couple and suppress arrhythmias in injured hearts.** *Nature* (2012) **489**(7415):322-325.
53. Chong JJ, Yang X, Don CW, Minami E, Liu YW, Weyers JJ, Mahoney WM, Van Biber B, Cook SM, Palpant NJ, Gantz JA *et al*: **Human embryonic-stem-cell-derived cardiomyocytes regenerate non-human primate hearts.** *Nature* (2014) **510**(7504):273-277.
54. Mayfield AE, Tilokee EL, Davis DR: **Resident cardiac stem cells and their role in stem cell therapies for myocardial repair.** *The Canadian journal of cardiology* (2014) **30**(11):1288-1298.
55. Urbanek K, Quaini F, Tasca G, Torella D, Castaldo C, Nadal-Ginard B, Leri A, Kajstura J, Quaini E, Anversa P: **Intense myocyte formation from cardiac stem cells in human cardiac hypertrophy.** *Proceedings of the National Academy of Sciences of the United States of America* (2003) **100**(18):10440-10445.
56. Bergmann O, Bhardwaj RD, Bernard S, Zdunek S, Barnabe-Heider F, Walsh S, Zupicich J, Alkass K, Buchholz BA, Druid H, Jovinge S *et al*: **Evidence for cardiomyocyte renewal in humans.** *Science* (2009) **324**(5923):98-102.
57. Unno K, Jain M, Liao R: **Cardiac side population cells: Moving toward the center stage in cardiac regeneration.** *Circulation research* (2012) **110**(10):1355-1363.
58. Liang SX, Khachigian LM, Ahmadi Z, Yang M, Liu S, Chong BH: **In vitro and in vivo proliferation, differentiation and migration of cardiac endothelial progenitor cells (sca1+/cd31+ side-population cells).** *Journal of thrombosis and haemostasis : JTH* (2011) **9**(8):1628-1637.

59. Liang SX, Tan TY, Gaudry L, Chong B: **Differentiation and migration of sca1+/cd31- cardiac side population cells in a murine myocardial ischemic model.** *International journal of cardiology* (2010) **138**(1):40-49.
60. Oyama T, Nagai T, Wada H, Naito AT, Matsuura K, Iwanaga K, Takahashi T, Goto M, Mikami Y, Yasuda N, Akazawa H *et al*: **Cardiac side population cells have a potential to migrate and differentiate into cardiomyocytes in vitro and in vivo.** *The Journal of cell biology* (2007) **176**(3):329-341.
61. Pfister O, Mouquet F, Jain M, Summer R, Helmes M, Fine A, Colucci WS, Liao R: **Cd31- but not cd31+ cardiac side population cells exhibit functional cardiomyogenic differentiation.** *Circulation research* (2005) **97**(1):52-61.
62. Wang X, Hu Q, Nakamura Y, Lee J, Zhang G, From AH, Zhang J: **The role of the sca-1+/cd31- cardiac progenitor cell population in postinfarction left ventricular remodeling.** *Stem cells* (2006) **24**(7):1779-1788.
63. Keith MC, Bolli R: **"String theory" of c-kit(pos) cardiac cells: A new paradigm regarding the nature of these cells that may reconcile apparently discrepant results.** *Circulation research* (2015) **116**(7):1216-1230.
64. Kazakov A, Meier T, Werner C, Hall R, Klemmer B, Korbel C, Lammert F, Maack C, Bohm M, Laufs U: **C-kit(+) resident cardiac stem cells improve left ventricular fibrosis in pressure overload.** *Stem cell research* (2015) **15**(3):700-711.
65. Bolli R, Tang XL, Sanganalmath SK, Rimoldi O, Mosna F, Abdel-Latif A, Jneid H, Rota M, Leri A, Kajstura J: **Intracoronary delivery of autologous cardiac stem cells improves cardiac function in a porcine model of chronic ischemic cardiomyopathy.** *Circulation* (2013) **128**(2):122-131.
66. Vicinanza C, Aquila I, Scalise M, Cristiano F, Marino F, Cianflone E, Mancuso T, Marotta P, Sacco W, Lewis FC, Couch L *et al*: **Adult cardiac stem cells are multipotent and robustly myogenic: C-kit expression is necessary but not sufficient for their identification.** *Cell death and differentiation* (2017) **24**(12):2101-2116.
67. Ellison GM, Vicinanza C, Smith AJ, Aquila I, Leone A, Waring CD, Henning BJ, Stirparo GG, Papait R, Scarfo M, Agosti V *et al*: **Adult c-kit(pos) cardiac stem cells are necessary and sufficient for functional cardiac regeneration and repair.** *Cell* (2013) **154**(4):827-842.

68. Rota M, Padin-Iruegas ME, Misao Y, De Angelis A, Maestroni S, Ferreira-Martins J, Fiumana E, Rastaldo R, Arcarese ML, Mitchell TS, Boni A *et al*: **Local activation or implantation of cardiac progenitor cells rescues scarred infarcted myocardium improving cardiac function.** *Circulation research* (2008) **103**(1):107-116.
69. Tang XL, Rokosh G, Sanganalmath SK, Yuan F, Sato H, Mu J, Dai S, Li C, Chen N, Peng Y, Dawn B *et al*: **Intracoronary administration of cardiac progenitor cells alleviates left ventricular dysfunction in rats with a 30-day-old infarction.** *Circulation* (2010) **121**(2):293-305.
70. Chugh AR, Beache GM, Loughran JH, Mewton N, Elmore JB, Kajstura J, Pappas P, Tatooles A, Stoddard MF, Lima JA, Slaughter MS *et al*: **Administration of cardiac stem cells in patients with ischemic cardiomyopathy: The scipio trial: Surgical aspects and interim analysis of myocardial function and viability by magnetic resonance.** *Circulation* (2012) **126**(11 Suppl 1):S54-64.
71. D'Amario D, Fiorini C, Campbell PM, Goichberg P, Sanada F, Zheng H, Hosoda T, Rota M, Connell JM, Gallegos RP, Welt FG *et al*: **Functionally competent cardiac stem cells can be isolated from endomyocardial biopsies of patients with advanced cardiomyopathies.** *Circulation research* (2011) **108**(7):857-861.
72. van Berlo JH, Kanisicak O, Maillet M, Vagnozzi RJ, Karch J, Lin SC, Middleton RC, Marban E, Molkentin JD: **C-kit<sup>+</sup> cells minimally contribute cardiomyocytes to the heart.** *Nature* (2014) **509**(7500):337-341.
73. Sultana N, Zhang L, Yan J, Chen J, Cai W, Razzaque S, Jeong D, Sheng W, Bu L, Xu M, Huang GY *et al*: **Resident c-kit(+) cells in the heart are not cardiac stem cells.** *Nature communications* (2015) **6**(8701).
74. Nadal-Ginard B, Ellison GM, Torella D: **Absence of evidence is not evidence of absence: Pitfalls of cre knock-ins in the c-kit locus.** *Circulation research* (2014) **115**(4):415-418.
75. Fischer KM, Cottage CT, Wu W, Din S, Gude NA, Avitabile D, Quijada P, Collins BL, Fransioli J, Sussman MA: **Enhancement of myocardial regeneration through genetic engineering of cardiac progenitor cells expressing pim-1 kinase.** *Circulation* (2009) **120**(21):2077-2087.
76. Messina E, De Angelis L, Frati G, Morrone S, Chimenti S, Fiordaliso F, Salio M, Battaglia M, Latronico MV, Coletta M, Vivarelli E *et al*: **Isolation and expansion**

- of adult cardiac stem cells from human and murine heart.** *Circulation research* (2004) **95**(9):911-921.
77. Davis DR, Zhang Y, Smith RR, Cheng K, Terrovitis J, Malliaras K, Li TS, White A, Makkar R, Marban E: **Validation of the cardiosphere method to culture cardiac progenitor cells from myocardial tissue.** *PloS one* (2009) **4**(9):e7195.
78. Shen D, Cheng K, Marban E: **Dose-dependent functional benefit of human cardiosphere transplantation in mice with acute myocardial infarction.** *Journal of cellular and molecular medicine* (2012) **16**(9):2112-2116.
79. Malliaras K, Makkar RR, Smith RR, Cheng K, Wu E, Bonow RO, Marban L, Mendizabal A, Cingolani E, Johnston PV, Gerstenblith G *et al*: **Intracoronary cardiosphere-derived cells after myocardial infarction: Evidence of therapeutic regeneration in the final 1-year results of the caduceus trial (cardiosphere-derived autologous stem cells to reverse ventricular dysfunction).** *Journal of the American College of Cardiology* (2014) **63**(2):110-122.
80. Davis DR, Kizana E, Terrovitis J, Barth AS, Zhang Y, Smith RR, Miake J, Marban E: **Isolation and expansion of functionally-competent cardiac progenitor cells directly from heart biopsies.** *Journal of molecular and cellular cardiology* (2010) **49**(2):312-321.
81. Chimenti I, Smith RR, Li TS, Gerstenblith G, Messina E, Giacomello A, Marban E: **Relative roles of direct regeneration versus paracrine effects of human cardiosphere-derived cells transplanted into infarcted mice.** *Circulation research* (2010) **106**(5):971-980.
82. Malliaras K, Li TS, Luthringer D, Terrovitis J, Cheng K, Chakravarty T, Galang G, Zhang Y, Schoenhoff F, Van Eyk J, Marban L *et al*: **Safety and efficacy of allogeneic cell therapy in infarcted rats transplanted with mismatched cardiosphere-derived cells.** *Circulation* (2012) **125**(1):100-112.
83. Aminzadeh MA, Tseliou E, Sun B, Cheng K, Malliaras K, Makkar RR, Marban E: **Therapeutic efficacy of cardiosphere-derived cells in a transgenic mouse model of non-ischaemic dilated cardiomyopathy.** *European heart journal* (2015) **36**(12):751-762.
84. Johnston PV, Sasano T, Mills K, Evers R, Lee ST, Smith RR, Lardo AC, Lai S, Steenbergen C, Gerstenblith G, Lange R *et al*: **Engraftment, differentiation, and**

- functional benefits of autologous cardiosphere-derived cells in porcine ischemic cardiomyopathy.** *Circulation* (2009) **120**(12):1075-1083.
85. Aminzadeh MA, Rogers RG, Fournier M, Tobin RE, Guan X, Childers MK, Andres AM, Taylor DJ, Ibrahim A, Ding X, Torrente A *et al*: **Exosome-mediated benefits of cell therapy in mouse and human models of duchenne muscular dystrophy.** *Stem cell reports* (2018) **10**(3):942-955.
86. Wagner W: **Implications of long-term culture for mesenchymal stem cells: Genetic defects or epigenetic regulation?** *Stem cell research & therapy* (2012) **3**(6):54.
87. Tang Q, Chen Q, Lai X, Liu S, Chen Y, Zheng Z, Xie Q, Maldonado M, Cai Z, Qin S, Ho G *et al*: **Malignant transformation potentials of human umbilical cord mesenchymal stem cells both spontaneously and via 3-methylcholanthrene induction.** *PloS one* (2013) **8**(12):e81844.
88. Oskouei BN, Lamirault G, Joseph C, Treuer AV, Landa S, Da Silva J, Hatzistergos K, Dauer M, Balkan W, McNiece I, Hare JM: **Increased potency of cardiac stem cells compared with bone marrow mesenchymal stem cells in cardiac repair.** *Stem cells translational medicine* (2012) **1**(2):116-124.
89. Li TS, Cheng K, Malliaras K, Smith RR, Zhang Y, Sun B, Matsushita N, Blusztajn A, Terrovitis J, Kusuoka H, Marban L *et al*: **Direct comparison of different stem cell types and subpopulations reveals superior paracrine potency and myocardial repair efficacy with cardiosphere-derived cells.** *Journal of the American College of Cardiology* (2012) **59**(10):942-953.
90. Zwetsloot PP, Vegh AM, Jansen of Lorkeers SJ, van Hout GP, Currie GL, Sena ES, Gremmels H, Buikema JW, Goumans MJ, Macleod MR, Doevendans PA *et al*: **Cardiac stem cell treatment in myocardial infarction: A systematic review and meta-analysis of preclinical studies.** *Circulation research* (2016) **118**(8):1223-1232.
91. Valente M, Nascimento DS, Cumano A, Pinto-do OP: **Sca-1+ cardiac progenitor cells and heart-making: A critical synopsis.** *Stem cells and development* (2014) **23**(19):2263-2273.
92. Marban E: **Breakthroughs in cell therapy for heart disease: Focus on cardiosphere-derived cells.** *Mayo Clinic proceedings* (2014) **89**(6):850-858.

93. Chong JJ, Murry CE: **Cardiac regeneration using pluripotent stem cells--progression to large animal models.** *Stem cell research* (2014) **13**(3 Pt B):654-665.
94. Cao F, Wagner RA, Wilson KD, Xie X, Fu JD, Drukker M, Lee A, Li RA, Gambhir SS, Weissman IL, Robbins RC *et al*: **Transcriptional and functional profiling of human embryonic stem cell-derived cardiomyocytes.** *PloS one* (2008) **3**(10):e3474.
95. Kaneko S, Yamanaka S: **To be immunogenic, or not to be: That's the ipsc question.** *Cell stem cell* (2013) **12**(4):385-386.
96. Singla DK: **Embryonic stem cells in cardiac repair and regeneration.** *Antioxidants & redox signaling* (2009) **11**(8):1857-1863.
97. Taapken SM, Nisler BS, Newton MA, Sampsell-Barron TL, Leonhard KA, McIntire EM, Montgomery KD: **Karyotypic abnormalities in human induced pluripotent stem cells and embryonic stem cells.** *Nature biotechnology* (2011) **29**(4):313-314.
98. Martins-Taylor K, Xu RH: **Concise review: Genomic stability of human induced pluripotent stem cells.** *Stem cells* (2012) **30**(1):22-27.
99. Balsam LB, Wagers AJ, Christensen JL, Kofidis T, Weissman IL, Robbins RC: **Haematopoietic stem cells adopt mature haematopoietic fates in ischaemic myocardium.** *Nature* (2004) **428**(6983):668-673.
100. Schussler-Lenz M, Beuneu C, Menezes-Ferreira M, Jekerle V, Bartunek J, Chamuleau S, Celis P, Doevendans P, O'Donovan M, Hill J, Hystad M *et al*: **Cell-based therapies for cardiac repair: A meeting report on scientific observations and european regulatory viewpoints.** *European journal of heart failure* (2016) **18**(2):133-141.
101. Lin Y, Weisdorf DJ, Solovey A, Hebbel RP: **Origins of circulating endothelial cells and endothelial outgrowth from blood.** *The Journal of clinical investigation* (2000) **105**(1):71-77.
102. Lee PS, Poh KK: **Endothelial progenitor cells in cardiovascular diseases.** *World journal of stem cells* (2014) **6**(3):355-366.

103. Bolli R, Chugh AR, D'Amario D, Loughran JH, Stoddard MF, Ikram S, Beache GM, Wagner SG, Leri A, Hosoda T, Sanada F *et al*: **Cardiac stem cells in patients with ischaemic cardiomyopathy (scipio): Initial results of a randomised phase 1 trial.** *Lancet* (2011) **378**(9806):1847-1857.
104. The Lancet E: **Expression of concern: The scipio trial.** *Lancet* (2014) **383**(9925):1279.
105. **Notice of retraction.** *Circulation* (2014).
106. Makkar RR, Smith RR, Cheng K, Malliaras K, Thomson LE, Berman D, Czer LS, Marban L, Mendizabal A, Johnston PV, Russell SD *et al*: **Intracoronary cardiosphere-derived cells for heart regeneration after myocardial infarction (caduceus): A prospective, randomised phase 1 trial.** *Lancet* (2012) **379**(9819):895-904.
107. Malliaras K, Makkar RR, Smith RR, Cheng K, Wu E, Bonow RO, Marban L, Mendizabal A, Cingolani E, Johnston PV, Gerstenblith G *et al*: **Intracoronary cardiosphere-derived cells after myocardial infarction: Evidence of therapeutic regeneration in the final 1-year results of the caduceus trial (cardiosphere-derived autologous stem cells to reverse ventricular dysfunction).** *J Am Coll Cardiol* (2014) **63**(2):110-122.
108. Terrovitis J, Lautamäki R, Bonios M, Fox J, Engles JM, Yu J, Leppo MK, Pomper MG, Wahl RL, Seidel J, Tsui BM *et al*: **Noninvasive quantification and optimization of acute cell retention by in vivo positron emission tomography after intramyocardial cardiac-derived stem cell delivery.** *Journal of the American College of Cardiology* (2009) **54**(17):1619-1626.
109. Yee K, Malliaras K, Kanazawa H, Tseliou E, Cheng K, Luthringer DJ, Ho CS, Takayama K, Minamino N, Dawkins JF, Chowdhury S *et al*: **Allogeneic cardiospheres delivered via percutaneous transendocardial injection increase viable myocardium, decrease scar size, and attenuate cardiac dilatation in porcine ischemic cardiomyopathy.** *PloS one* (2014) **9**(12):e113805.
110. Inc. C: **Capricor therapeutics provides update on allstar trial.** (2017) 1).
111. Ishigami S, Ohtsuki S, Eitoku T, Ousaka D, Kondo M, Kurita Y, Hirai K, Fukushima Y, Baba K, Goto T, Horio N *et al*: **Intracoronary cardiac progenitor cells in single ventricle physiology: The perseus (cardiac progenitor cell infusion to**

- treat univentricular heart disease) randomized phase 2 trial. *Circulation research* (2017) **120**(7):1162-1173.
112. Stanley WC: **Changes in cardiac metabolism: A critical step from stable angina to ischaemic cardiomyopathy.** *European Heart Journal Supplements* (2001) **3**(suppl O):O2-O7.
113. Tune JD, Gorman MW, Feigl EO: **Matching coronary blood flow to myocardial oxygen consumption.** *Journal of applied physiology* (2004) **97**(1):404-415.
114. Kalogeris T, Baines CP, Krenz M, Korthuis RJ: **Cell biology of ischemia/reperfusion injury.** *International review of cell and molecular biology* (2012) **298**(229-317).
115. Nallamothu BK, Bradley EH, Krumholz HM: **Time to treatment in primary percutaneous coronary intervention.** *The New England journal of medicine* (2007) **357**(16):1631-1638.
116. Circu ML, Aw TY: **Reactive oxygen species, cellular redox systems, and apoptosis.** *Free radical biology & medicine* (2010) **48**(6):749-762.
117. Taverne YJ, Bogers AJ, Duncker DJ, Merkus D: **Reactive oxygen species and the cardiovascular system.** *Oxidative medicine and cellular longevity* (2013) **2013**(862423).
118. Poon BY, Ward CA, Cooper CB, Giles WR, Burns AR, Kubes P: **Alpha(4)-integrin mediates neutrophil-induced free radical injury to cardiac myocytes.** *The Journal of cell biology* (2001) **152**(5):857-866.
119. Prabhu SD, Frangogiannis NG: **The biological basis for cardiac repair after myocardial infarction: From inflammation to fibrosis.** *Circulation research* (2016) **119**(1):91-112.
120. Nian M, Lee P, Khaper N, Liu P: **Inflammatory cytokines and postmyocardial infarction remodeling.** *Circulation research* (2004) **94**(12):1543-1553.
121. Yan X, Anzai A, Katsumata Y, Matsushashi T, Ito K, Endo J, Yamamoto T, Takeshima A, Shinmura K, Shen W, Fukuda K *et al*: **Temporal dynamics of cardiac immune cell accumulation following acute myocardial infarction.** *Journal of molecular and cellular cardiology* (2013) **62**(24-35).

122. French BA, Kramer CM: **Mechanisms of post-infarct left ventricular remodeling.** *Drug discovery today Disease mechanisms* (2007) **4**(3):185-196.
123. Opitz CA, Litzemberger UM, Lutz C, Lanz TV, Tritschler I, Koppel A, Tolosa E, Hoberg M, Anderl J, Aicher WK, Weller M *et al*: **Toll-like receptor engagement enhances the immunosuppressive properties of human bone marrow-derived mesenchymal stem cells by inducing indoleamine-2,3-dioxygenase-1 via interferon-beta and protein kinase r.** *Stem cells* (2009) **27**(4):909-919.
124. Tomchuck SL, Zwezdaryk KJ, Coffelt SB, Waterman RS, Danka ES, Scandurro AB: **Toll-like receptors on human mesenchymal stem cells drive their migration and immunomodulating responses.** *Stem cells* (2008) **26**(1):99-107.
125. Lotfi R, Eisenbacher J, Solgi G, Fuchs K, Yildiz T, Nienhaus C, Rojewski MT, Schrezenmeier H: **Human mesenchymal stem cells respond to native but not oxidized damage associated molecular pattern molecules from necrotic (tumor) material.** *Eur J Immunol* (2011) **41**(7):2021-2028.
126. van den Akker F, de Jager SC, Sluijter JP: **Mesenchymal stem cell therapy for cardiac inflammation: Immunomodulatory properties and the influence of toll-like receptors.** *Mediators Inflamm* (2013) **2013**(181020).
127. van den Borne SW, Diez J, Blankesteyn WM, Verjans J, Hofstra L, Narula J: **Myocardial remodeling after infarction: The role of myofibroblasts.** *Nature reviews Cardiology* (2010) **7**(1):30-37.
128. Segers VF, Lee RT: **Biomaterials to enhance stem cell function in the heart.** *Circulation research* (2011) **109**(8):910-922.
129. Hodgkinson CP, Gomez JA, Payne AJ, Zhang L, Wang X, Dal-Pra S, Pratt RE, Dzau VJ: **Abi3bp regulates cardiac progenitor cell proliferation and differentiation.** *Circulation research* (2014) **115**(12):1007-1016.
130. Li Z, Guo X, Guan J: **An oxygen release system to augment cardiac progenitor cell survival and differentiation under hypoxic condition.** *Biomaterials* (2012) **33**(25):5914-5923.
131. Chen TG, Zhong ZY, Sun GF, Zhou YX, Zhao Y: **Effects of tumour necrosis factor-alpha on activity and nitric oxide synthase of endothelial progenitor cells from peripheral blood.** *Cell proliferation* (2011) **44**(4):352-359.

132. Hu X, Wang J, Chen J, Luo R, He A, Xie X, Li J: **Optimal temporal delivery of bone marrow mesenchymal stem cells in rats with myocardial infarction.** *European journal of cardio-thoracic surgery : official journal of the European Association for Cardio-thoracic Surgery* (2007) **31**(3):438-443.
133. Liu B, Duan CY, Luo CF, Ou CW, Wu ZY, Zhang JW, Ni XB, Chen PY, Chen MS: **Impact of timing following acute myocardial infarction on efficacy and safety of bone marrow stem cells therapy: A network meta-analysis.** *Stem cells international* (2016) **2016**(1031794).
134. Caveliers V, De Keulenaer G, Everaert H, Van Riet I, Van Camp G, Verheye S, Roland J, Schoors D, Franken PR, Schots R: **In vivo visualization of 111in labeled cd133+ peripheral blood stem cells after intracoronary administration in patients with chronic ischemic heart disease.** *The quarterly journal of nuclear medicine and molecular imaging : official publication of the Italian Association of Nuclear Medicine* (2007) **51**(1):61-66.
135. Dedobbeleer C, Blocklet D, Toungouz M, Lambermont M, Unger P, Degaute JP, Goldman S, Berkenboom G: **Myocardial homing and coronary endothelial function after autologous blood cd34+ progenitor cells intracoronary injection in the chronic phase of myocardial infarction.** *Journal of cardiovascular pharmacology* (2009) **53**(6):480-485.
136. Mayfield AE, Tilokee EL, Latham N, McNeill B, Lam BK, Ruel M, Suuronen EJ, Courtman DW, Stewart DJ, Davis DR: **The effect of encapsulation of cardiac stem cells within matrix-enriched hydrogel capsules on cell survival, post-ischemic cell retention and cardiac function.** *Biomaterials* (2014) **35**(1):133-142.
137. Anversa P, Leri A, Rota M, Hosoda T, Bearzi C, Urbanek K, Kajstura J, Bolli R: **Concise review: Stem cells, myocardial regeneration, and methodological artifacts.** *Stem cells* (2007) **25**(3):589-601.
138. Yaziji H, Barry T: **Diagnostic immunohistochemistry: What can go wrong?** *Advances in anatomic pathology* (2006) **13**(5):238-246.
139. Hong KU, Li QH, Guo Y, Patton NS, Moktar A, Bhatnagar A, Bolli R: **A highly sensitive and accurate method to quantify absolute numbers of c-kit+ cardiac stem cells following transplantation in mice.** *Basic research in cardiology* (2013) **108**(3):346.

140. Love C, Palestro CJ: **Radionuclide imaging of infection.** *Journal of nuclear medicine technology* (2004) **32**(2):47-57; quiz 58-49.
141. Wu C, Ma G, Li J, Zheng K, Dang Y, Shi X, Sun Y, Li F, Zhu Z: **In vivo cell tracking via (1)(8)f-fluorodeoxyglucose labeling: A review of the preclinical and clinical applications in cell-based diagnosis and therapy.** *Clinical imaging* (2013) **37**(1):28-36.
142. Moreira ML, da Costa Medeiros P, de Souza SA, Gutfilen B, Rosado-de-Castro PH: **In vivo tracking of cell therapies for cardiac diseases with nuclear medicine.** *Stem cells international* (2016) **2016**(3140120).
143. Kang WJ, Kang HJ, Kim HS, Chung JK, Lee MC, Lee DS: **Tissue distribution of 18f-fdg-labeled peripheral hematopoietic stem cells after intracoronary administration in patients with myocardial infarction.** *J Nucl Med* (2006) **47**(8):1295-1301.
144. Schachinger V, Aicher A, Dobert N, Rover R, Diener J, Fichtlscherer S, Assmus B, Seeger FH, Menzel C, Brenner W, Dimmeler S *et al.*: **Pilot trial on determinants of progenitor cell recruitment to the infarcted human myocardium.** *Circulation* (2008) **118**(14):1425-1432.
145. Campbell NG, Kaneko M, Shintani Y, Narita T, Sawhney V, Coppen SR, Yashiro K, Mathur A, Suzuki K: **Cell size critically determines initial retention of bone marrow mononuclear cells in the heart after intracoronary injection: Evidence from a rat model.** *PloS one* (2016) **11**(7):e0158232.
146. Fischer UM, Harting MT, Jimenez F, Monzon-Posadas WO, Xue H, Savitz SI, Laine GA, Cox CS, Jr.: **Pulmonary passage is a major obstacle for intravenous stem cell delivery: The pulmonary first-pass effect.** *Stem cells and development* (2009) **18**(5):683-692.
147. Doerschuk CM, Beyers N, Coxson HO, Wiggs B, Hogg JC: **Comparison of neutrophil and capillary diameters and their relation to neutrophil sequestration in the lung.** *Journal of applied physiology* (1993) **74**(6):3040-3045.
148. Freyman T, Polin G, Osman H, Crary J, Lu M, Cheng L, Palasis M, Wilensky RL: **A quantitative, randomized study evaluating three methods of mesenchymal stem cell delivery following myocardial infarction.** *European heart journal* (2006) **27**(9):1114-1122.

149. Kraitchman DL, Tatsumi M, Gilson WD, Ishimori T, Kedziorek D, Walczak P, Segars WP, Chen HH, Fritzges D, Izbudak I, Young RG *et al*: **Dynamic imaging of allogeneic mesenchymal stem cells trafficking to myocardial infarction.** *Circulation* (2005) **112**(10):1451-1461.
150. Bonios M, Terrovitis J, Chang CY, Engles JM, Higuchi T, Lautamaki R, Yu J, Fox J, Pomper M, Wahl RL, Tsui BM *et al*: **Myocardial substrate and route of administration determine acute cardiac retention and lung bio-distribution of cardiosphere-derived cells.** *Journal of nuclear cardiology : official publication of the American Society of Nuclear Cardiology* (2011) **18**(3):443-450.
151. Schrepfer S, Deuse T, Reichenspurner H, Fischbein MP, Robbins RC, Pelletier MP: **Stem cell transplantation: The lung barrier.** *Transplantation proceedings* (2007) **39**(2):573-576.
152. Aicher A, Brenner W, Zuhayra M, Badorff C, Massoudi S, Assmus B, Eckey T, Henze E, Zeiher AM, Dimmeler S: **Assessment of the tissue distribution of transplanted human endothelial progenitor cells by radioactive labeling.** *Circulation* (2003) **107**(16):2134-2139.
153. Johnston PV, Sasano T, Mills K, Evers R, Lee ST, Smith RR, Lardo AC, Lai S, Steenbergen C, Gerstenblith G, Lange R *et al*: **Engraftment, differentiation, and functional benefits of autologous cardiosphere-derived cells in porcine ischemic cardiomyopathy.** *Circulation* (2009) **120**(12):1075-1083, 1077 p following 1083.
154. Gyongyosi M, Dib N: **Diagnostic and prognostic value of 3d noga mapping in ischemic heart disease.** *Nature reviews Cardiology* (2011) **8**(7):393-404.
155. Rodrigo SF, van Ramshorst J, Beeres SL, Al Younis I, Dibbets-Schneider P, de Roos A, Fibbe WE, Zwaginga JJ, Schalij MJ, Bax JJ, Atsma DE: **Intramyocardial injection of bone marrow mononuclear cells in chronic myocardial ischemia patients after previous placebo injection improves myocardial perfusion and anginal symptoms: An intra-patient comparison.** *American heart journal* (2012) **164**(5):771-778.
156. Maeda K, Seymour R, Ruel M, Suuronen EJ: **Echocardiography-guided intramyocardial injection method in a murine model.** *Methods in molecular biology* (2017) **1553**(217-225).
157. Perin EC, Silva GV, Assad JA, Vela D, Buja LM, Sousa AL, Litovsky S, Lin J, Vaughn WK, Coulter S, Fernandes MR *et al*: **Comparison of intracoronary and**

- transendocardial delivery of allogeneic mesenchymal cells in a canine model of acute myocardial infarction.** *Journal of molecular and cellular cardiology* (2008) **44**(3):486-495.
158. Kanelidis A, Premer C, Lopez JG, Balkan W, Hare JM: **Route of delivery modulates the efficacy of mesenchymal stem cell therapy for myocardial infarction: A meta-analysis of preclinical studies and clinical trials.** *Circulation research* (2016).
159. van der Spoel TI, Vrijssen KR, Koudstaal S, Sluijter JP, Nijssen JF, de Jong HW, Hofer IE, Cramer MJ, Doevendans PA, van Belle E, Chamuleau SA: **Transendocardial cell injection is not superior to intracoronary infusion in a porcine model of ischaemic cardiomyopathy: A study on delivery efficiency.** *Journal of cellular and molecular medicine* (2012) **16**(11):2768-2776.
160. Vulliet PR, Greeley M, Halloran SM, MacDonald KA, Kittleson MD: **Intra-coronary arterial injection of mesenchymal stromal cells and microinfarction in dogs.** *Lancet* (2004) **363**(9411):783-784.
161. Tossios P, Krausgrill B, Schmidt M, Fischer T, Halbach M, Fries JW, Fahnenstich S, Frommolt P, Heppelmann I, Schmidt A, Schomacker K *et al*: **Role of balloon occlusion for mononuclear bone marrow cell deposition after intracoronary injection in pigs with reperfused myocardial infarction.** *European heart journal* (2008) **29**(15):1911-1921.
162. Grossman PM, Han Z, Palasis M, Barry JJ, Lederman RJ: **Incomplete retention after direct myocardial injection.** *Catheterization and cardiovascular interventions : official journal of the Society for Cardiac Angiography & Interventions* (2002) **55**(3):392-397.
163. Patel AN, Mittal S, Turan G, Winters AA, Henry TD, Ince H, Trehan N: **Revive trial: Retrograde delivery of autologous bone marrow in patients with heart failure.** *Stem cells translational medicine* (2015) **4**(9):1021-1027.
164. Vestweber D: **How leukocytes cross the vascular endothelium.** *Nature reviews Immunology* (2015) **15**(11):692-704.
165. Kavanagh DP, Kalia N: **Hematopoietic stem cell homing to injured tissues.** *Stem cell reviews* (2011) **7**(3):672-682.

166. Teo GS, Ankrum JA, Martinelli R, Boetto SE, Simms K, Sciuto TE, Dvorak AM, Karp JM, Carman CV: **Mesenchymal stem cells transmigrate between and directly through tumor necrosis factor-alpha-activated endothelial cells via both leukocyte-like and novel mechanisms.** *Stem cells* (2012) **30**(11):2472-2486.
167. Funcke F, Hoyer H, Brenig F, Steingen C, Ladage D, Muller-Ehmsen J, Schmidt A, Brixius K, Bloch W: **Characterisation of the interaction between circulating and in vitro cultivated endothelial progenitor cells and the endothelial barrier.** *European journal of cell biology* (2008) **87**(2):81-90.
168. Allen TA, Gracieux D, Talib M, Tokarz DA, Hensley MT, Cores J, Vandergriff A, Tang J, de Andrade JB, Dinh PU, Yoder JA *et al*: **Angiopeliosis as an alternative mechanism of cell extravasation.** *Stem cells* (2017) **35**(1):170-180.
169. Lam CK, Yoo T, Hiner B, Liu Z, Grutzendler J: **Embolus extravasation is an alternative mechanism for cerebral microvascular recanalization.** *Nature* (2010) **465**(7297):478-482.
170. Hinkel R, El-Aouni C, Olson T, Horstkotte J, Mayer S, Muller S, Willhauck M, Spitzweg C, Gildehaus FJ, Munzing W, Hannappel E *et al*: **Thymosin beta4 is an essential paracrine factor of embryonic endothelial progenitor cell-mediated cardioprotection.** *Circulation* (2008) **117**(17):2232-2240.
171. Li GH, Luo B, Lv YX, Zheng F, Wang L, Wei MX, Li XY, Zhang L, Wang JN, Chen SY, Tang JM *et al*: **Dual effects of vegf-b on activating cardiomyocytes and cardiac stem cells to protect the heart against short- and long-term ischemia-reperfusion injury.** *Journal of translational medicine* (2016) **14**(1):116.
172. Wang J, Nachtigal MW, Kardami E, Cattini PA: **Fgf-2 protects cardiomyocytes from doxorubicin damage via protein kinase c-dependent effects on efflux transporters.** *Cardiovascular research* (2013) **98**(1):56-63.
173. Xia P, Liu Y, Cheng Z: **Signaling pathways in cardiac myocyte apoptosis.** *BioMed research international* (2016) **2016**(9583268).
174. Barile L, Lionetti V, Cervio E, Matteucci M, Gherghiceanu M, Popescu LM, Torre T, Siclari F, Moccetti T, Vassalli G: **Extracellular vesicles from human cardiac progenitor cells inhibit cardiomyocyte apoptosis and improve cardiac function after myocardial infarction.** *Cardiovascular research* (2014) **103**(4):530-541.

175. Sahoo S, Klychko E, Thorne T, Misener S, Schultz KM, Millay M, Ito A, Liu T, Kamide C, Agrawal H, Perlman H *et al*: **Exosomes from human cd34(+) stem cells mediate their proangiogenic paracrine activity.** *Circulation research* (2011) **109**(7):724-728.
176. Malliaras K, Ibrahim A, Tseliou E, Liu W, Sun B, Middleton RC, Seinfeld J, Wang L, Sharifi BG, Marban E: **Stimulation of endogenous cardioblasts by exogenous cell therapy after myocardial infarction.** *EMBO molecular medicine* (2014) **6**(6):760-777.
177. Ellison GM, Torella D, Dellegrottaglie S, Perez-Martinez C, Perez de Prado A, Vicinanza C, Purushothaman S, Galuppo V, Iaconetti C, Waring CD, Smith A *et al*: **Endogenous cardiac stem cell activation by insulin-like growth factor-1/hepatocyte growth factor intracoronary injection fosters survival and regeneration of the infarcted pig heart.** *Journal of the American College of Cardiology* (2011) **58**(9):977-986.
178. Segers VF, Tokunou T, Higgins LJ, MacGillivray C, Gannon J, Lee RT: **Local delivery of protease-resistant stromal cell derived factor-1 for stem cell recruitment after myocardial infarction.** *Circulation* (2007) **116**(15):1683-1692.
179. Malliaras K, Zhang Y, Seinfeld J, Galang G, Tseliou E, Cheng K, Sun B, Aminzadeh M, Marban E: **Cardiomyocyte proliferation and progenitor cell recruitment underlie therapeutic regeneration after myocardial infarction in the adult mouse heart.** *EMBO molecular medicine* (2013) **5**(2):191-209.
180. Tseliou E, de Couto G, Terrovitis J, Sun B, Weixin L, Marban L, Marban E: **Angiogenesis, cardiomyocyte proliferation and anti-fibrotic effects underlie structural preservation post-infarction by intramyocardially-injected cardiospheres.** *PloS one* (2014) **9**(2):e88590.
181. Lang JK, Young RF, Ashraf H, Canty JM, Jr.: **Inhibiting extracellular vesicle release from human cardiosphere derived cells with lentiviral knockdown of nsmase2 differentially effects proliferation and apoptosis in cardiomyocytes, fibroblasts and endothelial cells in vitro.** *PloS one* (2016) **11**(11):e0165926.
182. Ramkisoensing AA, de Vries AA, Atsma DE, Schalij MJ, Pijnappels DA: **Interaction between myofibroblasts and stem cells in the fibrotic heart: Balancing between deterioration and regeneration.** *Cardiovascular research* (2014) **102**(2):224-231.

183. Kang JW, Kang KS, Koo HC, Park JR, Choi EW, Park YH: **Soluble factors-mediated immunomodulatory effects of canine adipose tissue-derived mesenchymal stem cells.** *Stem cells and development* (2008) **17**(4):681-693.
184. Hasan AS, Luo L, Yan C, Zhang TX, Urata Y, Goto S, Mangoura SA, Abdel-Raheem MH, Zhang S, Li TS: **Cardiosphere-derived cells facilitate heart repair by modulating m1/m2 macrophage polarization and neutrophil recruitment.** *PLoS one* (2016) **11**(10):e0165255.
185. Xie Y, Ibrahim A, Cheng K, Wu Z, Liang W, Malliaras K, Sun B, Liu W, Shen D, Cheol Cho H, Li T *et al*: **Importance of cell-cell contact in the therapeutic benefits of cardiosphere-derived cells.** *Stem cells* (2014) **32**(9):2397-2406.
186. Jing D, Fonseca AV, Alakel N, Fierro FA, Muller K, Bornhauser M, Ehninger G, Corbeil D, Ordemann R: **Hematopoietic stem cells in co-culture with mesenchymal stromal cells--modeling the niche compartments in vitro.** *Haematologica* (2010) **95**(4):542-550.
187. Yang WJ, Li SH, Weisel RD, Liu SM, Li RK: **Cell fusion contributes to the rescue of apoptotic cardiomyocytes by bone marrow cells.** *Journal of cellular and molecular medicine* (2012) **16**(12):3085-3095.
188. Ibrahim AG, Cheng K, Marban E: **Exosomes as critical agents of cardiac regeneration triggered by cell therapy.** *Stem cell reports* (2014) **2**(5):606-619.
189. Vrtovec B, Poglajen G, Lezaic L, Sever M, Domanovic D, Cernelc P, Socan A, Schrepfer S, Torre-Amione G, Haddad F, Wu JC: **Effects of intracoronary cd34+ stem cell transplantation in nonischemic dilated cardiomyopathy patients: 5-year follow-up.** *Circulation research* (2013) **112**(1):165-173.
190. Ziebart T, Yoon CH, Trepels T, Wietelmann A, Braun T, Kiessling F, Stein S, Grez M, Ihling C, Muhly-Reinholz M, Carmona G *et al*: **Sustained persistence of transplanted proangiogenic cells contributes to neovascularization and cardiac function after ischemia.** *Circulation research* (2008) **103**(11):1327-1334.
191. Yoon CH, Koyanagi M, Iekushi K, Seeger F, Urbich C, Zeiher AM, Dimmeler S: **Mechanism of improved cardiac function after bone marrow mononuclear cell therapy: Role of cardiovascular lineage commitment.** *Circulation* (2010) **121**(18):2001-2011.

192. Borrelli E, Heyman R, Hsi M, Evans RM: **Targeting of an inducible toxic phenotype in animal cells.** *Proc Natl Acad Sci U S A* (1988) **85**(20):7572-7576.
193. Ziebart T, Yoon CH, Trepels T, Wietelmann A, Braun T, Kiessling F, Stein S, Grez M, Ihling C, Muhly-Reinholz M, Carmona G *et al*: **Sustained persistence of transplanted proangiogenic cells contributes to neovascularization and cardiac function after ischemia.** *Circ Res* (2008) **103**(11):1327-1334.
194. Clark AJ, Iwobi M, Cui W, Crompton M, Harold G, Hobbs S, Kamalati T, Knox R, Neil C, Yull F, Gusterson B: **Selective cell ablation in transgenic mice expression e. Coli nitroreductase.** *Gene Ther* (1997) **4**(2):101-110.
195. Ramos CA, Asgari Z, Liu E, Yvon E, Heslop HE, Rooney CM, Brenner MK, Dotti G: **An inducible caspase 9 suicide gene to improve the safety of mesenchymal stromal cell therapies.** *Stem cells* (2010) **28**(6):1107-1115.
196. Palmiter R: **Interrogation by toxin.** *Nat Biotechnol* (2001) **19**(8):731-732.
197. Huang LH, Lavine KJ, Randolph GJ: **Cardiac lymphatic vessels, transport, and healing of the infarcted heart.** *JACC Basic to translational science* (2017) **2**(4):477-483.
198. Collantes M, Pelacho B, Garcia-Velloso MJ, Gavira JJ, Abizanda G, Palacios I, Rodriguez-Borlado L, Alvarez V, Prieto E, Ecay M, Larequi E *et al*: **Non-invasive in vivo imaging of cardiac stem/progenitor cell biodistribution and retention after intracoronary and intramyocardial delivery in a swine model of chronic ischemia reperfusion injury.** *Journal of translational medicine* (2017) **15**(1):56.
199. Ishikawa Y, Akishima-Fukasawa Y, Ito K, Akasaka Y, Tanaka M, Shimokawa R, Kimura-Matsumoto M, Morita H, Sato S, Kamata I, Ishii T: **Lymphangiogenesis in myocardial remodelling after infarction.** *Histopathology* (2007) **51**(3):345-353.
200. Mehlhorn U, Geissler HJ, Laine GA, Allen SJ: **Myocardial fluid balance.** *European journal of cardio-thoracic surgery : official journal of the European Association for Cardio-thoracic Surgery* (2001) **20**(6):1220-1230.
201. Perin EC, Tian M, Marini FC, 3rd, Silva GV, Zheng Y, Baimbridge F, Quan X, Fernandes MR, Gahremanpour A, Young D, Paolillo V *et al*: **Imaging long-term fate of intramyocardially implanted mesenchymal stem cells in a porcine myocardial infarction model.** *PLoS one* (2011) **6**(9):e22949.

202. Mangi AA, Noiseux N, Kong D, He H, Rezvani M, Ingwall JS, Dzau VJ: **Mesenchymal stem cells modified with akt prevent remodeling and restore performance of infarcted hearts.** *Nat Med* (2003) **9**(9):1195-1201.
203. Li W, Ma N, Ong LL, Nesselmann C, Klopsch C, Ladilov Y, Furlani D, Piechaczek C, Moebius JM, Lutzow K, Lendlein A *et al*: **Bcl-2 engineered mscs inhibited apoptosis and improved heart function.** *Stem cells* (2007) **25**(8):2118-2127.
204. Liang Y, Lin Q, Zhu J, Li X, Fu Y, Zou X, Liu X, Tan H, Deng C, Yu X, Shan Z *et al*: **The caspase-8 shrna-modified mesenchymal stem cells improve the function of infarcted heart.** *Mol Cell Biochem* (2014) **397**(1-2):7-16.
205. Fischer KM, Cottage CT, Wu W, Din S, Gude NA, Avitabile D, Quijada P, Collins BL, Fransioli J, Sussman MA: **Enhancement of myocardial regeneration through genetic engineering of cardiac progenitor cells expressing pim-1 kinase.** *Circulation* (2009) **120**(21):2077-2087.
206. Song H, Chang W, Lim S, Seo HS, Shim CY, Park S, Yoo KJ, Kim BS, Min BH, Lee H, Jang Y *et al*: **Tissue transglutaminase is essential for integrin-mediated survival of bone marrow-derived mesenchymal stem cells.** *Stem cells* (2007) **25**(6):1431-1438.
207. Huang J, Zhang Z, Guo J, Ni A, Deb A, Zhang L, Mirotsov M, Pratt RE, Dzau VJ: **Genetic modification of mesenchymal stem cells overexpressing ccr1 increases cell viability, migration, engraftment, and capillary density in the injured myocardium.** *Circulation research* (2010) **106**(11):1753-1762.
208. Ward MR, Thompson KA, Isaac K, Vecchiarelli J, Zhang Q, Stewart DJ, Kutryk MJ: **Nitric oxide synthase gene transfer restores activity of circulating angiogenic cells from patients with coronary artery disease.** *Mol Ther* (2011) **19**(7):1323-1330.
209. Wu Y, Ip JE, Huang J, Zhang L, Matsushita K, Liew CC, Pratt RE, Dzau VJ: **Essential role of icam-1/cd18 in mediating epc recruitment, angiogenesis, and repair to the infarcted myocardium.** *Circ Res* (2006) **99**(3):315-322.
210. Wang Y, Chen Q, Zhang Z, Jiang F, Meng X, Yan H: **Interleukin-10 overexpression improves the function of endothelial progenitor cells stimulated with tnf-alpha through the activation of the stat3 signaling pathway.** *International journal of molecular medicine* (2015) **35**(2):471-477.

211. Song H, Kwon K, Lim S, Kang SM, Ko YG, Xu Z, Chung JH, Kim BS, Lee H, Joung B, Park S *et al*: **Transfection of mesenchymal stem cells with the fgf-2 gene improves their survival under hypoxic conditions.** *Molecules and cells* (2005) **19**(3):402-407.
212. Gomez-Mauricio G, Moscoso I, Martin-Cancho MF, Crisostomo V, Prat-Vidal C, Baez-Diaz C, Sanchez-Margallo FM, Bernad A: **Combined administration of mesenchymal stem cells overexpressing igf-1 and hgf enhances neovascularization but moderately improves cardiac regeneration in a porcine model.** *Stem cell research & therapy* (2016) **7**(1):94.
213. Haider H, Jiang S, Idris NM, Ashraf M: **Igf-1-overexpressing mesenchymal stem cells accelerate bone marrow stem cell mobilization via paracrine activation of sdf-1alpha/cxcr4 signaling to promote myocardial repair.** *Circulation research* (2008) **103**(11):1300-1308.
214. Jackson R, Tilokee EL, Latham N, Mount S, Rafatian G, Strydhorst J, Ye B, Boodhwani M, Chan V, Ruel M, Ruddy TD *et al*: **Paracrine engineering of human cardiac stem cells with insulin-like growth factor 1 enhances myocardial repair.** *Journal of the American Heart Association* (2015) **4**(9):e002104.
215. Zhang M, Mal N, Kiedrowski M, Chacko M, Askari AT, Popovic ZB, Koc ON, Penn MS: **Sdf-1 expression by mesenchymal stem cells results in trophic support of cardiac myocytes after myocardial infarction.** *FASEB journal : official publication of the Federation of American Societies for Experimental Biology* (2007) **21**(12):3197-3207.
216. Das H, George JC, Joseph M, Das M, Abdulhameed N, Blitz A, Khan M, Sakthivel R, Mao HQ, Hoit BD, Kuppusamy P *et al*: **Stem cell therapy with overexpressed vegf and pdgf genes improves cardiac function in a rat infarct model.** *PLoS one* (2009) **4**(10):e7325.
217. Cerrada I, Ruiz-Sauri A, Carrero R, Trigueros C, Dorronsoro A, Sanchez-Puelles JM, Diez-Juan A, Montero JA, Sepulveda P: **Hypoxia-inducible factor 1 alpha contributes to cardiac healing in mesenchymal stem cells-mediated cardiac repair.** *Stem cells and development* (2013) **22**(3):501-511.
218. Wang X, Zhao T, Huang W, Wang T, Qian J, Xu M, Kranias EG, Wang Y, Fan GC: **Hsp20-engineered mesenchymal stem cells are resistant to oxidative stress via enhanced activation of akt and increased secretion of growth factors.** *Stem cells* (2009) **27**(12):3021-3031.

219. Mangi AA, Noiseux N, Kong D, He H, Rezvani M, Ingwall JS, Dzau VJ: **Mesenchymal stem cells modified with akt prevent remodeling and restore performance of infarcted hearts.** *Nature medicine* (2003) **9**(9):1195-1201.
220. O'Sullivan JF, Leblond AL, Kelly G, Kumar AH, Metharom P, Buneker CK, Alizadeh-Vikali N, Hristova I, Hynes BG, O'Connor R, Caplice NM: **Potent long-term cardioprotective effects of single low-dose insulin-like growth factor-1 treatment postmyocardial infarction.** *Circulation Cardiovascular interventions* (2011) **4**(4):327-335.
221. Jackson R, Tilokee EL, Latham N, Mount S, Rafatian G, Strydhorst J, Ye B, Boodhwani M, Chan V, Ruel M, Ruddy TD *et al*: **Paracrine engineering of human cardiac stem cells with insulin-like growth factor 1 enhances myocardial repair.** *J Am Heart Assoc* (2015) **4**(9).
222. Tilokee EL, Latham N, Jackson R, Mayfield AE, Ye B, Mount S, Lam BK, Suuronen EJ, Ruel M, Stewart DJ, Davis DR: **Paracrine engineering of human explant-derived cardiac stem cells to over-express stromal-cell derived factor 1alpha enhances myocardial repair.** *Stem cells* (2016).
223. Douglas KL: **Toward development of artificial viruses for gene therapy: A comparative evaluation of viral and non-viral transfection.** *Biotechnol Prog* (2008) **24**(4):871-883.
224. Gwizdala A, Rozwadowska N, Kolanowski TJ, Malcher A, Cieplucha A, Perek B, Seniuk W, Straburzynska-Migaj E, Oko-Sarnowska Z, Cholewinski W, Michalak M *et al*: **Safety, feasibility and effectiveness of first in-human administration of muscle-derived stem/progenitor cells modified with connexin-43 gene for treatment of advanced chronic heart failure.** *European journal of heart failure* (2017) **19**(1):148-157.
225. Behfar A, Yamada S, Crespo-Diaz R, Nesbitt JJ, Rowe LA, Perez-Terzic C, Gaussin V, Homsy C, Bartunek J, Terzic A: **Guided cardiopoiesis enhances therapeutic benefit of bone marrow human mesenchymal stem cells in chronic myocardial infarction.** *Journal of the American College of Cardiology* (2010) **56**(9):721-734.
226. Laflamme MA, Chen KY, Naumova AV, Muskheli V, Fugate JA, Dupras SK, Reinecke H, Xu C, Hassanipour M, Police S, O'Sullivan C *et al*: **Cardiomyocytes derived from human embryonic stem cells in pro-survival factors enhance function of infarcted rat hearts.** *Nat Biotechnol* (2007) **25**(9):1015-1024.

227. Bartunek J, Behfar A, Dolatabadi D, Vanderheyden M, Ostojic M, Dens J, El Nakadi B, Banovic M, Beleslin B, Vrolix M, Legrand V *et al*: **Cardiopoietic stem cell therapy in heart failure: The c-cure (cardiopoietic stem cell therapy in heart failure) multicenter randomized trial with lineage-specified biologics.** *Journal of the American College of Cardiology* (2013) **61**(23):2329-2338.
228. Tekin D, Dursun AD, Xi L: **Hypoxia inducible factor 1 (hif-1) and cardioprotection.** *Acta pharmacologica Sinica* (2010) **31**(9):1085-1094.
229. Hu X, Xu Y, Zhong Z, Wu Y, Zhao J, Wang Y, Cheng H, Kong M, Zhang F, Chen Q, Sun J *et al*: **A large-scale investigation of hypoxia-preconditioned allogeneic mesenchymal stem cells for myocardial repair in nonhuman primates: Paracrine activity without remuscularization.** *Circulation research* (2016) **118**(6):970-983.
230. Kubo M, Li TS, Suzuki R, Shirasawa B, Morikage N, Ohshima M, Qin SL, Hamano K: **Hypoxic preconditioning increases survival and angiogenic potency of peripheral blood mononuclear cells via oxidative stress resistance.** *American journal of physiology Heart and circulatory physiology* (2008) **294**(2):H590-595.
231. Tang YL, Zhu W, Cheng M, Chen L, Zhang J, Sun T, Kishore R, Phillips MI, Losordo DW, Qin G: **Hypoxic preconditioning enhances the benefit of cardiac progenitor cell therapy for treatment of myocardial infarction by inducing cxcr4 expression.** *Circulation research* (2009) **104**(10):1209-1216.
232. Wang X, Zhao T, Huang W, Wang T, Qian J, Xu M, Kranias EG, Wang Y, Fan GC: **Hsp20-engineered mesenchymal stem cells are resistant to oxidative stress via enhanced activation of akt and increased secretion of growth factors.** *Stem cells* (2009) **27**(12):3021-3031.
233. Feng Y, Huang W, Meng W, Jegga AG, Wang Y, Cai W, Kim HW, Pasha Z, Wen Z, Rao F, Modi RM *et al*: **Heat shock improves sca-1+ stem cell survival and directs ischemic cardiomyocytes toward a prosurvival phenotype via exosomal transfer: A critical role for hsf1/mir-34a/hsp70 pathway.** *Stem cells* (2014) **32**(2):462-472.
234. Cheng K, Blusztajn A, Shen D, Li TS, Sun B, Galang G, Zarembinski TI, Prestwich GD, Marban E, Smith RR, Marban L: **Functional performance of human cardiosphere-derived cells delivered in an in situ polymerizable hyaluronan-gelatin hydrogel.** *Biomaterials* (2012) **33**(21):5317-5324.

235. Danoviz ME, Nakamuta JS, Marques FL, dos Santos L, Alvarenga EC, dos Santos AA, Antonio EL, Schettert IT, Tucci PJ, Krieger JE: **Rat adipose tissue-derived stem cells transplantation attenuates cardiac dysfunction post infarction and biopolymers enhance cell retention.** *PloS one* (2010) **5**(8):e12077.
236. Suuronen EJ, Veinot JP, Wong S, Kapila V, Price J, Griffith M, Mesana TG, Ruel M: **Tissue-engineered injectable collagen-based matrices for improved cell delivery and vascularization of ischemic tissue using cd133+ progenitors expanded from the peripheral blood.** *Circulation* (2006) **114**(1 Suppl):I138-144.
237. Godier-Furnemont AF, Martens TP, Koeckert MS, Wan L, Parks J, Arai K, Zhang G, Hudson B, Homma S, Vunjak-Novakovic G: **Composite scaffold provides a cell delivery platform for cardiovascular repair.** *Proceedings of the National Academy of Sciences of the United States of America* (2011) **108**(19):7974-7979.
238. Ceccaldi C, Fullana SG, Alfarano C, Lairez O, Calise D, Cussac D, Parini A, Sallerin B: **Alginate scaffolds for mesenchymal stem cell cardiac therapy: Influence of alginate composition.** *Cell transplantation* (2012) **21**(9):1969-1984.
239. Lu S, Wang H, Lu W, Liu S, Lin Q, Li D, Duan C, Hao T, Zhou J, Wang Y, Gao S *et al*: **Both the transplantation of somatic cell nuclear transfer- and fertilization-derived mouse embryonic stem cells with temperature-responsive chitosan hydrogel improve myocardial performance in infarcted rat hearts.** *Tissue engineering Part A* (2010) **16**(4):1303-1315.
240. Wang T, Jiang XJ, Tang QZ, Li XY, Lin T, Wu DQ, Zhang XZ, Okello E: **Bone marrow stem cells implantation with alpha-cyclodextrin/mpeg-pcl-mpeg hydrogel improves cardiac function after myocardial infarction.** *Acta biomaterialia* (2009) **5**(8):2939-2944.
241. Lin YD, Yeh ML, Yang YJ, Tsai DC, Chu TY, Shih YY, Chang MY, Liu YW, Tang AC, Chen TY, Luo CY *et al*: **Intramyocardial peptide nanofiber injection improves postinfarction ventricular remodeling and efficacy of bone marrow cell therapy in pigs.** *Circulation* (2010) **122**(11 Suppl):S132-141.
242. Mihic A, Cui Z, Wu J, Vlacic G, Miyagi Y, Li SH, Lu S, Sung HW, Weisel RD, Li RK: **A conductive polymer hydrogel supports cell electrical signaling and improves cardiac function after implantation into myocardial infarct.** *Circulation* (2015) **132**(8):772-784.

243. Rane AA, Christman KL: **Biomaterials for the treatment of myocardial infarction: A 5-year update.** *Journal of the American College of Cardiology* (2011) **58**(25):2615-2629.
244. Chan BP, Hui TY, Yeung CW, Li J, Mo I, Chan GC: **Self-assembled collagen-human mesenchymal stem cell microspheres for regenerative medicine.** *Biomaterials* (2007) **28**(31):4652-4666.
245. Aguado BA, Mulyasasmita W, Su J, Lampe KJ, Heilshorn SC: **Improving viability of stem cells during syringe needle flow through the design of hydrogel cell carriers.** *Tissue engineering Part A* (2012) **18**(7-8):806-815.
246. Zhang W, Zhao S, Rao W, Snyder J, Choi JK, Wang J, Khan IA, Saleh NB, Mohler PJ, Yu J, Hund TJ *et al*: **A novel core-shell microcapsule for encapsulation and 3d culture of embryonic stem cells.** *Journal of materials chemistry B, Materials for biology and medicine* (2013) **2013**(7):1002-1009.
247. Lam J, Segura T: **The modulation of msc integrin expression by rgd presentation.** *Biomaterials* (2013) **34**(16):3938-3947.
248. Mao AS, Shin JW, Utech S, Wang H, Uzun O, Li W, Cooper M, Hu Y, Zhang L, Weitz DA, Mooney DJ: **Deterministic encapsulation of single cells in thin tunable microgels for niche modelling and therapeutic delivery.** *Nature materials* (2017) **16**(2):236-243.
249. Kuraitis D, Hou C, Zhang Y, Vulesevic B, Sofrenovic T, McKee D, Sharif Z, Ruel M, Suuronen EJ: **Ex vivo generation of a highly potent population of circulating angiogenic cells using a collagen matrix.** *Journal of molecular and cellular cardiology* (2011) **51**(2):187-197.
250. Silva NA, Moreira J, Ribeiro-Samy S, Gomes ED, Tam RY, Shoichet MS, Reis RL, Sousa N, Salgado AJ: **Modulation of bone marrow mesenchymal stem cell secretome by ecm-like hydrogels.** *Biochimie* (2013) **95**(12):2314-2319.
251. Ifkovits JL, Tous E, Minakawa M, Morita M, Robb JD, Koomalsingh KJ, Gorman JH, 3rd, Gorman RC, Burdick JA: **Injectable hydrogel properties influence infarct expansion and extent of postinfarction left ventricular remodeling in an ovine model.** *Proceedings of the National Academy of Sciences of the United States of America* (2010) **107**(25):11507-11512.

252. Cheng K, Malliaras K, Shen D, Tseliou E, Ionta V, Smith J, Galang G, Sun B, Houde C, Marban E: **Intramyocardial injection of platelet gel promotes endogenous repair and augments cardiac function in rats with myocardial infarction.** *Journal of the American College of Cardiology* (2012) **59**(3):256-264.
253. Chachques JC, Trainini JC, Lago N, Cortes-Morichetti M, Schussler O, Carpentier A: **Myocardial assistance by grafting a new bioartificial upgraded myocardium (magnum trial): Clinical feasibility study.** *The Annals of thoracic surgery* (2008) **85**(3):901-908.
254. Takehara N, Tsutsumi Y, Tateishi K, Ogata T, Tanaka H, Ueyama T, Takahashi T, Takamatsu T, Fukushima M, Komeda M, Yamagishi M *et al*: **Controlled delivery of basic fibroblast growth factor promotes human cardiosphere-derived cell engraftment to enhance cardiac repair for chronic myocardial infarction.** *Journal of the American College of Cardiology* (2008) **52**(23):1858-1865.
255. Yacoub MH, Terrovitis J: **Caduceus, scipio, alcadia: Cell therapy trials using cardiac-derived cells for patients with post myocardial infarction lv dysfunction, still evolving.** *Global cardiology science & practice* (2013) **2013**(1):5-8.
256. Kanda P, Davis DR: **Cellular mechanisms underlying cardiac engraftment of stem cells.** *Expert opinion on biological therapy* (2017) **17**(9):1127-1143.
257. de Couto G, Gallet R, Cambier L, Jaghatspanyan E, Makkar N, Dawkins JF, Berman BP, Marban E: **Exosomal microrna transfer into macrophages mediates cellular postconditioning.** *Circulation* (2017) **136**(2):200-214.
258. Gallet R, Dawkins J, Valle J, Simsolo E, de Couto G, Middleton R, Tseliou E, Luthringer D, Kreke M, Smith RR, Marban L *et al*: **Exosomes secreted by cardiosphere-derived cells reduce scarring, attenuate adverse remodelling, and improve function in acute and chronic porcine myocardial infarction.** *Eur Heart J* (2016) 201-211.
259. Ibrahim AG, Cheng K, Marban E: **Exosomes as critical agents of cardiac regeneration triggered by cell therapy.** *Stem cell reports* (2014) **2**(5):606-619.
260. Pelaz B, Alexiou C, Alvarez-Puebla RA, Alves F, Andrews AM, Ashraf S, Balogh LP, Ballerini L, Bestetti A, Brendel C, Bosi S *et al*: **Diverse applications of nanomedicine.** *ACS Nano* (2017) **11**(3):2313-2381.

261. Sugiura S, Oda T, Izumida Y, Aoyagi Y, Satake M, Ochiai A, Ohkohchi N, Nakajima M: **Size control of calcium alginate beads containing living cells using micro-nozzle array.** *Biomaterials* (2005) **26**(16):3327-3331.
262. Ross CJ, Chang PL: **Development of small alginate microcapsules for recombinant gene product delivery to the rodent brain.** *J Biomater Sci, Polym Ed* (2002) **13**(8):953-962.
263. Tang J, Cui X, Caranasos TG, Hensley MT, Vandergriff AC, Hartanto Y, Shen D, Zhang H, Zhang J, Cheng K: **Heart repair using nanogel-encapsulated human cardiac stem cells in mice and pigs with myocardial infarction.** *ACS Nano* (2017) **11**(10):9738-9749.
264. Mayfield AE, Tilokee EL, Latham N, McNeill B, Lam BK, Ruel M, Suuronen EJ, Courtman DW, Stewart DJ, Davis DR: **The effect of encapsulation of cardiac stem cells within matrix-enriched hydrogel capsules on cell survival, post-ischemic cell retention and cardiac function.** *Biomaterials* (2014) **35**(1):133-142.
265. Karoubi G, Ormiston ML, Stewart DJ, Courtman DW: **Single-cell hydrogel encapsulation for enhanced survival of human marrow stromal cells.** *Biomaterials* (2009) **30**(29):5445-5455.
266. Ahmadi A, McNeill B, Vulesevic B, Kordos M, Mesana L, Thorn S, Renaud JM, Manthorp E, Kuraitis D, Toeg H, Mesana TG *et al*: **The role of integrin alpha2 in cell and matrix therapy that improves perfusion, viability and function of infarcted myocardium.** *Biomaterials* (2014) **35**(17):4749-4758.
267. Mak WC, Olesen K, Sivler P, Lee CJ, Moreno-Jimenez I, Edin J, Courtman D, Skog M, Griffith M: **Controlled delivery of human cells by temperature responsive microcapsules.** *Journal of functional biomaterials* (2015) **6**(2):439-453.
268. Chaudhuri O, Gu L, Klumpers D, Darnell M, Bencherif SA, Weaver JC, Huebsch N, Lee HP, Lippens E, Duda GN, Mooney DJ: **Hydrogels with tunable stress relaxation regulate stem cell fate and activity.** *Nat Mater* (2016) **15**(3):326-334.
269. Engler A, Bacakova L, Newman C, Hategan A, Griffin M, Discher D: **Substrate compliance versus ligand density in cell on gel responses.** *Biophysical journal* (2004) **86**(1 Pt 1):617-628.

270. Engler AJ, Sen S, Sweeney HL, Discher DE: **Matrix elasticity directs stem cell lineage specification.** *Cell* (2006) **126**(4):677-689.
271. Chaudhuri O, Koshy ST, Branco da Cunha C, Shin JW, Verbeke CS, Allison KH, Mooney DJ: **Extracellular matrix stiffness and composition jointly regulate the induction of malignant phenotypes in mammary epithelium.** *Nat Mater* (2014) **13**(10):970-978.
272. Paszek MJ, Zahir N, Johnson KR, Lakins JN, Rozenberg GI, Gefen A, Reinhart-King CA, Margulies SS, Dembo M, Boettiger D, Hammer DA *et al*: **Tensional homeostasis and the malignant phenotype.** *Cancer cell* (2005) **8**(3):241-254.
273. Jutila AA, Zignego DL, Schell WJ, June RK: **Encapsulation of chondrocytes in high-stiffness agarose microenvironments for *in vitro* modeling of osteoarthritis mechanotransduction.** *Annals of biomedical engineering* (2015) **43**(5):1132-1144.
274. Shkumatov A, Thompson M, Choi KM, Sicard D, Baek K, Kim DH, Tschumperlin DJ, Prakash YS, Kong H: **Matrix stiffness-modulated proliferation and secretory function of the airway smooth muscle cells.** *American journal of physiology Lung cellular and molecular physiology* (2015) **308**(11):L1125-L1135.
275. Charras G, Sahai E: **Physical influences of the extracellular environment on cell migration.** *Nat Rev Mol Cell Biol* (2014) **15**(12):813-824.
276. Mao AS, Shin JW, Utech S, Wang H, Uzun O, Li W, Cooper M, Hu Y, Zhang L, Weitz DA, Mooney DJ: **Deterministic encapsulation of single cells in thin tunable microgels for niche modelling and therapeutic delivery.** *Nat Mater* (2017) **16**(2):236-243.
277. Canibano-Hernandez A, Saenz Del Burgo L, Espona-Noguera A, Orive G, Hernandez RM, Ciriza J, Pedraz JL: **Alginate microcapsules incorporating hyaluronic acid recreate closer *in vivo* environment for mesenchymal stem cells.** *Mol pharmaceutics* (2017) **14**(7):2390-2399.
278. Blocki A, Beyer S, Dewavrin JY, Goralczyk A, Wang Y, Peh P, Ng M, Moonshi SS, Vuddagiri S, Raghunath M, Martinez EC *et al*: **Microcapsules engineered to support mesenchymal stem cell (msc) survival and proliferation enable long-term retention of mscs in infarcted myocardium.** *Biomaterials* (2015) **53**(12-24).

279. Sakai S, Kawabata K, Ono T, Ijima H, Kawakami K: **Development of mammalian cell-enclosing subsieve-size agarose capsules (<100 microm) for cell therapy.** *Biomaterials* (2005) **26**(23):4786-4792.
280. Asano S, Ito S, Takahashi K, Furuya K, Kondo M, Sokabe M, Hasegawa Y: **Matrix stiffness regulates migration of human lung fibroblasts.** *Physiological reports* (2017) **5**(9):e13281.
281. Yeh YT, Hur SS, Chang J, Wang KC, Chiu JJ, Li YS, Chien S: **Matrix stiffness regulates endothelial cell proliferation through septin 9.** *PloS one* (2012) **7**(10):e46889.
282. Cavo M, Fato M, Penuela L, Beltrame F, Raiteri R, Scaglione S: **Microenvironment complexity and matrix stiffness regulate breast cancer cell activity in a 3d in vitro model.** *Scientific reports* (2016) **6**(35367).
283. Sun M, Chi G, Xu J, Tan Y, Xu J, Lv S, Xu Z, Xia Y, Li L, Li Y: **Extracellular matrix stiffness controls osteogenic differentiation of mesenchymal stem cells mediated by integrin alpha5.** *Stem cell research & therapy* (2018) **9**(1):52.
284. Abdeen AA, Weiss JB, Lee J, Kilian KA: **Matrix composition and mechanics direct proangiogenic signaling from mesenchymal stem cells.** *Tissue Eng, Part A* (2014) **20**(19-20):2737-2745.
285. Seib FP, Prewitz M, Werner C, Bornhauser M: **Matrix elasticity regulates the secretory profile of human bone marrow-derived multipotent mesenchymal stromal cells (mscs).** *Biochem Biophys Res Commun* (2009) **389**(4):663-667.
286. Latham N, Ye B, Jackson R, Lam BK, Kuraitis D, Ruel M, Suuronen EJ, Stewart DJ, Davis DR: **Human blood and cardiac stem cells synergize to enhance cardiac repair when cotransplanted into ischemic myocardium.** *Circulation* (2013) **128**(11 Suppl 1):S105-S112.
287. Jiang CY, Gui C, He AN, Hu XY, Chen J, Jiang Y, Wang JA: **Optimal time for mesenchymal stem cell transplantation in rats with myocardial infarction.** *Journal of Zhejiang University Science B* (2008) **9**(8):630-637.
288. Yang F, Liu YH, Yang XP, Xu J, Kapke A, Carretero OA: **Myocardial infarction and cardiac remodelling in mice.** *Experimental physiology* (2002) **87**(5):547-555.

289. Kulandavelu S, Karantalis V, Fritsch J, Hatzistergos KE, Loescher VY, McCall F, Wang B, Bagno L, Golpanian S, Wolf A, Grenet J *et al*: **Pim1 kinase overexpression enhances ckit+ cardiac stem cell cardiac repair following myocardial infarction in swine.** *J Am Coll Cardiol* (2016) **68**(22):2454-2464.
290. Tokita Y, Tang XL, Li Q, Wysoczynski M, Hong KU, Nakamura S, Wu WJ, Xie W, Li D, Hunt G, Ou Q *et al*: **Repeated administrations of cardiac progenitor cells are markedly more effective than a single administration: A new paradigm in cell therapy.** *Circ Res* (2016) **119**(5):635-651.
291. Reich H, Tseliou E, de Couto G, Angert D, Valle J, Kubota Y, Luthringer D, Mirocha J, Sun B, Smith RR, Marban L *et al*: **Repeated transplantation of allogeneic cardiosphere-derived cells boosts therapeutic benefits without immune sensitization in a rat model of myocardial infarction.** *J Heart Lung Transplant* (2016) **35**(11):1348-1357.
292. Narayanan J, Xiong J-Y, Liu X-Y: **Determination of agarose gel pore size: Absorbance measurements *vis a vis* other techniques.** *J Phys: Conf Ser* (2006) **28**(83-86).
293. Pluen A, Netti PA, Jain RK, Berk DA: **Diffusion of macromolecules in agarose gels: Comparison of linear and globular configurations.** *Biophysical journal* (1999) **77**(1):542-552.
294. Caliarì SR, Burdick JA: **A practical guide to hydrogels for cell culture.** *Nature methods* (2016) **13**(5):405-414.
295. Jackson R, Tilokee EL, Latham N, Mount S, Rafatian G, Strydhorst J, Ye B, Boodhwani M, Chan V, Ruel M, Ruddy TD *et al*: **Paracrine engineering of human cardiac stem cells with insulin-like growth factor 1 enhances myocardial repair.** *Journal of the American Heart Association* (2015) **4**(9):e002104.
296. Molgat ASD, Tilokee EL, Rafatian G, Vulesevic B, Ruel M, Milne R, Suuronen EJ, Davis DR: **Hyperglycemia inhibits cardiac stem cell-mediated cardiac repair and angiogenic capacity.** *Circulation* (2014) **130**(11 Suppl 1):S70-S76.
297. Tilokee EL, Latham N, Jackson R, Mayfield AE, Ye B, Mount S, Lam BK, Suuronen EJ, Ruel M, Stewart DJ, Davis DR: **Paracrine engineering of human explant-derived cardiac stem cells to over-express stromal-cell derived factor 1alpha enhances myocardial repair.** *Stem Cells* (2016) 1826-1835.

298. Patten RD, Hall-Porter MR: **Small animal models of heart failure: Development of novel therapies, past and present.** *Circ: Heart Failure* (2009) **2**(2):138-144.
299. Fantozzi A, Gruber DC, Pisarsky L, Heck C, Kunita A, Yilmaz M, Meyer-Schaller N, Cornille K, Hopfer U, Bentires-Alj M, Christofori G: **Vegf-mediated angiogenesis links emt-induced cancer stemness to tumor initiation.** *Cancer research* (2014) **74**(5):1566-1575.
300. Hendrayani SF, Al-Khalaf HH, Aboussekhra A: **The cytokine il-6 reactivates breast stromal fibroblasts through transcription factor stat3-dependent up-regulation of the rna-binding protein auf1.** *The Journal of biological chemistry* (2014) **289**(45):30962-30976.
301. Orimo A, Gupta PB, SgROI DC, Arenzana-Seisdedos F, Delaunay T, Naeem R, Carey VJ, Richardson AL, Weinberg RA: **Stromal fibroblasts present in invasive human breast carcinomas promote tumor growth and angiogenesis through elevated sdf-1/cxcl12 secretion.** *Cell* (2005) **121**(3):335-348.
302. Rudisch A, Dewhurst MR, Horga LG, Kramer N, Harrer N, Dong M, van der Kuip H, Wernitznig A, Bernthaler A, Dolznig H, Sommergruber W: **High emt signature score of invasive non-small cell lung cancer (nsclc) cells correlates with nfkappab driven colony-stimulating factor 2 (csf2/gm-csf) secretion by neighboring stromal fibroblasts.** *PloS one* (2015) **10**(4):e0124283.
303. Rechartd O, Elomaa O, Vaalamo M, Paakkonen K, Jahkola T, Hook-Nikanne J, Hembry RM, Hakkinen L, Kere J, Saarialho-Kere U: **Stromelysin-2 is upregulated during normal wound repair and is induced by cytokines.** *J Invest Dermatol* (2000) **115**(5):778-787.
304. Visse R, Nagase H: **Matrix metalloproteinases and tissue inhibitors of metalloproteinases: Structure, function, and biochemistry.** *Circ Res* (2003) **92**(8):827-839.
305. House SL, Wang J, Castro AM, Weinheimer C, Kovacs A, Ornitz DM: **Fibroblast growth factor 2 is an essential cardioprotective factor in a closed-chest model of cardiac ischemia-reperfusion injury.** *Physiological reports* (2015) **3**(1):e12278.
306. Mayfield AE, Kanda P, Nantsios A, Parent S, Mount S, Dixit S, Ye B, Seymour R, Stewart DJ, Davis DR: **Interleukin-6 mediates post-infarct repair by cardiac explant-derived stem cells.** *Theranostics* (2017) **7**(19):4850-4861.

307. Mayfield AE, Fitzpatrick ME, Latham N, Tilokee EL, Villanueva M, Mount S, Lam BK, Ruel M, Stewart DJ, Davis DR: **The impact of patient co-morbidities on the regenerative capacity of cardiac explant-derived stem cells.** *Stem Cell Res Ther* (2016) **7**(1):60.
308. Schneider CA, Rasband WS, Eliceiri KW: **Nih image to imagej: 25 years of image analysis.** *Nature methods* (2012) **9**(7):671-675.
309. Ravichandran R, Islam MM, Alarcon EI, Samanta A, Wang S, Lundstrom P, Hilborn J, Griffith M, Phopase J: **Functionalised type-i collagen as a hydrogel building block for bio-orthogonal tissue engineering applications.** *J Mater Chem B* (2016) **4**(2):318-326.
310. Rezende CA, Lee L-T, Galembeck F: **Surface mechanical properties of thin polymer films investigated by afm in pulsed force mode.** *Langmuir* (2009) **25**(17):9938-9946.
311. Tolde O, Rosel D, Vesely P, Folk P, Brabek J: **The structure of invadopodia in a complex 3d environment.** *Eur J Cell Biol* (2010) **89**(9):674-680.
312. Jorgens DM, Inman JL, Wojcik M, Robertson C, Palsdottir H, Tsai WT, Huang H, Bruni-Cardoso A, Lopez CS, Bissell MJ, Xu K *et al*: **Deep nuclear invaginations are linked to cytoskeletal filaments - integrated bioimaging of epithelial cells in 3d culture.** *J Cell Sci* (2017) **130**(1):177-189.
313. Xie JL, Grahl N, Sless T, Leach MD, Kim SH, Hogan DA, Robbins N, Cowen LE: **Signaling through Irg1, rho1 and pkc1 governs candida albicans morphogenesis in response to diverse cues.** *PLoS genetics* (2016) **12**(10):e1006405.
314. Tam S, de Borja R, Tsao MS, McPherson JD: **Robust global microrna expression profiling using next-generation sequencing technologies.** *Laboratory investigation; a journal of technical methods and pathology* (2014) **94**(3):350-358.
315. Hyder CL, Kemppainen K, Isoniemi KO, Imanishi SY, Goto H, Inagaki M, Fazeli E, Eriksson JE, Tornquist K: **Sphingolipids inhibit vimentin-dependent cell migration.** *J Cell Sci* (2015) **128**(11):2057-2069.

316. Zilionis R, Nainys J, Veres A, Savova V, Zemmour D, Klein AM, Mazutis L: **Single-cell barcoding and sequencing using droplet microfluidics.** *Nature protocols* (2017) **12**(1):44-73.
317. Kanda P, Alarcon EI, Yeuchyk T, Parent S, de Kemp RA, Variola F, Courtman D, Stewart DJ, Davis DR: **Deterministic encapsulation of human cardiac stem cells in variable composition nanoporous gel cocoons to enhance therapeutic repair of injured myocardium.** *ACS Nano* (2018) **12**(5):4338-4350.
318. Gomez-Mauricio RG, Acarregui A, Sanchez-Margallo FM, Crisostomo V, Gallo I, Hernandez RM, Pedraz JL, Orive G, Martin-Cancho MF: **A preliminary approach to the repair of myocardial infarction using adipose tissue-derived stem cells encapsulated in magnetic resonance-labelled alginate microspheres in a porcine model.** *European journal of pharmaceuticals and biopharmaceutics : official journal of Arbeitsgemeinschaft fur Pharmazeutische Verfahrenstechnik eV* (2013) **84**(1):29-39.
319. Roche ET, Hastings CL, Lewin SA, Shvartsman D, Brudno Y, Vasilyev NV, O'Brien FJ, Walsh CJ, Duffy GP, Mooney DJ: **Comparison of biomaterial delivery vehicles for improving acute retention of stem cells in the infarcted heart.** *Biomaterials* (2014) **35**(25):6850-6858.
320. Tan RP, Lee BSL, Chan AHP, Yuen SCG, Hung J, Wise SG, Ng MKC: **Non-invasive tracking of injected bone marrow mononuclear cells to injury and implanted biomaterials.** *Acta biomaterialia* (2017) **53**(378-388).
321. Cho HJ, Lee HJ, Youn SW, Koh SJ, Won JY, Chung YJ, Cho HJ, Yoon CH, Lee SW, Lee EJ, Kwon YW *et al*: **Secondary sphere formation enhances the functionality of cardiac progenitor cells.** *Molecular therapy : the journal of the American Society of Gene Therapy* (2012) **20**(9):1750-1766.
322. Qazi TH, Mooney DJ, Duda GN, Geissler S: **Biomaterials that promote cell-cell interactions enhance the paracrine function of mscs.** *Biomaterials* (2017) **140**(103-114).
323. Fang Y, Zhao Y, He S, Guo T, Song Q, Guo N, Yuan Z: **Overexpression of fgf19 alleviates hypoxia/reoxygenation-induced injury of cardiomyocytes by regulating gsk-3beta/nrf2/are signaling.** *Biochemical and biophysical research communications* (2018) **503**(4):2355-2362.
324. Li X, Zhao D, Guo Z, Li T, Qili M, Xu B, Qian M, Liang H, E X, Chege Gitau S, Wang L *et al*: **Overexpression of serpine2/protease nexin-1 contribute to**

- pathological cardiac fibrosis via increasing collagen deposition.** *Scientific reports* (2016) **6**(37635).
325. Xia Y, Frangogiannis NG: **Mcp-1/ccl2 as a therapeutic target in myocardial infarction and ischemic cardiomyopathy.** *Inflammation & allergy drug targets* (2007) **6**(2):101-107.
326. Suthahar N, Meijers WC, Sillje HHW, de Boer RA: **From inflammation to fibrosis-molecular and cellular mechanisms of myocardial tissue remodelling and perspectives on differential treatment opportunities.** *Current heart failure reports* (2017) **14**(4):235-250.
327. Fornai F, Carrizzo A, Forte M, Ambrosio M, Damato A, Ferrucci M, Biagioni F, Busceti C, Puca AA, Vecchione C: **The inflammatory protein pentraxin 3 in cardiovascular disease.** *Immunity & ageing : I & A* (2016) **13**(1):25.
328. Velasquez IM, Frumento P, Johansson K, Berglund A, de Faire U, Leander K, Gigante B: **Association of interleukin 8 with myocardial infarction: Results from the stockholm heart epidemiology program.** *International journal of cardiology* (2014) **172**(1):173-178.
329. Latham N, Ye B, Jackson R, Lam BK, Kuraitis D, Ruel M, Suuronen EJ, Stewart DJ, Davis DR: **Human blood and cardiac stem cells synergize to enhance cardiac repair when cotransplanted into ischemic myocardium.** *Circulation* (2013) **128**(11 Suppl 1):S105-112.
330. Molgat ASD, Tilokee EL, Rafatian G, Vulesevic B, Ruel M, Milne R, Suuronen EJ, Davis DR: **Hyperglycemia inhibits cardiac stem cell-mediated cardiac repair and angiogenic capacity.** *Circulation* (2014) **130**(11 Suppl 1):S70-76.
331. Kai F, Laklai H, Weaver VM: **Force matters: Biomechanical regulation of cell invasion and migration in disease.** *Trends in cell biology* (2016) **26**(7):486-497.
332. Lange JR, Fabry B: **Cell and tissue mechanics in cell migration.** *Experimental cell research* (2013) **319**(16):2418-2423.
333. Haeger A, Wolf K, Zegers MM, Friedl P: **Collective cell migration: Guidance principles and hierarchies.** *Trends in cell biology* (2015) **25**(9):556-566.
334. Pironti G, Strachan RT, Abraham D, Mon-Wei Yu S, Chen M, Chen W, Hanada K, Mao L, Watson LJ, Rockman HA: **Circulating exosomes induced by cardiac**

- pressure overload contain functional angiotensin ii type 1 receptors.** *Circulation* (2015) **131**(24):2120-2130.
335. Villasante A, Marturano-Kruik A, Ambati SR, Liu Z, Godier-Furnemont A, Parsa H, Lee BW, Moore MA, Vunjak-Novakovic G: **Recapitulating the size and cargo of tumor exosomes in a tissue-engineered model.** *Theranostics* (2016) **6**(8):1119-1130.
336. Previtiera ML, Sengupta A: **Substrate stiffness regulates proinflammatory mediator production through tlr4 activity in macrophages.** *PloS one* (2015) **10**(12):e0145813.
337. Takehara N, Tsutsumi Y, Tateishi K, Ogata T, Tanaka H, Ueyama T, Takahashi T, Takamatsu T, Fukushima M, Komeda M, Yamagishi M *et al*: **Controlled delivery of basic fibroblast growth factor promotes human cardiosphere-derived cell engraftment to enhance cardiac repair for chronic myocardial infarction.** *Journal of the American College of Cardiology* (2008) **52**(23):1858-1865.
338. Ren RM, Liu H, Zhao SH, Cao JH: **Targeting of mir-432 to myozenin1 to regulate myoblast proliferation and differentiation.** *Genetics and molecular research : GMR* (2016) **15**(4):gmr15049313.
339. Gururajan M, Josson S, Chu GC, Lu CL, Lu YT, Haga CL, Zhau HE, Liu C, Lichterman J, Duan P, Posadas EM *et al*: **Mir-154\* and mir-379 in the dlk1-dio3 microrna mega-cluster regulate epithelial to mesenchymal transition and bone metastasis of prostate cancer.** *Clinical cancer research : an official journal of the American Association for Cancer Research* (2014) **20**(24):6559-6569.
340. Chen J, Crawford R, Chen C, Xiao Y: **The key regulatory roles of the pi3k/akt signaling pathway in the functionalities of mesenchymal stem cells and applications in tissue regeneration.** *Tissue Eng, Part B* (2013) **19**(6):516-528.
341. Sharma S, Mishra R, Simpson D, Wehman B, Colletti EJ, Deshmukh S, Datla SR, Balachandran K, Guo Y, Chen L, Siddiqui OT *et al*: **Cardiosphere-derived cells from pediatric end-stage heart failure patients have enhanced functional activity due to the heat shock response regulating the secretome.** *Stem cells* (2015) **33**(4):1213-1229.
342. Fisher SA, Zhang H, Doree C, Mathur A, Martin-Rendon E: **Stem cell treatment for acute myocardial infarction.** *The Cochrane database of systematic reviews* (2015) 9):CD006536.

343. Pieters T, van Roy F: **Role of cell-cell adhesion complexes in embryonic stem cell biology.** *Journal of cell science* (2014) **127**(Pt 12):2603-2613.
344. Li TS, Cheng K, Lee ST, Matsushita S, Davis D, Malliaras K, Zhang Y, Matsushita N, Smith RR, Marban E: **Cardiospheres recapitulate a niche-like microenvironment rich in stemness and cell-matrix interactions, rationalizing their enhanced functional potency for myocardial repair.** *Stem cells* (2010) **28**(11):2088-2098.
345. Kanazawa H, Tseliou E, Malliaras K, Yee K, Dawkins JF, De Couto G, Smith RR, Kreke M, Seinfeld J, Middleton RC, Gallet R *et al*: **Cellular postconditioning: Allogeneic cardiosphere-derived cells reduce infarct size and attenuate microvascular obstruction when administered after reperfusion in pigs with acute myocardial infarction.** *Circulation Heart failure* (2015) **8**(2):322-332.
346. Cassani DAD, Altomare L, De Nardo L, Variola F: **Physicochemical and nanomechanical investigation of electrodeposited chitosan:Peo blends.** *J Mater Chem B* (2015) **3**(13):2641-2650.
347. Tang J, Shen D, Caranasos TG, Wang Z, Vandergriff AC, Allen TA, Hensley MT, Dinh PU, Cores J, Li TS, Zhang J *et al*: **Therapeutic microparticles functionalized with biomimetic cardiac stem cell membranes and secretome.** *Nat Commun* (2017) **8**(13724).
348. Badr CE: **Bioluminescence imaging: Basics and practical limitations.** *Methods in molecular biology* (2014) **1098**(1-18).
349. Boehler RM, Graham JG, Shea LD: **Tissue engineering tools for modulation of the immune response.** *BioTechniques* (2011) **51**(4):239-240, 242, 244 passim.
350. Grainger DW: **All charged up about implanted biomaterials.** *Nature biotechnology* (2013) **31**(6):507-509.
351. Kirkpatrick FH, Dumais MM, White HW, Guiseley KB: **Influence of the agarose matrix in pulsed-field electrophoresis.** *Electrophoresis* (1993) **14**(4):349-354.
352. Brodbeck WG, Patel J, Voskerician G, Christenson E, Shive MS, Nakayama Y, Matsuda T, Ziats NP, Anderson JM: **Biomaterial adherent macrophage apoptosis is increased by hydrophilic and anionic substrates in vivo.** *Proceedings of the National Academy of Sciences of the United States of America* (2002) **99**(16):10287-10292.

353. Almond A: **Hyaluronan**. *Cellular and molecular life sciences : CMLS* (2007) **64**(13):1591-1596.
354. Gerecht S, Burdick JA, Ferreira LS, Townsend SA, Langer R, Vunjak-Novakovic G: **Hyaluronic acid hydrogel for controlled self-renewal and differentiation of human embryonic stem cells**. *Proceedings of the National Academy of Sciences of the United States of America* (2007) **104**(27):11298-11303.
355. Flynn L, Prestwich GD, Semple JL, Woodhouse KA: **Adipose tissue engineering in vivo with adipose-derived stem cells on naturally derived scaffolds**. *Journal of biomedical materials research Part A* (2009) **89**(4):929-941.
356. Zhong J, Chan A, Morad L, Kornblum HI, Fan G, Carmichael ST: **Hydrogel matrix to support stem cell survival after brain transplantation in stroke**. *Neurorehabilitation and neural repair* (2010) **24**(7):636-644.
357. Gaetani R, Feyen DA, Verhage V, Slaats R, Messina E, Christman KL, Giacomello A, Doevendans PA, Sluijter JP: **Epicardial application of cardiac progenitor cells in a 3d-printed gelatin/hyaluronic acid patch preserves cardiac function after myocardial infarction**. *Biomaterials* (2015) **61**(339-348).
358. Donegan GC, Hunt JA, Rhodes N: **Investigating the importance of flow when utilizing hyaluronan scaffolds for tissue engineering**. *Journal of tissue engineering and regenerative medicine* (2010) **4**(2):83-95.
359. Young JL, Tuler J, Braden R, Schup-Magoffin P, Schaefer J, Kretchmer K, Christman KL, Engler AJ: **In vivo response to dynamic hyaluronic acid hydrogels**. *Acta biomaterialia* (2013) **9**(7):7151-7157.
360. Mo W, Yang C, Liu Y, He Y, Wang Y, Gao F: **The influence of hyaluronic acid on vascular endothelial cell proliferation and the relationship with ezrin/merlin expression**. *Acta biochimica et biophysica Sinica* (2011) **43**(12):930-939.
361. Richette P, Chevalier X, Ea HK, Eymard F, Henrotin Y, Ornetti P, Sellam J, Cucherat M, Marty M: **Hyaluronan for knee osteoarthritis: An updated meta-analysis of trials with low risk of bias**. *RMD open* (2015) **1**(1):e000071.
362. Longinotti C: **The use of hyaluronic acid based dressings to treat burns: A review**. *Burns & trauma* (2014) **2**(4):162-168.

363. Stawicki SP, Green JM, Martin ND, Green RH, Cipolla J, Seamon MJ, Eiferman DS, Evans DC, Hazelton JP, Cook CH, Steinberg SM *et al*: **Results of a prospective, randomized, controlled study of the use of carboxymethylcellulose sodium hyaluronate adhesion barrier in trauma open abdomens.** *Surgery* (2014) **156**(2):419-430.
364. Vrijland WW, Tseng LN, Eijkman HJ, Hop WC, Jakimowicz JJ, Leguit P, Stassen LP, Swank DJ, Haverlag R, Bonjer HJ, Jeekel H: **Fewer intraperitoneal adhesions with use of hyaluronic acid-carboxymethylcellulose membrane: A randomized clinical trial.** *Annals of surgery* (2002) **235**(2):193-199.
365. Prestwich GD: **Evaluating drug efficacy and toxicology in three dimensions: Using synthetic extracellular matrices in drug discovery.** *Accounts of chemical research* (2008) **41**(1):139-148.
366. Varoni E, Tschon M, Palazzo B, Nitti P, Martini L, Rimondini L: **Agarose gel as biomaterial or scaffold for implantation surgery: Characterization, histological and histomorphometric study on soft tissue response.** *Connective tissue research* (2012) **53**(6):548-554.
367. Scarano A, Carinci F, Piattelli A: **Lip augmentation with a new filler (agarose gel): A 3-year follow-up study.** *Oral surgery, oral medicine, oral pathology, oral radiology, and endodontics* (2009) **108**(2):e11-15.
368. Gonzalez-Andrades M, Mata R, Gonzalez-Gallardo MDC, Medialdea S, Arias-Santiago S, Martinez-Atienza J, Ruiz-Garcia A, Perez-Fajardo L, Lizana-Moreno A, Garzon I, Campos A *et al*: **A study protocol for a multicentre randomised clinical trial evaluating the safety and feasibility of a bioengineered human allogeneic nanostructured anterior cornea in patients with advanced corneal trophic ulcers refractory to conventional treatment.** *BMJ open* (2017) **7**(9):e016487.
369. Gupta A, Bhat S, Jagdale PR, Chaudhari BP, Lidgren L, Gupta KC, Kumar A: **Evaluation of three-dimensional chitosan-agarose-gelatin cryogel scaffold for the repair of subchondral cartilage defects: An in vivo study in a rabbit model.** *Tissue engineering Part A* (2014) **20**(23-24):3101-3111.
370. Yin Z, Yang X, Jiang Y, Xing L, Xu Y, Lu Y, Ding P, Ma J, Xu Y, Gui J: **Platelet-rich plasma combined with agarose as a bioactive scaffold to enhance cartilage repair: An in vitro study.** *Journal of biomaterials applications* (2014) **28**(7):1039-1050.

371. Selmi TA, Verdonk P, Chambat P, Dubrana F, Potel JF, Barnouin L, Neyret P: **Autologous chondrocyte implantation in a novel alginate-agarose hydrogel: Outcome at two years.** *The Journal of bone and joint surgery British volume* (2008) **90**(5):597-604.
372. Gao M, Lu P, Bednark B, Lynam D, Conner JM, Sakamoto J, Tuszynski MH: **Templated agarose scaffolds for the support of motor axon regeneration into sites of complete spinal cord transection.** *Biomaterials* (2013) **34**(5):1529-1536.
373. Holdcraft RW, Gazda LS, Circle L, Adkins H, Harbeck SG, Meyer ED, Bautista MA, Martis PC, Laramore MA, Vinerean HV, Hall RD *et al*: **Enhancement of in vitro and in vivo function of agarose-encapsulated porcine islets by changes in the islet microenvironment.** *Cell transplantation* (2014) **23**(8):929-944.
374. Yoo SJ, Kim J, Lee CS, Nam Y: **Simple and novel three dimensional neuronal cell culture using a micro mesh scaffold.** *Experimental neurobiology* (2011) **20**(2):110-115.
375. Pandey R, Yang Y, Jackson L, Ahmed RP: **Micrnas regulating meis1 expression and inducing cardiomyocyte proliferation.** *Cardiovascular regenerative medicine* (2016) **3**(e1468).
376. Wang X, Ha T, Zou J, Ren D, Liu L, Zhang X, Kalbfleisch J, Gao X, Williams D, Li C: **Microrna-125b protects against myocardial ischaemia/reperfusion injury via targeting p53-mediated apoptotic signalling and traf6.** *Cardiovasc Res* (2014) **102**(3):385-395.
377. Cheng J, Zhang P, Jiang H: **Let-7b-mediated pro-survival of transplanted mesenchymal stem cells for cardiac regeneration.** *Stem Cell Res Ther* (2015) **6**(216).
378. Lesizza P, Prosdocimo G, Martinelli V, Sinagra G, Zacchigna S, Giacca M: **Single-dose intracardiac injection of pro-regenerative micrnas improves cardiac function after myocardial infarction.** *Circ Res* (2017) **120**(8):1298-1304.
379. Xiao J, Pan Y, Li XH, Yang XY, Feng YL, Tan HH, Jiang L, Feng J, Yu XY: **Cardiac progenitor cell-derived exosomes prevent cardiomyocytes apoptosis through exosomal mir-21 by targeting pdcd4.** *Cell death & disease* (2016) **7**(6):e2277.

380. Jakob P, Doerries C, Briand S, Mocharla P, Krankel N, Besler C, Mueller M, Manes C, Templin C, Baltés C, Rudin M *et al*: **Loss of angiomiR-126 and 130a in angiogenic early outgrowth cells from patients with chronic heart failure: Role for impaired *in vivo* neovascularization and cardiac repair capacity.** *Circulation* (2012) **126**(25):2962-2975.
381. van Rooij E, Sutherland LB, Thatcher JE, DiMaio JM, Naseem RH, Marshall WS, Hill JA, Olson EN: **Dysregulation of miRNAs after myocardial infarction reveals a role of miR-29 in cardiac fibrosis.** *Proc Natl Acad Sci USA* (2008) **105**(35):13027-13032.
382. Hong Y, Cao H, Wang Q, Ye J, Sui L, Feng J, Cai X, Song H, Zhang X, Chen X: **Mir-22 may suppress fibrogenesis by targeting tgfbeta1 in cardiac fibroblasts.** *Cellular physiology and biochemistry : international journal of experimental cellular physiology, biochemistry, and pharmacology* (2016) **40**(6):1345-1353.
383. Wang S, Aurora AB, Johnson BA, Qi X, McAnally J, Hill JA, Richardson JA, Bassel-Duby R, Olson EN: **The endothelial-specific microRNA miR-126 governs vascular integrity and angiogenesis.** *Developmental cell* (2008) **15**(2):261-271.
384. Ke ZP, Xu P, Shi Y, Gao AM: **Microrna-93 inhibits ischemia-reperfusion induced cardiomyocyte apoptosis by targeting pten.** *Oncotarget* (2016) **7**(20):28796-28805.
385. Banerjee S, Cui H, Xie N, Tan Z, Yang S, Icyuz M, Thannickal VJ, Abraham E, Liu G: **Mir-125a-5p regulates differential activation of macrophages and inflammation.** *The Journal of biological chemistry* (2013) **288**(49):35428-35436.
386. Joshi S, Wei J, Bishopric NH: **A cardiac myocyte-restricted lin28/let-7 regulatory axis promotes hypoxia-mediated apoptosis by inducing the akt signaling suppressor pik3ip1.** *Biochimica et biophysica acta* (2016) **1862**(2):240-251.
387. Liu X, Xiao J, Zhu H, Wei X, Platt C, Damilano F, Xiao C, Bezzerides V, Bostrom P, Che L, Zhang C *et al*: **Mir-222 is necessary for exercise-induced cardiac growth and protects against pathological cardiac remodeling.** *Cell metabolism* (2015) **21**(4):584-595.
388. Xing Y, Hou J, Guo T, Zheng S, Zhou C, Huang H, Chen Y, Sun K, Zhong T, Wang J, Li H *et al*: **Microrna-378 promotes mesenchymal stem cell survival and**

- vascularization under hypoxic-ischemic conditions *in vitro*. *Stem Cell Res Ther* (2014) 5(6):130.**
389. Katare R, Riu F, Mitchell K, Gubernator M, Campagnolo P, Cui Y, Fortunato O, Avolio E, Cesselli D, Beltrami AP, Angelini G *et al*: **Transplantation of human pericyte progenitor cells improves the repair of infarcted heart through activation of an angiogenic program involving micro-rna-132.** *Circ Res* (2011) **109**(8):894-906.
390. Guo C, Deng Y, Liu J, Qian L: **Cardiomyocyte-specific role of mir-24 in promoting cell survival.** *J Cell Mol Med* (2015) **19**(1):103-112.
391. Wang K, Liu F, Liu CY, An T, Zhang J, Zhou LY, Wang M, Dong YH, Li N, Gao JN, Zhao YF *et al*: **The long noncoding rna nrf regulates programmed necrosis and myocardial injury during ischemia and reperfusion by targeting mir-873.** *Cell Death Differ* (2016) **23**(8):1394-1405.
392. Eulalio A, Mano M, Dal Ferro M, Zentilin L, Sinagra G, Zacchigna S, Giacca M: **Functional screening identifies mirnas inducing cardiac regeneration.** *Nature* (2012) **492**(7429):376-381.
393. Vlachos IS, Zagganas K, Paraskevopoulou MD, Georgakilas G, Karagkouni D, Vergoulis T, Dalamagas T, Hatzigeorgiou AG: **Diana-mirpath v3.0: Deciphering microrna function with experimental support.** *Nucleic acids research* (2015) **43**(W1):W460-W466.